# THE FUNCTION OF SYMPATHETIC INNERVATION IN THE SPLEEN AND THE ROLE OF ENDOGENOUS CB1/CB2 RECEPTOR SIGNALING

By

Tyrell Jonathan Simkins

A DISSERTATION

Submitted to
Michigan State University
in partial fulfillment of the requirements
for the degree of

Neuroscience - Environmental Toxicology – Doctor of Philosophy

2014

ABSTRACT

THE FUNCTION OF SYMPATHETIC INNERVATION IN THE SPLEEN AND THE ROLE OF ENDOGENOUS CB1/CB2 RECEPTOR SIGNALING

By

Tyrell Jonathan Simkins

The spleen is a multifunction organ that sits at a unique intersection between the circulatory, immune, and neurologic systems. The work in this dissertation endeavored to shed light on the interaction of the sympathetic nervous system in the spleen with these other vital biologic systems. In addition, the role of signaling by the cannabinoid receptors 1 and 2 was explored as it relates the function of splenic sympathetic innervation. Specifically, it was found that splenic noradrenergic neurons do not play a role in T cell independent humoral immunity, and that both norepinephrine and adenosine mediate spleen contraction. It was discovered that splenic sympathetic noradrenergic neurons are likely not regulated by CB1 and that cannabinoid-mediated immunosuppression of humoral immunity is likely due solely to CB2 on immune cells. It was also found that CB1/CB2 play a permissive role in maintaining the relationship between NE release from splenic sympathetic neurons and spleen contraction. These findings add to the knowledge base regarding both the spleen and extra-CNS cannabinoid effects and can be built upon for a more complete understanding of these systems.

Dedicated to my Dad -
“Education is never a waste.”

# ACKNOWLEDGEMENTS

The completion of a dissertation, much like raising children, takes “a village”. There are far too many people that have contributed in some respect to this dissertation, whether directly or indirectly, to list here. Therefore, this will be short and broad.

I have been directly surrounded by an amazing group of people during my life. At home this is my amazing partner, Jensie, without whom I would be lost. I also wish to thank my children, Lucie and Asher, for always making me smile and giving me perspective. My parents, Vione and Paul, raised me right. They are the origin for my own family’s motto: Work hard, play hard. Thank you, thank you. I also wish to thank my siblings for support, teasing, encouragement, and the perfect amount of brotherly competition.

My research colleagues have been amazing. This could be a VERY long list, but I wish to specifically thank a few people. This dissertation really is as much mine as is it Keith Lookingland’s. Thank you for pushing me, guiding me, and being a great mentor. Barb Kaplan, this project was your whole idea in the beginning. Thank you for the guidance, laughs, and keeping me in line. John Goudreau, thank you for showing me that it can be done and for being there when I needed it. There have been a host of Goud-Looking lab mates that have come and gone over the course of my time here: Dr. Bahareh Behrouz, Dr. Kelly

Janis, Hae-Young Hawong, Joe Patterson, Teri Lansdell, Brittany Winner, Kelly McGregor, Ethan Edwin, and Kevin Parihk. But I need to especially thank Dr. Sam Pappas, Dr. Matthew Benskey, and Dr. Chelsea Tiernan. Whew! We all made it.

Lastly I would like to broadly thank and acknowledge the contribution of all the other people I have worked with over the years. Of particular note are Dr. Justin McCormick, Dr. Veronica Maher, Dr. Norbert Kaminski, Dr. James Galligan, Dr. Cheryl Sisk, Bob Crawford, Shawna D'Ingillo, David Fried, Brian Jespersen, and Jim Stockmeyer. Thank you to the Stephanie Watts and the Watts Lab for their help with smooth muscle physiology and quantification. Other notable entities I need to acknowledge are the Neuroscience Program, the Center for Integrative Toxicology, the NIH NRSA program, the College of Osteopathic Medicine, and the DO/PhD program. And to everybody who I was unable to list here: Thank you! You are not forgotten. Thank you one and all. I did it.

TABLE OF CONTENTS

LIST OF TABLES

LIST OF FIGURES

# KEY TO ABBREVIATIONS

| | |
|---|---|
| 2-AG | 2-arachidonylglyceride |
| ABTS | 2,2'-Azino-di-[3-ethylbenzthiazoline sulfonate |
| NSD-1015 | 3-hydroxybenzylhyrdazine |
| MHPG | 3-methoxy-3-hydroxyphenylglycol |
| DOPAL | 3,4-dihydroxyphenylacetaldehyde |
| DHPG | 3,4-dihydroxyphenylglycol |
| 5HT | 5-hydroxytryptamine |
| DPCPX | 8-Cyclopentyl-1,3-dipropylxanthine |
| Ach | Acetylcholine |
| ADP | Adenosine diphosphate |
| AMP | Adenosine monophosphate |
| ATP | Adenosine triphosphate |
| AD | Alcohol dehydrogenase |
| ALD | Aldehyde dehydrogenase |
| ADR | Aldehyde reductase |
| AR | Adrenergic receptor |
| aMT | $\alpha$-Methyl-DL-tyrosine methyl ester hydrochloride |
| A | Amps |
| AEA | Arachidonoylethanolamide or anandamide |
| BCR | B cell receptor |

| | |
|---|---|
| 2-ME | β-Mercaptoethanol |
| BCA | Bicinchoninic acid |
| BCS | Bovine calf serum |
| BSA | Bovine serum albumin |
| BDNF | Brain derived neurotrophic factor |
| CBD | Cannabidiol |
| CB1 | Cannabinoid receptor 1 |
| CB2 | Cannabinoid receptor 2 |
| COMT | Catechol-o-methyl transferase |
| KO | Knockout |
| CNS | Central nervous system |
| cAMP | Cyclic adenosine monophosphate |
| CRH | Corticotropin releasing hormone |
| THC | $\Delta^9$-Tetrahydrocannabinol |
| DMSO | Dimethyl sulfoxide |
| DTT | Dithiothreitol |
| DA | Dopamine |
| DBH | Dopamine-β-hydroxylase |
| DRG | Dorsal root ganglion |
| EFS | Electrical field stimulation |
| ELISA | Enzyme linked immunosorbant assay |
| ELISPOT | Enzyme Linked Immunosorbent Spot Assay |

| | |
|---|---|
| RBC | Erythrocyte(s) |
| EDTA | Ethylenediaminetetraacetic acid |
| FAAH | Fatty acid amide hydrolase |
| FACS | Fluorescence activated cell sorting |
| FDA | Food and Drug Agency |
| GABA | γ-Aminobutyric acid |
| GAPDH | Glyceraldehyde 3-phosphate dehydrogenase |
| HBSS | Hank's Buffered Saline Solution |
| Hz | Hertz |
| HPLC-ED | High performance liquid chromatography coupled with electrochemical detection |
| HRP | Gorseradish peroxidase |
| HCl | Hydrochloric acid |
| HPA | Hypothalamic-pituitary-adrenal |
| Ig | Immunoglobulin |
| IP3 | Inositol 1,4,5-triphosphate |
| IL | Interleukin |
| IML | Intermediolateral cell column of the spinal cord |
| i.p. | Intraperitoneal |
| L-AAAD | L-aromatic amino acid decarboxylase |
| DOPA | L-dihydroxyphenylalanine |
| LPS | Bacterial lipopolysaccharide |

| | |
|---|---|
| MHC | Major histocompatibility complex |
| MFI | Mean fluorescence intensity |
| MAGL | Monoacylglyceride lipase |
| MAPK | Mitogen activated protein kinase |
| MAO | Monoamine oxidase |
| BIBP3226 | N2-(Diphenylacetyl)-N-[(4-hydroxyphenyl)methyl]-D-arginine amide |
| NPY | Neuropeptide Y |
| NE | Norepinephrine |
| PVN | Paraventricular nucleus of the hypothalamus |
| PALS | Periarteriolar lymphatic sheath |
| PNS | Peripheral nervous system |
| PMSF | Phenylmethylsulfonyl fluoride |
| PBS | Phosphate buffered saline |
| PLC | Phospholipase C |
| PCR | Polymerase chain reaction |
| KCl | Potassium chloride |
| $KH_2PO_4$ | Postassium phosphate monobasic |
| PPADS | Pyridoxal phosphate-6-azo(benzene-2,4-disulfonic acid |
| RCF | Relative centrifugal force |
| RDU | Relative density unit |
| RT | Room temperature |

| | |
|---|---|
| Ser | Serine |
| sRBC | Sheep erythrocytes |
| $NaHCO_3$ | Sodium bicarbonate |
| NaCl | Sodium chloride |
| SDS-PAGE | Sodium dodecyl sulfate poly-acrylamide gel electrophoresis |
| NaOH | Sodium hydroxide |
| $Na_2HPO_4$ | Sodium phosphate dibasic |
| sIPSCs | Spontaneous inhibitory postsynaptic currents |
| SEM | Standard error of the mean |
| TCR | T cell receptor |
| $T_H$ | T helper cell |
| TTX | Tetrodotoxin |
| TH | Tyrosine hydroxylase |
| VMA | Vanillylmandelic acid |
| VMAT | Vesicular monoamine transporter |
| V | Volts |
| WT | Wild-type |

## Chapter 1: General Introduction

### 1.1: Statement of Purpose

The spleen is a visceral organ with both hematologic and immune functions. Hematologically the spleen serves as a site to remove foreign material and dead, dying, or damaged erythrocytes from circulation. It also serves as a storage site for erythrocytes, which are released upon demand by contraction of the splenic capsule to increase hematocrit. Immunologically, the spleen is the largest secondary lymphoid organ and plays a significant role in the adaptive immune response by housing leukocytes and providing easy access to the circulation and blood-borne antigens. Innervation of the spleen is via the sympathetic nervous system. The impact of sympathetic neuronal activity on the multifunctional role of the spleen is not entirely clear and is the major purpose of this work.

The legalization and use of marijuana, as well as related cannabinoid compounds, for medicinal and a recreational purposes is increasing in the United States and worldwide. Despite this increasing approval and popularity, the biological ramifications of cannabinoid use are not completely understood. This is particularly true for the actions of cannabinoids outside the brain. Cannabinoid receptors are not only in the central nervous system, but also throughout the body of mammals. The presence of peripheral located cannabinoid receptors suggests a role for both exogenous (marijuana and cannabinoid based drugs) and endogenous cannabinoids (endocannabinoids). Understanding the role of endocannabinoid signaling is significant

by itself, but can also informs the scientific and medical community of the possible ramifications of cannabinoid use and/or abuse.

## 1.2: Spleen

The spleen is a visceral organ with both hematologic and immune functions. The major hematological purpose of the spleen is to remove foreign material and dead, dying, or damaged erythrocytes from circulation. It also serves as a storage site for erythrocytes and iron as well as a site for limited hematopoiesis. Immunologically, the spleen is the largest secondary lymphoid organ and plays a significant role in the adaptive immune response by housing leukocytes and providing easy access to the bloodstream, and thus to blood-borne antigens.

### 1.2.1: Splenic Organization

The spleen is divided into two major parenchymal compartments and one major structural component (Davies and Withrington, 1973; Cesta, 2006). The parenchymal compartments of the spleen are the red and white pulp, which serve the hematologic and immunologic functions of the spleen, respectively. The major structural component of the spleen is the capsule, which gives rise to parenchyma penetrating trabeculae, which also serves a structural function.

1.2.1.1: Red Pulp

The red pulp is composed of a meshwork of reticular cells and fibers, in the midst of which are contained mostly erythrocytes (RBC) and macrophages. The reticular cells in the red pulp are considered myofibroblasts as they contain contractile elements and likely contribute to the contraction of the spleen (Blue and Weiss, 1981; Pinkus et al., 1986; Saito et al., 1988). Red pulp reticular fibers are multi-component structures composed of collagen fibers, elastic fibers, micofibrils, and unmyelinated noradrenergic axons (Saito et al., 1988), all of which is ensheathed by reticular cells and their processes (Cesta, 2006). Within this reticular meshwork are largely RBC entering from branches of central arterioles in the red pulp, or through the white pulp marginal zone to red pulp (Schmidt et al., 1985; Satodate et al., 1986; Schmidt et al., 1993; Mebius and Kraal, 2005). The concentration of RBC within the splenic red pulp, the likely site of RBC storage, is double that of the general circulation (Groom et al., 1991). This area is also where macrophages actively phagocytize dead and damaged erythrocytes (Cesta, 2006). Macrophages within the red pulp are also constantly exposed to foreign particulate matter in the circulation, thus facilitating the speed and efficacy of immune responses (Cesta, 2006).

1.2.1.2: White Pulp

1.2.1.2.1: Structure

The white pulp is composed of T cells, B cells, and macrophages in a reticular framework similar to the red pulp (Saito et al., 1988). As central arterioles enter the spleen they are surrounded the periarteriolar lymphatic sheath (PALS), which is composed of lymphocytes, T and B cells (Mebius and Kraal, 2005; Cesta, 2006), and concentric layers of reticular fibers and cells, which have contractile machinery (Pinkus et al., 1986; Satodate et al., 1986; Cesta, 2006). The PALS is roughly divided into the inner and outer zones. The inner PALS is largely composed of $CD4^+$ T cells, also known as T helper cells ($T_H$), whereas the outer PALS is a mixture of T cells, B cells, macrophages, and plasma cells (B cells differentiated into dedicated antibody producing cells) (Matsuno et al., 1989; Mebius and Kraal, 2005; Cesta, 2006). Collectively, the PALS is considered to be a site for plasma cell differentiation (Matsuno et al., 1989). The marginal zone is a portion of the white pulp at the interface between the red and white pulp of the spleen. It is composed largely of macrophages and functions as a site where the blood is screened for systemic circulating antigens and pathogens (Mebius and Kraal, 2005; Cesta, 2006)

1.2.1.2.2: Function

The spleen is the largest secondary lymphoid organ and the white pulp of the spleen mediates the immune function of the spleen. The full complement of cells required for immune responses, particularly for humoral immunity, are found within the

splenic white pulp. The immune system produces highly complex, multi-cellular, coordinated responses that act to protect organisms from harmful infectious diseases and cancer. The presence of foreign particles, pathogens, or tumor cells ellicit distinct actions with their own particular set of cells and signaling molecules. In general there are two broad divisions of the immune system: innate and adaptive.

Innate immunity is an intrinsic system that is ever present and provides an early and rapid defense against microbes (Oikonomopoulou et al., 2001; Quah and Parish, 2001). The innate immune system does not confer long-term immunity to a pathogen, however it can help the adaptive immune system respond more efficaciously to microbes (Meager and Wadhwa, 2001). The cells mediating the innate immune response include natural killer cells, neutrophils, monocytes/macrophages, and dendritic cells (Quah and Parish, 2001).

The adaptive immune system is directed by lymphocytes comprised of two major types: B cells and T cells (P Kane, 2001), and is activated when an antigen is recognized by epitope specific receptors on lymphocytes (P Kane, 2001). Both B cells and T cells express epitope specific receptors composed of surface expressed immunoglobulin (Ig), termed the B cell receptor (BCR) and T cell receptor (TCR), respectively (Ferrero et al., 2001; P Kane, 2001; Kurosaki and Hikida). An important difference between these receptors is the types of antigens to which they respond. BCRs recognize a vast array of antigens such as proteins, polysaccharides, lipids, nucleic acids, and soluble antigens including small chemicals, whereas TCRs only recognize peptide fragments presented by host cells in the major histocompatibility

complex (MHC) (Ferrero et al., 2001; Saha, 2001; Kurosaki and Hikida). The activation of these receptors results in highly specific responses centered about the ability of these cells to recognize the epitope on the inciting antigen. These responses are divided into cell-mediated and humoral immunity (Saha, 2001).

T cells implement cell-mediated adaptive immune responses once an antigen has been recognized (Ademokun and Dunn-Walters, 2001). Two major classes of T cells exist (Nath, 2001; Saha, 2001). $CD8^+$ cells, also known as cytotoxic T cells, aid in the removal of cells infected with intracellular pathogens such as viruses and intracellular bacteria (Gotch, 2001; Nath, 2001). $CD4^+$ T cells, or $T_H$ cells, aid in the removal of extracellular pathogens (Ademokun and Dunn-Walters, 2001; Ferrero et al., 2001). There are several $T_H$ cell subtypes; the $T_H1$ subtype is involved in the stimulation of macrophages to more effectively phagocytize and lyse bacteria, whereas the $T_H2$ subtype is especially involved in the immune response against helminthes and parasites (Ferrero et al., 2001). Another more recently recognized subtype of $T_H$ cell is the follicular $T_H$ cell, which are antigen experienced $T_H$ cells that reside within B-cell follicles of secondary lymphoid organs, such as the spleen, and assist in the production of antibodies, especially the IgG isotype (Fazilleau et al., 2009).

T cells also participate in humoral immune responses. Many of the $T_H$ subtypes ($T_H1$, $T_H2$, and follicular $T_H$ cells) assist in stimulating B cells to produce antibodies (Ademokun and Dunn-Walters, 2001; Ferrero et al., 2001). Once activated by exposure to an extracellular antigen, $T_H$ cell types begin expressing CD40-ligand, also known as CD154, on their cell surface and release cytokines (i.e. interferon-γ, interleukin-2, and

interleukin-4) in response to interaction with CD40 expressing B cells that recognize the same antigen (Ademokun and Dunn-Walters, 2001; Néron et al., 2011). The antigen specific interaction between B cells and $T_H$ cells, including CD40/CD40-ligand interaction and cytokine stimulation, induces B cells to produce antibodies directed against the commonly recognized antigen (Néron et al., 2011).

Antibodies are composed of two distinct portions: the heavy chain and the light chain. Each heavy and light chain has a constant and variable region (Kenter, 2005). The variable region of each chain confers the ability of the antibody to recognize a unique antigenic site (Zouali, 2001a). The constant portion of the heavy chain determines the subtype of antibody, of which there are 5 types: IgA, IgD, IgE, IgM, and IgG (Zouali, 2001a; Kenter, 2005). The subtype of antibody plays a major role in determining its function as the heavy chain constant portion of the each antibody is the site recognized by receptors throughout the body, such as by $F_c$ receptors on macrophages or by complement (Daëron, 1997; Stavnezer et al., 2008).

IgM is a pentameric Ig with relatively low specificity, but high capacity, and is the first type of antibody produced in response to a novel antigen (Ademokun and Dunn-Walters, 2001; Zouali, 2001a; Czajkowsky and Shao, 2009). Additionally, low specificity IgM is constitutively produced as a form of innate-type immunity (Zouali, 2001b; Czajkowsky and Shao, 2009; Baumgarth, 2013). These antibodies are termed ‘natural antibodies’ and are produced largely in the spleen and bone marrow (Zouali, 2001b; Baumgarth, 2013). The effector mechanism of IgM is complement activation (Czajkowsky and Shao, 2009; Baumgarth, 2013). Over the course of a humoral immune

response the isotype of antibody changes from IgM to IgG (Ademokun and Dunn-Walters, 2001; Schroeder and Cavacini, 2010). This process is termed class switching. IgG is a monomeric Ig with a high specificity, but relatively low capacity (Zouali, 2001a; Schroeder and Cavacini, 2010). IgG is the predominant antibody type produced several days (3-4) following an initial immune exposure and during repeated exposure to the same antigen (Ademokun and Dunn-Walters, 2001). Effector mechanisms of IgG include complement activation, neutralization of toxins, and facilitation of phagocytosis (Daëron, 1997; Schroeder and Cavacini, 2010).

There are certain types of antigens that stimulate humoral responses that do not require T cells. These antigens are termed thymus-independent antigens, or T cell independent antigens, and stimulate B cells to produce antibodies by replacing the secondary stimulation provided by $T_H$ cells (Ademokun and Dunn-Walters, 2001). These secondary signals come from either cross linking of BCRs or stimulation of toll-like receptors (TLR) that recognize specific pathogen associated molecules. A prime example of this type of antigen is bacterial lipopolysaccharide (LPS) (Moller, 2001; Lanzavecchia and Sallusto, 2007; Bekeredjian-Ding and Jego, 2009). LPS is a component of the cell wall of many types of pathogenic bacteria (Miller et al., 2005). Upon entering the circulation, LPS is recognized by TLR4 receptors on the surface of B cells (Moller, 2001; Lanzavecchia and Sallusto, 2007; Bekeredjian-Ding and Jego, 2009). In addition, because of its large size and repeating subunits, LPS can be simultaneously be recognized by many BCRs on the same lymphocyte, termed crosslinking (Moller, 2001; Lanzavecchia and Sallusto, 2007; Bekeredjian-Ding and

Jego, 2009). Together these two unique features of LPS are able to stimulate B cells to produce antibodies in the absence of $T_H$ cell involvement (Moller, 2001).

1.2.1.3: Spleen Capsule

The spleen is encapsulated by a tissue layer with three major components: connective tissue, elastic tissue, and smooth muscle (Cesta, 2006). Immunohistochemical detection of smooth muscle specific myosin, one of the core components required for muscle contraction (Squire, 2001), is demonstrative of the large amount of smooth muscle contained within the spleen capsule (Pinkus et al., 1986) and confirms histologic evaluation (Davies and Withrington, 1973; Cesta, 2006). However as mentioned above, contractile elements have also been observed in trabeculae of connective tissue that penetrate the spleen (Pinkus et al., 1986). These trabeculae carry with them branches of the incoming arterioles with contractile components in their walls, and axons of noradrenergic sympathetic neurons (Davies and Withrington, 1973; Pinkus et al., 1986; Cesta, 2006).

Contraction of smooth muscle in the spleen serves two hematologic purposes. First, the spleen acts as a reservoir for RBC (Cesta, 2006). Due to the reticular mesh network parenchyma surrounded by a fibromuscular spleen capsule (Davies and Withrington, 1973; Cesta, 2006), contraction of the spleen capsule reduces the overall size and volume of the spleen (Sandler et al., 1984; Richardson et al., 2009; Seifert et al., 2012). This contraction expels the cells contained within the spleen into the general circulation thereby increasing the content of RBC, or hematocrit of the blood.

Contraction of the spleen can increase the hematocrit of the blood by as much as 5% in humans (Sandler et al., 1984; Bakovic et al., 2005; Richardson et al., 2007; 2009), 10% in rats (Kuwahira et al., 1999), and 16% in dogs (Sato et al., 1995), thereby increasing its oxygen carrying capacity. This effect is considered the primary function of spleen contraction. In addition to being a reservoir for RBC, the spleen is the largest secondary lymphoid organ and contains a large number of immune cells (macrophages, leukocytes, and lymphocytes) (Mebius and Kraal, 2005; Cesta, 2006). Thus, the immune cells of the spleen are also released during splenic contraction (Schaffner, 1985; Seifert et al., 2012), but the consequences of this effect are essentially unknown.

### 1.2.2: Splenic Blood supply

#### 1.2.2.1: Anatomy

Blood enters the spleen via the splenic artery which branches into a number of trabecular arteries that follow connective tissue trabeculae into the spleen parenchyma (Cesta, 2006). These vessels branch further and enter the red pulp of the spleen where they are termed central arterioles and are surrounded by the PALS within the white pulp (Cesta, 2006). Branches from central arterioles have several destinations including capillary beds within the white pulp (marginal zone) and the red pulp of the spleen (Schmidt et al., 1985; Satodate et al., 1986; Schmidt et al., 1993). This distribution of blood vessels leads to two defined pathways of blood flow through the spleen: the ‘fast’ and ‘slow’ pathways. Blood that flows through the white pulp marginal zone and directly into venous sinuses is considered the ‘fast’ pathway (Cesta, 2006). As much as 90% of

splenic blood flow travels through this 'fast' pathway (Schmidt et al., 1985; 1993; Cesta, 2006). Alternatively, the 'slow' pathway is where blood enters the reticular meshwork of the red pulp (Schmidt et al., 1993) through terminal capillaries arising from central arterioles terminating within the reticular meshwork of the red pulp (Mebius and Kraal, 2005). Blood flow through the red pulp is collected into venous sinuses, which coalesce into venous collecting veins and ultimately exit the spleen via the splenic vein to drain into the hepatic portal system, traveling in the same neurovascular bundle as the splenic artery (Mebius and Kraal, 2005; Cesta, 2006).

1.2.2.2: Regulation of Splenic Blood Flow

Blood flow through the spleen is regulated by both arteriolar/capillary endothelial cells and red pulp reticular cell contraction (Blue and Weiss, 1981; Pinkus et al., 1986; Saito et al., 1988; Groom et al., 1991). Contraction of endothelial cells in capillaries within the red pulp serve to decrease blood flow to the reticular meshwork, thereby shunting more blood flow through the 'fast' pathway (Blue and Weiss, 1981; Groom et al., 1991). Reticular cells in the red pulp, which contain contractile elements, likely further prevent blood from entering by decreasing the size of passages through this area (Blue and Weiss, 1981; Pinkus et al., 1986; Saito et al., 1988). Contraction of red pulp reticular cells also likely participates in ejection of the cells contained within this compartment (Blue and Weiss, 1981; Pinkus et al., 1986; Saito et al., 1988). Hypoxia is the most well researched condition that causes spleen contraction and shuttling of blood to the 'fast' pathway within the spleen (Sandler et al., 1984; Sato et al., 1997; Kuwahira

et al., 1999; Bakovic et al., 2003; Richardson et al., 2007; 2009). Spleen contraction has also been found to occur in response to both stroke and exercise (Schaffner, 1985; Seifert et al., 2012).

### 1.2.3: Splenic Innervation

#### 1.2.3.1: Sympathetic Innervation

##### 1.2.3.1.1: Brain Nuclei Associated with Spleen Innervation

Sympathetic neuronal activity in the periphery is controlled primarily by five brain nuclei. These nuclei are the A5 cell group, rostral ventrolateral medulla, ventromedial medulla, caudal raphe nuclei, and paraventricular nucleus of the hypothalamus (PVN) (Strack et al., 1989; Cano et al., 2001; Sved et al., 2001). These nuclei all have direct descending connections with spinal cord pre-ganglionic neurons (Strack et al., 1989; Cano et al., 2001). Furthermore all of these brain nuclei are the first nuclei to become infected after injection of retrogradely transported reporter-viruses into known sympathetic targets such as the spleen, kidney, adrenal gland, tail artery, and sympathetic ganglia (Strack et al., 1989; Li et al., 1992; Schramm et al., 1993; Smith et al., 1998; Weiss and Chowdhury, 1998; Cano et al., 2001). Despite the common circuitry to all these peripheral targets, different subsets of nuclei are specifically involved in the control of each organ (Sved et al., 2001). For example, both retroviral tracing studies (Cano et al., 2001) and microinjection studies (Katafuchi et al., 1993) demonstrate that the PVN is an upstream regulator of splenic sympathetic neuronal activity.

The PVN is a bilateral nucleus located at the dorsal aspect of the 3rd ventricle of the brain. The PVN has a multitude of functions which are aimed at maintaining the homeostasis of the body, particularly cardiovascular function (Pyner, 2009). The PVN is regarded as one of five canonical central pre-sympathetic nuclei, and has direct descending efferent projections to the intermediolateral cell column of the spinal cord (IML) where they synapse on pre-ganglionic sympathetic neurons (Strack et al., 1989; Schramm et al., 1993; Cano et al., 2001; Sved et al., 2001; Pyner, 2009). These descending spinal projecting neurons specifically express vasopressin, oxytocin, or dopamine (DA), and terminate at virtually every thoracic level (Sawchenko and Swanson, 1982; Strack et al., 1989; Sved et al., 2001; Pyner, 2009). Both oxytocin and vasopressin are stimulatory to pre-ganglionic sympathetic neurons, whereas dopamine has mixed effects on pre-ganglionic sympathetic neurons, likely due to a combination of direct and indirect interactions (Pyner, 2009).

The PVN receives noradrenergic innervation from several brain nuclei, including the A1, A5, and A6 (locus coeruleus) noradrenergic cell groups (Byrum and Guyenet, 1987; Pacak et al., 1995; Samuels and Szabadi, 2008). The PVN is divided into three magnocellular and five parvocellular subdivisions (Pyner, 2009). The majority of noradrenergic innervation to the PVN terminates in the parvocellular portion, which is also the region where the cells bodies of pre-sympathetic spinal projecting neurons reside (Byrum and Guyenet, 1987; Cunningham and Sawchenko, 1988; Strack et al., 1989; Samuels and Szabadi, 2008; Pyner, 2009). These descending pre-sympathetic neurons synapse upon the cell bodies of pre-ganglionic acetylcholine (Ach) expressing

neurons in the IML of the spinal cord to control sympathetic outflow in the periphery (Kandel et al., 2000). Stimulation of the PVN by direct intracerebral glutamate injection stimulates splenic sympathetic activity (Katafuchi et al., 1993). Norepinephrine (NE) release in the PVN, in turn, stimulates glutamate releasing neurons in the parvocellular regions of the PVN to contribute to the control of sympathetic outflow (Daftary et al., 2000).

Noradrenergic signaling in the PVN is mediated by α1, α2, and β-adrenergic receptors (AR) (Leibowitz and Hor, 1982; Goldman et al., 1985; Daftary et al., 2000; Chong et al., 2004). Within the parvocellular regions, α1AR increase spontaneous inhibitory post-synaptic currents (sIPSC) in gamma-aminobutyric acid expressing (GABA) interneurons and stimulate the activity of glutamatergic interneurons, both of which synapse upon effector parvocellular neurons, such as directly descending pre-sympathetic neurons (Daftary et al., 2000; Chong et al., 2004). Conversely, α2AR decrease sIPSCs in GABAergic interneurons (Chong et al., 2004). Other parvocellular neurons are directly inhibited via βAR (Daftary et al., 2000).

Afferent PVN noradrenergic axon terminals are known to be regulated by pre-synaptic α2-adrenergic auto-receptors (Lookingland et al., 1991). The rate of NE turnover (an estimate of noradrenergic neuronal activity) is generally higher in central nervous system (CNS) noradrenergic neurons compared to noradrenergic neurons in the peripheral nervous system (PNS). For instance, the half-life of NE turnover in the PVN and amygdala is $<1.5$ h, whereas NE turnover in the heart and pancreas is $>3$ h (Levin, 1995). A well known and well studied cause for higher NE release in the PVN is

stress, serving to activate the hypothalamic-pituitary-adrenal (HPA) axis by the inducing the production of stress-related corticosteroids, such as cortisol, as well as increasing sympathetic outflow (Pacak et al., 1995; Itoi and Sugimoto, 2010; Inoue et al., 2013).

1.2.3.1.2: Post-Ganglionic Innervation of the Spleen

Sympathetic pre-ganglionic neurons innervating the spleen arise from the thoracic spinal cord, specifically $T_3$-$T_{12}$ (Bellinger et al., 1987; Cano et al., 2001). Upon exiting the spinal cord at these levels, axons of pre-ganglionic neurons regulating splenic sympathetic activity largely terminate in the celiac-mesenteric plexus (Bellinger et al., 1987; Nance and Sanders, 2007). There is, however, a minor (<15%) sympathetic innervation contribution to the spleen from sources other than the celiac-mesenteric ganglion, perhaps from splanchnic nerves emanating directly from sympathetic chain ganglia (Bellinger et al., 1987; Nance and Burns, 1989). Post-ganglionic sympathetic neuron axons travel to the spleen via the splenic neurovascular bundle, which contains the splenic artery, vein, and nerve, to terminate diffusely in the spleen capsule and periarteriolar regions (Felten et al., 1987; Felten and Olschowka, 1987; Kohm and Sanders, 2001; Cesta, 2006). Unmyelinated nerves are present in reticular fibers of the red and white pulp, presumably controlling the contraction of reticular cells in these areas (Pinkus et al., 1986; Satodate et al., 1986; Saito et al., 1988; Cesta, 2006). Axon terminals have also been identified in lymphocyte-rich areas, such as the PALS, terminating in very close proximity (less than 8 microns) to immune cells (Felten et al., 1987; Felten and Olschowka, 1987).

1.2.3.1.3: Sympathetic Neurotransmitters

1.2.3.1.3.1: Norepinephrine

1.2.3.1.3.1.1: Synthesis

NE is synthesized within the axon terminal of post-ganglionic sympathetic neurons through a multistep process (**Figure 1.1**) (Eisenhofer et al., 2004). Dietary tyrosine is taken in to the cell via the L-neutral amino acid transporter (Oxender and Christensen, 1963). Once inside the cell tyrosine is converted to L-3,4-dihydroxyphenylalanine (L-DOPA) by the rate-limited enzyme in catecholamine synthesis, tyrosine hydroxylase (TH) (Levitt et al., 1965; Eisenhofer et al., 2004). L-DOPA is then rapidly converted to DA by the actions of L-aromatic amino acid decarboxylase (L-AAAD), such that L-DOPA is normally undetectable within the neuron (Blaschko, 1942; Lookingland and Moore, 2005). DA is then taken up into vesicles by the vesicular monoamine transporter (VMAT), where is it converted to NE by way of DA-β-hydroxylase (DBH) (Kaufman, 1974; Weinshilboum, 1977; Kumer and Vrana, 1996; Eisenhofer et al., 2004)

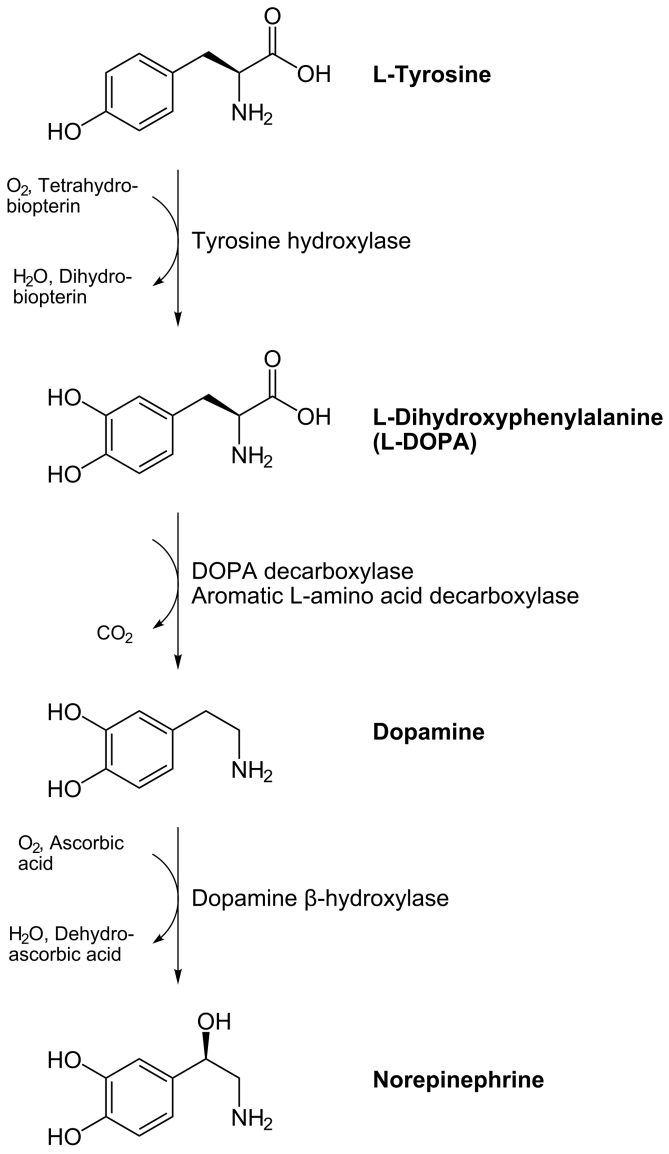


**Figure 1.1. Synthetic pathway of NE.** Dietary tyrosine is hydroxylated to DOPA via TH, the rate-limiting enzyme in NE synthesis. DOPA is rapidly decarboxylated to DA by L-AAAD. DA is then hydroxylated by DβH to form NE. Figure adapted from Marino and Cosentino (Marino and Cosentino, 2013).

The synthesis of NE is largely regulated by the activity of TH. Short-term regulation of TH is accomplished by phosphorylation (Kumer and Vrana, 1996). Phosphorylation of serine (Ser) residues (Ser19, Ser31, and Ser40) located on the N-terminus of TH can increase enzyme efficiency (Haycock, 1990; Daubner et al., 2011). Phosphorylation at Ser40, the most important site of phosphorylation, decreases end-product feedback inhibition (Daubner et al., 1992; Ribeiro et al., 1992; Ramsey and Fitzpatrick, 1998). Phosphorylation of Ser19 and Ser31 have modest direct effects on TH activity, but also increase the rate of Ser40 phosphorylation to indirectly potentiate TH activity (Bevilaqua et al., 2001; Lehmann et al., 2006). Interestingly, the phosphorylation of TH to increase catalytic activity also reduces the stability of the phosphorylated enzyme, but not due to degradation of the entire protein (Lazar et al., 1981; Vrana et al., 1981; Vrana and Roskoski, 1983). Thus, while more catalytically active, the half-life of phosphorylated TH protein is decreased relative to non-phosphorylated TH (Gahn and Roskoski, 1995). On the other hand, TH stability can be increased by both tyrosine and feedback inhibitors (i.e., catecholamines) (Kumer and Vrana, 1996). A number of $Ca^{2+}$-dependent pathways mediate TH phosphorylation including $Ca^{2+}$/phospholipid-dependent protein kinase C and $Ca^{2+}$/calmodulin-dependent multi-protein kinase (Yamauchi and Fujisawa, 1981; Albert et al., 1984; Vulliet et al., 1985). Phosphorylation of TH is also activity dependent, such that activated neurons increase the amount of phosphorylated enzyme (Kumer and Vrana, 1996).

1.2.3.1.3.1.2: Metabolism

NE is converted to 3-methoxy-4-hydroxyphenylglycol (MHPG), the major metabolite of NE in the brain, by successive processing of monoamine oxidase (MAO), catechol-O-methyltransferase (COMT) and aldehyde reductase (ADR) (**Figure 1.2**) (Lookingland et al., 1991; Hayley et al., 2001; Eisenhofer et al., 2004). More specifically, in the brain NE is converted to 3,4-dihydroxyphenylglycoaldehyde (DOPEGAL), by MAO, which diffuses out of the neuron to glia cells where it is converted to MHPG via COMT and ADR (Lookingland et al., 1991; Eisenhofer et al., 2004). In the spleen, MHPG is produced by MAO/ADR conversion of NE to 3,4-dihydroxyphenylglycol (DHPG) in sympathetic neurons followed by the conversion of DHPG to MPHG by COMT in macrophages within the white pulp of the spleen (Karhunen et al., 1994; Eisenhofer et al., 2004; Myöhänen et al., 2010). MHPG is then released from the spleen into circulation and further metabolized to vanillylmandelic acid (VMA) in the liver by alcohol dehydrogenase (ADH) and aldehyde dehydrogenase (AD) (Oh-hashi et al., 2001; Eisenhofer et al., 2004; Siraskar et al., 2011).

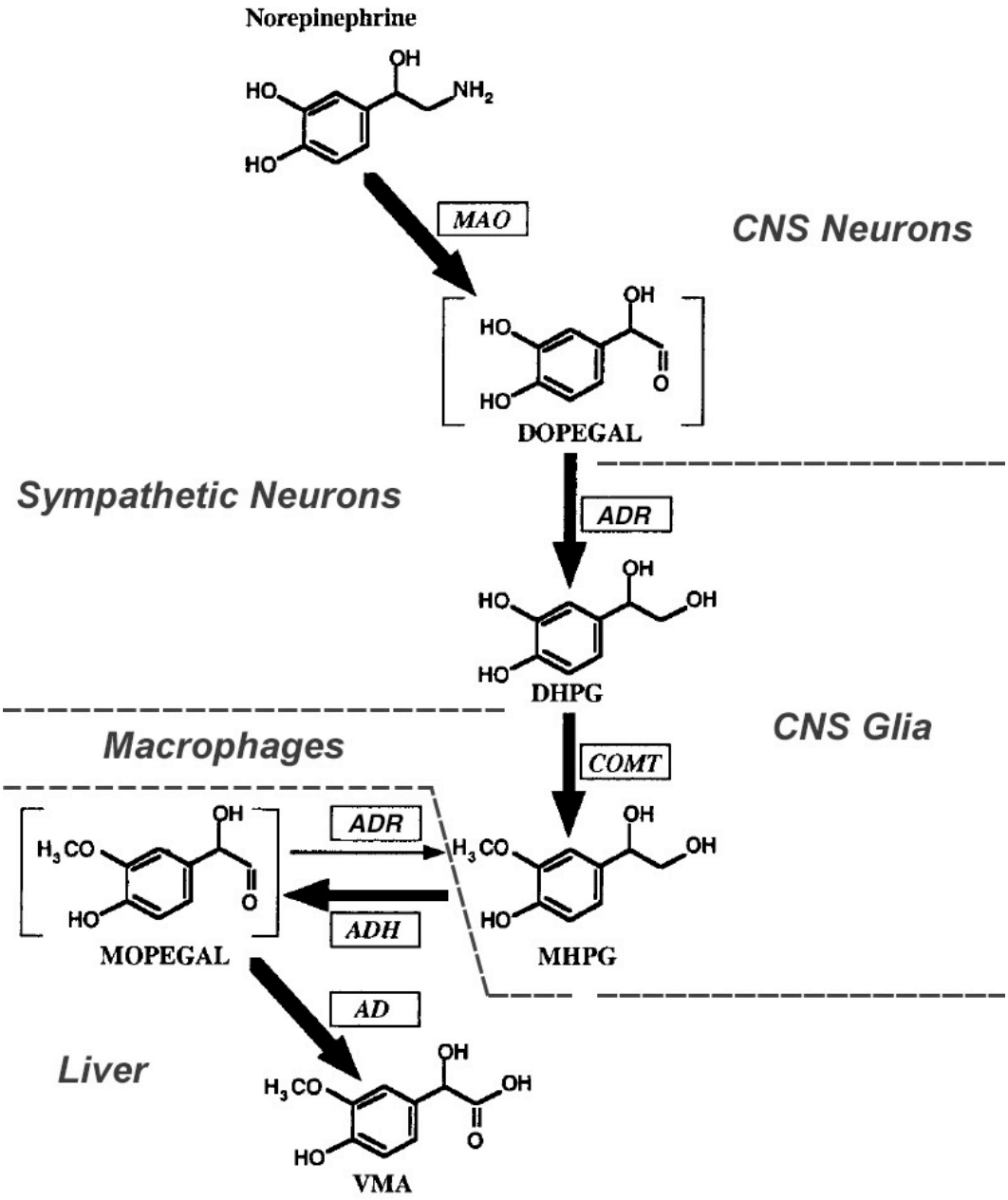


**Figure 1.2. Metabolic pathway of NE**. NE is converted to the major brain metabolite MHPG in neurons and glia/macrophages by successive deamination-hydroxylation, reduction, and methylation by MAO, ADR, and COMT, respectively. MHPG can the be converted in the liver to VMA, the major metabolite of NE found in the blood, by dehydrogenation and hydroxylation via ADH and AD. Figure adapted from Eisenhofer, et al (Eisenhofer et al., 2004).

1.2.3.1.3.1.3: Receptors

AR mediate the effects of NE released from sympathetic axon terminals. These receptors, which are also activated by epinephrine, are divided into two major types, $\alpha$ and $\beta$ (Malbon and Wang, 2001). There are 2 identified subtypes of $\alpha$ AR and 3 $\beta$ subtypes (Marino and Cosentino, 2013).

The two $\alpha$ AR are designated $\alpha$1 and $\alpha$2. The $\alpha$1AR is a G-protein coupled receptor that activates the $G_q$ pathway (Eltze, 1996; Aboud et al., 2012). This pathway results in the activation of phospholipase C and generation of inositol 1,4,5-triphosphate (IP3) by the hydrolysis of phospholipid precursors (Bootman et al., 2001; Malbon and Wang, 2001). IP3 then acts upon the IP3 receptor found on intracellular $Ca^{2+}$ storage sites, such as the endoplasmic or sarcoplasmic reticulum, leading to the release and elevation of intracellular $Ca^{2+}$ causing contraction of smooth muscle (Bootman et al., 2001; Malbon and Wang, 2001). Contraction of smooth muscle is the major physiologic action of $\alpha$1AR at sites such as the urethra, vascular smooth muscle, and in the spleen. This specific subtype receptor has been demonstrated to undergo phosphorylation-mediated desensitization and internalization occurring as quickly as 5 min after NE binding (Leeb-Lundberg et al., 1987; Fonseca et al., 1995; Malbon and Wang, 2001).

The $\alpha$2AR is also a G-protein coupled receptor, but this receptor activates the $G_{i/o}$ pathway whose primary effects upon are to inhibit cyclic adenosine monophosphate (cAMP) production via inhibition of adenylyl cyclase (Howlett and Mukhopadhyay, 2000; Marino and Cosentino, 2013). Activation of these G-proteins also leads to the inhibition of $Ca^{2+}$ ion channels and increases in $K^+$ conductance (Bockaert, 2001; Khan et al.,

2002). These effects result in a decrease in the firing of neurons and explains the physiological role of these receptors, which is to inhibit the release of NE from the axon terminals of noradrenergic neurons as a form of autoregulatory feedback (Khan et al., 2002; Marino and Cosentino, 2013). Thus, $\alpha$2AR are largely expressed on pre-synaptic axon terminals of noradrenergic neurons in the brain and periphery, particularly in the spleen and kidney (Marino and Cosentino, 2013).

The three $\beta$AR are designated $\beta$1, $\beta$2, and $\beta$3. All these receptors are G-coupled proteins that activate the $G_s$ pathway (Malbon and Wang, 2001; Marino and Cosentino, 2013). Activation of the $G_s$ pathway stimulates adenylyl cyclase leading to an increase in the production intracellular cAMP, and therefore increased activity of protein kinase A (Bockaert, 2001; Malbon and Wang, 2001; Marino and Cosentino, 2013). The most well known physiologic effect of $\beta$1AR is to increase cardiac output via increasing heart rate and contractility (Malbon and Wang, 2001; Marino and Cosentino, 2013). However, this receptor is known to stimulate the release of renin from the juxtaglomerular apparatus of the kidney as well. $\beta$1, along with $\beta$3AR, also regulates the lipolysis adipose tissue (Marino and Cosentino, 2013).

The most well studied effect of $\beta$2AR is to induce the relaxation of smooth muscle (Malbon and Wang, 2001; Marino and Cosentino, 2011). $\beta$2AR are also known to have an number of other actions including the regulation of glycogenolysis, aqueous humor production, and insulin secretion (Marino and Cosentino, 2013). However, $\beta$2AR are also expressed by cells of the immune system, the highest expression being on B cells,

suggesting an immunologic function role for these receptors (Kin and Sanders, 2006; Sanders, 2012).

1.2.3.1.3.1.4: NE Function in Spleen:

1.2.3.1.3.1.4.1: Splenic Blood Flow and Contraction

Spleen contraction is controlled by the sympathetic nervous system. NE was first found to bind to receptors located on smooth muscle cells within the spleen by Gillespie and Hamilton in 1966 (Gillespie and Hamilton, 1966). These receptors were later identified as $\alpha$1AR, more specifically the $\alpha 1_B$AR subtype (Eltze, 1996; Aboud et al., 2012). In congruence with the ability of NE to stimulate splenic smooth muscle contraction, noradrenergic axons densely innervate the spleen capsule, periarteriolar regions of the spleen, and in reticular fibers of the splenic white and red pulp (Davies and Withrington, 1973; Blue and Weiss, 1981; Pinkus et al., 1986; Felten et al., 1987; Felten and Olschowka, 1987; Saito et al., 1988; Elenkov and Vizi, 1991; Cesta, 2006).

1.2.3.1.3.1.4.2: NE Effects on the Immune System

Interactions between the immune and nervous systems are coordinated within the spleen. The sympathetic nervous system is activated following the presentation of an immune challenge (Kohm et al., 2000; Meltzer et al., 2003; Hefco et al., 2004), and sympathetic post-ganglionic noradrenergic axon terminal activity increases in the spleen following the injection of soluble protein antigens (Kohm et al., 2000; Sanders, 2012).

Pro-inflammatory cytokines are likely the activators of sympathetic neuronal activity during an immune challenge. The most studied of these early inflammatory factors are interleukin (IL)-1β and IL-6. Both of these cytokines are produced by phagocytic monocytes early in inflammatory events (Dinarello, 2004). The production of IL-1β and IL-6 in response to an immune challenge occurs within hours (Kakizaki et al., 1999). This makes these cytokines prime candidates to mediate rapid and early changes in sympathetic activity. In support of this, intraperitoneal (i.p.) injection of IL-1β increases the release of NE in the spleen (Shimizu et al., 1994; Kohm and Sanders, 2001). This suggests that IL-1β is the sympatho-stimulatory mediator *in vivo*. However, IL-1β is also able to stimulate the production of IL-6 from a myriad of cell types (Kauma et al., 1994; Spangelo et al., 1994; Parikh et al., 1997). This leaves open the possibility that the effects of IL-1β on sympathetic activity may be due to IL-6. Plasma and brain levels of IL-6 peak within 1-3 h following an immune challenge (Kakizaki et al., 1999). Intraventricular injection of IL-6 produces increased firing of spleen capsule sympathetic neurons (Helwig et al., 2008), suggesting IL-6 may act centrally to increase NE release during an immune challenge. Taken together, these data strongly suggest that one, or both, of these cytokines are stimulating the sympathetic nervous system during an immune challenge.

Splenic B cells express functional β2AR and respond to NE both *in vitro* and *in vivo* (Nance and Sanders, 2007; Sanders, 2012). Engagement of NE with β2AR on B cells within 24 h of an antigen exposure increases the amount of secreted IgM and IgG in response to a humoral immune challenge (Sanders, 2012). Conversely, blockade of

β2AR on B cells during an immune challenge decreases the amount of secreted antibody (Sanders, 2012).

Transcriptional activity of the 3'-Ig heavy chain enhancer (3'-IgH) and the actions of the transcription factor OCA-B are critically important to antibody production (Stevens et al., 2000; Pinaud et al., 2001; Vincent-Fabert et al., 2010). Activation of β2AR on B cells, through a protein-kinase A dependent mechanism, up-regulates OCA-B and OCA-B binding to the 3'-IgH, thereby connecting β2AR stimulation to increased antibody production (Podojil et al., 2004). Increased antibody production by B cells in response to NE is likely temporally dependent. Only exposure to NE at early time points (<24 h) following antigen exposure has been shown to increase B cell proliferation and antibody production (Kohm and Sanders, 2000; 2001). Exposure to NE prior to or 24 h after an immune challenge has no effect on the resulting antibody response. However, there is also evidence that β2AR stimulation may decrease proliferation in lymphocytes (Marino and Cosentino, 2011).

1.2.3.1.3.2: ATP/Adenosine

1.2.3.1.3.2.1: Synthesis

Adenosine 5’-triphosphate (ATP) is the universal energy currency for biological systems. It is synthesized by the combination of three chemically distinct parts: the adenine ring, the ribose moiety, and the triphosphate chain (Sperlágh and Vizi, 1996). Each of these components are synthesized via independent pathways and assembled

to form ATP. Adenine rings are formed during *de novo* purine synthesis by combining the carbon and nitrogen atoms derived from glycine, $N^5$, $N^{10}$-methenyltetrahydrofolate, glutamine, $N^{10}$-formyltetrahydrofolate, aspartate and respiratory $CO_2$ (Sperlágh and Vizi, 1996). The ribose moiety, synthesized in the pentose phosphate pathway, is attached to the adenine ring and the ultimate end product of purine synthesis is inosine monophosphate, which can be converted to adenosine monophosphate (AMP) via a two-step amination process (Sperlágh and Vizi, 1996). AMP can also be scavenged through the purine salvage pathway, by the phosphorylation of scavenged adenosine by adenosine kinase (Sperlágh and Vizi, 1996). AMP is then again phosphorylated by nucleotide diphosphate kinase to create adenosine diphosphate (ADP). ADP is the major substrate for ATP synthase which is powered by the generation of a hydrogen ion concentration through the process of oxidative phosphorylation in mitochondria to generate ATP (Sperlágh and Vizi, 1996).

ATP is exported from the mitochondria by adenine nucleotide transporters, driven by the exchange of ATP for ADP (Sperlágh and Vizi, 1996). ATP is found in virtually all synaptic vesicles, but it is assumed there is a specific ADP/ATP translocase, believed to be structurally and functionally similar to the transporter used to export ATP from mitochondria, that allows for the accumulation of ATP in synaptic vesicles (Dowdall et al., 1974; Lagercrantz and Stajärne, 1974; Winkler and Westhead, 1980; Sperlágh and Vizi, 1996; Gualix et al., 1999; Pankratov et al., 2006).

1.2.3.1.3.2.2: Metabolism

After release, extracellular ATP is quickly degraded to AMP by extracellular phosphatases followed by conversion to adenosine by 5′-nucleosidase (Pearson et al., 1980; Welford et al., 1987; Juul et al., 1991). Adenosine is rapidly cleared from the interstitium, at least in part, by re-uptake through pre-synaptic nucleoside transporters (Van Belle, 1993). Recaptured adenosine can then be metabolized or recycled through the purine salvage pathway to generate new AMP, ADP, and ATP (Sperlágh and Vizi, 1996).

1.2.3.1.3.2.3: Receptors

Purinergic receptors are divided into two broad categories: P1 and P2. P1 receptors are all G-coupled protein receptors that are agonized by adenosine (Ralevic, 2009). Of the four subtypes, the A1 and A3 activate the $G_{i/o}$ pathway, whereas the two isotypes of A2 both activate $G_s$ pathway (Ralevic, 2009). The A1 receptor has been identified as being able to modulate the release of sympathetic neurotransmitters (Rongen et al., 1996; Ralevic and Kendall, 2002). Specifically, A1 receptors are expressed on the pre-synaptic axon terminal of post-ganglionic sympathetic neurons and activation of these receptors inhibits the release of neurotransmitters (Rubino et al., 1991; 1993; Rongen et al., 1996). Activation of A2 receptors has been shown to induce relaxation of vascular smooth muscle (Ralevic, 2009).

There are two major categories of P2 receptors. P2X receptors are ligand-gated ion channels that when activated by ATP cause membrane depolarization and

extracellular $Ca^{2+}$ entry into cells (Sedaa et al., 1990; Ren and Burnstock, 1997; North, 2002; Burnstock and Ralevic). P2Y receptors are G-protein coupled receptors and depending upon which of the 8 subtypes activate either the $G_s$ or $G_q$ pathway (Ralevic, 2009). All P2 receptors recognize ATP, as well other nucleotides such as ADP, uridine triphosphate, and uridine diphosphate (Ralevic, 2009). P2X receptors are known to induce the contraction of vascular smooth muscle when released from sympathetic neurons (Ralevic and Kendall, 2002; Macarthur et al., 2011). Activation of pre-synaptically expressed P2X receptors has been demonstrated to induce depolarization, whereas pre-synaptically expressed P2Y receptors are inhibitory to neurotransmitter release (Ralevic, 2009). P2Y and P1-type A1 receptors have been shown to form a heterodimer, suggesting that the actions of one of these receptors may be assisted or mediated by the other (Yoshioka et al., 2002; Ralevic, 2009).

1.2.3.1.3.2.4: ATP/Adenosine Function in Spleen:

1.2.3.1.3.2.4.1: Splenic Blood Flow and Contraction

Purinergic receptors likely regulate two different aspects of splenic contraction. Adenosine has largely been known to inhibit NE release from sympathetic neurons via acting on pre-synaptic A1 adenosine receptors (Kubo and Su, 1983; Wennmalm et al., 1988; Kügelgen et al., 1992; Rongen et al., 1996; Ralevic, 2009; Macarthur et al., 2011; Burnstock and Ralevic). Interestingly, there is some precedence that activation of A1 receptors can stimulate vascular smooth muscle contraction and contraction of the spleen (Fozard and Milavec-Krizman, 1993; Tawfik et al., 2005). ATP released from

sympathetic neurons is also able to induce the constriction of vascular smooth muscle in a variety of tissues (vas deferens, aorta, splenic nerve) through P2X receptors (Sedaa et al., 1990; Ren and Burnstock, 1997; Burnstock and Ralevic), however, a specific role for P2X receptors in inducing splenic contraction has not been described.

1.2.3.1.3.2.4.2: ATP/Adenosine Effects on The Immune System

The role of purine in the immune response is relatively unknown. The most well researched aspect of purinergic effects on the immune system involved P2X receptors. P2X receptors have been identified on nearly every cell type of the immune system (Jacob et al., 2013). The role of these receptors is largely undefined, but it appears to be mostly involved in chemotaxis of inflammatory cells, such as neutrophils, macrophages, and eosinophils, as well as stimulating granular release from these latter cells (Jacob et al., 2013). In addition to this direct effect, the role of purinergic receptor modulation of neurotransmitter release from sympathetic neurons may also affect immune responses, such as those mediated by NE.

1.2.3.1.3.3: Neuropeptide Y

1.2.3.1.3.3.1: Synthesis

Neuropeptide Y (NPY) is a 36 amino acid peptide expressed by many post-ganglionic sympathetic neurons, including those projecting to the spleen, kidney, and mesentery (Lundberg et al., 1990; Romano et al., 1991; Chevendra and Weaver, 1992). NPY was named as such due to the many tyrosine residues, designated by the letter

"Y", in its linear sequence (Tatemoto, 2004). NPY is generated from a 97 amino acid that is cleaved at two sites producing NPY as well as a 28 amino acid peptide, termed "signal peptide", and a 30 amino acid peptide, termed "COOH-terminal peptide" (Tatemoto, 2004). NPY distribution largely parallels that of TH and DBH and is considered the major signaling peptide of sympathetic neurotransmission (Lundberg et al., 1990).

1.2.3.1.3.3.2: Metabolism

After release, NPY signal is terminated by proteolytic cleavage. This proteolysis is accomplished by ectopeptidases located on the cell surface of neurons, as has been described for other neuropeptides, such as enkephalins (Turner and Barnes, 1994). Specifically, NPY is degraded predominantly by dipeptidyl peptidase IV, neutral endopeptidase-24.11, and by aminopeptidase P (Mentlein et al., 1993; Medeiros and Turner, 1996).

1.2.3.1.3.3.3: Receptors

To date, five different NPY receptors have been identified including Y1, Y2, Y4, Y5, and Y6 subtypes (Tatemoto, 2004). All NPY receptors are G-protein coupled receptors that activate the $G_{i/o}$ pathway (Michel et al., 1998). Y1 receptors are expressed by vascular smooth muscle and can induce contraction and vasoconstriction (Westfall et al., 1987; 1990; Zukowska-Grojec et al., 1996; Michel et al., 1998; Wiest et

al., 2006). Y2 receptors are expressed on the pre-synaptic terminal of post-ganglionic sympathetic neurons and inhibit the release of sympathetic neurotransmitters (Westfall et al., 1987; 1990; Michel et al., 1998). Y4 receptors primarily bind a NPY related peptide called pancreatic polypeptide and only has significant affinity for a mutated form of NPY, [Leu31, Pro34]NPY (Michel et al., 1998). Y5 receptor pharmacological and physiological actions are very similar to that of Y1 receptors, and in fact may be considered a subtype of Y1 receptors (Michel et al., 1998). While the Y6 receptor has been cloned and identified, a physiologic effect of the receptor has yet to be identified (Michel et al., 1998).

1.2.3.1.3.3.4: NPY Function in Spleen

1.2.3.1.3.3.4.1: Splenic Blood Flow and Contraction

Y1 receptors are expressed by vascular smooth muscle and can induce vasoconstriction, while Y2 receptors inhibit the release of sympathetic neurotransmitters (Westfall et al., 1987; 1990; Zukowska-Grojec et al., 1996; Michel et al., 1998; Wiest et al., 2006). Thus it is likely that NPY may act to regulate the flow of arterial blood and thus modify blood flow through the spleen. Regarding spleen contraction, only one study has shown NPY capable of inducing spleen contraction, albeit very weakly in comparison to NE (Corder et al., 1987).

1.2.3.1.3.3.4.2: NPY Effects on The Immune System

NPY has been demonstrated to modulate a number of immune responses, and most cells in the immune system express NPY receptors, the predominant type being Y1 and Y2 (Bedoui et al., 2003; Wheway et al., 2005; Dimitrijević and Stanojević, 2013). While the consensus effect of NPY on immunity is not clear at this time, NPY acts generally to promote migration, inhibiting proliferation, and skew immune responses to a $T_H2$-type (la Fuente et al., 1993; Levite, 1998; Puerto et al., 2005; Dimitrijević and Stanojević, 2013). In addition to these direct effects, the role of Y2 receptor modulation of neurotransmitter release from sympathetic neurons may also affect immune responses, such as those mediated by NE.

1.2.3.2: Parasympathetic Innervation

Parasympathetic innervation of the spleen is somewhat controversial. A number of anatomical studies have failed to demonstrate cholinergic parasympathetic innervation of the spleen (Bellinger et al., 1993; Schäfer et al., 1998; Cano et al., 2001; Nance and Sanders, 2007; Olofsson et al., 2012), yet the spleen is known to contain acetylcholine (Ach), and activation of muscarinic cholinergic receptors induces contraction of the spleen capsule through an action independent of $\alpha$1AR (Davies and Withrington, 1973; Wong, 1990; Olofsson et al., 2012). In addition, the vagus nerve plays a vital role in controlling the inflammatory response (i.e., tumor necrosis factor

production) of splenocytes to an immune challenge, an effect believed to be mediated by $\alpha$7 nicotinic Ach receptors on macrophage immune cells (Olofsson et al., 2012).

The prevailing thought as to the source of splenic Ach is from T cells (Fujii et al., 2008). This finding, combined with the identification of vagus stimulation of spleen projecting sympathetic neurons of the celiac ganglion plexus provides a potential mechanism whereby vagal and cholinergic signaling can cause effects in the absence of direct parasympathetic innervation of the spleen (Vida et al., 2011; Olofsson et al., 2012). The final piece of this puzzle will then be to confirm the production of Ach from T cells in response to sympathetic activity in the spleen (Vida et al., 2011; Olofsson et al., 2012).

## 1.3: Cannabinoids

Cannabinoids are a class of lipophilic compounds defined by their ability to bind to two identified cannabinoid receptors designated CB1 and CB2. The most widely known cannabinoid, $\Delta$9-tetrahydrocannabinol (THC), is derived from plants of the genus *cannabis*, a.k.a. marijuana. THC is known mainly for its psychoactive properties when either ingested or inhaled (Pertwee, 2008). Cannabinoid derivatives have been widely used throughout history for both medicinal and recreational purposes. In the U.S.A., dronabinol (synthetic THC) is approved by the Federal Drug Administration for the control of nausea and vomiting in cancer patients undergoing chemotherapy as well as an appetite stimulant in patients with AIDS (Galal et al., 2009). In the United Kingdom, a drug named nabiximols (Sativex®), which is a mixture of THC and another *cannabis*-

derived cannabinoid called cannabidiol (CBD), is approved for the control of spasticity in multiple sclerosis patients (Pharmaceuticals, 2011). In the U.S.A., 20 states and District of Columbia have approved measures allowing the possession and growing of marijuana for medicinal purposes (WhiteHouse.gov). Furthermore, two of these states have legalized the recreational use of marijuana, which is an indicator of increasing popular support for the use of marijuana (drugpolicy.org; Wollner).

The effects of exogenous cannabinoids, such as THC, are mediated by modulation of the endocannabinoid system (**Figure 1.3**). The endocannabinoid system has largely been identified as modulating the release of neurotransmitters from axon terminals as a form of negative feed back. The two most well researched receptors of the endocannabinoid system are CB1 and CB2 (Mackie, 2008; Alger and Kim, 2011). Endogenous ligands for CB1 and CB2, termed “endocannabinoids”, were identified in the mid 1990's, of which the two most widely studied endocannabinoids are *N*-arachidonoyl-ethanolamide (anandamide) and 2-arachidonoyl glycerol (2-AG) (Di Marzo, 2008; Alger and Kim, 2011).

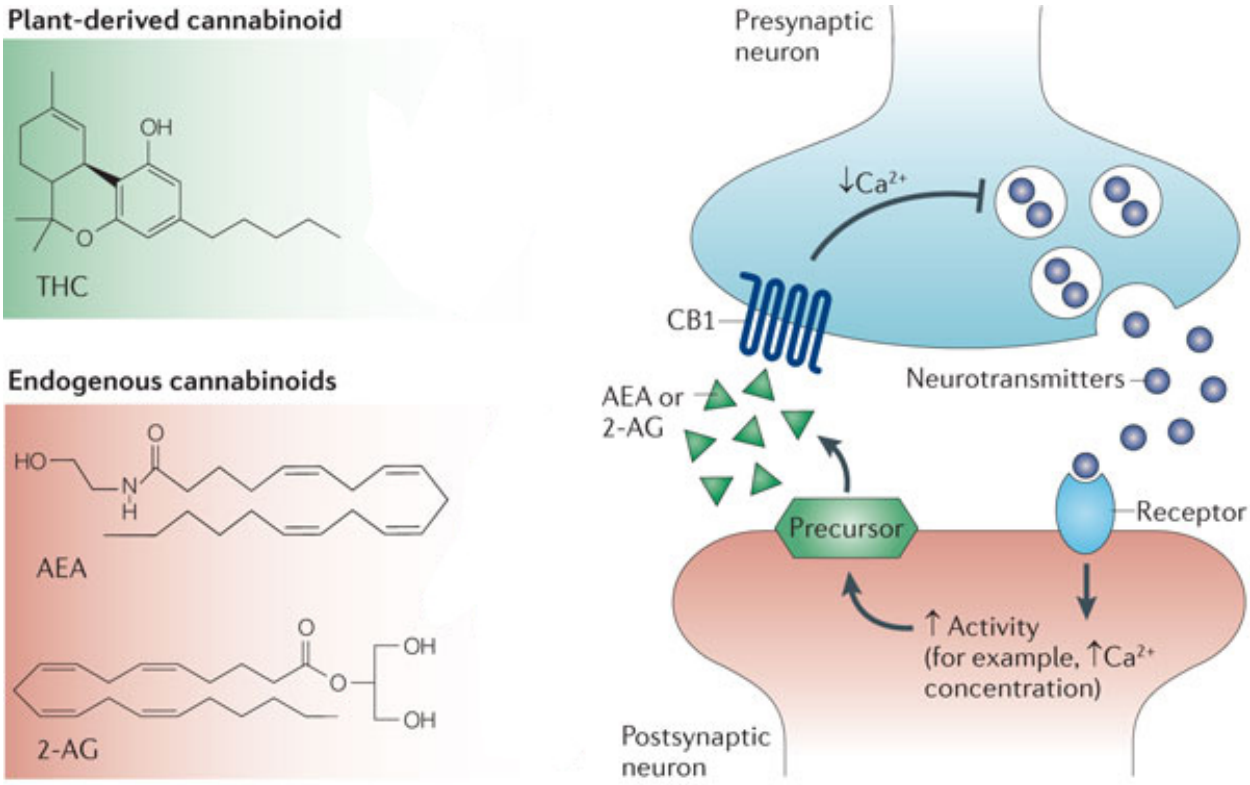


**Figure 1.3. Schematic representation of the endocannabinoid system.** The endogenous cannabinoid ligands AEA and 2-AG can be synthesized from precursors in the post-synaptic membrane in response to binding of released neurotransmitters. CB1 activation by AEA or 2-AG then results in the inhibition of neurotransmitter release via through a variety of mechanisms, including a decrease in voltage-gated $Ca^{2+}$ channel conductance. THC, the major cannabinoid congener found in *cannabis*, is also CB1 agonist, and it through this action that its psychotropic actions are believed to be mediated. Figure adapted from Guzman (Guzmán, 2003).

### 1.3.1: Cannabinoid Receptors

#### 1.3.1.1: CB1

Structure and Signaling

CB1 is considered to be the major neuronal cannabinoid receptor. CB1 is a G protein-coupled receptor consisting of seven-transmembrane domains, with an intracellular C terminus and an extracellular amino terminus (Mackie, 2008). CB1 predominantly couples with the $G_{i/o}$ subtype, whose primary effects upon activation are to inhibit cAMP production via inhibition of adenylyl cyclase (Howlett and Mukhopadhyay, 2000). Inhibition of cAMP production leads to inhibition of protein kinase A which then leads to a number of downstream consequences, including a positive shift in the voltage-dependence of A-current $K^+$ channels (Childers and Deadwyler, 1996). Activation of these G-proteins also leads to the inhibition of N-type (Felder et al., 1993; Mackie et al., 1993), Q-type (Mackie et al., 1995), and L-type $Ca^{2+}$ channels (Gebremedhin et al., 1999). Calcium influx through voltage-gated calcium channels, especially Q- and N-type, is essential for the release of neurotransmitters from axon terminals (Sheng et al., 1998). CB1 receptor agonism also activates inwardly rectifying $K^+$ channels, which play a significant role in determining the resting membrane potential of neurons (Mackie et al., 1995). It is by these mechanisms that CB1 inhibits neurotransmitter release from axon terminals. Additional effects of CB1 activation includes activation of the MAPK pathway, leading to increased glucose and fatty-acid oxidation, and well-characterized intracellular calcium transients mediated by $IP_3$ (Howlett and Mukhopadhyay, 2000).

Location

CB1 is localized to the pre-synaptic axon terminals of neurons (Nyíri et al., 2005). CB1 is found abundantly in CNS areas such as the cortex, basal ganglia, cerebellum, and brainstem emetic center, but expressed at very low levels in brainstem respiratory control centers and the thalamus (Herkenham et al., 1991; Mackie, 2008). There is also evidence for functional CB1 on autonomic sympathetic axon terminals. Functional evidence for CB1 has been identified in sympathetic axon terminals of the atria, vas deferens, and mesenteric arteries (Ishac et al., 1996; Niederhoffer and Szabo, 1999; Ralevic and Kendall, 2002). Interestingly, CB1 mRNA has also been found in the superior celiac ganglion, vas deferens, and the spleen (Ishac et al., 1996; Schatz et al., 1997). In addition, CB1 is expressed by immune cells, including splenic lymphocytes, but to a much lesser extent than CB2 (Galiegue et al., 1995; Kaplan, 2012). The role of CB1 on immune cells remains somewhat controversial, but a handful of studies have shown CB1 to mediate, at least partially, some immune effects (Kaplan, 2012). For example, CB1 transcription is induced by IL-4, a $T_H2$ cytokine, and once up-regulated CB1 stimulation inhibits cAMP formation and IL-2 production, a cytokine critical for T cell responses *in vivo* (Ferrero et al., 2001; Börner et al., 2008).

Ligands

CB1 is activated by both exogenous and endogenous cannabinoids. THC is a partial agonist of the CB1 receptor ($K_i$ ~40 nM) compared to compounds such as WIN55212, a full agonist ($K_i$ ~2 nM) (Kuster et al., 1993; Pertwee, 2008). The two most

well characterized endocannabinoid compounds that bind to CB1 are AEA and 2-AG. Neither of these compounds are stored in the neuron, but instead are made on demand from phospholipid components found in the membrane of post-synaptic neurons (Giuffrida and Mcmahon, 2010). AEA is derived from the deacylation of N-arachidonoyl phosphatidylethanolamine, a phospholipid precursor, in a $Ca^{2+}$-dependent process (Okamoto et al., 2004). 2-AG is synthesized by sequential hydrolysis of inositol phospholipids containing arachidonic acid by PLCβ and diacylglycerol lipase (Giuffrida and Mcmahon, 2010). Following *de novo* synthesis, endocannabinoids are released and travel retrogradely across the synapse to act on presynaptic CB1. Both AEA and 2-AG are partial agonists of CB1, however AEA is more selective for CB1 than 2-AG (Alger and Kim, 2011). AEA and 2-AG are rapidly degraded within minutes by the enzymes FAAH (primarily AEA) and MAGL (primarily 2-AG), thereby terminating their actions (Gerra et al., 2010; Giuffrida and Mcmahon, 2010).

1.3.1.2: CB2

Structure and Signaling

CB2 is considered to be the major peripheral cannabinoid receptor. CB2 was first discovered in the HL60 cell line, a pro-myelocytic cell line (Munro et al., 1993). It was subsequently discovered that CB2 mRNA is abundant in peripheral tissues, such as the spleen, but relatively absent from the brain (Shire et al., 1996; Griffin et al., 2000; Brown et al., 2002). Like CB1, CB2 is a seven-transmembrane protein that couples to $G_{i/o}$ subtype G-proteins and inhibit adenylyl cyclase, preventing the formation of cAMP

(Felder et al., 1995). CB2 also activates the MAPK/ERK pathway (modulating inflammation in microglia), the PI3K/AKT signaling pathway (promoting survival in oligodendrocyte precursors), and ceramide synthesis (inducing the apoptosis of tumor cells) (Molina-Holgado et al., 2002; Carracedo et al., 2006; Herrera et al., 2006; Romero-Sandoval et al., 2009). Very different from CB1, CB2 agonism does not inhibit Q-type $Ca^{2+}$ channels, nor activate inwardly rectifying $K^{+}$ channels (Felder et al., 1995).

Location

CB2 is expressed primarily on cells with an immunologic function. As mentioned above, the spleen was among the first organs shown to have abundant CB2 expression (Brown et al., 2002). CB2 is found on T cells, B cells, macrophages, and natural killer cells of the immune system, with B-cells having the highest expression (Galiegue et al., 1995; Schatz et al., 1997; Cabral and Griffin-Thomas, 2009). Microglia, the resident macrophage of the brain, also express CB2 (Cabral et al., 2008; Romero-Sandoval et al., 2009).

Ligands

Much like CB1, THC is a partial agonist of CB2 ($K_i$ ~20 nM) and WIN55212 is a full agonist ($K_i$ ~10 nM), although the difference in selectivity for these two ligands is less for CB2 as compared with CB1 (Shire et al., 1996; Griffin et al., 2000). Both AEA and 2-AG are also agonists for CB2, but 2-AG is a more selective and potent agonist

than AEA and is expressed in higher quantities in the spleen, bone marrow, and gut (Tanasescu and Constantinescu, 2010; Basu et al., 2011).

1.3.1.3: Non-CB1/CB2 Receptors

While CB1 and CB2 are the most well-known cannabinoid receptors, there are number of other receptors that bind cannabinoids with varying strength. These receptors can be divided broadly into two broad categories: G-protein coupled receptors and transient receptor potential (TRP) channels (De Petrocellis and Di Marzo, 2010). GPR55 is a G-protein coupled receptors that binds 2-AG, THC, and AEA, listed in order of affinity from highest to lowest (Ryberg et al., 2007). Activation of GPR55 has been shown to activate the $G_{13}$ pathways which leads to the activation of rhoA, cdc42, and rac1 (Ryberg et al., 2007). However, there is also evidence that GPR55 activation can increase intracellular $Ca^{2+}$ and increase neuronal excitability, via activation of IP3 receptors (Lauckner et al., 2008). In humans these receptors are found in only in the striatum (Sawzdargo et al., 1999), however in mice GPR55 has been found to be expressed in the spleen, adrenals, and distribution in the brain parallels that of CB1, although at lower levels (Ryberg et al., 2007). Functionally, GPR55 has been shown to be critical in inducing inflammatory hyperalgesia, as it failed to occur in a model in GPR55 knockout mice, and to induce an increase in intracellular $Ca^{2+}$ in dorsal root ganglion (DRG) cells (De Petrocellis and Di Marzo, 2010).

The other known G-protein coupled receptor to which cannabinoids bind is GPR119, which is an orphan receptor expressed primarily in the pancreas and

gastrointestinal tract that activates the $G_s$ pathway (De Petrocellis and Di Marzo, 2010). GPR119 is activated by the endocannabinoid oleoylethanolamide and may enhance glucose-dependent insulin release (De Petrocellis and Di Marzo, 2010).

TRP channels are six-domain transmembrane channels that gate the passage of ions, including $Ca^{2+}$ (Latorre et al., 2007). These channels are activated by physical stimuli, such as temperature or mechanical pressure, or chemical stimuli, such as acid, alkali, and lipids (Latorre et al., 2007). TRP channels are divided into several subcategories: TRPC (canonical), TRPA (ankyrin type),TRPM (melastatin-type), TRPP (polycystin-like), TRPML (mucolipin-like), and TRPV (vanilloid-type) channels (De Petrocellis and Di Marzo, 2010).

At least two TRPV channels are activated by cannabinoid compounds: TRPV1 and TRPV2. TRPV1 was originally described as the target for capsaicin and mediates the burning sensation of this compound (Julius et al., 1997). This receptor is found in afferent nociceptive neurons of the DRG as well as in the brain, which interestingly corresponds with many of the same places as CB1 receptors (Julius et al., 1997; Zygmunt et al., 1999; Mezey et al., 2000; Cristino et al., 2006). However, unlike CB1, TRPV1 is typically located on the post-synaptic membranes (Maccarrone et al., 2008). AEA and CBD are the known agonists of TRPV1 (Bisogno et al., 2001; de Petrocellis et al., 2001). The TRPV2 channel shares 50% homology with TRPV1 and is activated by high temperatures (~52° C) and cell swelling (Caterina et al., 1999; De Petrocellis and Di Marzo, 2010). TRPV2 is also found within DRG sensory ganglia (Qin et al., 2008).

TRPV2 channels are agonized by both AEA and CBD, but unlike TRPV1 channels, can be agonized by THC (De Petrocellis and Di Marzo, 2010).

Besides the TRPV1 and TRPV2 receptors, two other TRP channels are known to bind cannabinoids. The TRPM8 is gated by low temperatures (<25°C) and natural or synthetic cooling compounds, such as menthol, eucalyptol, spearmint (De Petrocellis and Di Marzo, 2010). These receptors are expressed on nociceptors, trigeminal neurons, and a small proportion of DRG neurons (Peier et al., 2002; Nealen et al., 2003; Kobayashi et al., 2005; Xing et al., 2006; De Petrocellis and Di Marzo, 2010). Contrary to the TRPV receptors, AEA and THC are antagonists of the TRPM8 receptor (De Petrocellis et al., 2007; 2008).

The TRPA1 receptor is expressed in unmyelinated peptidergic polymodal nociceptors of the trigeminal ganglion and DRG, distinct from those expressing TRPM8, but overlapping with nociceptive neurons expressing TRPV1, substance P, CGRP, and bradykinin receptors (Story et al., 2003; Bandell et al., 2004; Bautista et al., 2005; Kobayashi et al., 2005). These receptors are activated by a variety of stimuli including bradykinin, cold (≤17° C), formalin, aldehydes found in smoke, and plant oils, such as those from mustard, cinnamon, garlic, wintergreen, cloves, and ginger (Story et al., 2003; Bandell et al., 2004; De Petrocellis and Di Marzo, 2010). Activation of TRPA1 induces burning, prickling, or aching pain in humans (Morin and Bushnell, 1998). THC and AEA are agonists of TRPA1, although the binding for AEA is very weak ($EC_{50}$ = ~5 μM) (Jordt et al., 2004; De Petrocellis and Di Marzo, 2009).

### 1.3.2: Cannabinoid Effects

#### 1.3.2.1: Neuronal Effects of CB1 Stimulation

As discussed above, CB1 is located on the pre-synaptic axon terminals (Nyíri et al., 2005). The activation of CB1 induces a number of effects on ion channels that play critical roles in the release of neurotransmitters. These effects include a positive shift in the voltage-dependence of A-current $K^+$ channels (Childers and Deadwyler, 1996), inhibition of N-, Q-, and L-type $Ca^{2+}$ channels (Felder et al., 1993; Mackie et al., 1993; 1995; Gebremedhin et al., 1999), and activation of inwardly rectifying $K^+$ channels (Mackie et al., 1995). These mechanisms result in the inhibition of neurotransmitter release from axon terminals. This effect was first described in CNS neurons (Mackie, 2008), however, CB1 expression and regulation of neurotransmitter release in post-ganglionic sympathetic neurons has also been described (Ishac et al., 1996; Niederhoffer and Szabo, 1999; Ralevic and Kendall, 2002).

#### 1.3.2.2: Immune effects of CB2 Stimulation

Cannabinoids are known immunosuppressive compounds. This can be seen as a decrease in the immune profile, particularly of lymphocytes, obtained from humans who consume cannabis (Pacifici et al., 2003; Gohary and Eid, 2004). Further, cannabinoids decrease serum antibody concentrations in humans consuming cannabinoids, in this case THC (Klein et al., 1998). Interestingly, epidemiologic studies have yet to fully identify the consequences of cannabinoid-mediated immunosuppression, despite the wealth of information in animal studies (Greineisen and Turner, 2010; Tashkin, 2013).

The most well researched cannabinoid compound in this regard is THC, which is known to suppress both cell-mediated (Lu et al., 2009; Karmaus et al., 2012; 2013) and humoral (Schatz et al., 1993; Jan et al., 2003) adaptive immune responses in animal models. For example, THC was recently shown to broadly inhibit the immune response of mice to influenza infection (Karmaus et al., 2013). The results of this study strongly suggest a major site of action in this regard is inhibition of antigen presenting cell function. THC also inhibits the humoral response in mice, as demonstrated by decreasing the number of antibody producing cells in the spleen in response to sheep RBC (sRBC) injection (Schatz et al., 1993).

THC is a known agonist of both CB1 and CB2. Therefore experiments using THC do not provide information regarding the specific immunosuppressive role of CB1 or CB2. However, the expression of CB2 on immune cells makes it likely that at least part of THC-induced immunosuppression is mediated by CB2 (Schatz et al., 1997). A number of *in vitro* studies summarized here have been used to assess the effect of CB2 receptor activation on a variety of immune cell functions. Stimulation of the CB2 receptor by 2-AG induces the migration of immune cell types, including B cells, monocytes/macrophages, and microglia (Basu and Dittel, 2011). However, migration of mouse macrophages in response to common chemotactants is inhibited by synthetic CB2 agonists (Ghosh et al., 2006; Montecucco et al., 2008; Raborn et al., 2008). To date there is no consensus regarding the effect of CB2 on immune cell migration, but it is clear from these studies that CB2 can modulate immune cell chemotaxis. CB2 can also affect immune cell proliferation, however there is no clear consensus with studies

showing stimulatory effects in microglia (Carrier et al., 2004) and suppressive effect in $CD4^+$ T cells (Maresz et al., 2007). More clear data is available regarding the ability of CB2 to inhibit cytokine production, especially pro-inflammatory cytokines (IL-10 and IL-23) (Basu et al., 2011).

In addition to studies using CB agonists, a number of studies have used mice genetically manipulated to lack CB1 and CB2. These mice appear phenotypically normal and have normal immune cell profiles (Springs et al., 2008). Yet, in accordance with the immunosuppression observed with CB receptor stimulation, these mice demonstrate enhanced immunity. CB1/CB2 knockout (KO) mice show increased numbers of antibody producing cells from the spleen in response to sRBC injection (Springs et al., 2008). CB1/CB2 KO mice also demonstrate enhanced T cell immunity in response to influenza infection, which is associated with augmented antigen presenting cell function (Karmaus et al., 2011). While these mice are useful in establishing the immunomodulatory role of the CB1 and/or CB2, they do not provide specific details regarding the contribution of the individual receptors.

## 1.4: Summary

Sympathetic noradrenergic innervation of the spleen has multiple roles. It controls the contraction of the spleen, which serves the dual purposes of modulating the pathway of blood through this highly perfused organ as well as releasing the cellular contents of the splenic parenchyma, such as RBC and lymphocytes. Splenic

innervation also serves an immunologic purpose. NE released from spleen projecting noradrenergic post-ganglionic sympathetic neurons can increase the production of antibodies in response to an immune challenge inducing a humoral immune response.

Cannabinoids have multiple effects in the mammalian system. The most widely studied effect is the inhibition of neurotransmitter release caused by agonism of pre-synaptic CB1, which represents an emerging field in the immunologic effects of cannabinoids. It is assumed that most effects of cannabinoids are meditated by CB2, which are expressed on immune cells. However, there has yet to be a consensus on the effect of CB2 on immunity, despite the consistent ability of cannabinoids to be immunosuppressive. Furthermore, the contribution of CB1 to this effect is unclear.

The interaction between sympathetic noradrenergic innervation and the effect of cannabinoid receptor signaling is relatively unknown. The experiments in this dissertation were designed to investigate the role of CB1 and CB2 on the function of splenic sympathetic innervation.

## 1.5: Thesis Objective

The studies described in this dissertation were developed in order to test the central hypothesis that the genetic knockout of the CB1 and CB2 in mice will enhance splenic sympathetic neuronal function. The following specific aims and hypotheses were designed to test this central hypothesis:

***Specific Aim 1:*** Characterize the physiology and function of splenic sympathetic innervation

*Hypothesis:* Splenic sympathetic innervation augments splenic humoral immune responses by NE agonism of the β2AR on splenic B cells and controls spleen contraction through NE agonism of α1AR on capsular smooth muscle.

***Specific Aim 2:*** Investigate the role of endogenous CB1/CB2 signaling in the interaction between NE and splenic humoral immune responses

*Hypothesis:* Enhanced humoral immunity in mice lacking the CB1 and CB2 is due to increased splenic sympathetic NE release and activation of β2AR on splenic B cells.

***Specific Aim 3:*** Investigate the role of endogenous CB1/CB2 signaling in sympathetic nervous system control of spleen contraction

*Hypothesis:* Spleen contraction in mice lacking the CB1 and CB2 is attenuated due to decreased α1AR expression secondary to chronically increased noradrenergic sympathetic neuron activity.

The following chapters outline the research performed to address the above Specific Aims. The reader is referred to **Chapter 2** for detailed methodology. **Chapters 3-6** describe findings as they relate to the central hypothesis and the thesis objectives. **Chapter 7** provides a general discussion on the relevance and the importance of this research as it relates to the previous findings and information in the literature.

# REFERENCES

# REFERENCES


Aboud R, Shafii M, Docherty JR. Investigation of the subtypes of α1-adrenoceptor mediating contractions of rat aorta, vas deferens and spleen. Br J Pharmacol. 2012 Jul 19;109(1):80–7.

Ademokun AA, Dunn-Walters D. Immune Responses: Primary and Secondary. els.net. Chichester, UK: John Wiley & Sons, Ltd; 2001.

Albert KA, Helmer-Matyjek E, Nairn AC, Müller TH, Haycock JW, Greene LA, et al. Calcium/phospholipid-dependent protein kinase (protein kinase C) phosphorylates and activates tyrosine hydroxylase. Proc Natl Acad Sci USA. 1984 Dec;81(24):7713–7. PMCID: PMC392222

Alger B, Kim J. Supply and demand for endocannabinoids. Trends Neurosci. 2011 Jun 1;34(6):304–15.

Bakovic D, Eterovic D, Saratlija-Novaković Z, Palada I, Valic Z, Bilopavlović N, et al. Effect of human splenic contraction on variation in circulating blood cell counts. Clin Exp Pharmacol Physiol. 2005 Nov;32(11):944–51.

Bakovic D, Valic Z, Eterovic D, Vukovic I, Obad A, Marinović-Terzić I, et al. Spleen volume and blood flow response to repeated breath-hold apneas. J. Appl. Physiol. 2003 Oct;95(4):1460–6.

Bandell M, Story GM, Hwang SW, Viswanath V, Eid SR, Petrus MJ, et al. Noxious cold ion channel TRPA1 is activated by pungent compounds and bradykinin. Neuron. 2004 Mar 25;41(6):849–57.

Basu S, Dittel BN. Unraveling the complexities of cannabinoid receptor 2 (CB2) immune regulation in health and disease. Immunol. Res. 2011 Oct;51(1):26–38.

Basu S, Ray A, Dittel BN. Cannabinoid receptor 2 is critical for the homing and retention of marginal zone B lineage cells and for efficient T-independent immune responses. The Journal of Immunology. 2011 Dec 1;187(11):5720–32. PMCID: PMC3226756

Baumgarth N. Innate-Like B Cells and Their Rules of Engagement. link.springer.com.proxy2.cl.msu.edu. New York, NY: Springer New York; 2013. p. 57–66.

Bautista DM, Movahed P, Hinman A, Axelsson HE, Sterner O, Högestätt ED, et al. Pungent products from garlic activate the sensory ion channel TRPA1. Proc Natl Acad Sci USA. 2005 Aug 23;102(34):12248–52. PMCID: PMC1189336

Bedoui S, Miyake S, Lin Y, Miyamoto K, Oki S, Kawamura N, et al. Neuropeptide Y (NPY) suppresses experimental autoimmune encephalomyelitis: NPY1 receptor-specific inhibition of autoreactive Th1 responses in vivo. J Immunol. 2003 Oct 1;171(7):3451–8.

Bekeredjian-Ding I, Jego G. Toll-like receptors--sentries in the B-cell response. Immunology. 2009 Nov;128(3):311–23. PMCID: PMC2770679

Bellinger D, Felten S, Collier T, Felten D. Noradrenergic sympathetic innervation of the spleen: IV. Morphometric analysis in adult and aged F344 rats. J Neurosci Res. 1987;18(1):55–63, 126–9.

Bellinger DL, Lorton D, Hamill RW, Felten SY, Felten DL. Acetylcholinesterase staining and choline acetyltransferase activity in the young adult rat spleen: lack of evidence for cholinergic innervation. Brain Behav Immun. 1993 Sep;7(3):191–204.

Bevilaqua LR, Graham ME, Dunkley PR, Nagy-Felsobuki von EI, Dickson PW. Phosphorylation of Ser(19) alters the conformation of tyrosine hydroxylase to increase the rate of phosphorylation of Ser(40). J Biol Chem. 2001 Nov 2;276(44):40411–6.

Bisogno T, Hanus L, de Petrocellis L, Tchilibon S, Ponde DE, Brandi I, et al. Molecular targets for cannabidiol and its synthetic analogues: effect on vanilloid VR1 receptors and on the cellular uptake and enzymatic hydrolysis of anandamide. Br J Pharmacol. 2001 Oct;134(4):845–52. PMCID: PMC1573017

Blaschko H. The activity of l (—)-dopa decarboxylase. J. Physiol. (Lond.). 1942.

Blue J, Weiss L. Electron microscopy of the red pulp of the dog spleen including vascular arrangements, periarterial macrophage sheaths (Ellipsoids), and the contractile, innervated reticular meshwork. Am. J. Anat. 1981 Jun;161(2):189–218.

Bockaert JL. G Protein-coupled Receptors. onlinelibrary.wiley.com. Chichester: John Wiley & Sons, Ltd; 2001.

Bootman MD, Rietdorf K, Hardy H, Dautova Y, Corps E, Pierro C, et al. Calcium Signalling and Regulation of Cell Function. els.net. Chichester, UK: John Wiley & Sons, Ltd; 2001.

Börner C, Bedini A, Höllt V, Kraus J. Analysis of promoter regions regulating basal and interleukin-4-inducible expression of the human CB1 receptor gene in T lymphocytes. Mol Pharmacol. 2008 Mar;73(3):1013–9.

Brown SM, Wager-Miller J, Mackie K. Cloning and molecular characterization of the rat CB2 cannabinoid receptor. Biochim Biophys Acta. 2002 Jul 19;1576(3):255–64.

Burnstock G, Ralevic V. Purinergic Signaling and Blood Vessels in Health and Disease.

Byrum CE, Guyenet PG. Afferent and efferent connections of the A5 noradrenergic cell group in the rat. J Comp Neurol. 1987 Jul 22;261(4):529–42.

Cabral GA, Griffin-Thomas L. Emerging role of the cannabinoid receptor CB2 in immune regulation: therapeutic prospects for neuroinflammation. Expert Rev Mol Med. 2009;11:e3. PMCID: PMC2768535

Cabral GA, Raborn ES, Griffin L, Dennis J, Marciano-Cabral F. CB 2receptors in the brain: role in central immune function. Br J Pharmacol. 2008 Jan;153(2):240–51. PMCID: PMC2219530

Cano G, Sved AF, Rinaman L, Rabin BS, Card JP. Characterization of the central nervous system innervation of the rat spleen using viral transneuronal tracing. J Comp Neurol. 2001 Oct 8;439(1):1–18.

Carracedo A, Gironella M, Lorente M, Garcia S, Guzmán M, Velasco G, et al. Cannabinoids induce apoptosis of pancreatic tumor cells via endoplasmic reticulum stress-related genes. Cancer Res. 2006 Jul 1;66(13):6748–55.

Carrier EJ, Kearn CS, Barkmeier AJ, Breese NM, Yang W, Nithipatikom K, et al. Cultured rat microglial cells synthesize the endocannabinoid 2-arachidonylglycerol, which increases proliferation via a CB2 receptor-dependent mechanism. Mol Pharmacol. 2004 Apr;65(4):999–1007.

Caterina MJ, Rosen TA, Tominaga M, Brake AJ, Julius D. A capsaicin-receptor homologue with a high threshold for noxious heat. Nature. 1999 Apr 1;398(6726):436–41.

Cesta M. Normal Structure, Function, and Histology of the Spleen. Toxicol Pathol. 2006;34(5):455–65.

Chevendra V, Weaver LC. Distributions of neuropeptide Y, vasoactive intestinal peptide and somatostatin in populations of postganglionic neurons innervating the rat kidney, spleen and intestine. Neuroscience. 1992 Oct;50(3):727–43.

Childers SR, Deadwyler SA. Role of cyclic AMP in the actions of cannabinoid receptors. Biochem Pharmacol. 1996 Sep 27;52(6):819–27.

Chong W, Li LH, Lee K, Lee MH, Park JB, Ryu PD. Subtypes of alpha1- and alpha2-adrenoceptors mediating noradrenergic modulation of spontaneous inhibitory postsynaptic currents in the hypothalamic paraventricular nucleus. J. Neuroendocrinol. 2004 May;16(5):450–7.

Corder R, Lowry PJ, Withrington PG. The actions of the peptides, neuropeptide Y and

peptide YY, on the vascular and capsular smooth muscle of the isolated, blood-perfused spleen of the dog. Br J Pharmacol. 1987 Apr;90(4):785–90. PMCID: PMC1917199

Cristino L, de Petrocellis L, Pryce G, Baker D, Guglielmotti V, Di Marzo V. Immunohistochemical localization of cannabinoid type 1 and vanilloid transient receptor potential vanilloid type 1 receptors in the mouse brain. Neuroscience. 2006;139(4):1405–15.

Cunningham ET, Sawchenko PE. Anatomical specificity of noradrenergic inputs to the paraventricular and supraoptic nuclei of the rat hypothalamus. J Comp Neurol. 1988 Aug 1;274(1):60–76.

Czajkowsky DM, Shao Z. The human IgM pentamer is a mushroom-shaped molecule with a flexural bias. Proc Natl Acad Sci USA. 2009 Sep 1;106(35):14960–5.

Daëron M. Fc RECEPTOR BIOLOGY - Annual Review of Immunology, 15(1):203. Annu. Rev. Immunol. 1997.

Daftary SS, Boudaba C, Tasker JG. Noradrenergic regulation of parvocellular neurons in the rat hypothalamic paraventricular nucleus. Neuroscience. 2000 Mar;96(4):743–51.

Daubner SC, Lauriano C, Haycock JW, Fitzpatrick PF. Site-directed mutagenesis of serine 40 of rat tyrosine hydroxylase. Effects of dopamine and cAMP-dependent phosphorylation on enzyme activity. J Biol Chem. 1992 Jun 25;267(18):12639–46.

Daubner SC, Le T, Wang S. Tyrosine hydroxylase and regulation of dopamine synthesis. Arch. Biochem. Biophys. 2011 Apr 1;508(1):1–12. PMCID: PMC3065393

Davies BN, Withrington PG. The actions of drugs on the smooth muscle of the capsule and blood vessels of the spleen. Pharmacol Rev. 1973 Sep;25(3):373–413.

de Petrocellis L, Bisogno T, Maccarrone M, Davis JB, Finazzi-Agro A, Di Marzo V. The activity of anandamide at vanilloid VR1 receptors requires facilitated transport across the cell membrane and is limited by intracellular metabolism. J Biol Chem. 2001 Apr 20;276(16):12856–63.

De Petrocellis L, Di Marzo V. Role of endocannabinoids and endovanilloids in Ca2+ signalling. Cell Calcium. 2009 Jun;45(6):611–24.

De Petrocellis L, Di Marzo V. Non-CB1, non-CB2 receptors for endocannabinoids, plant cannabinoids, and synthetic cannabimimetics: focus on G-protein-coupled receptors and transient receptor potential channels. J Neuroimmune Pharmacol. 2010 Mar;5(1):103–21.

De Petrocellis L, Starowicz K, Moriello AS, Vivese M, Orlando P, Di Marzo V. Regulation of transient receptor potential channels of melastatin type 8 (TRPM8): Effect of cAMP, cannabinoid CB1 receptors and endovanilloids. Exp. Cell Res. 2007 May;313(9):1911–20.

De Petrocellis L, Vellani V, Schiano-Moriello A, Marini P, Magherini PC, Orlando P, et al. Plant-derived cannabinoids modulate the activity of transient receptor potential channels of ankyrin type-1 and melastatin type-8. Journal of Pharmacology and Experimental Therapeutics. 2008 Jun;325(3):1007–15.

Di Marzo V. Endocannabinoids: synthesis and degradation. Rev. Physiol. Biochem. Pharmacol. 2008;160:1–24.

Dimitrijević M, Stanojević S. The intriguing mission of neuropeptide Y in the immune system. Amino Acids. 2013 Jul;45(1):41–53.

Dinarello C. Infection, fever, and exogenous and endogenous pyrogens: some concepts have changed. J Endotoxin Res. 2004;10(4):201–22.

Dowdall MJ, Boyne AF, Whittaker VP. Adenosine triphosphate. A constituent of cholinergic synaptic vesicles. Biochem J. 1974 Apr;140(1):1–12. PMCID: PMC1167964

drugpolicy.org. Marijuana Legalization in Washington State and Colorado | Drug Policy Alliance [Internet]. drugpolicy.org. [cited 2013 Dec 31]. Retrieved from: http://www.drugpolicy.org/resource/marijuana-legalization-washington-state-and-colorado

Eisenhofer G, Kopin IJ, Goldstein DS. Catecholamine metabolism: a contemporary view with implications for physiology and medicine. 2004 Sep 1;56(3):331–49.

Elenkov I, Vizi E. Presynaptic modulation of release of noradrenaline from the sympathetic nerve terminals in the rat spleen. Neuropharmacology. 1991 Dec 1;30(12A):1319–24.

Eltze M. Functional evidence for an alpha 1B-adrenoceptor mediating contraction of the mouse spleen. Eur J Pharmacol. 1996 Sep 12;311(2-3):187–98.

Fazilleau N, Mark L, McHeyzer-Williams LJ, McHeyzer-Williams MG. Follicular helper T cells: lineage and location. Immunity. 2009 Mar 20;30(3):324–35. PMCID: PMC2731675

Felder CC, Briley EM, Axelrod J, Simpson JT, Mackie K, Devane WA. Anandamide, an endogenous cannabimimetic eicosanoid, binds to the cloned human cannabinoid receptor and stimulates receptor-mediated signal transduction. Proc Natl Acad Sci USA. 1993 Aug 15;90(16):7656–60. PMCID: PMC47201

Felder CC, Joyce KE, Briley EM, Mansouri J, Mackie K, Blond O, et al. Comparison of the pharmacology and signal transduction of the human cannabinoid CB1 and CB2 receptors. Mol Pharmacol. 1995 Sep;48(3):443–50.

Felten DL, Ackerman KD, Wiegand SJ, Felten SY. Noradrenergic sympathetic innervation of the spleen: I. Nerve fibers associate with lymphocytes and macrophages in specific compartments of the splenic white pulp. J Neurosci Res. 1987;18(1):28–36, 118–21.

Felten SY, Olschowka J. Noradrenergic sympathetic innervation of the spleen: II. Tyrosine hydroxylase (TH)-positive nerve terminals form synapticlike contacts on lymphocytes in the splenic white pulp. J Neurosci Res. 1987;18(1):37–48.

Ferrero I, Michelin O, Luescher I. Antigen Recognition by T Lymphocytes. onlinelibrary.wiley.com.proxy2.cl.msu.edu. Chichester, UK: John Wiley & Sons, Ltd; 2001.

Fonseca MI, Button DC, Brown RD. Agonist regulation of alpha 1B-adrenergic receptor subcellular distribution and function. J Biol Chem. 1995 Apr 14;270(15):8902–9.

Fozard JR, Milavec-Krizman M. Contraction of the rat isolated spleen mediated by adenosine A1 receptor activation. Br J Pharmacol. 1993 Jul 19;109(4):1059–63. PMCID: PMC2175713

Fujii T, Takada-Takatori Y, Kawashima K. Basic and clinical aspects of non-neuronal acetylcholine: expression of an independent, non-neuronal cholinergic system in lymphocytes and its clinical significance in immunotherapy. J. Pharmacol. Sci. 2008 Feb;106(2):186–92.

Gahn LG, Roskoski R. Thermal stability and CD analysis of rat tyrosine hydroxylase. Biochemistry. 1995 Jan 10;34(1):252–6.

Galal A, Slade D, Gul W, El-Alfy A, Ferreira D, Elsohly M. Naturally occurring and related synthetic cannabinoids and their potential therapeutic applications. Recent Pat CNS Drug Discov. 2009 Jun 1;4(2):112–36.

Galiegue S, Mary S, Marchand J, Dussossoy D, Carriere D, Carayon P, et al. Expression of Central and Peripheral Cannabinoid Receptors in Human Immune Tissues and Leukocyte Subpopulations. Eur J Biochem. 1995 Aug;232(1):54–61.

Gebremedhin D, Lange AR, Campbell WB, Hillard CJ, Harder DR. Cannabinoid CB1 receptor of cat cerebral arterial muscle functions to inhibit L-type Ca2+ channel current. Am J Physiol. 1999 Jun;276(6 Pt 2):H2085–93.

Gerra G, Zaimovic A, Gerra ML, Ciccocioppo R, Cippitelli A, Serpelloni G, et al. Pharmacology and toxicology of Cannabis derivatives and endocannabinoid

agonists. Recent Pat CNS Drug Discov. 2010 Jan;5(1):46–52.

Ghosh S, Preet A, Groopman JE, Ganju RK. Cannabinoid receptor CB2 modulates the CXCL12/CXCR4-mediated chemotaxis of T lymphocytes. Mol Immunol. 2006 Jul;43(14):2169–79.

Gillespie JS, Hamilton DN. Binding of noradrenaline to smooth muscle cells in the spleen. Nature. 1966 Oct 29;212(5061):524–5.

Giuffrida A, Mcmahon LR. In vivo pharmacology of endocannabinoids and their metabolic inhibitors: therapeutic implications in Parkinson's disease and abuse liability. Prostaglandins and Other Lipid Mediators. 2010 Apr 1;91(3-4):90–103.

Gohary ME, Eid MA. Effect of cannabinoid ingestion (in the form of bhang) on the immune system of high school and university students. Human & experimental toxicology. 2004.

Goldman CK, Marino L, Leibowitz SF. Postsynaptic α2-noradrenergic receptors mediate feeding induced by paraventricular nucleus injection of norepinephrine and clonidine. Eur J Pharmacol. 1985 Sep;115(1):11–9.

Gotch FM. T Lymphocytes: Cytotoxic. Chichester, UK: John Wiley & Sons, Ltd; 2001.

Greineisen WE, Turner H. Immunoactive effects of cannabinoids: considerations for the therapeutic use of cannabinoid receptor agonists and antagonists. Int Immunopharmacol. 2010 May;10(5):547–55. PMCID: PMC3804300

Griffin G, Tao Q, Abood ME. Cloning and pharmacological characterization of the rat CB(2) cannabinoid receptor. J Pharmacol Exp Ther. 2000 Mar;292(3):886–94.

Groom AC, Schmidt EE, MacDonald IC. Microcirculatory pathways and blood flow in spleen: new insights from washout kinetics, corrosion casts, and quantitative intravital videomicroscopy. Scanning Microsc. 1991 Mar;5(1):159–73– discussion173–4.

Gualix J, Pintor J, Miras-Portugal MT. Characterization of nucleotide transport into rat brain synaptic vesicles. J Neurochem. 1999 Sep;73(3):1098–104.

Guzmán M. Cannabinoids: potential anticancer agents. Nat Rev Cancer. Nature Publishing Group; 2003 Oct;3(10):745–55.

Haycock JW. Phosphorylation of tyrosine hydroxylase in situ at serine 8, 19, 31, and 40. J Biol Chem. 1990 Jul 15;265(20):11682–91.

Hayley S, Lacosta S, Merali Z, van Rooijen N, Anisman H. Central monoamine and plasma corticosterone changes induced by a bacterial endotoxin: sensitization and cross-sensitization effects. Eur J Neurosci. 2001 Mar;13(6):1155–65.

Hefco V, Olariu A, Hefco A, Nabeshima T. The modulator role of the hypothalamic paraventricular nucleus on immune responsiveness. Brain Behav Immun. 2004 Mar;18(2):158–65.

Helwig BG, Craig RA, Fels RJ, Blecha F, Kenney MJ. Central nervous system administration of interleukin-6 produces splenic sympathoexcitation. Autonomic Neuroscience. 2008 Aug;141(1-2):104–11.

Herkenham M, Lynn AB, Johnson MR, Melvin LS, de Costa BR, Rice KC. Characterization and localization of cannabinoid receptors in rat brain: a quantitative in vitro autoradiographic study. 1991 Feb 1;11(2):563–83.

Herrera B, Carracedo A, Diez-Zaera M, Gómez del Pulgar T, Guzmán M, Velasco G. The CB2 cannabinoid receptor signals apoptosis via ceramide-dependent activation of the mitochondrial intrinsic pathway. Exp. Cell Res. 2006 Jul 1;312(11):2121–31.

Howlett AC, Mukhopadhyay S. Cellular signal transduction by anandamide and 2-arachidonoylglycerol. Chemistry and Physics of Lipids. 2000 Nov;108(1-2):53–70.

Inoue W, Baimoukhametova DV, Füzesi T, Cusulin JIW, Koblinger K, Whelan PJ, et al. Noradrenaline is a stress-associated metaplastic signal at GABA synapses. Nat. Neurosci. 2013 May;16(5):605–12.

Ishac E, Jiang L, Lake K, Varga K, Abood M, Kunos G. Inhibition of exocytotic noradrenaline release by presynaptic cannabinoid CB1 receptors on peripheral sympathetic nerves. Br J Pharmacol. 1996 Aug 1;118(8):2023–8. PMCID: PMC1909901

Itoi K, Sugimoto N. The brainstem noradrenergic systems in stress, anxiety and depression. J. Neuroendocrinol. 2010 May;22(5):355–61.

Jacob F, Novo CP, Bachert C, Van Crombruggen K. Purinergic signaling in inflammatory cells: P2 receptor expression, functional effects, and modulation of inflammatory responses. Purinergic Signalling. Springer; 2013 Sep 1;9(3):285.

Jan T-R, Farraj AK, Harkema JR, Kaminski NE. Attenuation of the ovalbumin-induced allergic airway response by cannabinoid treatment in A/J mice. Toxicol Appl Pharmacol. 2003 Apr 1;188(1):24–35.

Jordt S-E, Bautista DM, Chuang H-H, McKemy DD, Zygmunt PM, Högestätt ED, et al. Mustard oils and cannabinoids excite sensory nerve fibres through the TRP channel ANKTM1. Nature. 2004 Jan 15;427(6971):260–5.

Julius D, Caterina MJ, Schumacher MA, Tominaga M, Rosen TA, Levine JD. The capsaicin receptor: a heat-activated ion channel in the pain pathway. Nature. Nature Publishing Group; 1997 Oct 23;389(6653):816–24.

Juul B, Lüscher ME, Aalkjaer C, Plesner L. Nucleotide hydrolytic activity of isolated intact rat mesenteric small arteries. Biochim Biophys Acta. 1991 Aug 26;1067(2):201–7.

Kakizaki Y, Watanobe H, Kohsaka A, Suda T. Temporal profiles of interleukin-1beta, interleukin-6, and tumor necrosis factor-alpha in the plasma and hypothalamic paraventricular nucleus after intravenous or intraperitoneal administration of lipopolysaccharide in the rat: estimation by push-pull perfusion. Endocr J. 1999 Aug 1;46(4):487–96.

Kandel E, Schwartz J, Jessell T. Principles of neural science. 2000.

Kaplan BLF. The Role of CB(1) in Immune Modulation by Cannabinoids. Pharmacol. Ther. 2012 Dec 19.

Karhunen T, Tilgmann C, Ulmanen I, Julkunen I, Panula P. Distribution of catechol-O-methyltransferase enzyme in rat tissues. … of Histochemistry & …. 1994.

Karmaus PWF, Chen W, (null), Kaplan BLF, Kaminski NE. Δ9-Tetrahydrocannabinol Impairs the Inflammatory Response to Influenza Infection: Role of Antigen-Presenting Cells and the Cannabinoid Receptors 1 and 2. Toxicological Sciences. 2013. PMCID: PMC3551428

Karmaus PWF, Chen W, Crawford RB, Harkema JR, Kaplan BLF, Kaminski NE. Deletion of cannabinoid receptors 1 and 2 exacerbates APC function to increase inflammation and cellular immunity during influenza infection. J Leukoc Biol. 2011 Nov;90(5):983–95. PMCID: PMC3206470

Karmaus PWF, Chen W, Kaplan BLF, Kaminski NE. Δ9-tetrahydrocannabinol suppresses cytotoxic T lymphocyte function independent of CB1 and CB 2, disrupting early activation events. J Neuroimmune Pharmacol. 2012 Dec;7(4):843–55. PMCID: PMC3266990

Katafuchi T, Ichijo T, Take S, Hori T. Hypothalamic modulation of splenic natural killer cell activity in rats. J. Physiol. (Lond.). 1993 Nov;471:209–21. PMCID: PMC1143959

Kaufman S. Dopamine-beta-hydroxylase. J Psychiatr Res. 1974;11:303–16.

Kauma SW, Turner TT, Harty JR. Interleukin-1 beta stimulates interleukin-6 production in placental villous core mesenchymal cells. Endocrinology. 1994;134(1):457–60.

Kenter AL. Class Switch Recombination: An Emerging Mechanism - Springer. Molecular Analysis of B Lymphocyte Development and …. 2005.

Khan ZP, Ferguson CN, Jones RM. Alpha-2 and imidazoline receptor agonistsTheir pharmacology and therapeutic role. Anaesthesia. 2002 Apr 6;54(2):146–65.

Kin NW, Sanders VM. It takes nerve to tell T and B cells what to do. J Leukoc Biol. 2006 Jun;79(6):1093–104.

Klein TW, Friedman H, Specter S. Marijuana, immunity and infection. J Neuroimmunol. 1998 Mar 15;83(1-2):102–15.

Kobayashi K, Fukuoka T, Obata K, Yamanaka H, Dai Y, Tokunaga A, et al. Distinct expression of TRPM8, TRPA1, and TRPV1 mRNAs in rat primary afferent neurons with adelta/c-fibers and colocalization with trk receptors. J Comp Neurol. 2005 Dec 26;493(4):596–606.

Kohm AP, Sanders VM. Norepinephrine: a messenger from the brain to the immune system. Immunology Today. 2000 Nov;21(11):539–42.

Kohm AP, Sanders VM. Norepinephrine and beta 2-adrenergic receptor stimulation regulate CD4+ T and B lymphocyte function in vitro and in vivo. Pharmacol Rev. 2001 Dec;53(4):487–525.

Kohm AP, Tang Y, Sanders VM, Jones SB. Activation of antigen-specific CD4+ Th2 cells and B cells in vivo increases norepinephrine release in the spleen and bone marrow. 2000 Jul 15;165(2):725–33.

Kubo T, Su C. Effects of adenosine on [3H]norepinephrine release from perfused mesenteric arteries of SHR and renal hypertensive rats. Eur J Pharmacol. 1983 Feb 18;87(2-3):349–52.

Kumer SC, Vrana KE. Intricate regulation of tyrosine hydroxylase activity and gene expression. J Neurochem [Internet]. 1996 Aug 1;67(2):443–62. Retrieved from: https://mail.google.com/mail/ca/u/0/?ui=2&view=bsp&ver=ohhl4rw8mbn4

Kurosaki T, Hikida M. B Lymphocytes: Receptors. eLS.

Kuster JE, Stevenson JI, Ward SJ, D'Ambra TE, Haycock DA. Aminoalkylindole binding in rat cerebellum: selective displacement by natural and synthetic cannabinoids. J Pharmacol Exp Ther. 1993 Mar;264(3):1352–63.

Kuwahira I, Kamiya U, Iwamoto T, Moue Y, Urano T, Ohta Y, et al. Splenic contraction-induced reversible increase in hemoglobin concentration in intermittent hypoxia. J. Appl. Physiol. 1999 Jan;86(1):181–7.

Kügelgen von I, Späth L, Starke K. Stable adenine nucleotides inhibit [3H]-noradrenaline release in rabbit brain cortex slices by direct action at presynaptic adenosine A1-receptors. Naunyn-Schmied Arch Pharmacol. 1992 Aug;346(2):187–96.

la Fuente De M, Bernaez I, Del Rio M, Hernanz A. Stimulation of murine peritoneal macrophage functions by neuropeptide Y and peptide YY. Involvement of protein

kinase C. Immunology. 1993 Oct;80(2):259–65. PMCID: PMC1422192

Lagercrantz H, Stajärne L. Evidence that most noradrenaline is stored without ATP in sympathetic large dense core nerve vesicles. Nature. 1974 Jun 28;249(460):843–5.

Lanzavecchia A, Sallusto F. Toll-like receptors and innate immunity in B-cell activation and antibody responses. Curr Opin Immunol. 2007 Jun;19(3):268–74.

Latorre R, Brauchi S, Orta G, Zaelzer C, Vargas G. ThermoTRP channels as modular proteins with allosteric gating. Cell Calcium. 2007 Oct;42(4-5):427–38.

Lauckner JE, Jensen JB, Chen H-Y, Lu H-C, Hille B, Mackie K. GPR55 is a cannabinoid receptor that increases intracellular calcium and inhibits M current. Proc Natl Acad Sci USA. 2008 Feb 19;105(7):2699–704. PMCID: PMC2268199

Lazar MA, Truscott RJW, Raese JD, Barchas JD. Thermal Denaturation of Native Striatal Tyrosine Hydroxylase: Increased Thermolability of the Phosphorylated Form of the Enzyme. J Neurochem. 1981 Feb;36(2):677–82.

Leeb-Lundberg LM, Cotecchia S, DeBlasi A, Caron MG, Lefkowitz RJ. Regulation of adrenergic receptor function by phosphorylation. I. Agonist-promoted desensitization and phosphorylation of alpha 1-adrenergic receptors coupled to inositol phospholipid metabolism in DDT1 MF-2 smooth muscle cells. J Biol Chem. 1987 Mar 5;262(7):3098–105.

Lehmann IT, Bobrovskaya L, Gordon SL, Dunkley PR, Dickson PW. Differential regulation of the human tyrosine hydroxylase isoforms via hierarchical phosphorylation. J Biol Chem. 2006 Jun 30;281(26):17644–51.

Leibowitz SF, Hor L. Endorphinergic and α-noradrenergic systems in the paraventricular nucleus: Effects on eating behavior. Peptides. 1982 May;3(3):421–8.

Levin BE. Reduced norepinephrine turnover in organs and brains of obesity-prone rats l Regulatory, Integrative and Comparative Physiology. … Journal of Physiology-Regulatory. 1995.

Levite M. Neuropeptides, by direct interaction with T cells, induce cytokine secretion and break the commitment to a distinct T helper phenotype. Proc Natl Acad Sci USA. 1998 Oct 13;95(21):12544–9. PMCID: PMC22867

Levitt M, Spector S, Sjoerdsma A, Udenfriend S. Elucidation of the rate-limiting step in norepinephrine biosynthesis in the perfused guinea-pig heart. J Pharmacol Exp Ther. 1965 Apr;148:1–8.

Li YW, Ding ZQ, Wesselingh SL, Blessing WW. Renal and adrenal sympathetic preganglionic neurons in rabbit spinal cord: tracing with herpes simplex virus. Brain

Res. 1992 Feb 21;573(1):147–52.

Lookingland KJ, Ireland LM, Gunnet JW, Manzanares J, Tian Y, Moore KE. 3-Methoxy-4-hydroxyphenylethyleneglycol concentrations in discrete hypothalamic nuclei reflect the activity of noradrenergic neurons. Brain Res. 1991 Sep 13;559(1):82–8.

Lookingland KJ, Moore KE. Chapter VIII Functional neuroanatomy of hypothalamic dopaminergic neuroendocrine systems. Handbook of chemical neuroanatomy. 2005.

Lu H, Kaplan BLF, Ngaotepprutaram T, Kaminski NE. Suppression of T cell costimulator ICOS by Delta9-tetrahydrocannabinol. J Leukoc Biol. 2009 Feb;85(2):322–9. PMCID: PMC2631366

Lundberg JM, Franco-Cereceda A, Lacroix JS, Pernow J. Neuropeptide Y and sympathetic neurotransmission. Ann N Y Acad Sci. 1990;611:166–74.

Macarthur H, Wilken GH, Westfall TC, Kolo LL. Neuronal and non-neuronal modulation of sympathetic neurovascular transmission. Acta Physiol (Oxf). 2011 Sep;203(1):37–45. PMCID: PMC3139802

Maccarrone M, Rossi S, Bari M, De Chiara V, Fezza F, Musella A, et al. Anandamide inhibits metabolism and physiological actions of 2-arachidonoylglycerol in the striatum. Nat. Neurosci. 2008 Feb;11(2):152–9.

Mackie K. Signaling via CNS cannabinoid receptors. Mol. Cell. Endocrinol. 2008 Apr 16;286(1-2 Suppl 1):S60–5. PMCID: PMC2435200

Mackie K, Devane WA, Hille B. Anandamide, an endogenous cannabinoid, inhibits calcium currents as a partial agonist in N18 neuroblastoma cells. Mol Pharmacol. 1993 Sep;44(3):498–503.

Mackie K, Lai Y, Westenbroek R, Mitchell R. Cannabinoids activate an inwardly rectifying potassium conductance and inhibit Q-type calcium currents in AtT20 cells transfected with rat brain cannabinoid receptor. J Neurosci. 1995 Oct;15(10):6552–61.

Malbon CC, Wang H-Y. Adrenergic Receptors. onlinelibrary.wiley.com. Chichester, UK: John Wiley & Sons, Ltd; 2001.

Maresz K, Pryce G, Ponomarev ED, Marsicano G, Croxford JL, Shriver LP, et al. Direct suppression of CNS autoimmune inflammation via the cannabinoid receptor CB1 on neurons and CB2 on autoreactive T cells. Nat. Med. 2007 Apr;13(4):492–7.

Marino F, Cosentino M. Adrenergic modulation of immune cells: an update. Amino Acids. 2011 Dec 8.

Marino F, Cosentino M. Adrenergic modulation of immune cells: an update. Amino

Acids. 2013 Jul;45(1):55–71.

Matsuno K, Ezaki T, Kotani M. Splenic outer periarterial lymphoid sheath (PALS): an immunoproliferative microenvironment constituted by antigen-laden marginal metallophils and ED2-positive macrophages in the rat. Cell Tissue Res. 1989 Sep;257(3):459–70.

Meager A, Wadhwa M. An Overview of Cytokine Regulation of Inflammation and Immunity. onlinelibrary.wiley.com. Chichester, UK: John Wiley & Sons, Ltd; 2001.

Mebius RE, Kraal G. Structure and function of the spleen. Nat Rev Immunol. Nature Publishing Group; 2005 Aug;5(8):606–16.

Medeiros MDS, Turner AJ. Metabolism and functions of neuropeptide Y. Neurochem Res. 1996 Sep;21(9):1125–32.

Meltzer JC, MacNeil BJ, Sanders V, Pylypas S, Jansen AH, Greenberg AH, et al. Contribution of the adrenal glands and splenic nerve to LPS-induced splenic cytokine production in the rat. Brain Behav Immun. 2003 Dec;17(6):482–97.

Mentlein R, Dahms P, Grandt D, Krüger R. Proteolytic processing of neuropeptide Y and peptide YY by dipeptidyl peptidase IV. Regul. Pept. 1993 Dec 10;49(2):133–44.

Mezey E, Tóth ZE, Cortright DN, Arzubi MK, Krause JE, Elde R, et al. Distribution of mRNA for vanilloid receptor subtype 1 (VR1), and VR1-like immunoreactivity, in the central nervous system of the rat and human. Proc Natl Acad Sci USA. 2000 Mar 28;97(7):3655–60. PMCID: PMC16295

Michel MC, Beck-Sickinger A, Cox H, Doods HN, Herzog H, Larhammar D, et al. XVI. International Union of Pharmacology recommendations for the nomenclature of neuropeptide Y, peptide YY, and pancreatic polypeptide receptors. Pharmacol Rev. 1998 Mar;50(1):143–50.

Miller SI, Ernst RK, Bader MW. LPS, TLR4 and infectious disease diversity. Nat. Rev. Microbiol. 2005 Jan;3(1):36–46.

Molina-Holgado E, Vela JM, Arévalo-Martín A, Almazán G, Molina-Holgado F, Borrell J, et al. Cannabinoids promote oligodendrocyte progenitor survival: involvement of cannabinoid receptors and phosphatidylinositol-3 kinase/Akt signaling. Journal of Neuroscience. 2002 Nov 15;22(22):9742–53.

Moller G. Antigens: Thymus Independent. els.net.proxy2.cl.msu.edu. Chichester, UK: John Wiley & Sons, Ltd; 2001.

Montecucco F, Burger F, Mach F, Steffens S. CB2 cannabinoid receptor agonist JWH-015 modulates human monocyte migration through defined intracellular signaling

pathways. Am J Physiol Heart Circ Physiol. 2008 Mar;294(3):H1145–55.

Morin C, Bushnell MC. Temporal and qualitative properties of cold pain and heat pain: a psychophysical study. Pain. 1998 Jan;74(1):67–73.

Munro S, Thomas KL, Abu-Shaar M. Molecular characterization of a peripheral receptor for cannabinoids. Nature. Nature Publishing Group; 1993 Sep 2;365(6441):61–5.

Myöhänen TT, Schendzielorz N, Männistö PT. Distribution of catechol-O-methyltransferase (COMT) proteins and enzymatic activities in wild-type and soluble COMT deficient mice. J Neurochem. 2010 Mar 31;:no–no.

Nance DM, Burns J. Innervation of the spleen in the rat: Evidence for absence of afferent innervation. Brain Behav Immun. 1989 Dec;3(4):281–90.

Nance DM, Sanders VM. Autonomic innervation and regulation of the immune system (1987-2007). Brain Behav Immun. 2007 Aug;21(6):736–45. PMCID: PMC1986730

Nath I. Immune Mechanisms against Intracellular Pathogens. onlinelibrary.wiley.com.proxy2.cl.msu.edu. Chichester, UK: John Wiley & Sons, Ltd; 2001.

Nealen ML, Gold MS, Thut PD, Caterina MJ. TRPM8 mRNA is expressed in a subset of cold-responsive trigeminal neurons from rat. J Neurophysiol. 2003 Jul;90(1):515–20.

Néron S, Nadeau PJ, Darveau A, Leblanc J-F. Tuning of CD40-CD154 interactions in human B-lymphocyte activation: a broad array of in vitro models for a complex in vivo situation. Arch. Immunol. Ther. Exp. (Warsz.). 2011 Feb;59(1):25–40.

Niederhoffer N, Szabo B. Effect of the cannabinoid receptor agonist WIN55212-2 on sympathetic cardiovascular regulation. Br J Pharmacol. 1999 Jan;126(2):457–66.

North RA. Molecular physiology of P2X receptors. Physiol. Rev. 2002 Oct;82(4):1013–67.

Nyíri G, Cserép C, Szabadits E, Mackie K, Freund TF. CB1 cannabinoid receptors are enriched in the perisynaptic annulus and on preterminal segments of hippocampal GABAergic axons. Neuroscience. 2005;136(3):811–22.

Oh-hashi Y, Shindo T, Kurihara Y, Imai T, Wang Y, Morita H, et al. Elevated Sympathetic Nervous Activity in Mice Deficient in CGRP. Circ. Res. 2001 Nov 23;89(11):983–90.

Oikonomopoulou K, Reis ES, Lambris JD. Complement System and Its Role in Immune Responses. onlinelibrary.wiley.com. Chichester, UK: John Wiley & Sons, Ltd; 2001.

Okamoto Y, Morishita J, Tsuboi K, Tonai T, Ueda N. Molecular characterization of a

phospholipase D generating anandamide and its congeners. J Biol Chem. 2004 Feb 13;279(7):5298–305.

Olofsson PS, Rosas-Ballina M, Levine YA, Tracey KJ. Rethinking inflammation: neural circuits in the regulation of immunity. Immunol. Rev. 2012 Jul;248(1):188–204.

Oxender D, Christensen H. Distinct Mediating Systems for the Transport of Neurtral Amino Acids by the Ehrlich Cell. J Biol Chem. 1963 Nov;238:3686–99.

P Kane L. Lymphocyte Activation: Signal Transduction. onlinelibrary.wiley.com. Chichester, UK: John Wiley & Sons, Ltd; 2001.

Pacak K, Palkovits M, Kopin IJ, Goldstein DS. Stress-Induced Norepinephrine Release in the Hypothalamic Paraventricular Nucleus and Pituitary-Adrenocortical and Sympathoadrenal Activity: In Vivo Microdialysis Studies. Frontiers in …. 1995.

Pacifici R, Zuccaro P, Pichini S, Roset PN, Poudevida S, Farré M, et al. Modulation of the immune system in cannabis users. JAMA. 2003 Apr 16;289(15):1929–31.

Pankratov Y, Lalo U, Verkhratsky A, North RA. Vesicular release of ATP at central synapses. Pflügers Archiv. 2006.

Parikh AA, Salzman AL, Kane CD, Fischer JE, Hasselgren PO. IL-6 production in human intestinal epithelial cells following stimulation with IL-1 beta is associated with activation of the transcription factor NF-kappa B. J Surg Res. 1997 Apr 1;69(1):139–44.

Pearson JD, Carleton JS, Gordon JL. Metabolism of adenine nucleotides by ectoenzymes of vascular endothelial and smooth-muscle cells in culture. Biochem J. 1980 Aug 15;190(2):421–9. PMCID: PMC1162107

Peier AM, Moqrich A, Hergarden AC, Reeve AJ, Andersson DA, Story GM, et al. A TRP channel that senses cold stimuli and menthol. Cell. 2002 Mar 8;108(5):705–15.

Pertwee RG. The diverse CB1 and CB2 receptor pharmacology of three plant cannabinoids: Δ9-tetrahydrocannabinol, cannabidiol and Δ9-tetrahydrocannabivarin. Br J Pharmacol [Internet]. 2008 Jan;153(2):199–215. Retrieved from: http://onlinelibrary.wiley.com.proxy2.cl.msu.edu/doi/10.1038/sj.bjp.0707442/full. PMCID: PMC2219532

Pharmaceuticals G. Sativex. 2011;(3/8/2012).

Pinaud E, Khamlichi A, Le Morvan C, Drouet M, Nalesso V, Le Bert M, et al. Localization of the 3' IgH locus elements that effect long-distance regulation of class switch recombination. Immunity. 2001 Aug 1;15(2):187–99.

Pinkus GS, Warhol MJ, O'Connor EM, Etheridge CL, Fujiwara K. Immunohistochemical

localization of smooth muscle myosin in human spleen, lymph node, and other lymphoid tissues. Unique staining patterns in splenic white pulp and sinuses, lymphoid follicles, and certain vasculature, with ultrastructural correlations. Am. J. Pathol. 1986 Jun;123(3):440–53. PMCID: PMC1888274

Podojil JR, Kin NW, Sanders VM. CD86 and beta2-adrenergic receptor signaling pathways, respectively, increase Oct-2 and OCA-B Expression and binding to the 3'-IgH enhancer in B cells. 2004 May 28;279(22):23394–404.

Puerto M, Guayerbas N, Alvarez P, la Fuente De M. Modulation of neuropeptide Y and norepinephrine on several leucocyte functions in adult, old and very old mice. J Neuroimmunol. 2005 Aug;165(1-2):33–40.

Pyner S. Neurochemistry of the paraventricular nucleus of the hypothalamus: Implications for cardiovascular regulation. J. Chem. Neuroanat. 2009.

Qin N, Neeper MP, Liu Y, Hutchinson TL, Lubin ML, Flores CM. TRPV2 is activated by cannabidiol and mediates CGRP release in cultured rat dorsal root ganglion neurons. Journal of Neuroscience. 2008 Jun 11;28(24):6231–8.

Quah BJ, Parish CR. Innate Immune Mechanisms: Nonself Recognition. els.net. Chichester, UK: John Wiley & Sons, Ltd; 2001.

Raborn ES, Marciano-Cabral F, Buckley NE, Martin BR, Cabral GA. The cannabinoid delta-9-tetrahydrocannabinol mediates inhibition of macrophage chemotaxis to RANTES/CCL5: linkage to the CB2 receptor. J Neuroimmune Pharmacol. 2008 Jun;3(2):117–29. PMCID: PMC2677557

Ralevic V. Purines as Neurotransmitters and Neuromodulators in Blood Vessels. CVP. 2009 Jan 1;7(1):3–14.

Ralevic V, Kendall DA. Cannabinoids inhibit pre- and postjunctionally sympathetic neurotransmission in rat mesenteric arteries. Eur J Pharmacol. 2002 May 31;444(3):171–81.

Ramsey AJ, Fitzpatrick PF. Effects of phosphorylation of serine 40 of tyrosine hydroxylase on binding of catecholamines: evidence for a novel regulatory mechanism. Biochemistry. 1998 Jun 23;37(25):8980–6.

Ren LM, Burnstock G. Prominent sympathetic purinergic vasoconstriction in the rabbit splenic artery: potentiation by 2,2′-pyridylisatogen tosylate - Ren - 2009 - British Journal of Pharmacology - Wiley Online Library. Br J Pharmacol. 1997.

Ribeiro P, Wang Y, Citron BA, Kaufman S. Regulation of recombinant rat tyrosine hydroxylase by dopamine. Proc Natl Acad Sci USA. 1992 Oct 15;89(20):9593–7. PMCID: PMC50178

Richardson MX, de Bruijn R, Schagatay E. Hypoxia augments apnea-induced increase in hemoglobin concentration and hematocrit. Eur. J. Appl. Physiol. 2009 Jan;105(1):63–8.

Richardson MX, Lodin A, Reimers J, Schagatay E. Short-term effects of normobaric hypoxia on the human spleen. Eur. J. Appl. Physiol. Springer-Verlag; 2007 Nov 28;104(2):395–9.

Romano TA, Felten SY, Felten DL, Olschowka JA. Neuropeptide-Y innervation of the rat spleen: another potential immunomodulatory neuropeptide. Brain Behav Immun. 1991 Mar;5(1):116–31.

Romero-Sandoval EA, Horvath R, Landry RP, DeLeo JA. Cannabinoid receptor type 2 activation induces a microglial anti-inflammatory phenotype and reduces migration via MKP induction and ERK dephosphorylation. Mol Pain. 2009;5:25. PMCID: PMC2704199

Rongen GA, Lenders JW, Lambrou J, Willemsen JJ, Van Belle H, Thien T, et al. Presynaptic inhibition of norepinephrine release from sympathetic nerve endings by endogenous adenosine. Hypertension. 1996 Apr;27(4):933–8.

Rubino A, Amerini S, Mantelli L, Ledda F. Adenosine receptors involved in the inhibitory control of non-adrenergic non-cholinergic neurotransmission in guinea-pig atria belong to the A1 subtype. … -Schmiedeberg's archives of …. 1991.

Rubino A, Ralevic V, Burnstock G. The P1-purinoceptors that mediate the prejunctional inhibitory effect of adenosine on capsaicin-sensitive nonadrenergic noncholinergic neurotransmission in the rat mesenteric arterial bed are of the A1 subtype. J Pharmacol Exp Ther. 1993 Dec;267(3):1100–4.

Ryberg E, Larsson N, Sjögren S, Hjorth S, Hermansson N-O, Leonova J, et al. The orphan receptor GPR55 is a novel cannabinoid receptor. Br J Pharmacol. 2007 Dec;152(7):1092–101. PMCID: PMC2095107

Saha B. Antigens. els.net.proxy2.cl.msu.edu. Chichester, UK: John Wiley & Sons, Ltd; 2001.

Saito H, Yokoi Y, Watanabe S, Tajima J, Kuroda H, Namihisa T. Reticular meshwork of the spleen in rats studied by electron microscopy. Am. J. Anat. 1988 Mar;181(3):235–52.

Samuels ER, Szabadi E. Functional neuroanatomy of the noradrenergic locus coeruleus: its roles in the regulation of arousal and autonomic function part I: principles of functional organisation. Curr Neuropharmacol. 2008 Sep;6(3):235–53. PMCID: PMC2687936

Sanders VM. The beta2-adrenergic receptor on T and B lymphocytes: Do we understand it yet? Brain Behav Immun. 2012 Feb;26(2):195–200. PMCID: PMC3243812

Sandler MP, Kronenberg MW, Forman MB, Wolfe OH, Clanton JA, Partain CL. Dynamic fluctuations in blood and spleen radioactivity: splenic contraction and relation to clinical radionuclide volume calculations. J. Am. Coll. Cardiol. 1984 May;3(5):1205–11.

Sato N, Shen YT, Kiuchi K, Shannon RP, Vatner SF. Splenic contraction-induced increases in arterial O2 reduce requirement for CBF in conscious dogs. American Journal of Physiology - Heart and Circulatory Physiology. American Physiological Society; 1995 Aug 1;269(2):H491–H503.

Sato S, Steeber DA, Jansen PJ, Tedder TF. CD19 expression levels regulate B lymphocyte development: human CD19 restores normal function in mice lacking endogenous CD19. J Immunol. 1997 May 15;158(10):4662–9.

Satodate R, Tanaka H, Sasou S, Sakuma T, Kaizuka H. Scanning electron microscopical studies of the arterial terminals in the red pulp of the rat spleen. Anat. Rec. 1986 Jul;215(3):214–6.

Sawchenko PE, Swanson LW. Immunohistochemical identification of neurons in the paraventricular nucleus of the hypothalamus that project to the medulla or to the spinal cord in the rat. J Comp Neurol. 1982 Mar 1;205(3):260–72.

Sawzdargo M, Nguyen T, Lee DK, Lynch KR, Cheng R, Heng HH, et al. Identification and cloning of three novel human G protein-coupled receptor genes GPR52, PsiGPR53 and GPR55: GPR55 is extensively expressed in human brain. Brain Res Mol Brain Res. 1999 Feb 5;64(2):193–8.

Schaffner A. The Hypersplenic SpleenA Contractile Reservoir of Granulocytes and Platelets. Arch Intern Med. 1985 Apr 1;145(4):651.

Schatz A, Lee M, Condie R, Pulaski J, Kaminski N. Cannabinoid receptors CB1 and CB2: a characterization of expression and adenylate cyclase modulation within the immune system. Toxicol Appl Pharmacol. 1997 Feb 1;142(2):278–87.

Schatz AR, Koh WS, Kaminski NE. Delta 9-tetrahydrocannabinol selectively inhibits T-cell dependent humoral immune responses through direct inhibition of accessory T-cell function. Immunopharmacology. 1993 Sep;26(2):129–37.

Schäfer MK, Eiden LE, Weihe E. Cholinergic neurons and terminal fields revealed by immunohistochemistry for the vesicular acetylcholine transporter. II. The peripheral nervous system. Neuroscience. 1998 May;84(2):361–76.

Schmidt EE, MacDonald IC, Groom AC. Microcirculation in mouse spleen (nonsinusal) studied by means of corrosion casts. Journal of morphology. 1985.

Schmidt EE, MacDonald IC, Groom AC. Comparative aspects of splenic microcirculatory pathways in mammals: the region bordering the white pulp. Scanning Microsc. 1993 Jun;7(2):613–28.

Schramm LP, Strack AM, Platt KB, Loewy AD. Peripheral and central pathways regulating the kidney: a study using pseudorabies virus. Brain Res. 1993 Jul 9;616(1-2):251–62.

Schroeder HW Jr., Cavacini L. Structure and function of immunoglobulins. Journal of Allergy and Clinical Immunology. Elsevier; 2010 Feb;125(2):S41–S52.

Sedaa KO, Bjur RA, Shinozuka K, Westfall DP. Nerve and drug-induced release of adenine nucleosides and nucleotides from rabbit aorta. J Pharmacol Exp Ther. 1990 Mar;252(3):1060–7.

Seifert HA, Hall AA, Chapman CB, Collier LA, Willing AE, Pennypacker KR. A transient decrease in spleen size following stroke corresponds to splenocyte release into systemic circulation. J Neuroimmune Pharmacol. 2012 Dec;7(4):1017–24. PMCID: PMC3518577

Sheng ZH, Westenbroek RE, Catterall WA. Physical link and functional coupling of presynaptic calcium channels and the synaptic vesicle docking/fusion machinery. J. Bioenerg. Biomembr. 1998 Aug;30(4):335–45.

Shimizu N, Hori T, Nakane H. An interleukin-1 beta-induced noradrenaline release in the spleen is mediated by brain corticotropin-releasing factor: an in vivo microdialysis study in conscious rats. Brain Behav Immun. 1994 Mar 1;8(1):14–23.

Shire D, Calandra B, Rinaldi-Carmona M, Oustric D, Pessègue B, Bonnin-Cabanne O, et al. Molecular cloning, expression and function of the murine CB2 peripheral cannabinoid receptor. Biochim Biophys Acta. 1996 Jun 7;1307(2):132–6.

Siraskar B, Völkl J, Ahmed MSE, Hierlmeier M, Gu S, Schmid E, et al. Enhanced catecholamine release in mice expressing PKB/SGK-resistant GSK3. Pflugers Arch. 2011 Dec;462(6):811–9.

Smith JE, Jansen AS, Gilbey MP, Loewy AD. CNS cell groups projecting to sympathetic outflow of tail artery: neural circuits involved in heat loss in the rat. Brain Res. 1998 Mar 9;786(1-2):153–64.

Spangelo BL, deHoll PD, Kalabay L, Bond BR, Arnaud P. Neurointermediate pituitary lobe cells synthesize and release interleukin-6 in vitro: effects of lipopolysaccharide and interleukin-1 beta. Endocrinology. 1994 Aug 1;135(2):556–63.

Sperlágh B, Vizi SE. Neuronal synthesis, storage and release of ATP. Seminars in Neuroscience. 1996 Aug;8(4):175–86.

Springs AEB, Karmaus PWF, Crawford RB, Kaplan BLF, Kaminski NE. Effects of targeted deletion of cannabinoid receptors CB1 and CB2 on immune competence and sensitivity to immune modulation by Delta9-tetrahydrocannabinol. J Leukoc Biol. 2008 Dec;84(6):1574–84. PMCID: PMC2614598

Squire JM. Muscle Contraction: Regulation. els.net. Chichester, UK: John Wiley & Sons, Ltd; 2001.

Stavnezer J, Guikema JEJ, Schrader CE. Mechanism and Regulation of Class Switch Recombination. Annu. Rev. Immunol. 2008 Apr;26(1):261–92.

Stevens S, Ong J, Kim U, Eckhardt L, Roeder R. Role of OCA-B in 3'-IgH enhancer function. J Immunol. 2000 May 15;164(10):5306–12.

Story GM, Peier AM, Reeve AJ, Eid SR, Mosbacher J, Hricik TR, et al. ANKTM1, a TRP-like channel expressed in nociceptive neurons, is activated by cold temperatures. Cell. 2003 Mar 21;112(6):819–29.

Strack AM, Sawyer WB, Hughes JH, Platt KB, Loewy AD. A general pattern of CNS innervation of the sympathetic outflow demonstrated by transneuronal pseudorabies viral infections. Brain Res. 1989 Jul 3;491(1):156–62.

Sved AF, Cano G, Card JP. Neuroanatomical specificity of the circuits controlling sympathetic outflow to different targets. Clin Exp Pharmacol Physiol. 2001;28(1-2):115–9.

Tanasescu R, Constantinescu C. Cannabinoids and the immune system: an overview. Immunobiology. 2010 Aug 1;215(8):588–97.

Tashkin DP. Effects of marijuana smoking on the lung. Ann Am Thorac Soc. 2013 Jun;10(3):239–47.

Tatemoto K. Neuropeptide Y and related peptides. Alfalah M, Michel MC, editors. 2004.

Tawfik HE, Schnermann J, Oldenburg PJ, Mustafa SJ. Role of A1 adenosine receptors in regulation of vascular tone. Am J Physiol Heart Circ Physiol. 2005 Mar;288(3):H1411–6.

Turner AJ, Barnes K. Neuropeptidases: candidate enzymes and techniques for study. Biochem. Soc. Trans. 1994 Feb;22(1):122–7.

Van Belle H. Nucleoside transport inhibition: a therapeutic approach to cardioprotection via adenosine? Cardiovasc. Res. 1993 Jan;27(1):68–76.

Vida G, Pena G, Deitch EA, Ulloa L. α7-cholinergic receptor mediates vagal induction of splenic norepinephrine. The Journal of Immunology. 2011 Apr 1;186(7):4340–6. PMCID: PMC3083451

Vincent-Fabert C, Fiancette R, Cogné M, Pinaud E, Denizot Y. The IgH 3' regulatory region and its implication in lymphomagenesis. Eur J Immunol. 2010 Dec 1;40(12):3306–11.

Vrana KE, Allhiser CL, Roskoski R. Tyrosine hydroxylase activation and inactivation by protein phosphorylation conditions. J Neurochem. 1981 Jan;36(1):92–100.

Vrana KE, Roskoski R. Tyrosine hydroxylase inactivation following cAMP-dependent phosphorylation activation. J Neurochem. 1983 Jun;40(6):1692–700.

Vulliet PR, Woodgett JR, Ferrari S, Hardie DG. Characterization of the sites phosphorylated on tyrosine hydroxylase by Ca2+ and phospholipid-dependent protein kinase, calmodulin-dependent multiprotein kinase and cyclic AMP-dependent protein kinase. FEBS Lett. 1985 Mar 25;182(2):335–9.

Weinshilboum RM. Serum dopamine-beta-hydroxylase activity and blood pressure. Mayo Clin. Proc. 1977 Jun;52(6):374–8.

Weiss ML, Chowdhury SI. The renal afferent pathways in the rat: a pseudorabies virus study. Brain Res. 1998 Nov 23;812(1-2):227–41.

Welford LA, Cusack NJ, Hourani SM. The structure-activity relationships of ectonucleotidases and of excitatory P2-purinoceptors: evidence that dephosphorylation of ATP analogues reduces pharmacological potency. Eur J Pharmacol. 1987 Sep 2;141(1):123–30.

Wennmalm M, Fredholm BB, Hedqvist P. Adenosine as a modulator of sympathetic nerve-stimulation-induced release of noradrenaline from the isolated rabbit heart. Acta Physiol. Scand. 1988 Apr;132(4):487–94.

Westfall TC, Carpentier S, Chen X, Beinfeld MC, Naes L, Meldrum MJ. Prejunctional and postjunctional effects of neuropeptide Y at the noradrenergic neuroeffector junction of the perfused mesenteric arterial bed of the rat. Journal of Cardiovascular Pharmacology. 1987 Dec;10(6):716–22.

Westfall TC, Chen XL, Ciarleglio A, Henderson K, Del Valle K, Curfman-Falvey M, et al. In vitro effects of neuropeptide Y at the vascular neuroeffector junction. Ann N Y Acad Sci. 1990;611:145–55.

Wheway J, Mackay CR, Newton RA, Sainsbury A, Boey D, Herzog H, et al. A fundamental bimodal role for neuropeptide Y1 receptor in the immune system. J Exp Med. 2005 Dec 5;202(11):1527–38. PMCID: PMC2213323

WhiteHouse.gov. Marijuana Resource Center: State Laws Related to Marijuana | The White House [Internet]. whitehouse.gov. [cited 2013 Dec 31]. Retrieved from: http://www.whitehouse.gov/ondcp/state-laws-related-to-marijuana

Wiest R, Jurzik L, Moleda L, Froh M, Schnabl B, Hörsten SV, et al. Enhanced Y1-receptor-mediated vasoconstrictive action of neuropeptide Y (NPY) in superior mesenteric arteries in portal hypertension. Journal of Hepatology. 2006 Mar;44(3):512–9.

Winkler H, Westhead E. The molecular organization of adrenal chromaffin granules. Neuroscience. 1980;5(11):1803–23.

Wollner A. Public Support For Marijuana Legalization Hits Record High : It's All Politics : NPR [Internet]. npr.org. [cited 2014 Jan 4]. Retrieved from: http://www.npr.org/blogs/itsallpolitics/2013/10/22/239847084/public-support-for-marijuana-legalization-hits-record-high

Wong KK. Bethanechol induced contraction in mouse spleen. Chin J Physiol. 1990;33(2):161–7.

Xing H, Ling J, Chen M, Gu JG. Chemical and cold sensitivity of two distinct populations of TRPM8-expressing somatosensory neurons. J Neurophysiol. 2006 Feb;95(2):1221–30.

Yamauchi T, Fujisawa H. Tyrosine 3-monoxygenase is phosphorylated by Ca2+-, calmodulin-dependent protein kinase, followed by activation by activator protein. Biochemical and Biophysical Research Communications. 1981 May 29;100(2):807–13.

Yoshioka K, Hosoda R, Kuroda Y, Nakata H. Hetero-oligomerization of adenosine A1 receptors with P2Y1 receptors in rat brains. FEBS Lett. 2002 Nov 6;531(2):299–303.

Zouali M. Antibodies. els.net. Chichester, UK: John Wiley & Sons, Ltd; 2001a.

Zouali M. Natural Antibodies. els.net. Chichester, UK: John Wiley & Sons, Ltd; 2001b.

Zukowska-Grojec Z, Dayao EK, Karwatowska-Prokopczuk E, Hauser GJ, Doods HN. Stress-induced mesenteric vasoconstriction in rats is mediated by neuropeptide Y Y1 receptors. Am J Physiol. 1996 Feb;270(2 Pt 2):H796–800.

Zygmunt PM, Petersson J, Andersson DA, Chuang H, Sørgård M, Di Marzo V, et al. Vanilloid receptors on sensory nerves mediate the vasodilator action of anandamide. Nature. 1999 Jul 29;400(6743):452–7.

## Chapter 2: General Materials and Methods

### 2.1: Mice

C57BL/6 WT female mice (NCI/Charles River, Portage, MI) and female CB1/CB2 KO mice were used in all experiment unless otherwise indicated. CB1/CB2 KO mice, on a C57BL/6 background, were created by Dr. Andreas Zimmer at the University of Bonn, Germany as previously described (Jarai et al., 1999; Zimmer et al., 1999; Buckley et al., 2000; Gerald et al., 2006). CB1/CB2 KO mice for these studies were obtained from Drs. Norbert Kaminski and Barbara Kaplan who maintain a breeding colony of CB1/CB2 KO mice at Michigan State University. All animals were housed two to five per cage and maintained in a sterile, temperature (22 ± 1 °C) and light controlled (12L:12D) room, and provided with irradiated food and bottled tap water *ad libitum*. All experiments used the minimal number of animals required for statistical analyses, minimized suffering, and followed the guidelines of the National Institutes of Health Guide for the Care and Use of Laboratory Animals. The Michigan State Institutional Animal Care and Use Committee approved all drug administrations and methods of euthanasia (AUF# 03/12-060-00).

#### 2.1.1: CB1/CB2 KO Mouse Genotyping

PCR was used to confirm knockout of CB1 and CB2 receptor genes. Genomic DNA was isolated from ~0.5 cm tail snips using 100 $\mu$l DirectPCR Lysis Reagent

(Viagen Biotech, Los Angeles, CA) plus 0.1 mg/ml proteinase K. Tails were incubated overnight at 55°C followed by a 45 min incubation at 85°C. Crude DNA extract was obtained following centrifugation at 300 RCF for 1 min. One μl of extract was used in a Taqman PCR reaction using *Cnr1* stock primers (CB1 receptor gene) or *Cnr2* (CB2 receptor gene) custom primers (Life Technologies/Applied Biosystems, Foster City, CA) (Kaplan et al., 2010). PCR primers for CB1 receptors were forward 5'-AGGAGCAAGGACCTGAGACA-3', reverse 5'-GGTCACCTTGGCGATCTTAA-3', for CB2 receptor were forward 5'-CCTGATAGGCTGGAAGAAGTATCTAC-3', reverse 5'-ACATCAGCCTCTGTTTCTGTAACC-3', neomycin cassette primers were forward 5'-ACCGCTGTTGACCGCTACCTATGTCT-3', and reverse 5'-TAAAGCGCATGCTCCAGACTGCCTT-3'. The average ± standard deviation Ct values for *Cnr1* and *Cnr2* in WT mice were 25.0 ± 0.54 and 26.0 ± 1.22, respectively. All samples obtained from CB1/CB2 KO tail snips resulted in an "undetermined" Ct value, indicating lack of expression of both *Cnr1* and *Cnr2*.

## 2.2: General Materials and Drugs

All drug concentrations were calculated as free-base. All chemicals were prepared fresh for each experiment. **Table 2.1** summarizes the pharmacologic action of drugs listed in this section.

3-hydroxybenzylhyrdazine (NSD-1015): NSD-1015 (Molekula) was dissolved in 0.9% isotonic saline to a final concentration of 10 mg/ml and administered at dose of 100 mg/kg.

8-Cyclopentyl-1,3-dipropylxanthine (DPCPX): DPCPX (Sigma) was dissolved in DMSO to a concentration of 100 μM and used at a final concentration of 100 nM.

α-Methyl-DL-tyrosine methyl ester hydrochloride (aMT): aMT ester (Sigma, St. Louis, MO) was dissolved in 0.9% isotonic saline to a final concentration of 30 mg/ml and administered at dose of 300 mg/kg.

Butoxamine: Butoxamine (B1385, Sigma) was dissolved in sterile isotonic saline at a concentration of 5 mg/ml and administered at doses ranging from 1-10 mg/kg (i.p.).

Hank's Buffered Saline Solution (HBSS): 10x HBSS powder (Gibco) was diluted with ultra-pure $H_2O$ (NaCl 138 mM, KCl 5.3 mM, $Na_2HPO_4$ 0.3 mM, $NaHCO_3$ 4.2 mM, $KH_2PO_4$ 0.4 mM, and glucose 5.6 mM), autoclaved, and stored at $4^{\circ}$ C.

Idazoxan: Idazoxan (Sigma, St. Louis, MO) was dissolved in 0.9% isotonic saline to a final concentration of 0.4 mg/ml and administered at dose of 4 mg/kg.

Isotonic Saline: 1 L of 0.9% saline was prepared using ultra-pure $H_2O$ and 9 grams of NaCl. The solution was autoclaved and kept closed at room temperature.

Krebs bicarbonate buffer: NaCl 120.0 mM, KCl 5.5 mM, $CaCl_2$ 2.5 mM, $NaH_2PO_4$ 1.2 mM, $MgCl_2$ 1.2 mM, $NaHCO_3$ 20.0 mM, and glucose 11.0 mM in ultra-pure $H_2O$.

LPS: LPS (*E. coli* 055:B5 catalog L2880, lot 066K4096, 5 EU/ng (Limulus lysate assay) and 10 EU/ng (chromogenic assay), Sigma, St. Louis, MO) was dissolved in RPMI-1640 at used at a final concentration of 10 µg/ml for *in vitro* studies. For *in vivo* experiments, LPS was dissolved in HBSS to a concentration of 50 µg/ml and injected at 25 µg per mouse (i.p.).

N2-(Diphenylacetyl)-N-[(4-hydroxyphenyl)methyl]-D-arginine amide (BIBP3226): BIBP3226 (Tocris) was dissolved in DMSO to a concentration of 1 mM and used at a final concentration of 1 µM.

Norepinephrine (NE): NE (Cat# A7257, Sigma) was dissolved in RPMI media to a concentration of 1 mM and used at a final concentration between 20-80 µM. For spleen contraction studies, NE was dissolved in less than 20 ml of Krebs

bicarbonate buffer that was acidified by a single drop of concentrated (18 M) HCl to a concentration of 1 mM.

Paraformaldehyde: 4% Paraformaldehyde, buffered with 0.1 M phosphate at pH 7.4, was made by combining 1:1 an 8% paraformaldehyde stock solution prepared from prills (Sigma) and a 0.2 M phosphate buffer (pH 7.4) followed by adjustment with either sodium hydroxide or concentrated phosphoric acid.

Phosphate Buffere Saline (PBS): NaCl 137 mM, KCl 2.7 mM, $Na_2HPO_4$ 10 mM, and $KH_2PO_4$ 1.8 mM in ultra-pure $H_2O$.

Prazosin: Prazosin (Sigma) was dissolved in DMSO to concentration of 1 mM and used at a final concentration of 1 μM.

Pyridoxal phosphate-6-azo(benzene-2,4-disulfonic acid (PPADS): PPADS (Sigma) was dissolved in $H_2O$ to a concentration of 10 mM and used at a final concentration of 10 μM.

RPMI-1640: RPMI-1640 stock solution (Life Technologies) was supplemented with 15 ml of 1 M HEPES per 0.5 L prior to sterile filtration. Sterile bottles were stored under sterile conditions at 4° C.

sRBC: An aliquot of sRBC was placed in a 50-ml conical tube. 25 ml of HBSS was added to the sRBC and centrifuged at 300 RCF for 5 min. The supernatant was removed from the concentrated sRBC pellet. This process was performed 3 additional times. sRBC were then counted and adjusted to 2 x $10^9$ cells/ml in HBSS. In experiments using sRBC, mice received 1x $10^9$ cells via a single i.p. injection.

Tetrodotoxin (TTX): TTX (Sigma) was dissolved in $H_2O$ at a concentration of 0.3 mM and used at a final concentration of 0.3 µM.

**Table 2.1. Summary of Drug Actions.**

| Drug | Action | Reference |
|---|---|---|
| 3-Hydroxybenzylhydrazine dihydrochloride (NSD-1015) | L-aromatic amino acid decarboxylase inhibitor | (Carlsson et al., 1972) |
| 8-Cyclopentyl-1,3-dipropylxanthine (DPCPX) | Adenosine A1 receptor antagonist | (Fozard and Milavec-Krizman, 1993) |
| α-Methyl-DL-tyrosine (aMT) | Tyrosine hydroxylase inhibitor | (Brodie et al., 1966) |
| Butoxamine | β2-adrenergic receptor antagonist | (Burns et al., 1967) |
| Idazoxan | α2-adrenergic receptor antagonist | (Doxey et al., 2012) |
| N2-(Diphenylacetyl)-N-[(4-hydroxyphenyl)methyl]-D-arginine amide (BIBP3226) | Neuropeptide Y Y1 receptor antagonist | (Rudolf et al., 1994) |
| Norepinephrine (NE) | Adrenergic receptor agonist (α1, α2, and β2) | (Furchgott, 1967) |
| Prazosin | α1AR antagonist | (Cambridge and Davey, 1977) |
| Pyridoxal phosphate-6-azo(benzene-2,4-disulfonic acid) (PPADS) | Adenosine P2X receptor antagonist | (Lambrecht et al., 1992) |
| Tetrodotoxin (TTX) | Voltage-gated sodium channel blocker | (Hille, 1975) |

2.3: Isolation of the Spleen Capsule and Splenocytes

After euthanasia spleens were removed by an incision in the left lateral abdomen under sterile conditions, which entails spraying the area of removal with 70% ethanol and using ethanol cleaned scissors and forceps to cut through the skin, and underlying muscle and connective tissue. The spleen was placed in a 6-well plate and mechanically crushed with the blunt end of a 10 ml syringe in 2 ml of HBSS to separate the spleen capsule (insoluble tissue) from the splenocytes (contained in the disruption supernatant). The spleen capsule was removed from the supernatant using forceps and taken whole or divided into two parts using ethanol-cleaned scissors depending on the needs of the experiment. Splenocytes were separated from the disruption supernatant by centrifugation at 300 RCF for 5 min and the supernatant was decanted. The separated splenocytes were then re-suspended in differing buffers and taken whole or divided into two parts depending on the needs of the experiment.

2.4: Preparation of Brain Tissue for Neurochemical Analyses

Following sacrifice by decapitation, the brains were rapidly removed and quick-frozen on dry ice and stored at -80° C until sectioning. Coronal sections of the brain (500 µm) were prepared by cryostat (-10° C) for micropunching according to the method of Palkovits (Palkovits, 1973). For the PVN a 21 g oval shaped tool was used to take a single midline punch.

2.5: Neurochemistry

All samples were placed in ice-cold tissue buffer following isolation or dissection and kept frozen at -80°C until analysis. Samples were thawed on the day of analysis and sonicated with 3 one-sec bursts (Sonicator Cell Disruptor, Heat Systems-Ultrasonic, Plainview, NY, USA) and centrifuged at 18,000 RCF for 5 min in a Beckman-Coulter Microfuge 22R centrifuge. The supernatant of brain samples was removed and brought up to 65 µl (q.s.) with fresh cold tissue buffer. The supernatant from the first centrifugation of the spleen capsule was removed and spun again at 18,000 RCF for 5 min in a Beckman-Coulter Microfuge 22R centrifuge before being brought up to 100 µl (q.s.) with fresh cold tissue buffer. Spleen samples were then filtered using a 0.2 µM syringe driven Millex-LG filter (Millipore, Billerica, MA).

All samples were analyzed for NE, MHPG, VMA, and/or DOPA content using high performance liquid chromatography coupled with electrochemical detection (HPLC-ED) (Lindley et al., 1990; Eaton et al., 1994) using C18 reverse phase columns (ESA Inc., Sunnyvale, CA) combined with a low pH buffered mobile phase (0.05 M Sodium Phosphate, 0.03 M Citrate, 0.1 mM EDTA at a pH of 2.65) composed of 5-15% methanol and 0.03-0.05% sodium octyl sulfate. Oxidation of monoamines was measured at a constant potential of -0.4 V by coulometric detection using a Coulochem Electrochemical Detector (Thermo Scientific). The amount of each substance in the samples was determined by comparing peak height values (as determined by a Hewlett Packard Integrator,

Model 3395) with those obtained from known standards run on the same day. Representative HPLC tracings from a standard solution (**Figure 2.1**), the spleen capsule (**Figure 2.2**) and PVN (**Figure 2.3**) are provided as a reference. Tissue pellets remaining from preparation were dissolved in 1 N NaOH and assayed for protein using the BCA method (Noble and Bailey, 2009).

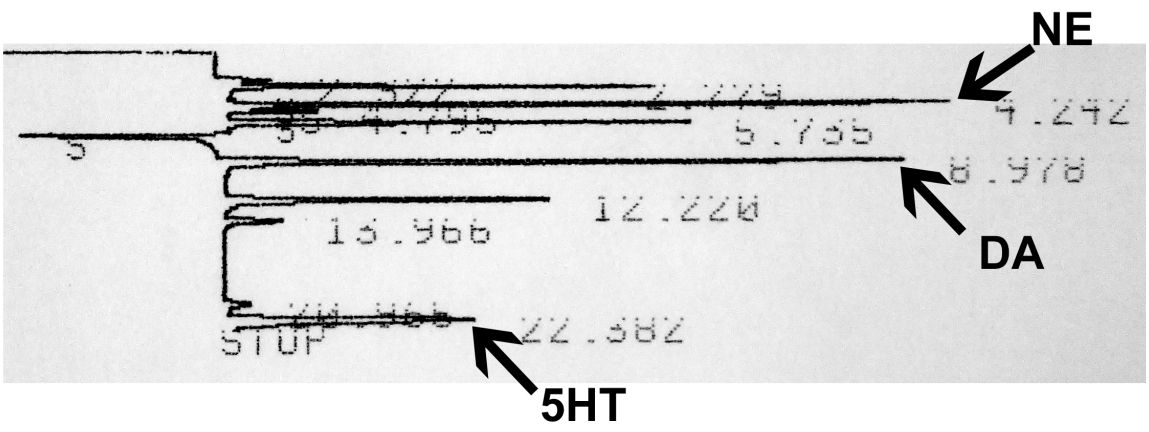


**Figure 2.1. Representative image from HPLC detection of biogenic amines in a standard solution.** HPLC-ED can be used to separate and quantify the amount of biogenic amines in prepared solutions. The biogenic amines NE, DA, and 5HT can be separated and identified based upon their retention time. The values obtained from known standards, such as this, run on the same day were used to quantify the amount of in experimental samples from various tissues.

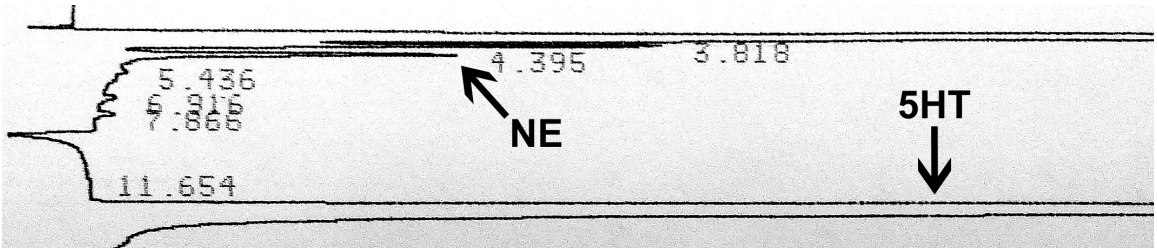


**Figure 2.2. Representative image of NE detection by HPLC in the spleen capsule.** HPLC-ED was used to separate and quantify the amount of NE from spleen capsule samples prepared as described. The two biogenic amines found in the spleen capsule, NE and 5HT, can be separated and identified based upon their retention time. The values obtained from HPLC standards run on the same day were used to quantify the amount of NE and normalized to the amount of protein per sample.

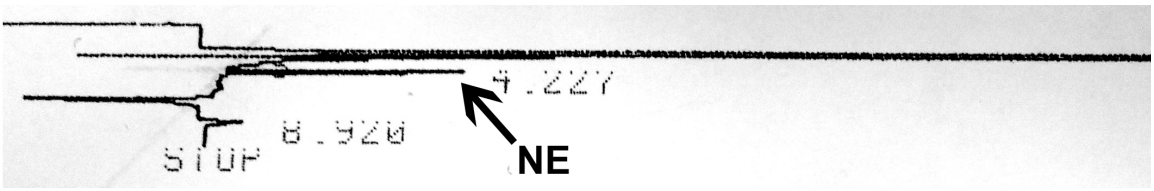


**Figure 2.3. Representative image of NE dectection by HPLC in the PVN.** HPLC-ED was used to separate and quantify the amount of NE from PVN samples prepared as described. The values obtained from HPLC standards run on the same day were used to quantify the amount of NE and normalized to the amount of protein per sample.

2.6: Western Blot

All samples were placed in ice-cold lysis buffer (water containing 1% Triton-x 100, 250 mM sucrose, 50 mM NaCl, 20 mM tris-HCl, 1 mM EDTA, 1 mM PMSF protease inhibitor cocktail, 1 mM DTT) immediately following isolation and kept frozen at -80° C until analysis. On the day of analysis samples were thawed, heated for 30 min at 100° C, sonicated for 8 sec, and spun at 12,000 RCF for 5 min. The supernatant was collected and a BCA protein assay performed (Noble and Bailey, 2009). Equal amounts of protein were separated using SDS-PAGE and transferred to PVDF-FL membranes (Millipore, Billerica, MA). The resulting membranes were reacted against antibodies for TH (AB152 1:2000, Millipore, Billerica, MA), smooth muscle α-actin (CP47 1:5000, Millipore, Billerica, MA), or α1AR (A270 1:400, Sigma) whose intensities were normalized to β-Actin (8H10D10 1:8000, Cell Signaling, Danvers, MA) or GAPDH (G8795, 1:2000, Sigma) to account for loading variability. Each PVDF-FL membrane contained samples representing all experimental conditions to avoid variability due to run, transfer, or antibody exposure conditions. Blots were visualized and quantified using an Odyssey Fc Infrared Imaging system (Li-Cor, Lincoln, NE) by utilization of IRDye conjugated secondary antibodies (goat anti-Mouse 800CW (1:20,000) or goat anti-rabbit 680LT (1:20,000)) and/or HRP-conjugated anti-rabbit antibodies (1:5000; Cell Signaling) visualized using SuperSignal West Pico Chemiluminescent Substrate kit (Thermo Scientific, Rockford, IL).

## 2.7: Immunohistochemistry

### 2.7.1: Brain Tissue Immunohistochemistry

Mice were anesthetized with a lethal dose of ketamine:xylazine (244 mg/kg:36 mg/kg; i.p.) and transcardially perfused first with ~5 ml of 0.9% isotonic saline immediately followed by ~100 ml of 4% paraformaldehyde prepared fresh that day. Perfused brains were removed and placed in vials of 4% paraformaldehyde and transferred to 20% sucrose in PBS after 24 h in paraformaldehyde and stored at 4° C until processing. Sections of the rostral 3rd ventricle containing the PVN (20 µm) were prepared in a cryostat at –20 C°. Sections were immunostained for TH (1:2,000 AB152, Millipore) using free-floating sections. Biotin conjugated goat anti-rabbit secondary antibodies (1:500) (Vector Laboratories, Burlingame, CA) were reacted with an avidin-biotin complex using an ABC Vectastain kit (Vector Laboratories), followed by 3,3′-diaminobenzidine (Sigma-Aldrich) to visual immunospecific staining for TH.

### 2.7.2: Spleen Immunohistochemistry

Freshly dissected spleens were quick frozen on dry ice and then stored at -80 C° for not more that 1 week. For sectioning spleens were embedded in Tissue-Tek OCT compound (VWR) and horizontal sections (8 µm) prepared in a cryostat at -20 C° and directly mounted onto gelatin-coated slides. The sections were then allowed to dry at room temperature for one h. Sections were soaked in

50% ethanol for 5 min to remove residual OCT compound and then fixed in 4 $C^{\circ}$ acetone prior to immunostaining. The sections were then immunostained for TH (1:250 AB152, Millipore). Biotin conjugated goat anti-rabbit secondary antibodies (1:500) (Vector Laboratories, Burlingame, CA) were reacted with an avidin-biotin complex using an ABC Vectastain kit (Vector Laboratories), followed by 3,3′-diaminobenzidine (Sigma-Aldrich) to visualize immunospecific staining for TH.

2.8: Preparation and Culture of Splenocytes

Two mice were killed by decapitation and their spleens removed aseptically via a single ethanol incision in the left flank, which was wetted with 70% ethanol, using ethanol-cleaned scissors. Single-cell suspensions were prepared by disrupting the spleen capsule with the blunt end of a sterile disposable 5-ml syringe in a 6-well plate in ~2 ml of RPMI-1640 media. The isolated splenocytes were then cultured in RPMI-1640 media supplemented with BCS (percentage of BCS dependent on length of culture and assay; Hyclone, Logan, UT, USA), 100 units penicillin/ml (Gibco), 100 µg streptomycin/ml (Gibco), and 50 µM 2-ME (Gibco). Splenocytes were cultured in a humidified atmosphere at 37$^{\circ}$C and 5% $CO_2$.

## 2.9: Flow Cytometry

### 2.9.1: Surface antibody labeling for flow cytometry

All staining protocols were performed in 96-well round bottom plates (BD Falcon, Franklin Lakes, NJ). Splenocytes were washed 3x with HBSS by centrifugation at 1000 RCF for 5 min, the supernatant was decanted, and the cells re-suspended in HBSS. Cultured splenocytes were then incubated for 30 min on ice in the dark in a 1x solution of near IR (APY-Cy7) live/dead stain (#L10119, Invitrogen, Grand Island, NY), a step which was omitted for splenocytes obtained directly from spleens. Following a wash in HBSS (as described above), splenocytes were then washed with FACS buffer (HBSS, 1% bovine serum albumin, 0.1% sodium azide, pH 7.6) as was done with HBSS. Surface Fc receptors were then blocked with anti-mouse CD16/CD32 [0.5 mg/ml] (#553142, BD Biosciences, Franklin Lakes, NJ) at 0.5 µl/well, IgM was blocked with anti-IgM [0.5 mg/ml] (#553425, BD Biosciences) at 1 µl/well, and IgG was blocked with anti-IgG [1.3 mg/ml] (#115-006-071, Jackson Immunoresearch, West Grove, PA) at 0.5 µl/well for 15 min each at RT. Cells were stained for 30 min at RT with the following antibody clones: CD19 (clone 6D5) [0.2 mg/ml] (Biolegend, San Diego, CA) at 1.25 µl/well and β2AR [0.25 mg/ml] (#AP7263d, Abgent, San Diego, CA) at 2 µl/ well. Cells were then washed 3x with FACS buffer. A secondary antibody for β2AR, donkey anti-rabbit DyLight 649 (clone Poly4064) [0.5 mg/ml] (Biolegend), at 0.5 µl/well was incubated for 30 min at RT. Subsequently cells were washed with FACS buffer, fixed with Cytofix (BD

Biosciences) for 15 min at RT, washed 3x with FACS buffer, and finally suspended in FACS buffer for intracellular staining. Stained and fixed cells were stored in the dark at 4°C for up to 2 weeks.

2.9.2: Intracellular antibody labeling for flow cytometry

Within 2 weeks of surface staining (described above), cells were washed 2x with Perm/Wash (BD) and incubated with Perm/Wash for 30 min at RT. Fluorescently labeled antibodies for IgM (Clone II/41) [0.5 mg/mL] (Biolegend) and/or IgG [0.5 mg/mL] (#115-606-071, Jackson Immunoresearch, West Grove, PA) were added at 1 µl/well (IgM) or 0.5 *µ*l/well (IgG) for 30 min. Cells were washed 2x with Perm/Wash and suspended in FACS buffer. After intracellular staining, cells were analyzed the same day.

2.9.3: Flow Cytometry Analysis

Fluorescent staining was analyzed using a BD Biosciences FACSCanto II flow cytometer. Data were analyzed using Kaluza (Beckman Coulter Inc., Brea, CA) or FlowJo software (Tree Star Inc., Ashland, OR). Compensation and voltage settings of fluorescent parameters were performed using fluorescence-minus-one controls. Cells were gated on singlets (forward scatter height versus area) (**Figure 2.4**) followed by determination of live cells (low APC-Cy7 signal) only in samples obtained from splenocyte culture (**Figure 2.5**). Cells were then gated to select lymphocytes using forward versus side scatter (**Figure 2.6**). For

some analyses, an additional gate was created for CD19 expression to select for B cells (**Figure 2.7**). These sequential gates were used to identify IgM producing B cells (**Figure 2.8**) and IgM producing B cells that express β2AR (**Figure 2.9**). The percentage of cells gated to individual populations relative to the entire population were collected and analyzed. Additionally, the numerical intensity of the fluorescent signal, termed the mean fluorescence intensity (MFI), was also quantified and analyzed.

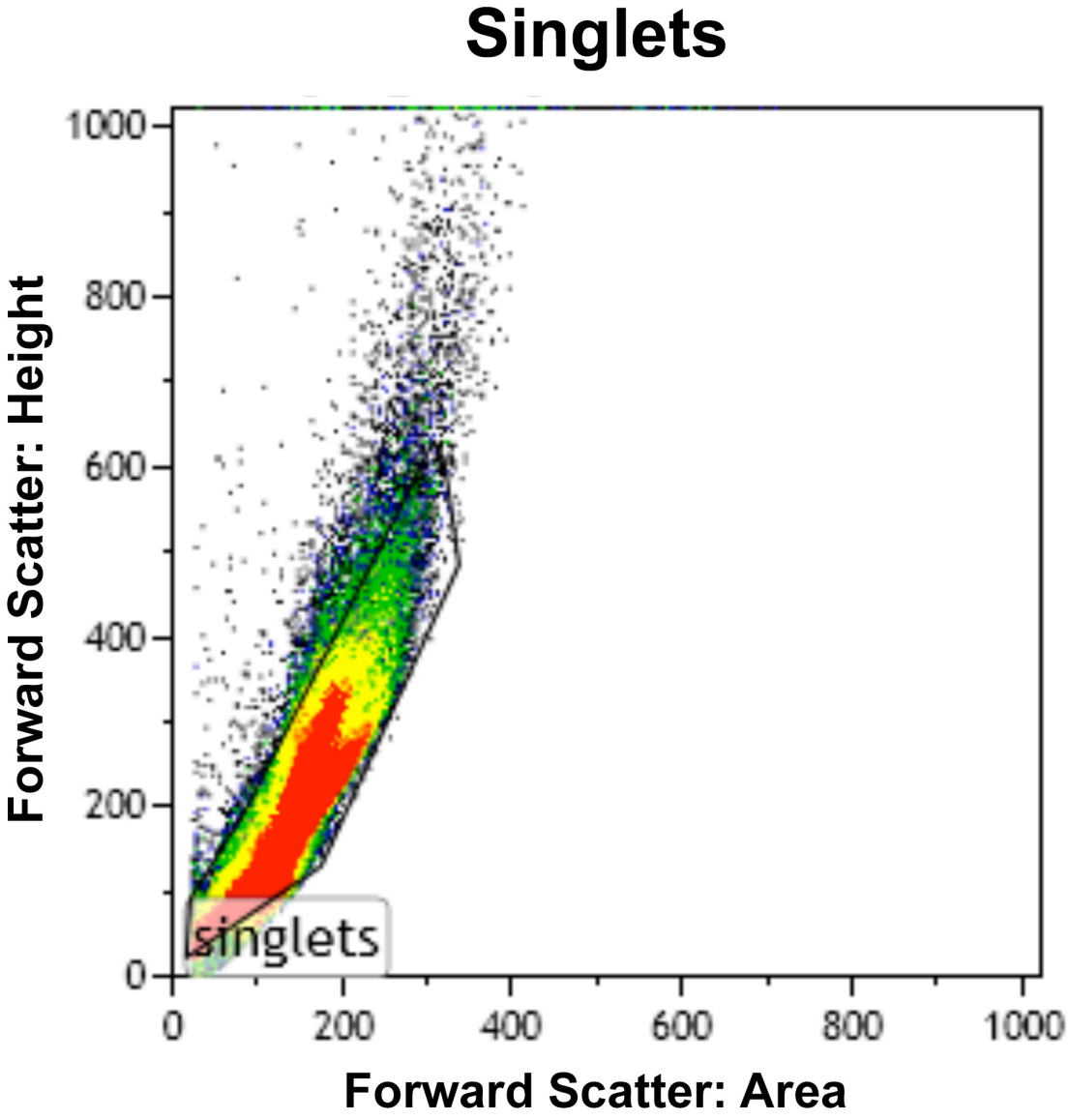


**NOTE:** For interpretation of the references to color in this and all other figures, the reader is referred to the electronic version of this dissertation.

**Figure 2.4. Representative gating of singlets in splenocytes prepared for flow cytometry.** The cells with a linear relationship when comparing the forward scatter area and height is encircled in black. This is the population single cells in solution, termed singlets.

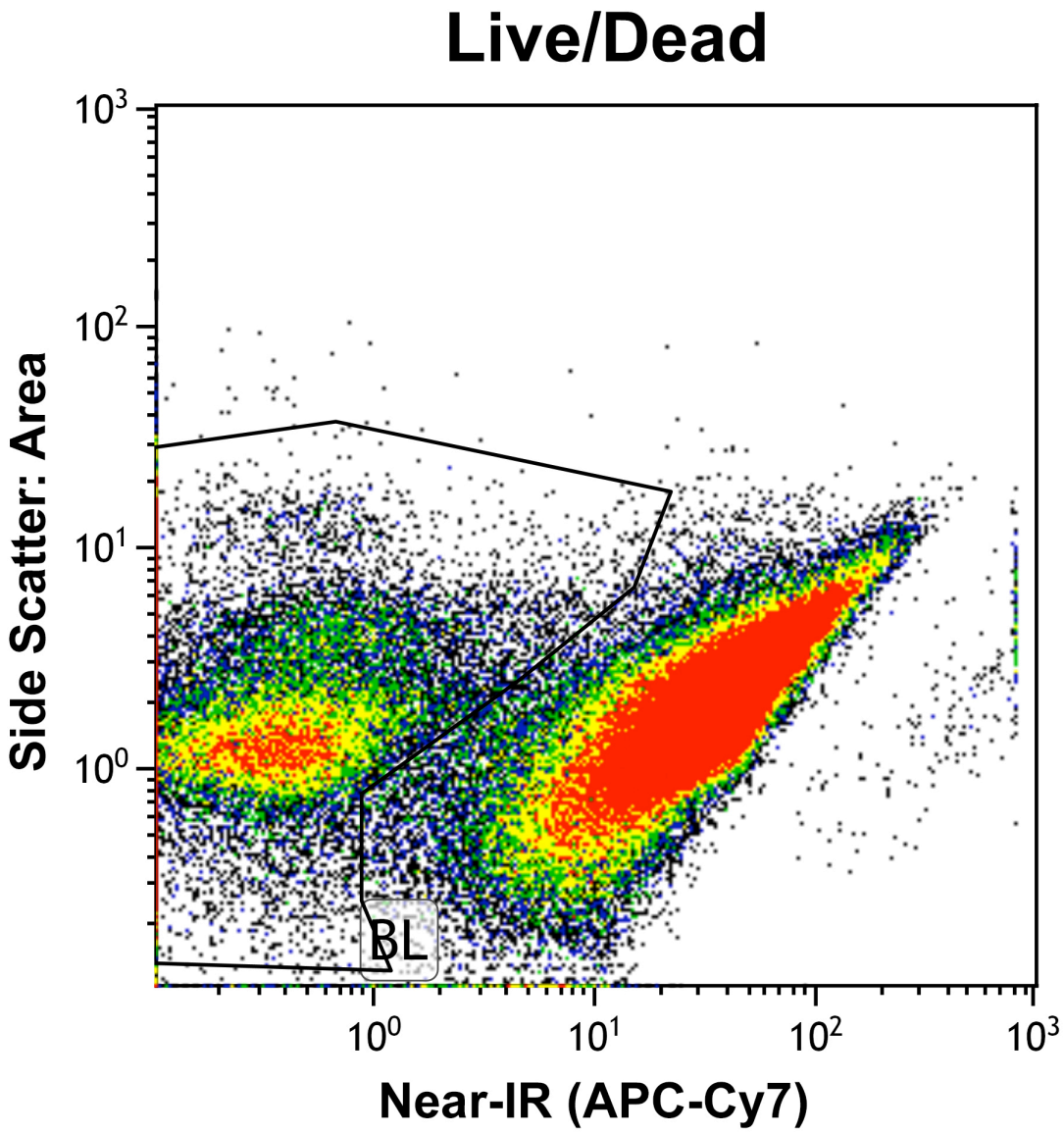


**Figure 2.5. Representative gating of live cells in preparations of cultured splenocytes for flow cytometry.** Within the singlet population, cells having low APC-Cy7 are encircled in black. This is the population singlets that are alive following isolation and preparation.

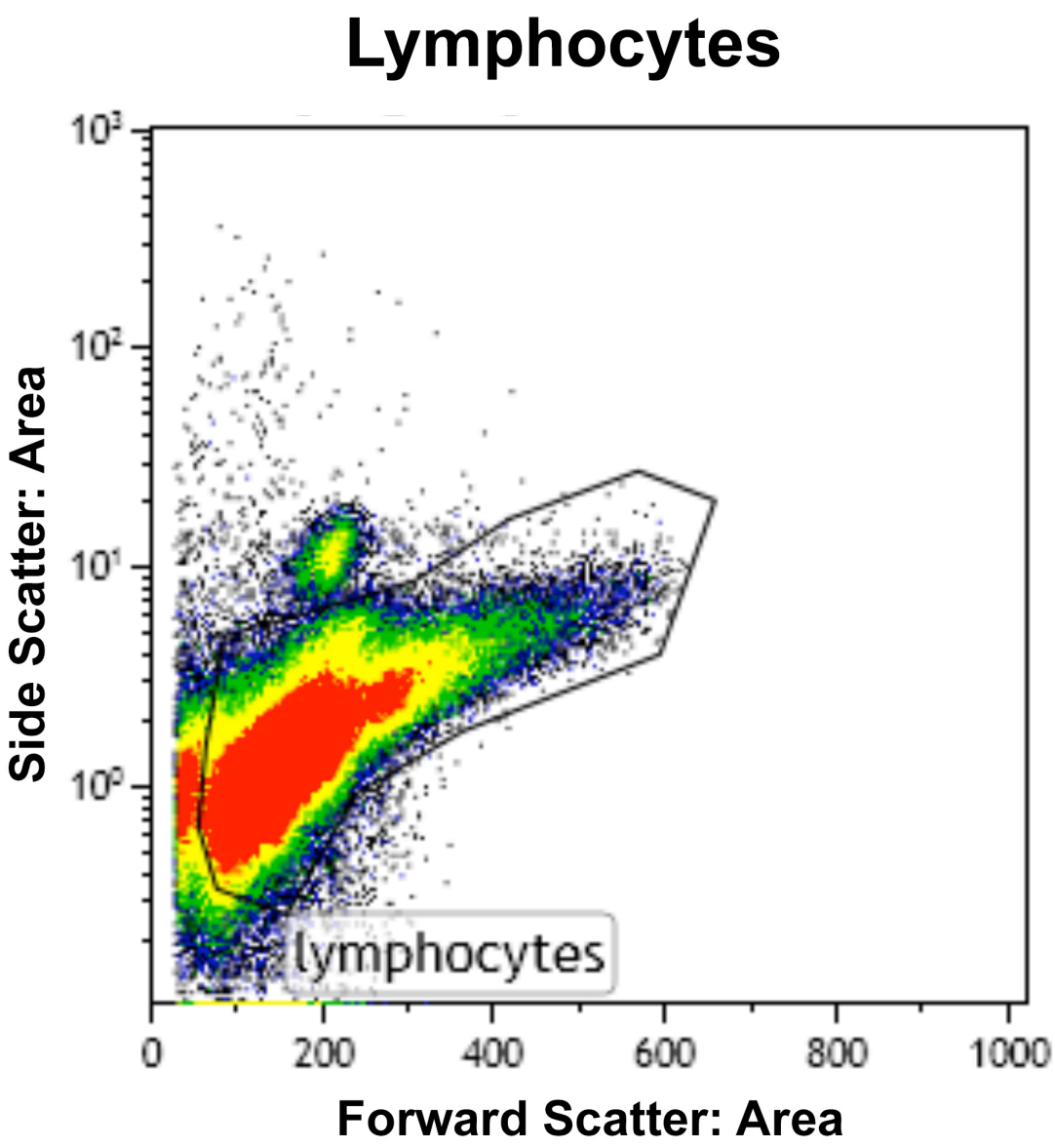


**Figure 2.6. Representative gating for spleen derived lymphocytes in preparations for flow cytometry.** Within the singlet/live cells, the population of lymphocytes in the spleen (encircled in black) was identified as cells having a relatively high forward scatter and low side scatter profile.

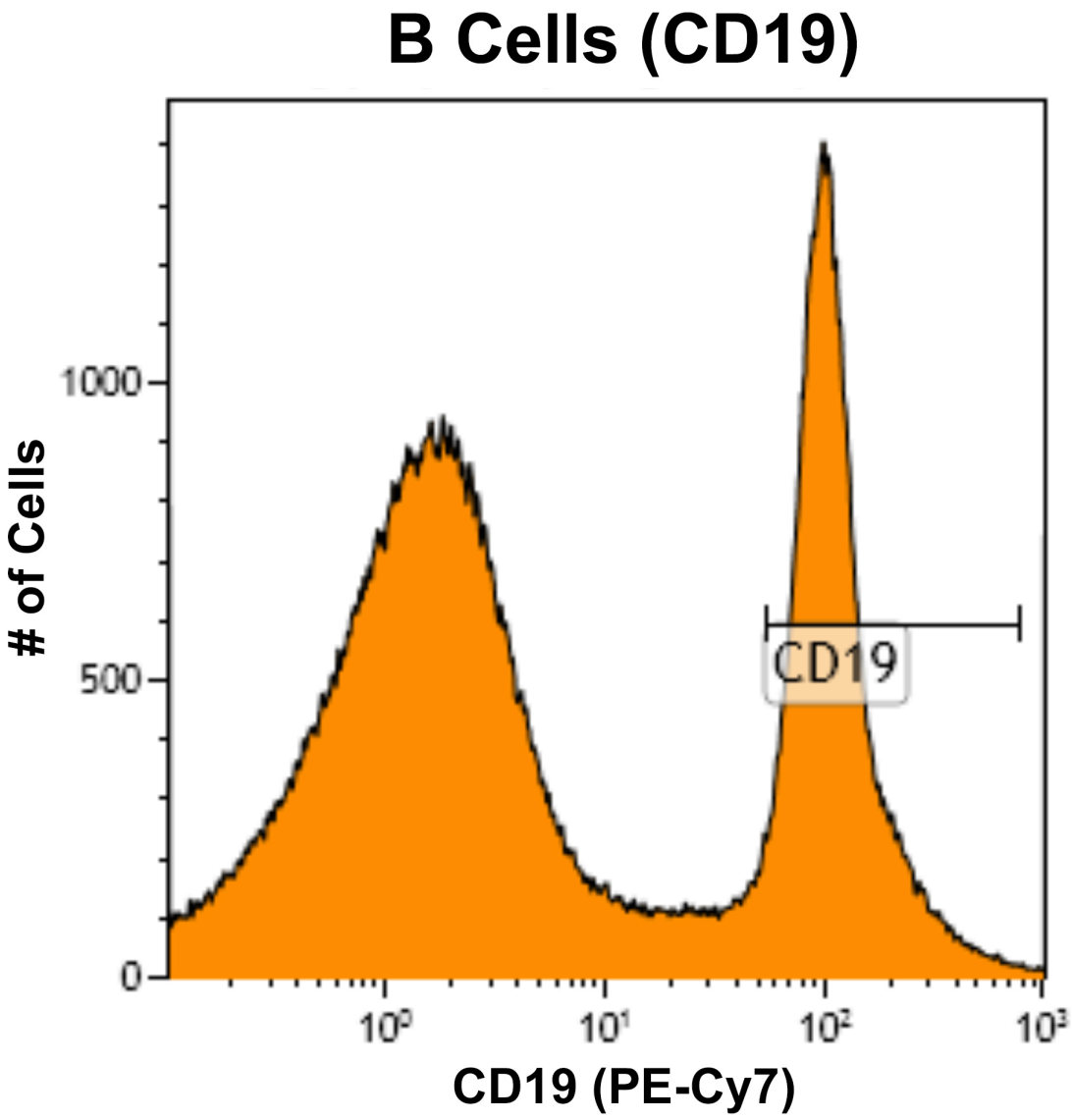


**Figure 2.7. Representative gating for splenic B cells by flow cytometry.** Among splenic lymphocytes, the population of B cells was identified by high CD19 expression (indicated by the brackets).

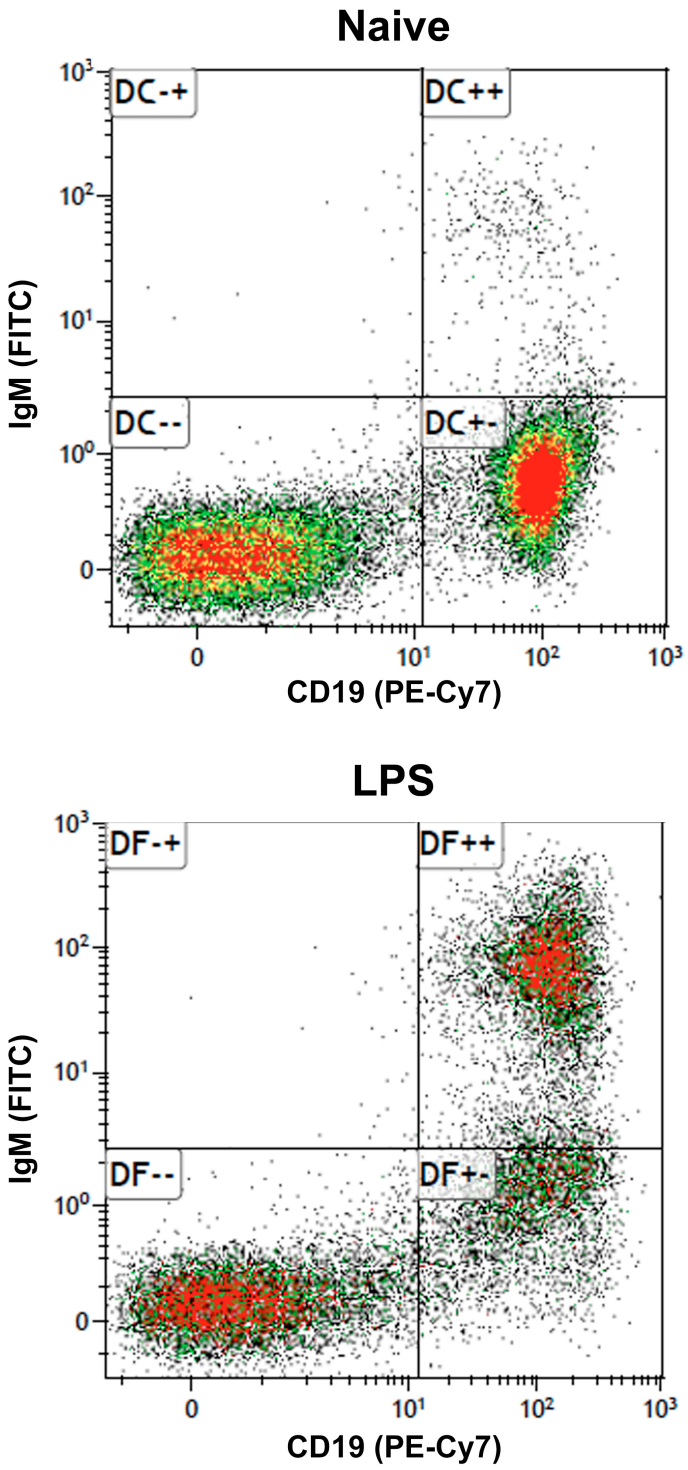


**Figure 2.8. Representative images from flow cytometric analysis of IgM producing splenic B cells.** Among splenic lymphocytes, IgM producing B cells were identified as cells with high IgM and CD19 expression (upper right quadrant). An image from both immunologically naïve and LPS treated splenocytes is provided for comparison.

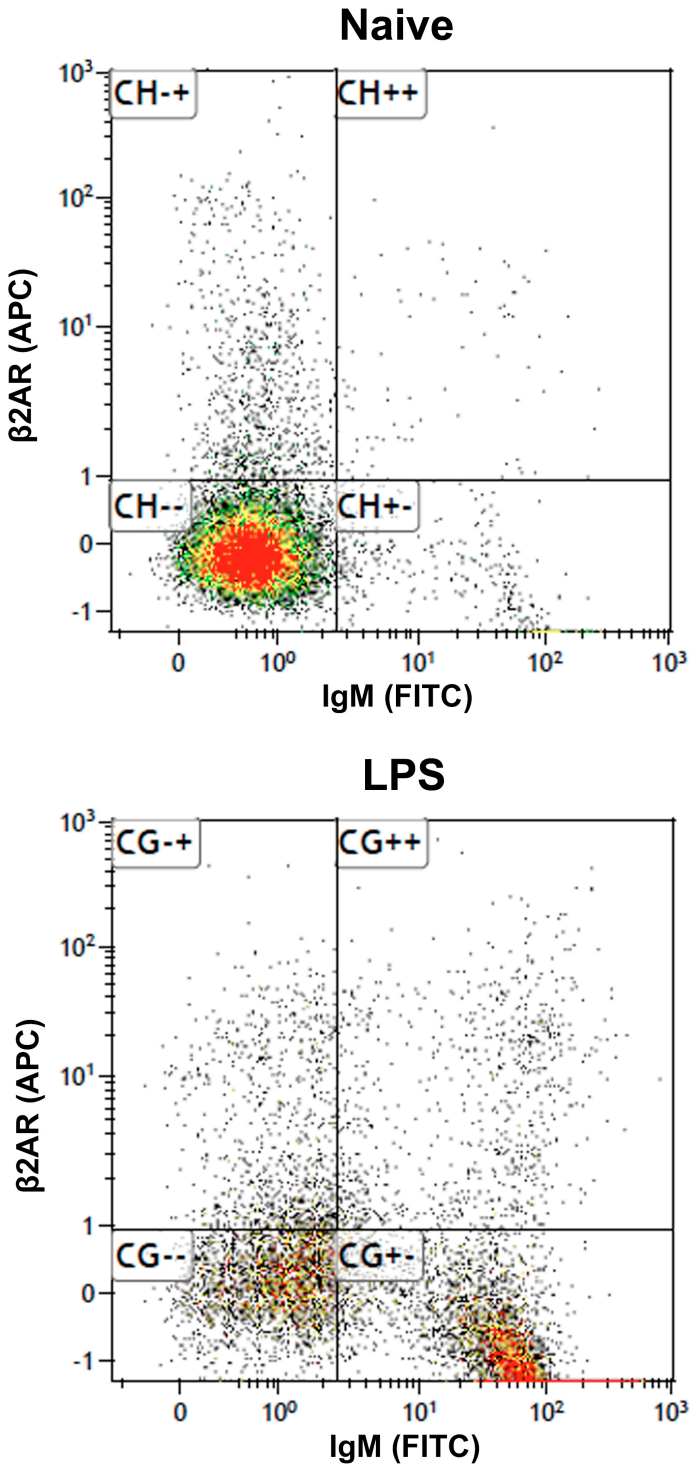


**Figure 2.9. Representative images from flow cytometric analysis of IgM producing splenic B cells expressing β2AR.** Among gated splenic B cells, IgM producing cells expressing β2AR were identified (upper right quadrant). An image from both immunologically naïve and LPS treated splenocytes is provided for comparison.

2.10: Enzyme Linked Immunosorbant Assay (ELISA)

Serum IgM and IgG were detected by sandwich ELISA. In preparation, 100 µl of 1 µg/ml anti-mouse IgM (Sigma-Aldrich, St. Louis, MO) or 1 µg/ml anti-mouse IgG (Sigma-Aldrich) was added to wells of a 96-well microtiter plate and stored at 4$^{o}$C overnight. After the pre-coating step, the plate was washed twice with 0.05% Tween-20 in PBS and three times with $H_2O$. Following this, 200 µl of 3% BSA-PBS was added to the wells and incubated at RT for 1.5 h to block nonspecific binding followed by the same washing steps described above. Serum samples were diluted and added to the coated plate (100 µl) for 1.5 h at RT. After the incubation, the plate was washed again, followed by addition of 100 µl of HRP-conjugated goat anti-mouse IgM (A8786, Sigma-Aldrich) or HRP-conjugated goat IgG (A3673, Sigma-Aldrich). Following the HRP incubation for 1.5 h at RT, any unbound detection antibody was washed away from the plate, and 100 µl ABTS (Roche Applied Science, Indianapolis, IN) added. The detection of the HRP substrate reaction was conducted over a 1 h period using a plate reader with a 405-nm filter (Bio-Tek). The KC4 computer analysis program (Bio-Tek) calculated the concentration of IgM or IgG in each sample based on a standard curve generated from the absorbance readings of known concentrations of IgM (range 6-1600 pg/ml, clone TEPC 183, Sigma-Aldrich) or IgG (range 3-800 pg/ml, Sigma-Aldrich).

## 2.11: Enzyme Linked Immunosorbent Spot Assay (ELISPOT)

ELISPOT was performed as described previously (Lu et al., 2009). ELISPOT wells were coated with purified anti-mouse (Sigma-Aldrich) IgM antibody and blocked with 5% BSA. Splenocytes from freshly disrupted spleens were washed, via centrifugation as described for flow cytometry, and incubated in the ELISPOT wells for 16–20 h. Biotin-conjugated anti-mouse IgM antibody (Sigma-Aldrich, St. Louis, MO) and streptavidin-horseradish peroxidase (Sigma-Aldrich, St. Louis, MO) were sequentially added to the wells. The spots were developed with the aminoethylcarbazole staining kit (Sigma-Aldrich, St. Louis, MO). Data were collected and analyzed using the CTL ImmunoSpot system (Cellular Technology Ltd, Shaker Heights, OH).

## 2.12: Spleen Contraction Studies

### 2.12.1: Preparation of Spleen Tissue for Spleen Contraction Studies

Spleens were obtained from mice euthanized via isoflurane (primary death by cervical dislocation results in less contractile responses and necessitates prolonged equilibration of the tissue (Eltze, 1996). Spleens were removed and connected via loops of nylon string to an isometric force transducer (Radnoti, Monrovia, CA) and placed in a 20-ml organ bath (Norman D. Erway Glass Blowing) under a resting tension of 0.8 g (7.84 mN) for recording isometric contractile responses in Krebs bicarbonate buffer maintained at 37°C and gassed with 95% $0_2$ - 5% $CO_2$ (**Figure 2.10**).

2.12.2: Spleen Contraction Measurement

Isometric contractions were recorded in response to EFS or direct injection of NE into the bath medium. EFS was produced by two ~1 cm platinum ring electrodes (custom built), above and below the spleen, connected to a Grass S48 Stimulator (Grass Technologies, Warwick, RI). All spleens were simultaneously stimulated using a Med-Lab Stimu-Splitter II (Med-Lab Instruments). The EFS consisted of square wave pulses 0.2-0.25 ms in duration with the following characteristics: 30 V, 25 hertz (Hz), and 3 s train duration. Prior to any testing, each spleen was given at least 45 min of undisturbed time to acclimate to the *ex vivo* environment. Increased tension on the nylon string from spleen contraction resulted in deflection of a post on the isometric force transducer, the deflection of which is read as a change in voltage (**Figure 2.11**). This change in voltage is converted to grams at a rate of 0.28 volts equaling 1 gram. All data was then converted to and expressed as mN by multiplying the gram data output by 9.8 $m/s^2$ and then multiplying by 1000.

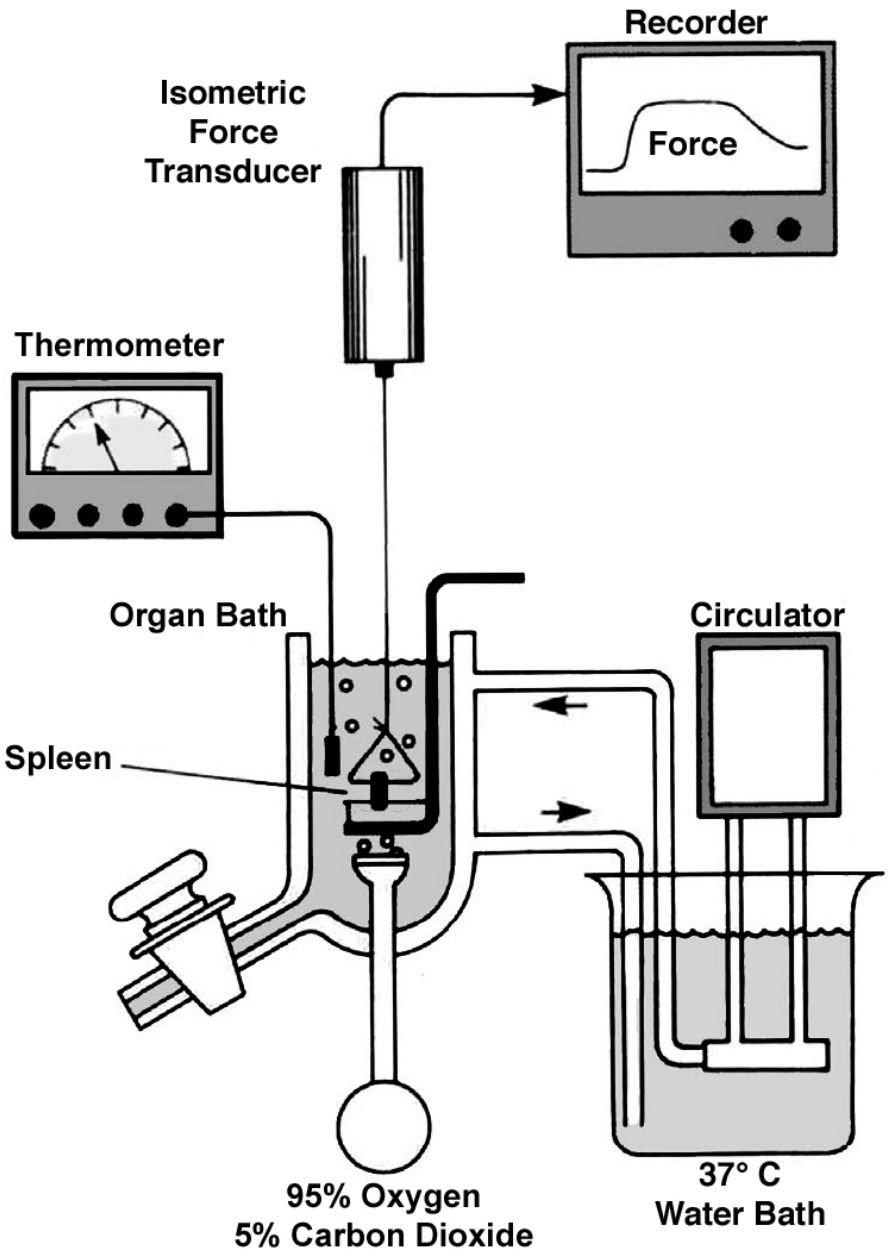


**Figure 2.10. Schematic of equipment setup used to record spleen contractile force.** Isolated spleens connected by nylon string to an isometric force transducer while residing in a physiological bath aerated with 95% oxygen and 5% carbon dioxide maintained at 37° C. Spleen contractile force was recorded by the tension generated on the nylon string. Figure adapted from Evora, et al (Evora et al., 2007).

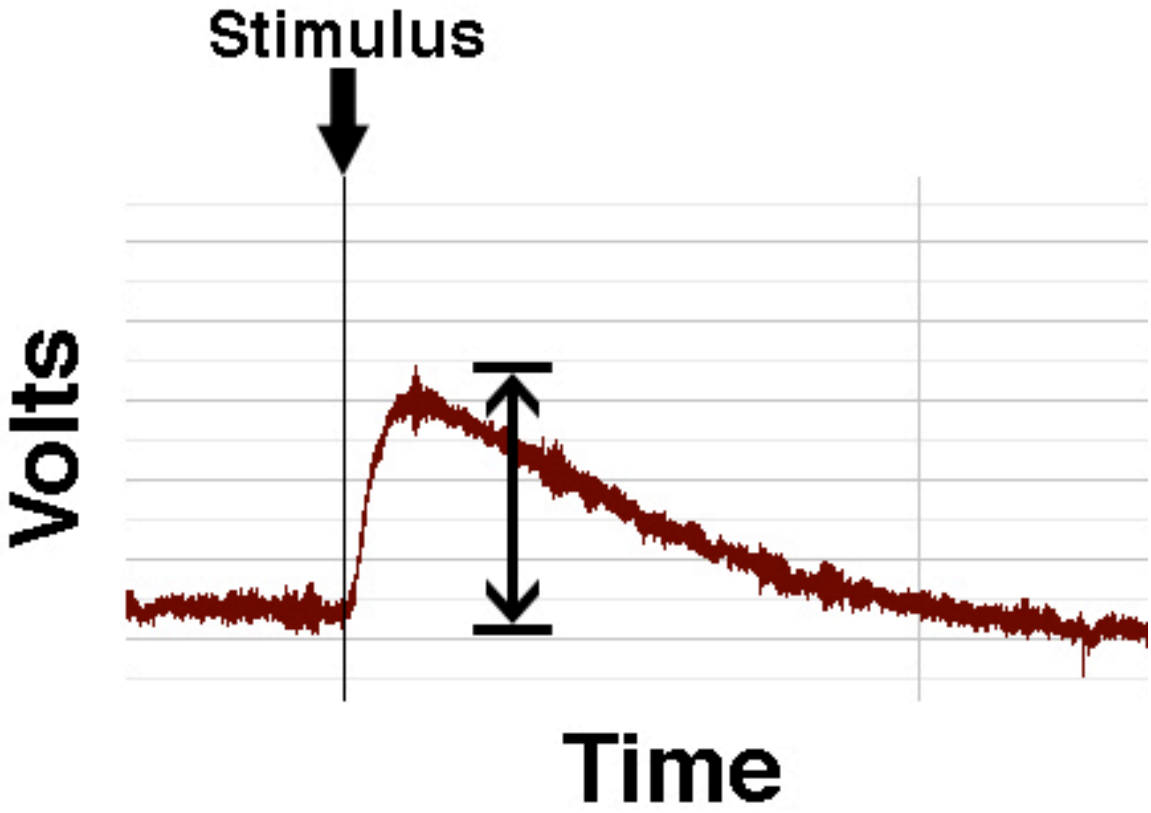


**Figure 2.11. Representative image of the raw data obtained from spleen contraction experiments.** The force of spleen contraction was measured by the tension generated on nylon strings connected from the spleen to the post of an isometric force transduction unit. The force of contraction was defined as the maximum voltage change, as indicated by the bracketed arrow, in response to a contractile stimulus.

## 2.13: Spleen Capsule Width Measurement

### 2.13.1: Hematoxylin and Eosin Staining

Mice were given a lethal dose of ketamine:xylazine (244 mg/kg:36 mg/kg; i.p.) and the spleen removed and dropped fixed in 4% paraformaldehyde. Fixed spleens were then taken to the Michigan State University Department of Pathology Histology Laboratory where they were paraffin embedded, sectioned at 4 µm, and stained with hematoxylin and eosin using standard accepted methodology.

### 2.13.2: Quantification of Spleen Capsule Thickness

Stained spleen sections were imaged at 40x magnification using a Nikon TE2000-S Inverted Microscope (Nikon, Melville, NY) with a Spot Insight QE camera (SPOT Imaging, Sterling Heights, MI) with SPOT 3.5.8 Imaging software (SPOT Imaging) (**Figure 2.12**). Each spleen was imaged, focused on the spleen capsule, two times at random locations on both the internal and external side of the spleen. ImageJ software (National Institutes of Health, USA) was used to measure the width of the spleen capsule, in pixels, at four evenly spaced locations on each image. All 12 values from each spleen were then averaged and this number used as a single n for comparison between genotypes.

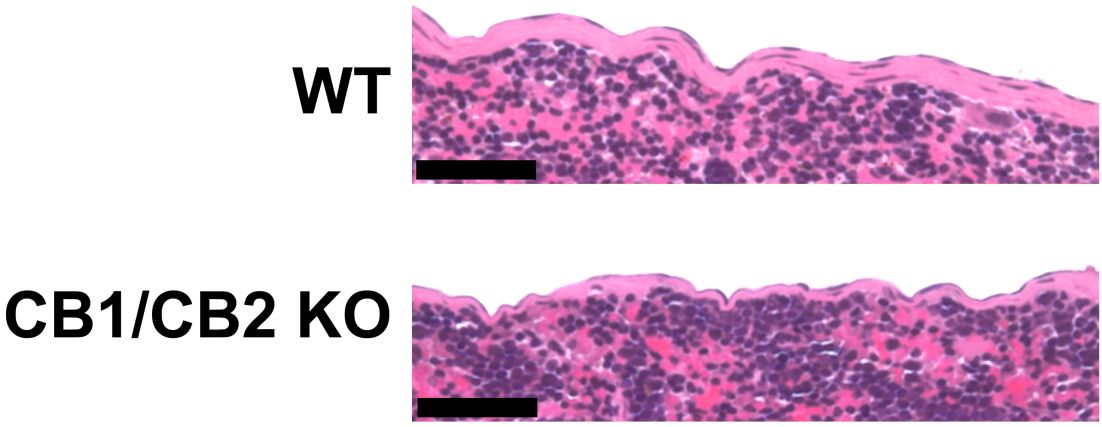


**Figure 2.12. Representative images comparing the spleen capsule thickness between WT and CB1/CB2 KO mice.** Spleens from WT and CB1/CB2 KO mice were fixed, stained with hematoxylin and eosin, and imaged at 40x magnification. Representative images from each genotype are presented. The black bar in the images is 50 μm in length.

## 2.14: Statistical Analysis

### 2.14.1: Statistical Comparisons

Prism software version 4.0a was used to make statistical comparisons between groups using the appropriate statistical test. Differences with a probability of error of less than 5% ($p<0.05$) were considered statistically significant. Two group comparisons were done using the Student's *t*-test. Two group comparisons where in one group had more than one degree or factor were done using a One-way ANOVA followed by a Bonferroni or Tukey's post-test for multiple comparisons. Experiments in which there were two groups with more than one degree or factor in each group, such as a 2x2 design, were analyzed using a Two-way ANOVA followed by Bonferroni post-test for multiple comparisons. Consideration for repeated measurements, as in spleen contraction studies, was given in analysis where appropriate.

### 2.14.2: aMT Experimentation

In experiments in which aMT was used to assess neuronal activity, NE concentrations from aMT treated and non-aMT (saline) treated mice were used for a regression analysis with saline animals acting as the 0 time control and aMT animals a 4 h time point. The rate constant was determined using this formula: $=(Log_{10}[B]-Log_{10}[A])/(-0.434*t)$. Where B is the concentration of NE after aMT, A is the concentration of A in saline treated animals, and t is the time of aMT treatment (Brodie et al., 1966). The slopes were compared via t-test using the

mean slope, SEM, and an n equal to the total number of data points used in the analysis to account for the total number of independent measurements used to generate the regression equations. Differences with a probability of error of less than 5% were considered statistically significant.

### 2.14.3: Flow Cytometry Data Handling

Population percentage data was transformed in Excel (Microsoft Corporation, Redmond, WA) to a parametric form before ANOVA analysis using the formula: =arcsin(sqrt(DATA/100)) (Ahrens et al., 1990). Raw percentage data was used for visual representations, while statistical significance indicated on these figures was performed on the transformed data.

# REFERENCES

# REFERENCES


Ahrens WH, Cox DJ, Budhwar G. Use of the arcsine and square root transformations for subjectively determined percentage data. Weed Science. 1990.

Brodie BB, Costa E, Dlabac A, Neff NH, Smookler HH. Application of steady state kinetics to the estimation of synthesis rate and turnover time of tissue catecholamines. J Pharmacol Exp Ther. 1966 Dec;154(3):493–8.

Buckley N, McCoy K, Mezey E, Bonner T, Zimmer A, Felder C, et al. Immunomodulation by cannabinoids is absent in mice deficient for the cannabinoid CB(2) receptor. Eur J Pharmacol. 2000 May 19;396(2-3):141–9.

Burns JJ, Salvador RA, Lemberger L. METABOLIC BLOCKADE BY METHOXAMINE AND ITS ANALOGS. Ann NY Acad Sci. 1967 Feb;139(3 New Adrenergi):833–40.

Cambridge D, Davey MJ. Prazosin, a selective antagonist of post-synaptic alpha-adrenoceptors [proceedings]. British journal of …. 1977.

Carlsson A, Davis JN, Kehr W, Lindqvist M, Atack CV. Simultaneous measurement of tyrosine and tryptophan hydroxylase activities in brain in vivo using an inhibitor of the aromatic amino acid decarboxylase. Naunyn-Schmied Arch Pharmacol. 1972;275(2):153–68.

Doxey JC, Roach AG, Smith CFC. Studies on RX 781094: a selective, potent and specific antagonist of α2-adrenoceptors. Br J Pharmacol. 2012 Jul 19;78(3):489–505.

Eaton MJ, Lookingland KJ, Moore KE. Effects of the selective dopaminergic D2 agonist quinelorane on the activity of dopaminergic and noradrenergic neurons projecting to the diencephalon of the rat. 1994 Feb 1;268(2):645–52.

Eltze M. Functional evidence for an alpha 1B-adrenoceptor mediating contraction of the mouse spleen. Eur J Pharmacol. 1996 Sep 12;311(2-3):187–98.

Evora PRB, Cable DG, Chua YL, Rodrigues AJ, Pearson PJ, Schaff HV. Nitric oxide and prostacyclin-dependent pathways involvement on in vitro induced hypothermia. Cryobiology. 2007 Feb;54(1):106–13.

Fozard JR, Milavec-Krizman M. Contraction of the rat isolated spleen mediated by adenosine A1 receptor activation. Br J Pharmacol. 1993 Jul 19;109(4):1059–63. PMCID: PMC2175713

Furchgott RF. The Pharmacological Differentiation of Adrenergic Receptors. Ann NY Acad Sci. 1967.

Gerald T, Ward G, Howlett A, Franklin S. CB1 knockout mice display significant changes in striatal opioid peptide and D4 dopamine receptor gene expression. Brain Res. 2006 Jun 6;1093(1):20–4.

Hille B. The receptor for tetrodotoxin and saxitoxin. A structural hypothesis. Biophysical Journal. The Biophysical Society; 1975 Jun 1;15(6):615.

Jarai Z, Wagner J, Varga K, Lake K, Compton D, Martin B, et al. Cannabinoid-induced mesenteric vasodilation through an endothelial site distinct from CB1 or CB2 receptors. Proc Natl Acad Sci U S A. 1999 Nov 23;96(24):14136–41.

Kaplan BLF, Lawver JE, Karmaus PWF, Ngaotepprutaram T, Birmingham NP, Harkema JR, et al. The effects of targeted deletion of cannabinoid receptors CB1 and CB2 on intranasal sensitization and challenge with adjuvant-free ovalbumin. Toxicol Pathol. 2010 Apr;38(3):382–92. PMCID: PMC2941344

Lambrecht G, Friebe T, Grimm U, Windscheif U, Bungardt E, Hildebrandt C, et al. PPADS, a novel functionally selective antagonist of P2 purinoceptor-mediated responses. Eur J Pharmacol. 1992 Jul 7;217(2-3):217–9.

Lindley SE, Gunnet JW, Lookingland KJ, Moore KE. 3,4-Dihydroxyphenylacetic acid concentrations in the intermediate lobe and neural lobe of the posterior pituitary gland as an index of tuberohypophysial dopaminergic neuronal activity. Brain Res. 1990 Jan 1;506(1):133–8.

Lu H, Kaplan BLF, Ngaotepprutaram T, Kaminski NE. Suppression of T cell costimulator ICOS by Delta9-tetrahydrocannabinol. J Leukoc Biol. 2009 Feb;85(2):322–9. PMCID: PMC2631366

Noble J, Bailey M. Quantitation of protein. Methods Enzymol. 2009;463:73–95.

Palkovits M. Isolated removal of hypothalamic or other brain nuclei of the rat. Brain Res. 1973 Sep 14;59:449–50.

Rudolf K, Eberlein W, Engel W, Wieland HA, Willim KD, Entzeroth M, et al. The first highly potent and selective non-peptide neuropeptide Y Y1 receptor antagonist: BIBP3226. Eur J Pharmacol. 1994 Dec 27;271(2-3):R11–3.

Zimmer A, Zimmer AM, Hohmann AG, Herkenham M, Bonner TI. Increased mortality, hypoactivity, and hypoalgesia in cannabinoid CB1 receptor knockout mice. Proc Natl Acad Sci USA. 1999 May 11;96(10):5780–5. PMCID: PMC21937

## Chapter 3: Comparison of the Noradrenergic Innervation in the Murine Spleen and the Paraventricular Nucleus of the Hypothalamus

### 3.1: Introduction

The PVN is a bilateral nucleus in the hypothalamus that has a multitude of functions that are aimed at maintaining the homeostasis of the body, particularly cardiovascular function. It is also regarded as one of five canonical central pre-sympathetic nuclei (Strack et al., 1989; Sved et al., 2001; Pyner, 2009). Like all central pre-sympathetic nuclei, the PVN has directly descending efferent projections to the IML of the spinal cord where they synapse on pre-ganglionic sympathetic neurons (Strack et al., 1989; Schramm et al., 1993; Cano et al., 2001; Sved et al., 2001; Pyner, 2009). The directly descending spinal projecting neurons of the PVN express vasopressin and oxytocin, which are stimulatory, or dopamine, which has mixed effects on pre-ganglionic sympathetic neurons (Sawchenko and Swanson, 1982; Strack et al., 1989; Sved et al., 2001; Pyner, 2009).

The PVN receives noradrenergic innervation from several brain nuclei, including the A1, A5, and A6 (locus coeruleus) noradrenergic systems (Byrum and Guyenet, 1987; Pacak et al., 1995; Samuels and Szabadi, 2008). Most noradrenergic innervation of the PVN is to the parvocellular portion, which is where the cells bodies of pre-autonomic spinal projecting neurons reside (Byrum and Guyenet, 1987; Cunningham and Sawchenko, 1988; Strack et al., 1989; Samuels and Szabadi, 2008; Pyner, 2009). Retroviral tracing and microinjection studies of the PVN demonstrate that this nucleus is

an upstream regulator of splenic sympathetic activity (Katafuchi et al., 1993; Cano et al., 2001). Stimulation of the PVN by direct intracerebral glutamate injection stimulates splenic sympathetic activity (Katafuchi et al., 1993).

Noradrenergic signaling in the PVN is mediated largely by α1 and α2AR (Leibowitz and Hor, 1982; Goldman et al., 1985; Daftary et al., 2000; Chong et al., 2004). Stimulation of α1AR on parvocellular neurons increase sIPSCs in GABAergic interneurons and stimulates the activity of glutamatergic interneurons, both of which synapse upon effector parvocellular neurons, including directly descending pre-autonomic neurons (Daftary et al., 2000; Chong et al., 2004). Conversely, α2AR decrease sIPSCs in GABAergic interneurons (Chong et al., 2004). Afferent PVN noradrenergic axon terminals have also known to be regulated by α2AR auto-receptors (Lookingland et al., 1991).

The rate of NE turnover (an estimate of noradrenergic neuronal activity) is generally higher in CNS noradrenergic neurons compared to noradrenergic neurons in the PNS. For instance, the half-life of NE turnover in the PVN is <1.5 h, whereas NE turnover in the heart and pancreas is >3 h (Levin, 1995). Stress is a well known cause for NE release in the PVN to activate the HPA-axis and induce the production of stress-related corticosteroids as well as increasing sympathetic outflow (Pacak et al., 1995; Itoi and Sugimoto, 2010; Inoue et al., 2013).

In comparison to the PVN, relatively little is known about the physiology of the splenic sympathetic neurons. The purpose of this chapter is to use the PVN, a central noradrenergic nucleus, as a comparator in evaluating the spleen projecting

noradrenergic sympathetic neurons. Not only are the noradrenergic neurons in the PVN well studied, but also are likely upstream in controlling the activity of splenic sympathetic neurons. Therefore, their activity is likely coupled with splenic sympathetic neurons and also likely share a number of physiological properties in common. Thus, identification of the similarities and differences between these two regions will be of use in identifying ways to study splenic noradrenergic neurons, the focus of this dissertation.
Furthermore many of the tools used to study PVN noradrenergic neurons will likely be useful for studying splenic noradrenergic neurons: including immunostaining, neurochemical analysis, and pharmacologic manipulation. The goal of the chapter is, therefore, to provide a basis of understanding and methodology necessary to interpret the findings in subsequent experimental paradigms with regard to the activity and function of splenic sympathetic neurons.

## 3.2: Materials and Methods

### 3.2.1:Mice

C57BL/6 WT female mice were housed two to five per cage and maintained in a temperature (22 ± 1 °C) and light controlled (12L:12D) room, and provided with food and water *ad libitum*.

### 3.2.2: Materials

NSD-1015: NSD-1015 (Molekula) was dissolved in 0.9% isotonic saline to a final concentration of 10 mg/ml and administered at dose of 100 mg/kg.

aMT: aMT ester (Sigma, St. Louis, MO) was dissolved in 0.9% isotonic saline to a final concentration of 30 mg/ml and administered at dose of 300 mg/kg.

HBSS: 10x HBSS powder (Gibco) was diluted with ultra-pure $H_2O$ (NaCl 138 mM, KCl 5.3 mM, $Na_2HPO_4$ 0.3 mM, $NaHCO_3$ 4.2 mM, $KH_2PO_4$ 0.4 mM, and glucose 5.6 mM), autoclaved, and stored at 4° C.

Idazoxan: Idazoxan (Sigma, St. Louis, MO) was dissolved in 0.9% isotonic saline to a final concentration of 0.4 mg/ml and administered at dose of 4 mg/kg.

Isotonic Saline: 1 L of 0.9% saline was prepared using ultra-pure $H_2O$ and 9 grams of NaCl. The solution was autoclaved and kept closed at room temperature.

Paraformaldehyde: 4% Paraformaldehyde, buffered with 0.1 M phosphate at pH 7.4, was made by combining 1:1 an 8% paraformaldehyde stock solution prepared from prills (Sigma) and a 0.2 M phosphate buffer (pH 7.4) followed by adjustment with either sodium hydroxide or concentrated phosphoric acid.

Phosphate Buffered Saline (PBS): NaCl 137 mM, KCl 2.7 mM, $Na_2HPO_4$ 10 mM, and $KH_2PO_4$ 1.8 mM in ultra-pure $H_2O$.

### 3.2.3: Isolation of the Spleen Capsule and Splenocytes

After euthanasia, spleens were removed by an incision in the left lateral abdomen under sterile conditions, which entails spraying the area of removal with 70% ethanol and using ethanol cleaned scissors and forceps to cut through the skin, and underlying muscle and connective tissue. The spleen was placed in a 6-well plate and mechanically crushed with the blunt end of a 10 ml syringe in 2 ml of HBSS to separate the spleen capsule (insoluble tissue) from the splenocytes (contained in the disruption supernatant). The spleen capsule was removed from the supernatant using forceps and taken whole or divided into two parts using ethanol-cleaned scissors depending on the needs of the experiment. Splenocytes were separated from the disruption supernatant by centrifugation at 300 RCF for 5 min and the supernatant was decanted. The separated splenocytes were then re-suspended in differing buffers and taken whole or divided into two parts depending on the needs of the experiment.

### 3.2.4: Preparation of Brain Tissue for Neurochemical Analyses

Following sacrifice by decapitation, the brains were rapidly removed and quick-frozen on dry ice and stored at -80° C until sectioning. Coronal sections of the brain (500 µm) were prepared by cryostat (-10° C) for micropunching according to the method of Palkovits (Palkovits, 1973). For the PVN a 21 g oval shaped tool was used to take a single midline punch.

3.2.5: Neurochemistry

All samples were placed in ice-cold tissue buffer following isolation or dissection and kept frozen at -80°C until analysis. Samples were thawed on the day of analysis and sonicated with 3 one-sec bursts (Sonicator Cell Disruptor, Heat Systems-Ultrasonic, Plainview, NY, USA) and centrifuged at 18,000 RCF for 5 min in a Beckman-Coulter Microfuge 22R centrifuge. The supernatant of brain samples was removed and brought up to 65 µl (q.s.) with fresh cold tissue buffer. The supernatant from the first centrifugation of the spleen capsule was removed and spun again at 18,000 RCF for 5 min in a Beckman-Coulter Microfuge 22R centrifuge before being brought up to 100 µl (q.s.) with fresh cold tissue buffer. Spleen samples were then filtered using a 0.2 µM syringe driven Millex-LG filter (Millipore, Billerica, MA).

All samples were analyzed for NE, MHPG, VMA, and/or DOPA content using HPLC-ED (Lindley et al., 1990; Eaton et al., 1994) using C18 reverse phase columns (ESA) combined with a low pH buffered mobile phase (0.05 M Sodium Phosphate, 0.03 M Citrate, 0.1 mM EDTA at a pH of 2.65) composed of 5-15% methanol and 0.03-0.05% sodium octyl sulfate. Oxidation of monoamines was measured at a constant potential of -0.4 V by coulometric detection using a Coulochem Electrochemical Detector (Thermo Scientific). The amount of each substance in the samples was determined by comparing peak height values (as determined by a Hewlett Packard Integrator, Model 3395) with those obtained from known standards run on the same day. Tissue pellets remaining from preparation were dissolved in 1 N NaOH and assayed for protein using the BCA method (Noble and Bailey, 2009).

3.2.6: Western Blot

All samples were placed in ice-cold lysis buffer (water containing 1% Triton-x 100, 250 mM sucrose, 50 mM NaCl, 20 mM tris-HCl, 1 mM EDTA, 1 mM PMSF protease inhibitor cocktail, 1 mM DTT) immediately following isolation and kept frozen at -80°C until analysis. On the day of analysis samples were thawed, heated for 30 min at 100° C, sonicated for 8 sec, and spun at 12,000 RCF for 5 min. The supernatant was collected and a BCA protein assay performed (Noble and Bailey, 2009). Equal amounts of protein were separated using SDS-PAGE and transferred to PVDF-FL membranes (Millipore, Billerica, MA). The resulting membranes were reacted against antibodies for TH (AB152 1:2000, Millipore, Billerica, MA), smooth muscle α-actin (CP47 1:5000, Millipore, Billerica, MA), or α1AR (A270 1:400, Sigma) whose intensities were normalized to Beta-Actin (8H10D10 1:8000, Cell Signaling, Danvers, MA) or GAPDH (G8795, 1:2000, Sigma) to account for loading variability. Each PVDF-FL membrane contained samples representing all experimental conditions to avoid variability due to run, transfer, or antibody exposure conditions. Blots were visualized and quantified using an Odyssey Fc Infrared Imaging system (Li-Cor, Lincoln, NE) by utilization of IRDye conjugated secondary antibodies, goat anti-Mouse 800CW (1:20,000) and/or goat anti-rabbit 680LT (1:20,000).

3.2.7: Immunohistochemistry

3.2.7.1: Brain Tissue Immunohistochemistry

Mice were anesthetized with a lethal dose of ketamine:xylazine (244 mg/kg: 36 mg/kg; i.p.) and transcardially perfused first with ~5 ml of 0.9% isotonic saline immediately followed by ~100 ml of 4% paraformaldehyde prepared fresh that day. Perfused brains were removed and placed in vials of 4% paraformaldehyde and transferred to 20% sucrose in PBS after 24 h in paraformaldehyde and stored at 4° C until processing. Sections of the rostral 3rd ventricle containing the PVN (20 µm) were prepared in a cryostat at –20 C°. Sections were immunostained for TH (1:2,000 AB152, Millipore) using free-floating sections. Biotin conjugated goat anti-rabbit secondary antibodies (1:500) (Vector Laboratories, Burlingame, CA) were reacted with an avidin-biotin complex using an ABC Vectastain kit (Vector Laboratories), followed by 3,3′-diaminobenzidine (Sigma-Aldrich) to visual immunospecific staining for TH.

3.2.7.2: Spleen Immunohistochemistry

Freshly dissected spleens were quick frozen on dry ice and then stored at -80 C° for not more that 1 week. For sectioning spleens were embedded in Tissue-Tek OCT compound (VWR) and horizontal sections (8 µm) prepared in a cryostat at -20 C° and directly mounted onto gelatin-coated slides. The sections were then allowed to dry at room temperature for one hour. Sections were soaked in 50% ethanol for 5 min to remove residual OCT compound and then fixed in 4 C° acetone prior to immunostaining. The sections were then immunostained for TH (1:250 AB152, Millipore). Biotin

conjugated goat anti-rabbit secondary antibodies (1:500) (Vector Laboratories, Burlingame, CA) were reacted with an avidin-biotin complex using an ABC Vectastain kit (Vector Laboratories), followed by 3,3′-diaminobenzidine (Sigma-Aldrich) to visual immunospecific staining for TH.

### 3.2.8: Statistical Analysis:

#### 3.2.8.1: Statistical Comparisons

Prism software version 4.0a was used to make statistical comparisons between groups using the appropriate statistical test. Differences with a probability of error of less than 5% ($p<0.05$) were considered statistically significant. Two group comparisons were done using the Student's *t*-test. Two group comparisons where in one group had more than one degree or factor were done using a One-way ANOVA followed by a Bonferroni or Tukey's post-test for multiple comparisons. Experiments in which there were two groups with more than one degree or factor in each group, such as a 2x2 design, were analyzed using a Two-way ANOVA followed by Bonferroni post-test for multiple comparisons. Consideration for repeated measurements, as in spleen contraction studies, was given in analysis where appropriate.

#### 3.2.8.2: aMT Experimentation

In experiments in which aMT was used to assess neuronal activity, NE concentrations from aMT treated and non-aMT (saline) treated mice were used for a regression analysis with saline animals acting as the 0 time control and aMT animals a

4 h time point. The rate constant was determined using this formula: $=(Log_{10}[B]-Log_{10}[A])/(-0.434*t)$. Where B is the concentration of NE after aMT, A is the concentration of A in saline treated animals, and t is the time of aMT treatment (Brodie et al., 1966). The slopes were compared via t-test using the mean slope, SEM, and an n equal to the total number of data points used in the analysis to account for the total number of independent measurements used to generate the regression equations. Differences with a probability of error of less than 5% were considered statistically significant.

## 3.3: Results

### 3.3.1: Noradrenergic innervation of the PVN and the spleen in mice

The noradrenergic innervation of the PVN and spleen can be visualized using immunohistochemical techniques. Immunostaining for TH demonstrates that the density of noradrenergic terminals differs greatly between these two areas. In the PVN, immunostaining for TH reveals dense noradrenergic axon terminal innervation largely in the dorsolateral portion of the PVN, with some axon terminals reaching periventricular areas of the PVN (**Figure 3.1**). These areas of the PVN are considered to be the lateral and dorsal parvocellular regions, respectively (Strack et al., 1989; Pacak et al., 1995; Daftary et al., 2000; Pyner, 2009). Neurons in this area are known to project to brain stem/spinal cord autonomic targets to control the activation of peripheral sympathetic neurons, as well as controlling CRH expressing neurons leading to HPA axis activation (Chong et al., 2004; Pyner, 2009). NE is reported to participate in the control of

sympathetic stimulation from this region, but interestingly only to certain types of stressors (Pacak et al., 1995).

Much like the PVN, TH staining in the spleen is heterogeneous and is localized to two regions within the spleen: the spleen capsule and plexus innervation of arterioles their surrounding areas, known as the PALS (**Figure 3.1**). This distribution is suggestive of the function of splenic sympathetic innervation, which is to control spleen contraction and the flow of blood through the spleen (Groom et al., 1991; Su et al., 1991; Eltze, 1996). Noradrenergic innervation of the PALS area immediately adjacent to splenic central arterioles is also supported by the staining demonstrated here (Felten et al., 1987; Felten and Olschowka, 1987). Western blot analysis for TH is congruent with immunohistochemical staining in showing that the majority of TH in the spleen is contained in the spleen capsule rather than the cellular parenchyma of the spleen, splenocytes (**Figure 3.2**). This distribution is further confirmed in that NE in the spleen is almost exclusively found in the spleen capsule as compared with splenocytes (**Figure 3.3**).

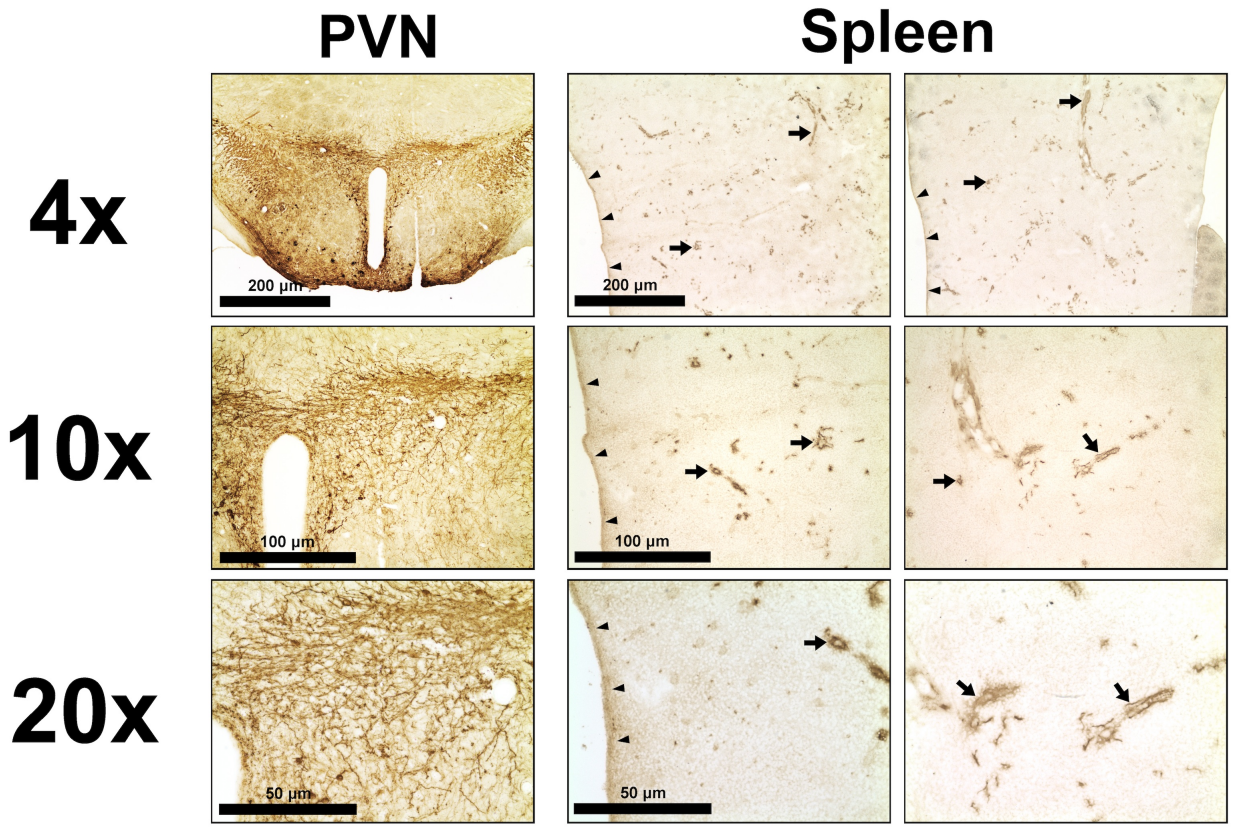


**Figure 3.1. Immunohistochemical staining for TH in the PVN and spleen of mice.** Fixed tissue from the PVN and spleen were stained for TH using standard immunohistochemical techniques (described in detail in Chapter 2). TH specific staining is shown as brown. Arrowheads denote TH immunostaining in the spleen capsule. Arrows denote TH immunostaining surrounding blood vessels. A scale bar for size reference is provided and represents the size denoted in the figure.

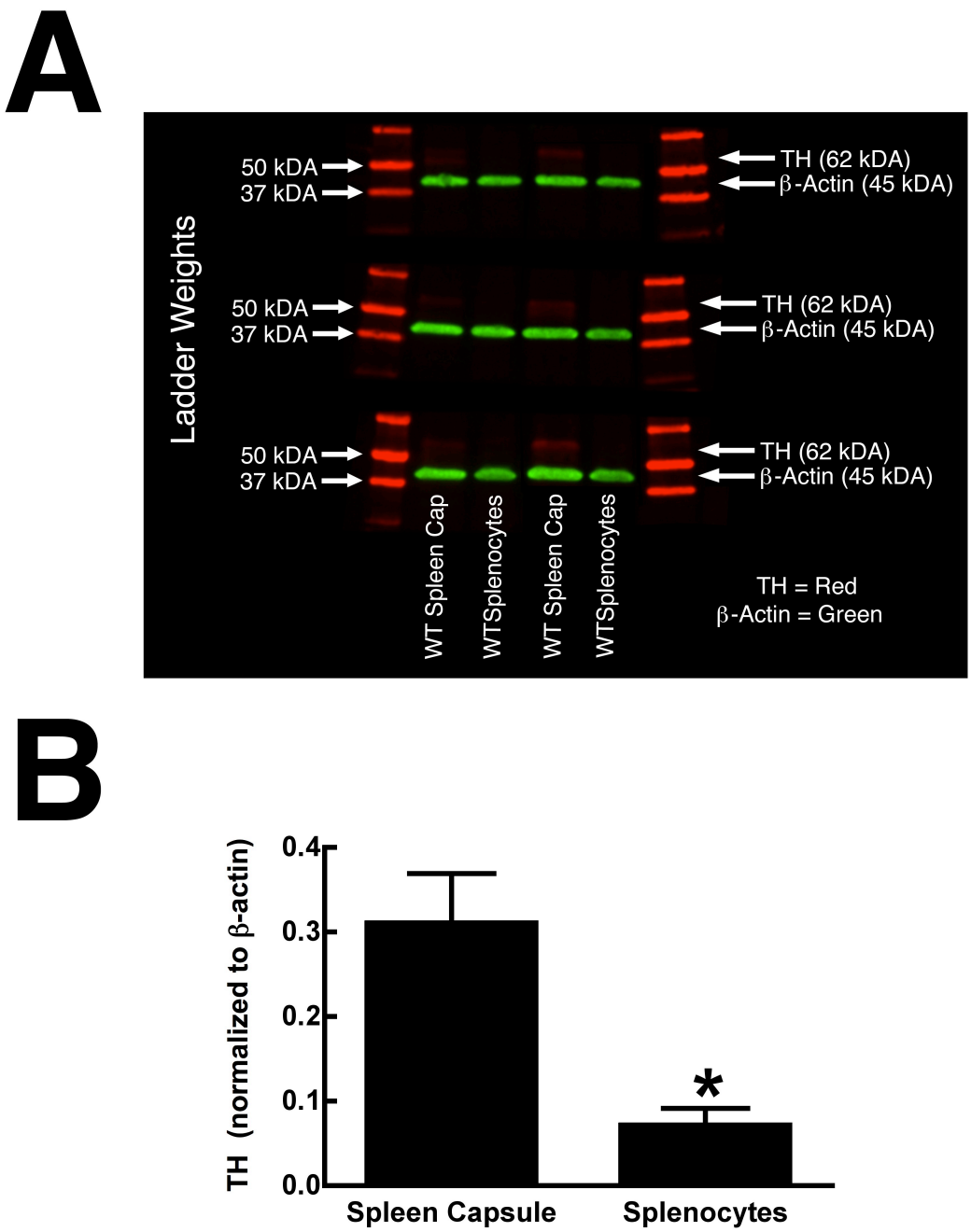


**Figure 3.2. Western blot analysis of TH in the spleen of mice.** Freshly removed mouse spleens were disrupted to separate the spleen capsule from the splenocytes. The tissue was then homogenized and lysed. Lysates were separated by SDS-PAGE then probed for TH and β-actin via Western blot. A) Labeled picture of the resulting image used for quantification. Red bands are TH and green bands are β-actin. B) Columns represent that mean TH RDU normalized to β-actin in the same sample + one SEM (n=6). * Differs from Spleen Capsule ($p<0.05$).

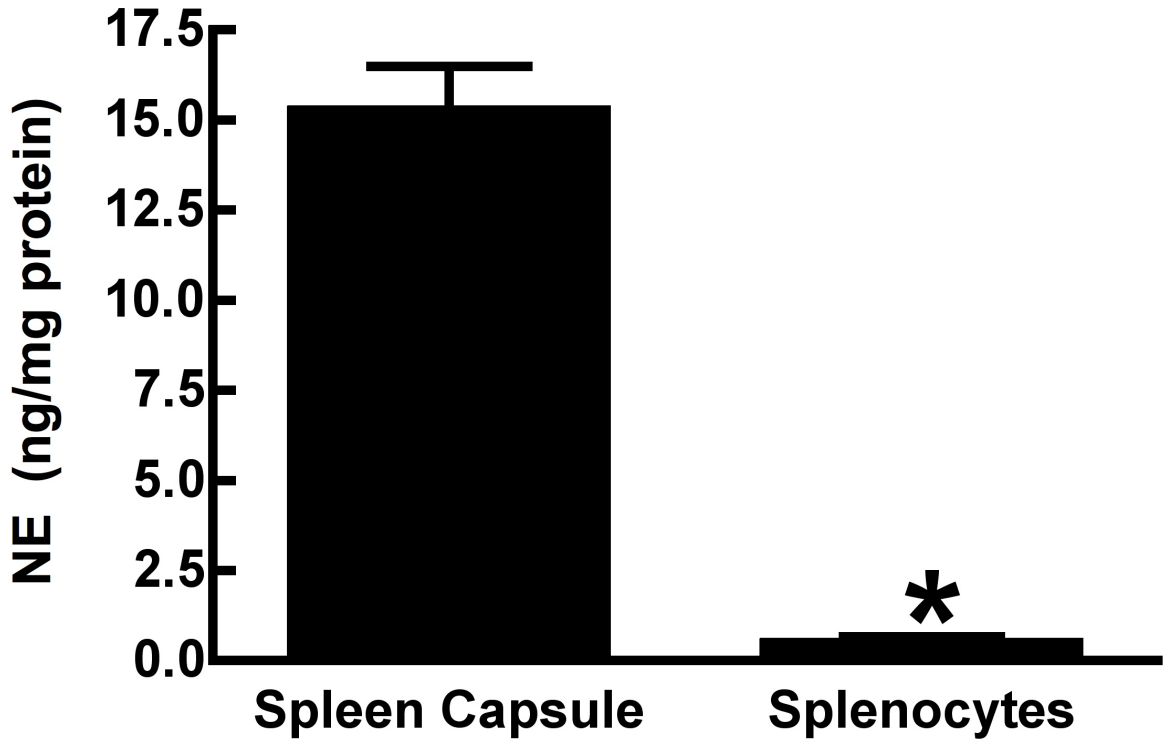


**Figure 3.3. Neurochemical analysis of NE in the murine spleen.** Freshly removed mouse spleens were disrupted to separate the spleen capsule from the splenocytes. The resulting samples were then prepared and analyzed via HPLC-ED for the amount of NE, which was normalized to the amount of protein per sample as determined by a BCA assay. Columns represent the mean concentration of NE + one SEM (n=7-8). * Differs from Spleen Capsule ($p<0.05$).

3.3.2: Noradrenergic neurochemical activity in the PVN and spleen of mice

Neurochemical analysis of noradrenergic axon terminals in the PVN and spleen capsule reveals a number of significant differences. First, there is a large difference in the concentration of NE, with the PVN having a significantly higher NE concentration than the spleen capsule (**Figure 3.4**). However, the total amount of NE in the spleen capsule is much greater (**Figure 3.5**). These findings are consistent with what was observed with TH immunostaining showing a higher density of TH fibers in the PVN versus the spleen. The relative proportion of axon terminals in relation to the size of the PVN appears to be much greater than the spleen capsule, but the spleen capsule is much larger than the PVN. Therefore, it is not surprising that the PVN has a higher concentration of NE, but less overall NE content than the spleen capsule.

The two major metabolites of NE, VMA and MHPG, were also measured in the PVN and spleen capsule. Commensurate with higher concentrations of NE in the PVN, the concentration of MHPG is higher in the PVN as compared with the spleen capsule (**Figure 3.6**). This difference is likely due to the relatively small size of the PVN compared to the spleen capsule, but may also be reflective of a higher metabolic rate in the PVN compared to the spleen capsule. The ratio of MHPG to NE can be used as an indirect index of the rate of NE release, re-uptake and metabolism (Lookingland et al., 1991). Successive processing of NE by MAO, COMT, and AR produces MHPG, which is considered to be the major metabolite of NE in the brain (Lookingland et al., 1991; Hayley et al., 2001; Eisenhofer et al., 2004). In the brain this metabolism takes place in both the neuron and glia cells, whereas in the spleen this conversion takes place in

neurons and macrophages (Karhunen et al., 1994; Eisenhofer et al., 2004; Myöhänen et al., 2010). The MHPG/NE ratio is higher in the PVN (**Figure 3.7**). These data, calculated using the content of each neurochemical, suggest that the PVN has a higher rate of metabolic activity.

NE is converted to MHPG locally and can then be further metabolized to VMA by AD and ALD (Eisenhofer, Kopin et al. 2004). In the periphery this occurs largely in the liver and VMA is considered the major end metabolite of NE outside the brain (Oh-hashi et al., 2001; Eisenhofer et al., 2004; Siraskar et al., 2011). Similar to MPHG, the concentration of VMA was observed to be higher in the PVN (**Figure 3.8**). However, the VMA/NE ratio was equivalent between the PVN and spleen capsule (**Figure 3.9**). These data suggests that the differences in VMA concentrations may be due largely to size difference, rather than increased metabolic activity. But since VMA is largely generated in non-neuronal cells it may not be a truly accurate indicator of neuronal metabolic activity.

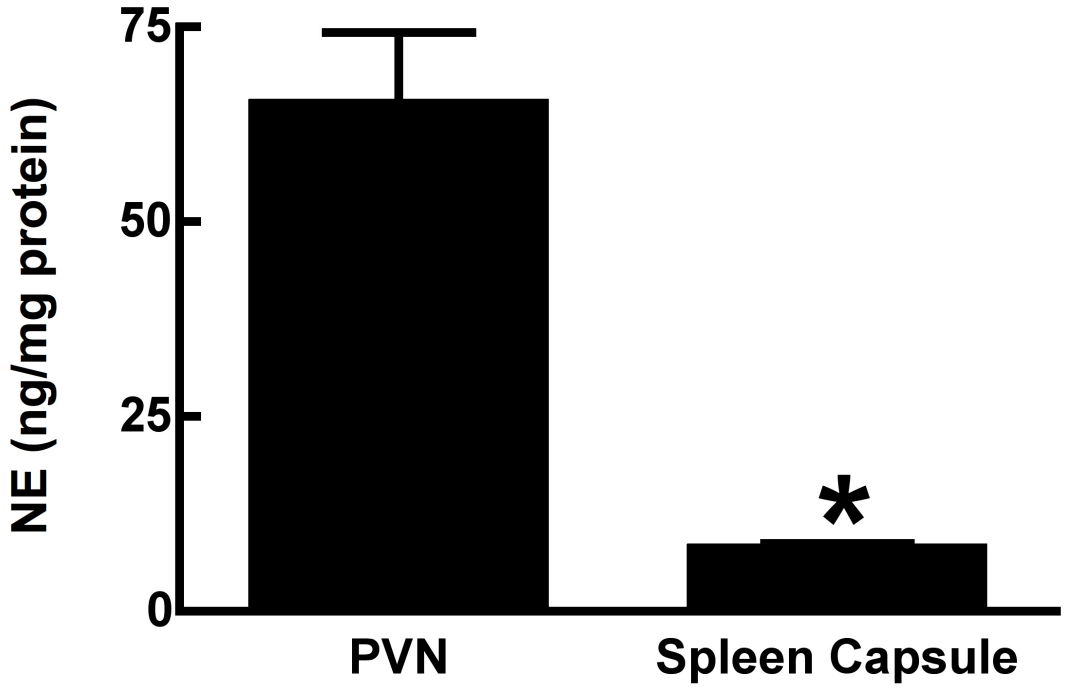


**Figure 3.4. Comparison of NE concentrations in the murine PVN and spleen capsule.** Immediately following sacrifice by decapitation, the spleens and brains of mice were rapidly removed and frozen on dry ice. The spleen capsule was isolated and brains were sliced at 500 μM and the PVN microdissected. The resulting PVN and spleen capsule samples were then prepared and analyzed via HPLC-ED for the amount of NE which was normalized to the amount of protein per sample as determined by a BCA assay. Columns represent the mean concentration of NE + one SEM (n=7). * Differs from PVN ($p<0.05$).

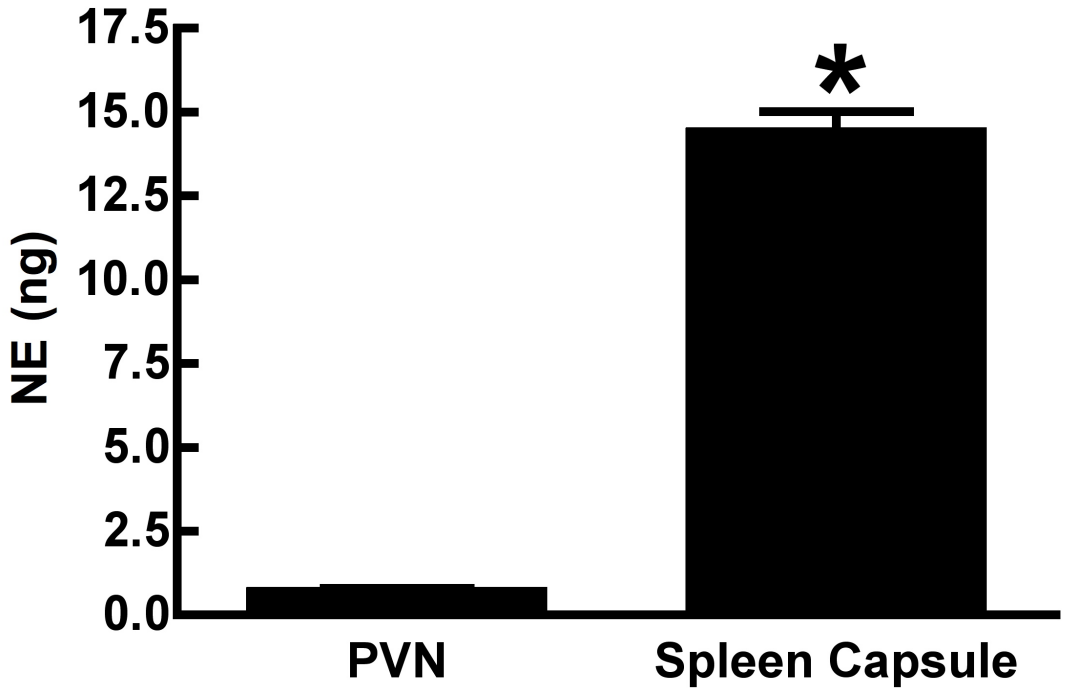


**Figure 3.5. Comparison of NE content in the murine PVN and spleen capsule.** Immediately following sacrifice by decapitation, the spleens and brains of mice were rapidly removed and frozen on dry ice. The spleen capsule was isolated and brains were sliced at 500 μM and the PVN microdissected. The resulting PVN and spleen capsule samples were then prepared and analyzed via HPLC-ED for the amount of NE. Columns represent the mean amount of NE per sample + one SEM (n=7). * Differs from PVN ($p<0.05$).

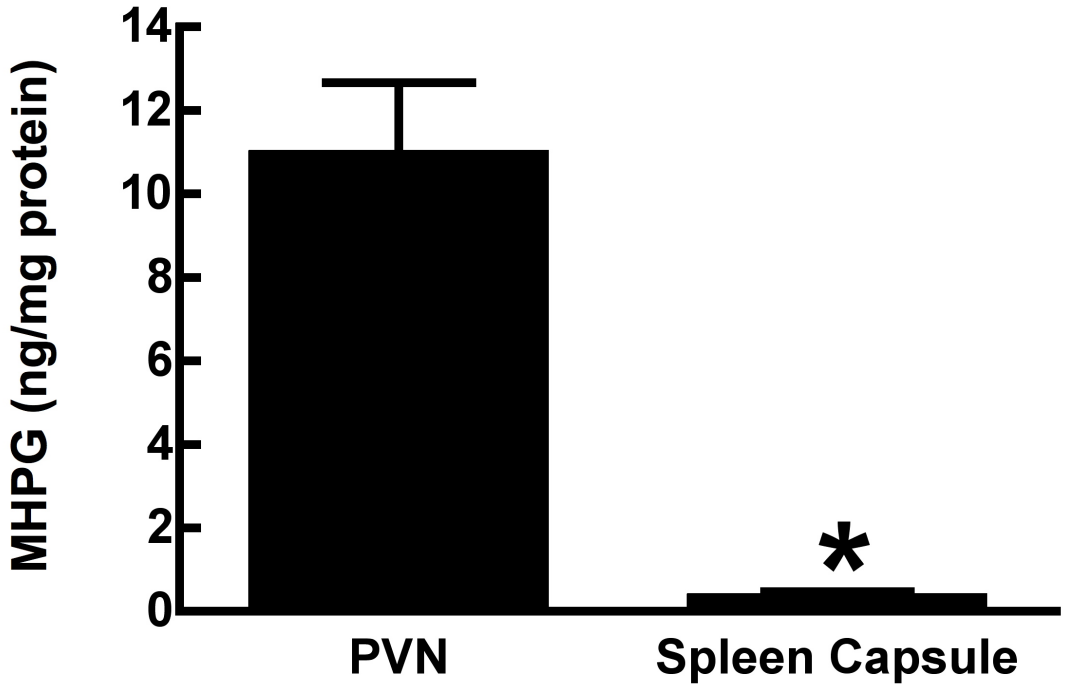


**Figure 3.6. Comparison of MHPG concentrations in the murine PVN and spleen capsule.** Immediately following sacrifice by decapitation, the spleens and brains of mice were rapidly removed and frozen on dry ice. The spleen capsule was isolated and brains were sliced at 500 μM and the PVN microdissected. The resulting PVN and spleen capsule samples were then prepared and analyzed via HPLC-ED for the amount of MHPG which was normalized to the amount of protein per sample as determined by a BCA assay. Columns represent the mean concentration of MHPG + one SEM (n=4-7). * Differs from PVN ($p<0.05$).

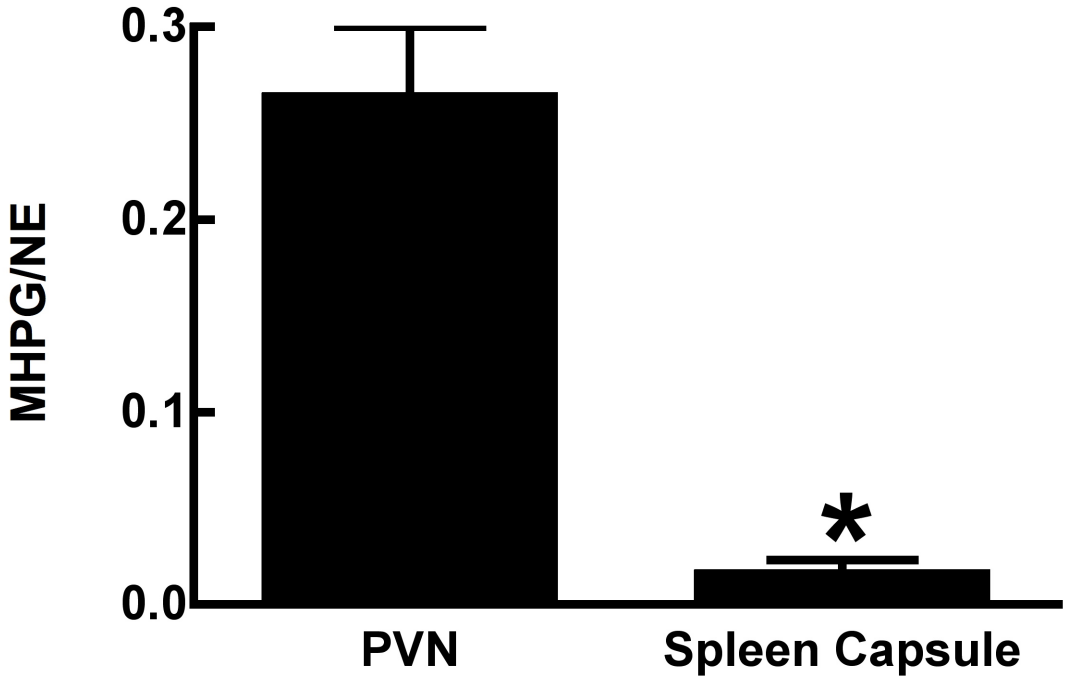


**Figure 3.7. The ratio of MHPG to NE in the murine PVN and spleen capsule.** Immediately following sacrifice by decapitation, the spleens and brains of mice were rapidly removed and frozen on dry ice. The spleen capsule was isolated and brains were sliced at 500 μM and the PVN microdissected. The resulting PVN and spleen capsule samples were then prepared and analyzed via HPLC-ED for the amount of MHPG and NE, which was normalized to the amount of protein per sample as determined by a BCA assay. Columns represent the mean ration of MHPG to NE + one SEM (n=4-7). * Differs from PVN ($p<0.05$).

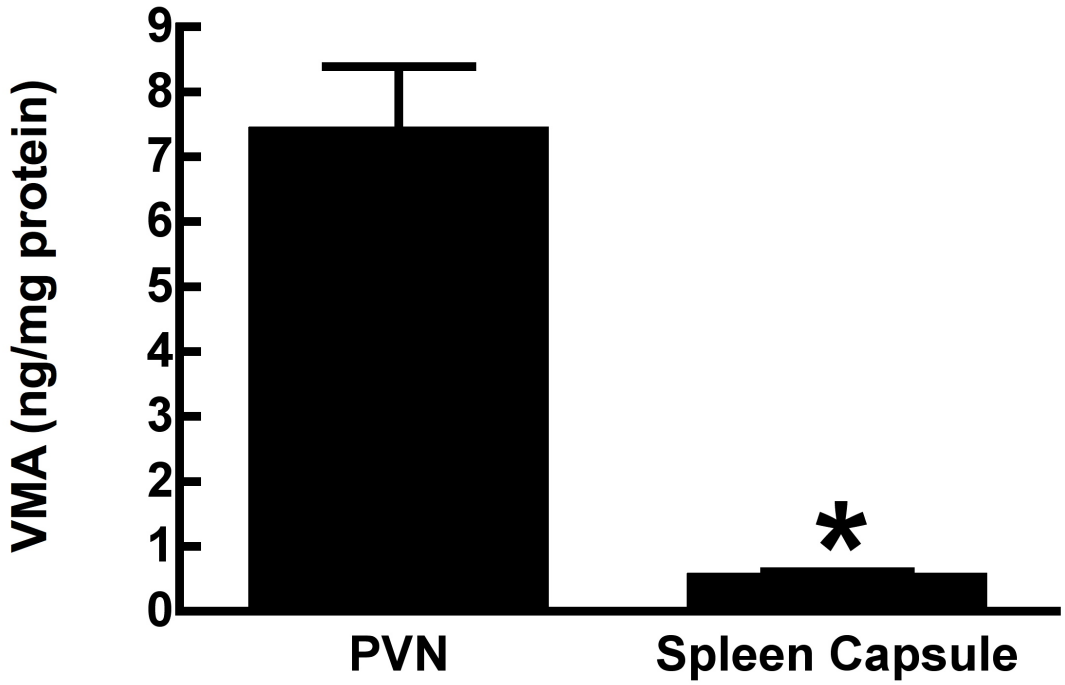


**Figure 3.8. Comparison of VMA concentrations in the murine PVN and spleen capsule.** Immediately following sacrifice by decapitation, the spleens and brains of mice were rapidly removed and frozen on dry ice. The spleen capsule was isolated and brains were sliced at 500 μM and the PVN microdissected. The resulting PVN and spleen capsule samples were then prepared and analyzed via HPLC-ED for the amount of VMA which was normalized to the amount of protein per sample as determined by a BCA assay. Columns represent the mean concentration of VMA + one SEM (n=4-7). * Differs from PVN ($p<0.05$).

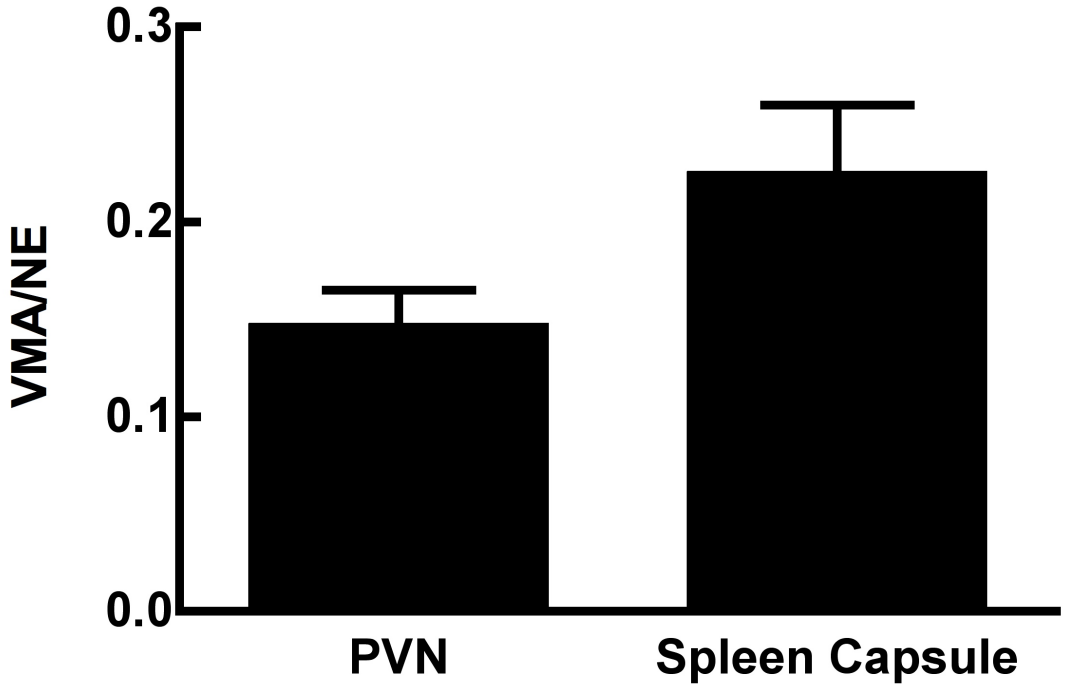


**Figure 3.9. The ratio of VMA to NE in the murine PVN and spleen capsule.** Immediately following sacrifice by decapitation, the spleens and brains of mice were rapidly removed and frozen on dry ice. The spleen capsule was isolated and brains were sliced at 500 μM and the PVN microdissected. The resulting PVN and spleen capsule samples were then prepared and analyzed via HPLC-ED for the amount of VMA and NE, which was normalized to the amount of protein per sample as determined by a BCA assay. Columns represent the mean ration of VMA to NE + one SEM (n=4-7).

The synthetic capacity of TH, the rate-limiting enzyme in NE synthesis, can be assessed utilizing an inhibitor of L-AAAD, the enzyme that catalyzes the conversion of DOPA to DA in noradrenergic axon terminals. Normally DOPA is undetectable due to its rapid conversion to DA following its synthesis (Lookingland and Moore, 2005). Therefore, during inhibition of L-AAAD the accumulation of DOPA is a way to assess the *in vivo* activity of TH. Using this methodology, it was shown that DOPA accumulation in the PVN occurs at a much higher rate than in the spleen capsule during the same time period (**Figure 3.10**). This reveals that NE synthesis in central noradrenergic axon terminals in the PVN is higher than in peripheral autonomic noradrenergic axon terminals in the spleen capsule. This data is in full agreement with the observed MPHG/NE ratio by indicating that PVN noradrenergic neurons terminating in the PVN have a higher metabolic rate than those in the spleen capsule.

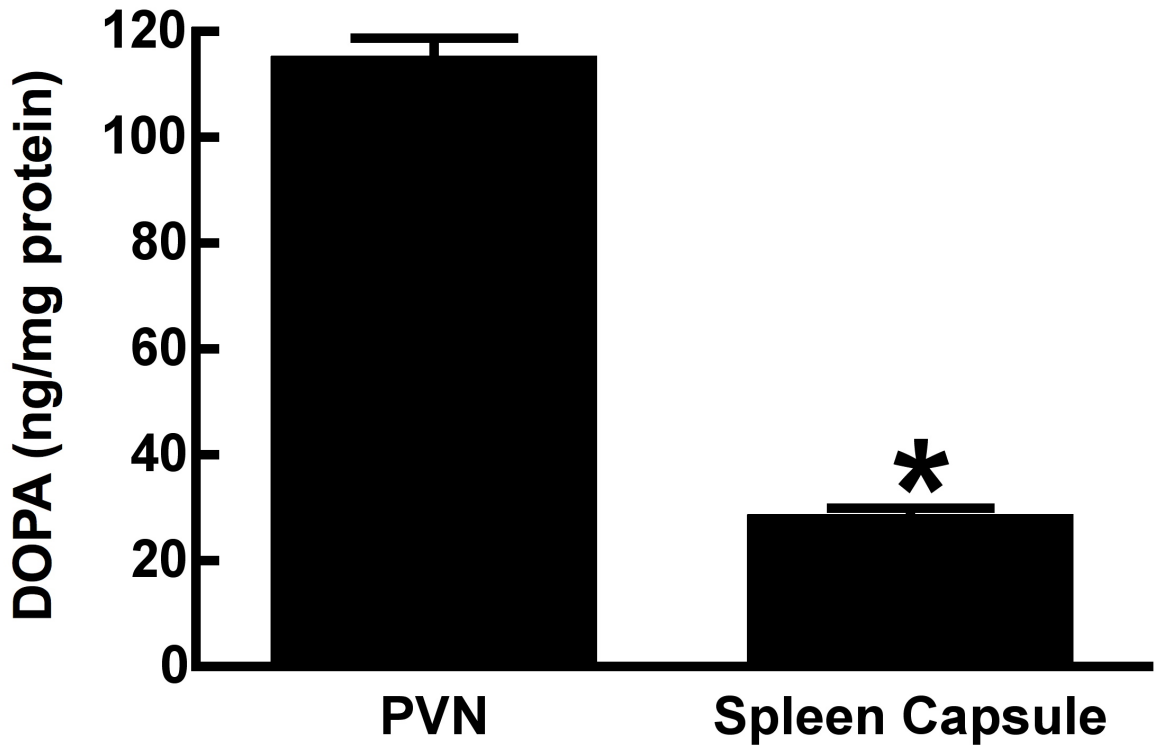


**Figure 3.10. Comparison of DOPA concentrations in the murine PVN and spleen capsule following treatment with NSD-1015.** Mice received a single i.p. injection of NSD-1015 (100 mg/kg) and sacrificed 30 min later. Freshly removed mouse spleens were disrupted to isolate the spleen capsule. In the same mice, the brain was rapidly removed and frozen on dry ice. Frozen brains were then sliced at 500 μM and the PVN microdissected. The resulting PVN and spleen capsule samples were then prepared and analyzed via HPLC-ED for the amount of DOPA which was normalized to the amount of protein per sample as determined by a BCA assay. Columns represent the mean concentration of DOPA + one SEM (n=4). * Differs from PVN ($p<0.05$).

The rate of NE utilization was also assessed in the PVN and spleen capsule, as an indirect index of NE release from axon terminals. Under normal conditions there is a tight coupling between catecholamine synthesis and release whereby newly synthesized NE is preferentially released from neurons before utilization of NE stores (Kopin et al., 1968). By blocking *de novo* synthesis of NE using an inhibitor of TH, aMT, and measuring the rate of decline of NE after a specified amount of time, the NE utilization rate, which is directly related to the release of NE, can be measured. Utilizing this methodology the rate of NE decline following aMT in the PVN was found to be much higher than the spleen under normal, quiescent conditions (**Figure 3.11**). The rate of spleen capsule NE utilization was also assessed following the administration of idazoxan, an α2AR antagonist. Antagonism of pre-junctional α2AR increases peripheral sympathetic neuron activity (Cheng et al., 2000; Khan et al., 2002; Doxey et al., 2012). In congruence, idazoxan significantly increased the rate of NE utilization in the spleen capsule (**Figure 3.12**). Increased NE utilization in the spleen capsule was accompanied by an increase in the concentration of NE in the spleen capsule (**Figure 3.12**).

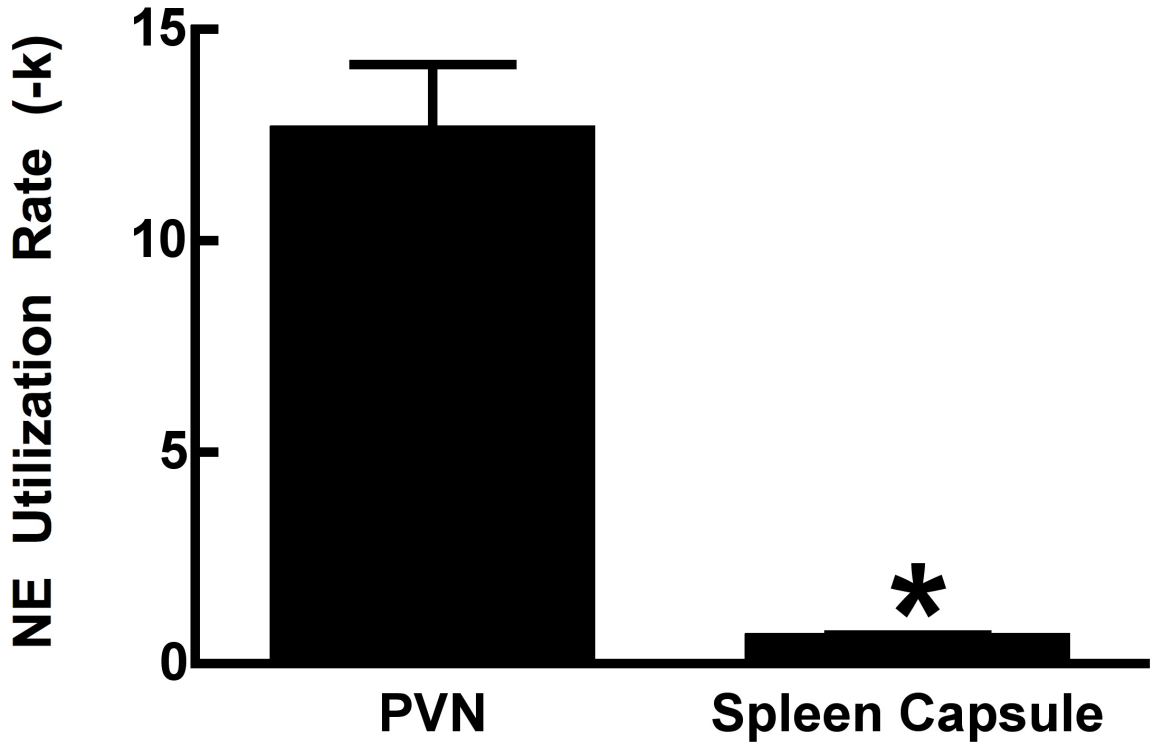


**Figure 3.11. Comparison of basal NE utilization rates in the murine PVN and spleen capsule.** Mice were injected with saline/aMT (300 mg/kg, i.p.) and sacrificed 4 h later. Freshly removed mouse spleens were disrupted to isolate the spleen capsule. In the same mice, the brain was rapidly removed and frozen on dry ice. Frozen brains were then sliced at 500 μM and the PVN microdissected. The resulting PVN and spleen capsule samples were then prepared and analyzed via HPLC-ED for the amount of NE which was normalized to the amount of protein per sample as determined by a BCA assay. Saline-treated mice were used for the 0 h time point and a linear regression analysis performed to determine the rate of NE utilization (the slope of the line generated). Columns depict the rate of NE utilization (absolute value of the slope of NE decline) + one SEM (n=14). * Differs from PVN ($p<0.05$).

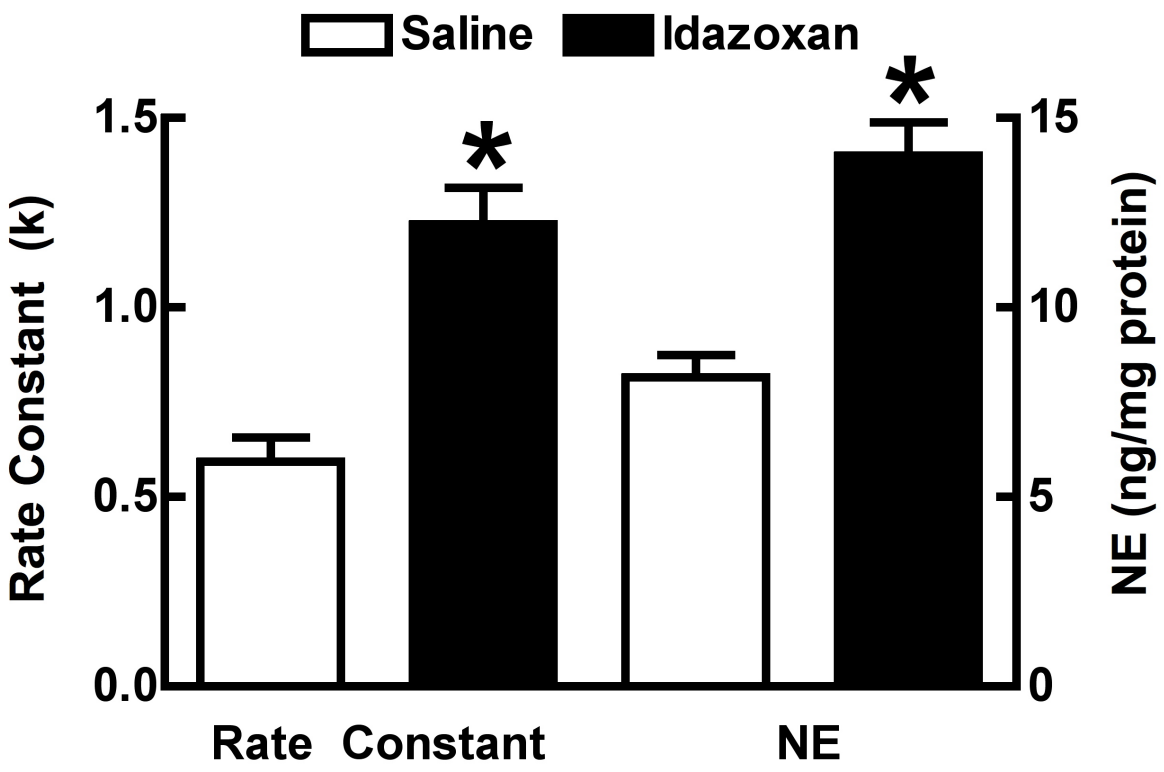


**Figure 3.12. Idazoxan increases the rate of NE utilization and NE concentrations in the murine spleen capsule.** Mice received a single injection saline/aMT (300 mg/kg, i.p.) immediately followed by saline/idazoxan (4 mg/kg, i.p.) and sacrificed 4 h later. HPLC-ED was used to determine amount of NE in the spleen capsule (A) normalized to the protein per sample. Non-aMT treated mice were used for the 0 h time point and a linear regression analysis performed to determine the rate of NE utilization (the slope of the line generated). Columns depict the rate of NE utilization or NE concentrations + one SEM (n=15-16). * Differs from saline ($p<0.05$).

## 3.4: Discussion

The data presented here demonstrate differences in noradrenergic innervation between the spleen, a peripheral organ receiving PNS sympathetic efferent axon terminals, with that of the PVN, a brain nucleus receiving CNS efferent axon terminals. Noradrenergic innervation of the PVN is heterogeneous. In agreement with other investigators, the data presented in this chapter demonstrate that only dorsal and periventricular portions of the parvocellular division receive noradrenergic innervation (Pacak et al., 1995; Chong et al., 2004). Innervation of the spleen is also heterogeneous, the targets of innervation being the spleen capsule and surrounding parenchymal arteriolar areas. While the spleen capsule contains more NE, due to it's relatively large size, the concentration of NE in the spleen capsule is less than that of the PVN. Noradrenergic activity in the spleen capsule is measurable and regulated, at least in part, by $\alpha$2AR. Interestingly, by comparison, the PVN has much a higher intrinsic rate of metabolism and activity compared to NE axon terminals in the spleen capsule.

### 3.4.1: Anatomic differences and consequences in noradrenergic innervation of the spleen and PVN

Noradrenergic terminals in the spleen and PVN can be visualized by TH immunostaining and are confirmed as being noradrenergic by a lack of finding significant amounts of either DA (see **Figures 2.2 and 2.3**) or epinephrine (data not shown) in the spleen and PVN by HPLC-ED, despite known adrenergic input to the PVN

from the C1, C2, and C3 nuclei (Cunningham et al., 1990). A major purpose of noradrenergic innervation of the spleen is to control smooth muscle contraction (Eltze, 1996). Thus, it is not surprising to find noradrenergic nerve terminals localized to the spleen capsule. The spleen capsule contains smooth muscle and contracts in response to a number of stimuli (Eltze, 1996; Cesta, 2006). It is also not surprising to find noradrenergic nerve terminals near arterioles in the spleen, as it is presumed that sympathetic innervation of these vessels is able to regulate blood flow through the spleen (Groom et al., 1991; Su et al., 1991).

The PALS is a spleen specific tissue surrounding incoming arterioles as they enter the spleen composed largely of lymphocytes, T and B cells (Cesta, 2006). Finding noradrenergic nerve terminals in this lymphocyte rich tissue, as well as reports of NE containing terminals in very close approximation to lymphocytes (Felten and Olschowka, 1987), supports the hypothesis that noradrenergic innervation of the spleen has a neuroimmune function. The paucity of noradrenergic nerve terminals, catecholamine synthetic machinery (TH), and NE in the remainder of the spleen parenchyma, including splenocytes, is suggestive of a major role for noradrenergic innervation in this compartment of the spleen.

Differences between the noradrenergic innervation of the spleen and PVN are reflective of differences in function. Noradrenergic innervation of the PVN has the purpose of regulating other neurons to cause down stream effects, such as participation in the activation of the HPA-axis during stress, hypoglycemia, and inflammation (Pyner, 2009). The PVN is also an upstream nucleus for sympathetic control of the spleen, with

the dorsal parvocellular region being one of the major areas in the brain labeled following retrograde tracers injection into the spleen (Cano et al., 2001). Stimulation of the PVN by glutamate injection is able to stimulate splenic sympathetic activity (Katafuchi et al., 1993). NE released in the PVN can stimulate glutamate releasing neurons in the parvocellular regions of the PVN to control sympathetic outflow (Daftary et al., 2000), thus establishing the link between NE release in the PVN and splenic sympathetic activity. Noradrenergic innervation of the spleen, on the other hand, is aimed at eliciting end-motor effects in smooth muscle and lymphocytes. Therefore, innervation distribution is localized specifically to those areas, as it is required that axon terminals end in direct opposition to the post-neuron target cell.

3.4.2: Noradrenergic neuron activity in the spleen capsule and PVN

The basal activity of noradrenergic neurons in the spleen is lower than the PVN. The differences observed between the spleen and PVN in the concentration of NE metabolites suggest NE axon terminals in the PVN are more metabolically active than those in the spleen. Differences in the concentration of these metabolites may simply be due to the size difference between the two regions. The ratio of total metabolite content to total primary catecholamine content is more suited for conclusions with regards to metabolic activity (Lookingland et al., 1991). It is interesting that the VMA/NE ratio was not different between these tissues, whereas the MHPG/NE ratio was. This difference may be due to differences in the site of NE metabolism. Briefly, NE is converted to DOPEGAL, by MAO, which diffuses out of the neuron to glia cells where is

it converted to MHPG via COMT and ADR (Lookingland et al., 1991; Eisenhofer et al., 2004).

In the spleen, MHPG is produced by MAO and ADR conversion of NE to DHPG in sympathetic neurons followed by the conversion of DHPG to MPHG in macrophages within the white pulp of the spleen by COMT (Karhunen et al., 1994; Eisenhofer et al., 2004; Myöhänen et al., 2010). MHPG is then released from the spleen into the circulation and further metabolized to VMA, by ADH and AD, in the liver (Oh-hashi et al., 2001; Eisenhofer et al., 2004; Siraskar et al., 2011). It is interesting that despite the obvious ability of VMA to be produced in the brain, as demonstrated above, MHPG is considered the major metabolite in the brain (Lookingland et al., 1991; Eisenhofer et al., 2004). However, VMA synthesis is mostly dependent upon extra-neuronal conversion of MHPG, whereas MHPG synthesis is largely dependent upon neuronal MAO activity. Therefore, MHPG is likely a better indicator of the metabolic capacity of the neurons. Thus, the large difference in the MHPG/NE ratio is more telling of a reduced metabolic rate in splenic sympathetic neurons.

In agreement with the assessment of the metabolic activity in the PVN and spleen using endogenous neurochemical concentrations, the higher accumulation of DOPA following blockade of NE synthesis with NDS-1015 suggests a faster rate of NE synthesis in axon terminals of the PVN versus the spleen capsule under basal conditions.

The rate of NE release was also indirectly assessed in the PVN and spleen. The most direct way to assess the firing activity of any set of neurons is using *in vivo*

electrophysiological techniques, such as patch-clamp and whole-cell recording (Kandel et al., 2000). While these techniques provide a great amount of detail (Katafuchi et al., 1993), they have several drawbacks. One of the most salient drawbacks is the inability to measuring the activity of two different sites in the body in the same animal (Lee et al., 1992; Helwig et al., 2008). Another significant drawback is that they are time intensive, typically only one to two specimens can be assessed in a single day. Lastly, the endpoint of electrophysiological studies is the neuronal activity itself, leaving out the possibility to measure physiologic endpoints related to the activity of the released neurotransmitters, especially with single-cell or slice preparations.

Alternative to electrophysiological methods is the use of site-specific microdialysis to measure released neurochemicals (Chefer et al., 2009). It is more plausible to assess multiple sites within a single animal with this technique, however this would require extensive animal surgery and manipulation. Additionally, the size of available probes presents a problem relative to the size of the areas being assessed. This is particularly true with reference to the dorsal parvocellular portion of the PVN, which is on the order of 100 x 50 microns in two dimensional area (**Figure 3.1**), and commercially available dialysis probes, on the order of 200+ microns in diameter (Olive et al., 2000; Ortega et al., 2012; CMA Microdialysis).

In this work, pharmacologic techniques were utilized to estimate the rate of neuronal activity. The activity rate of neurons in the PVN and spleen were measured using aMT, an inhibitor of tyrosine hydroxylase that prevents *de novo* NE synthesis (Brodie et al., 1966). Using this drug, and comparing treated mice with non-treated

mice after a set time period, the rate of NE utilization can be assessed. This technique has several advantages to those just mentioned. First, it easy to assess rates of neuronal NE utilization in multiple tissues within each animal. Second, many animals can be treated and assessed simultaneously. Lastly, the rate of NE utilization, indicated by the rate constant, is generated by comparing values within the same site of sampling, which leaves tissue endpoints in the rest of the body intact. This also allows for more valid comparison between areas with differences in size and innervation density, such as PVN and spleen.

Using this method, the rate of noradrenergic activity in the PVN was found to be much faster than that of the spleen. Further, it also demonstrated that increases in activity in the spleen could be induced and measured using the drug Idazoxan, an α2AR antagonist. Much like D2-dopamine receptors, α2AR act on presynaptic neuronal terminals to inhibit the synthesis and release of neurotransmitters (Khan et al., 2002). Therefore, antagonism of this receptor was expected to increase the synthesis and release of NE, measured as an increase in the rate constant of NE utilization.

Interestingly, the concentration of NE in the spleen capsule significantly increased in conjunction with increased neuronal activity. Normally, the coupling of NE synthesis and release maintains a steady-state amount of stored NE in the axon terminal. However, it appears that in splenic noradrenergic neurons the synthetic capacity of these neurons out-paces the release of NE leading to accumulation during activation. Activity dependent increases in the activity of TH is a known phenomenon in catecholaminergic neurons (Kumer and Vrana, 1996). These changes occur in

response to phosphorylation-induced increases in the catalytic-activity of TH (Kumer and Vrana, 1996). Thus, if the synthetic capacity of TH increases non-proportionally to increases in the rate of NE release this will lead to an accumulation of NE in the spleen capsule. This hypothesis needs further validation, but if true may provide an easily measured, albeit indirect, index of splenic noradrenergic activity.

### 3.4.3: Conclusion

The purpose of this chapter is aimed at understanding the noradrenergic innervation of the spleen as compared to a well-known CNS noradrenergic innervated nucleus. A number of important differences were observed between the PVN and spleen, including differences in the pattern of innervation, density of innervation, and rate of activity. The data presented here provide a comprehensive understanding of noradrenergic innervation of the spleen as compared to the PVN. PVN innervation by noradrenergic neurons is heterogeneous and site specific, indicating specific functional roles for NE in this nucleus. These observations in the PVN are paralleled in the spleen by finding NE containing terminals almost exclusively reside in the capsule and periarteriolar regions, indicating site-specific functions of these neurons, as well. This focuses further investigation to the impact of NE on the function carried out in these specific regions of the spleen. In addition, reliable methods of measuring splenic noradrenergic neuronal activity, such as aMT methodology, were identified and will be essential in ongoing pursuits to investigate the role of these neurons in the various aspects of spleen function.

# REFERENCES

# REFERENCES


Brodie BB, Costa E, Dlabac A, Neff NH, Smookler HH. Application of steady state kinetics to the estimation of synthesis rate and turnover time of tissue catecholamines. J Pharmacol Exp Ther. 1966 Dec;154(3):493–8.

Byrum CE, Guyenet PG. Afferent and efferent connections of the A5 noradrenergic cell group in the rat. J Comp Neurol. 1987 Jul 22;261(4):529–42.

Cano G, Sved AF, Rinaman L, Rabin BS, Card JP. Characterization of the central nervous system innervation of the rat spleen using viral transneuronal tracing. J Comp Neurol. 2001 Oct 8;439(1):1–18.

Cesta M. Normal Structure, Function, and Histology of the Spleen. Toxicol Pathol. 2006;34(5):455–65.

Chefer VI, Thompson AC, Zapata A, Shippenberg TS. Overview of brain microdialysis. Curr Protoc Neurosci. 2009 Apr;Chapter 7:Unit7.1. PMCID: PMC2953244

Cheng Y, Planta F, Ladure P, Julien C, Barres C. Acute cardiovascular effects of the alpha2-adrenoceptor antagonist, idazoxan, in rats: influence of the basal sympathetic tone. Journal of Cardiovascular Pharmacology. 2000 Jan;35(1):156–63.

Chong W, Li LH, Lee K, Lee MH, Park JB, Ryu PD. Subtypes of alpha1- and alpha2-adrenoceptors mediating noradrenergic modulation of spontaneous inhibitory postsynaptic currents in the hypothalamic paraventricular nucleus. J. Neuroendocrinol. 2004 May;16(5):450–7.

CMA Microdialysis. Microdialysis Probes [Internet]. CMA Microdialysis AB. [cited 2013 Dec 18]. Retrieved from: http://www.microdialysis.com/probe_brochure.pdf?cms_fileid=2772532331977349a4a942f6d40fafca

Cunningham ET, Bohn MC, Sawchenko PE. Organization of adrenergic inputs to the paraventricular and supraoptic nuclei of the hypothalamus in the rat. J Comp Neurol. 1990 Feb 22;292(4):651–67.

Cunningham ET, Sawchenko PE. Anatomical specificity of noradrenergic inputs to the paraventricular and supraoptic nuclei of the rat hypothalamus. J Comp Neurol. 1988 Aug 1;274(1):60–76.

Daftary SS, Boudaba C, Tasker JG. Noradrenergic regulation of parvocellular neurons in the rat hypothalamic paraventricular nucleus. Neuroscience. 2000 Mar;96(4):743–51.

Doxey JC, Roach AG, Smith CFC. Studies on RX 781094: a selective, potent and specific antagonist of α2-adrenoceptors. Br J Pharmacol. 2012 Jul 19;78(3):489–505.

Eaton MJ, Lookingland KJ, Moore KE. Effects of the selective dopaminergic D2 agonist quinelorane on the activity of dopaminergic and noradrenergic neurons projecting to the diencephalon of the rat. 1994 Feb 1;268(2):645–52.

Eisenhofer G, Kopin IJ, Goldstein DS. Catecholamine metabolism: a contemporary view with implications for physiology and medicine. 2004 Sep 1;56(3):331–49.

Eltze M. Functional evidence for an alpha 1B-adrenoceptor mediating contraction of the mouse spleen. Eur J Pharmacol. 1996 Sep 12;311(2-3):187–98.

Felten DL, Ackerman KD, Wiegand SJ, Felten SY. Noradrenergic sympathetic innervation of the spleen: I. Nerve fibers associate with lymphocytes and macrophages in specific compartments of the splenic white pulp. J Neurosci Res. 1987;18(1):28–36, 118–21.

Felten SY, Olschowka J. Noradrenergic sympathetic innervation of the spleen: II. Tyrosine hydroxylase (TH)-positive nerve terminals form synapticlike contacts on lymphocytes in the splenic white pulp. J Neurosci Res. 1987;18(1):37–48.

Goldman CK, Marino L, Leibowitz SF. Postsynaptic α2-noradrenergic receptors mediate feeding induced by paraventricular nucleus injection of norepinephrine and clonidine. Eur J Pharmacol. 1985 Sep;115(1):11–9.

Groom AC, Schmidt EE, MacDonald IC. Microcirculatory pathways and blood flow in spleen: new insights from washout kinetics, corrosion casts, and quantitative intravital videomicroscopy. Scanning Microsc. 1991 Mar;5(1):159–73– discussion173–4.

Hayley S, Lacosta S, Merali Z, van Rooijen N, Anisman H. Central monoamine and plasma corticosterone changes induced by a bacterial endotoxin: sensitization and cross-sensitization effects. Eur J Neurosci. 2001 Mar;13(6):1155–65.

Helwig BG, Craig RA, Fels RJ, Blecha F, Kenney MJ. Central nervous system administration of interleukin-6 produces splenic sympathoexcitation. Autonomic Neuroscience. 2008 Aug;141(1-2):104–11.

Inoue W, Baimoukhametova DV, Füzesi T, Cusulin JIW, Koblinger K, Whelan PJ, et al. Noradrenaline is a stress-associated metaplastic signal at GABA synapses. Nat. Neurosci. 2013 May;16(5):605–12.

Itoi K, Sugimoto N. The brainstem noradrenergic systems in stress, anxiety and depression. J. Neuroendocrinol. 2010 May;22(5):355–61.

Kandel E, Schwartz J, Jessell T. Principles of neural science. 2000.

Karhunen T, Tilgmann C, Ulmanen I, Julkunen I, Panula P. Distribution of catechol-O-methyltransferase enzyme in rat tissues. J. Histochem. Cytochem. 1994 Aug;42(8):1079–90.

Katafuchi T, Ichijo T, Take S, Hori T. Hypothalamic modulation of splenic natural killer cell activity in rats. J. Physiol. (Lond.). 1993 Nov;471:209–21. PMCID: PMC1143959

Khan ZP, Ferguson CN, Jones RM. Alpha-2 and imidazoline receptor agonistsTheir pharmacology and therapeutic role. Anaesthesia. 2002 Apr 6;54(2):146–65.

Kopin IJ, Breese GR, Krauss KR, Weise VK. Selective release of newly synthesized norepinephrine from the cat spleen during sympathetic nerve stimulation. J Pharmacol Exp Ther. 1968 Jun;161(2):271–8.

Kumer SC, Vrana KE. Intricate regulation of tyrosine hydroxylase activity and gene expression. J Neurochem. 1996 Aug 1;67(2):443–62.

Lee TH, Ellinwood EH Jr., Einstein G. Intracellular recording from dopamine neurons in the substantia nigra: double labelling for identification of projection site and morphological features. Journal of Neuroscience Methods. 1992 Jul;43(2-3):119–27.

Leibowitz SF, Hor L. Endorphinergic and α-noradrenergic systems in the paraventricular nucleus: Effects on eating behavior. Peptides. 1982 May;3(3):421–8.

Levin BE. Reduced norepinephrine turnover in organs and brains of obesity-prone rats l Regulatory, Integrative and Comparative Physiology. … Journal of Physiology-Regulatory. 1995.

Lindley SE, Gunnet JW, Lookingland KJ, Moore KE. 3,4-Dihydroxyphenylacetic acid concentrations in the intermediate lobe and neural lobe of the posterior pituitary gland as an index of tuberohypophysial dopaminergic neuronal activity. Brain Res. 1990 Jan 1;506(1):133–8.

Lookingland KJ, Ireland LM, Gunnet JW, Manzanares J, Tian Y, Moore KE. 3-Methoxy-4-hydroxyphenylethyleneglycol concentrations in discrete hypothalamic nuclei reflect the activity of noradrenergic neurons. Brain Res. 1991 Sep 13;559(1):82–8.

Lookingland KJ, Moore KE. Chapter VIII Functional neuroanatomy of hypothalamic dopaminergic neuroendocrine systems. Handbook of chemical neuroanatomy. 2005.

Myöhänen TT, Schendzielorz N, Männistö PT. Distribution of catechol-O-methyltransferase (COMT) proteins and enzymatic activities in wild-type and soluble COMT deficient mice. J Neurochem. 2010 Mar 31.

Noble J, Bailey M. Quantitation of protein. Methods Enzymol. 2009;463:73–95.

Oh-hashi Y, Shindo T, Kurihara Y, Imai T, Wang Y, Morita H, et al. Elevated Sympathetic Nervous Activity in Mice Deficient in CGRP. Circ. Res. 2001 Nov 23;89(11):983–90.

Olive MF, Mehmert KK, Hodge CW. Microdialysis in the mouse nucleus accumbens: a method for detection of monoamine and amino acid neurotransmitters with simultaneous assessment of locomotor activity. Brain Res. Brain Res. Protoc. 2000 Feb;5(1):16–24.

Ortega JE, Katner J, Davis R, Wade M, Nisenbaum L, Nomikos GG, et al. Modulation of neurotransmitter release in orexin/hypocretin-2 receptor knockout mice: a microdialysis study. J Neurosci Res. 2012 Mar;90(3):588–96.

Pacak K, Palkovits M, Kopin IJ, Goldstein DS. Stress-Induced Norepinephrine Release in the Hypothalamic Paraventricular Nucleus and Pituitary-Adrenocortical and Sympathoadrenal Activity: In Vivo Microdialysis Studies. Frontiers in …. 1995.

Palkovits M. Isolated removal of hypothalamic or other brain nuclei of the rat. Brain Res. 1973 Sep 14;59:449–50.

Pyner S. Neurochemistry of the paraventricular nucleus of the hypothalamus: Implications for cardiovascular regulation. J. Chem. Neuroanat. 2009.

Samuels ER, Szabadi E. Functional neuroanatomy of the noradrenergic locus coeruleus: its roles in the regulation of arousal and autonomic function part I: principles of functional organisation. Curr Neuropharmacol. 2008 Sep;6(3):235–53. PMCID: PMC2687936

Sawchenko PE, Swanson LW. Immunohistochemical identification of neurons in the paraventricular nucleus of the hypothalamus that project to the medulla or to the spinal cord in the rat. J Comp Neurol. 1982 Mar 1;205(3):260–72.

Schramm LP, Strack AM, Platt KB, Loewy AD. Peripheral and central pathways regulating the kidney: a study using pseudorabies virus. Brain Res. 1993 Jul 9;616(1-2):251–62.

Siraskar B, Völkl J, Ahmed MSE, Hierlmeier M, Gu S, Schmid E, et al. Enhanced catecholamine release in mice expressing PKB/SGK-resistant GSK3. Pflugers Arch. 2011 Dec;462(6):811–9.

Strack AM, Sawyer WB, Hughes JH, Platt KB, Loewy AD. A general pattern of CNS innervation of the sympathetic outflow demonstrated by transneuronal pseudorabies viral infections. Brain Res. 1989 Jul 3;491(1):156–62.

Su CY, Tsai AI, Liu HP, Chen LT, Chien S. Ultrastructural studies on splenic microcirculation of the rat. Chin J Physiol. 1991;34(2):223–34.

Sved AF, Cano G, Card JP. Neuroanatomical specificity of the circuits controlling sympathetic outflow to different targets. Clin Exp Pharmacol Physiol. 2001;28(1-2):115–9.

# Chapter 4: The Contribution of Norepinephrine to Humoral Immune Responses in the Spleen

## 4.1: Introduction

The immune system produces highly complex, multi-cellular, coordinated responses that act to protect organisms from harmful infectious diseases and cancer. The presence of foreign particles, pathogens, or tumor cells illicit distinct actions with their own particular set of cells and signaling molecules. In general there are two broad divisions of the immune system: innate and adaptive.

The innate immune response is an intrinsic system that is ever present and provides an early and rapid defense against microbes (Oikonomopoulou et al., 2001; Quah and Parish, 2001). The innate immune system does not confer long-term immunity to a pathogen, but can facilitate adaptive immune system responses (Meager and Wadhwa, 2001).

The adaptive immune system is activated when an antigen is recognized by epitope specific receptors on B cells and T cells (P Kane, 2001). BCRs recognize a vast array of antigens such as proteins, polysaccharides, lipids, nucleic acids, and soluble antigens including small chemicals, whereas TCRs only recognize peptide fragments presented by host cells in the MHC (Ferrero et al., 2001; Saha, 2001; Kurosaki and Hikida). The activation of these receptors results in highly specific responses centered around the recognition of specific epitopes on the inciting antigen.

T cells implement cell-mediated adaptive immune responses. $CD8^+$ cells, or cytotoxic T cells, aid in the removal of cells infected with intracellular pathogens, such as viruses and intracellular bacteria (Gotch, 2001; Nath, 2001). $CD4^+$ T cells, or $T_H$ cells, aid in the removal of extra-cellular pathogens by macrophages (Ademokun and Dunn-Walters, 2001; Ferrero et al., 2001). Important $T_H$ cell subtypes include the $T_H1$ subtype, (involved in the stimulation of macrophages to more effectively phagocytize and lyse bacteria), the $T_H2$ subtype (involved in the immune response against helminthes and parasites), and follicular $T_H$ cells (antigen experienced $T_H$ cells that reside within B-cell follicles of secondary lymphoid organs and assist in the production of antibodies) (Ferrero et al., 2001; Fazilleau et al., 2009).

T cells also participate in humoral immune responses. Many $T_H$ subtypes assist B cells to produce antibodies (Ademokun and Dunn-Walters, 2001; Ferrero et al., 2001). Once activated by exposure to an extracellular antigen, $T_H$ cells express CD154 on their cell surface and release cytokines (i.e. interferon-γ, IL-2, and IL-4) in response to interaction with CD40 expressing B cells recognizing the same antigen (Ademokun and Dunn-Walters, 2001; Néron et al., 2011). Antigen specific interaction between B cells and $T_H$ cells, including CD40-CD154 interaction and cytokine stimulation, induce B cells to produce antibodies directed against the commonly recognized antigen (Néron et al., 2011).

The isotype of antibody, determined by the constant portion of the heavy chain, plays a major role in determining the function of the antibody. This portion is the site recognized by receptors throughout the body, such as by $F_c$ receptors on macrophages or by complement (Daëron, 1997; Kenter, 2005; Stavnezer et al., 2008). IgM is the first type of antibody produced in response to a novel antigen (Ademokun and Dunn-Walters, 2001; Czajkowsky and Shao, 2009). Additionally, low specificity IgM, 'natural antibodies', are constitutively produced in the spleen and bone marrow as a form of innate-type immunity (Czajkowsky and Shao, 2009; Baumgarth, 2013). The effector mechanism of IgM is through complement activation (Czajkowsky and Shao, 2009; Baumgarth, 2013).

Over the course of an immune response the isotype of antibody changes from IgM to IgG (Ademokun and Dunn-Walters, 2001; Schroeder and Cavacini, 2010). IgG is a monomeric Ig with a high specificity, but relatively low capacity and is the predominant antibody type produced several days (3-4) following an initial immune exposure and during repeated exposure to the same antigen (Ademokun and Dunn-Walters, 2001; Schroeder and Cavacini, 2010). Effector mechanisms of IgG include complement activation, neutralization of toxins, and facilitation of phagocytosis (Daëron, 1997; Schroeder and Cavacini, 2010).

Certain types of antigens stimulate a humoral response, but do not require T cells. These T cell independent antigens stimulate B cells to produce antibodies by replacing the secondary stimulation provided by $T_H$ cells (Ademokun and Dunn-Walters, 2001). These secondary signals come from either cross linking of BCRs or stimulation of TLR

that recognize specific pathogen associated molecules. A prime example of this type of antigen is bacterial LPS (Moller, 2001; Lanzavecchia and Sallusto, 2007; Bekeredjian-Ding and Jego, 2009). Upon release, LPS can be recognized by TLR4 receptors on the surface of B cells (Moller, 2001; Lanzavecchia and Sallusto, 2007; Bekeredjian-Ding and Jego, 2009). In addition, because of its large size and repeating subunits, LPS is simultaneously recognized by many BCRs on the same lymphocyte (Moller, 2001; Lanzavecchia and Sallusto, 2007; Bekeredjian-Ding and Jego, 2009). The combination of these features serve to stimulate B cell antibody production in the absence of $T_H$ cell involvement (Moller, 2001).

Interactions between the immune and nervous systems are coordinated within the spleen. Sympathetic post-ganglionic axon terminal NE activity increases in the spleen following the injection of soluble protein antigens (Kohm et al., 2000; Sanders, 2012). These neurons have synaptic-like terminations in very close proximity (less than 8 microns) to immune cells in the spleen (Felten and Olschowka, 1987). Sympathetic axon terminals, visualized by immunostaining for the rate-limiting enzyme tyrosine hydroxylase (TH), are found in the PALS, which is composed of T cells, B cells, and macrophages (Felten et al., 1987; Felten and Olschowka, 1987; Cesta, 2006). This distribution is confirmed in **Chapter 3** by demonstrating that NE and TH exist in high concentrations within the splenic capsule, but are almost absent in splenocyte preparations. Splenic B cells express functional β2AR and respond to NE both *in vitro* and *in vivo* (Nance and Sanders, 2007; Sanders, 2012). Engagement of NE with β2AR on B cells within 24 h of an antigen exposure increases the amount of secreted

antibodies in response to a humoral immune challenge (Sanders, 2012). This effect is mediated by regulating the transcriptional activity of the 3'-IgH (Stevens et al., 2000; Pinaud et al., 2001; Vincent-Fabert et al., 2010). Activation of β2AR on B cells, through a protein-kinase A dependent mechanism, up-regulates 3'-IgH transcription leading to increased antibody production (Podojil et al., 2004). Interestingly, only exposure to NE at early time points (<24 h) following antigen exposure increases B cell antibody production (Kohm and Sanders, 2000; 2001).

The close proximity of sympathetic neurons to immune cells in the spleen along with the research showing NE can increase antibody production has led to the hypothesis that splenic sympathetic neurons are a source of immunomodulatory NE. Extended, it is believed that sympathetic nervous system activation during immune responses causes the release of NE from axon terminals in the spleen, which acts upon B cells expressing β2AR resulting in enhanced antibody production. The purpose of the research described in this chapter is to test this hypothesis. First, the correlation between splenic sympathetic noradrenergic neuronal activity and humoral immunity will be established. The expression of β2AR on splenic B cells will then be confirmed, thereby providing a mechanism by which these lymphocytes can sense NE. Finally, the effect of NE and β2AR stimulation will be tested with specific regards to the humoral immune response of splenic B cells.

## 4.2: Materials and Methods

### 4.2.1: Mice

C57BL/6 WT female mice (NCI/Charles River, Portage, MI) obtained from were used in all experiment unless otherwise indicated. All animals were housed two to five per cage and maintained in a sterile, temperature (22 ± 1 °C) and light controlled (12L:12D) room, and provided with irradiated food and bottled tap water *ad libitum*. All experiments used the minimal number of animals required for statistical analyses, minimized suffering, and followed the guidelines of the National Institutes of Health Guide for the Care and Use of Laboratory Animals. The Michigan State Institutional Animal Care and Use Committee approved all drug administrations and methods of euthanasia (AUF# 03/12-060-00).

### 4.2.2: Materials

aMT: aMT ester (Sigma, St. Louis, MO) was dissolved in 0.9% isotonic saline to a final concentration of 30 mg/ml and administered at dose of 300 mg/kg.

Butoxamine: Butoxamine (B1385, Sigma) was dissolved in sterile isotonic saline at a concentration of 5 mg/ml and administered at doses ranging from 1-10 mg/kg (i.p.).

HBSS: 10x HBSS powder (Gibco) was diluted with ultra-pure $H_2O$ (NaCl 138 mM, KCl 5.3 mM, $Na_2HPO_4$ 0.3 mM, $NaHCO_3$ 4.2 mM, $KH_2PO_4$ 0.4 mM, and glucose 5.6 mM), autoclaved, and stored at $4^{\circ}$ C.

Isotonic Saline: one L of 0.9% saline was prepared using ultra-pure $H_2O$ and 9 grams of NaCl. The solution was autoclaved and kept closed at room temperature.

LPS: LPS (*E. coli* 055:B5 catalog L2880, lot 066K4096, 5 EU/ng (Limulus lysate assay) and 10 EU/ng (chromogenic assay), Sigma, St. Louis, MO) was dissolved in RPMI-1640 at used at a final concentration of 10 µg/ml for *in vitro* studies. For *in vivo* experiments, LPS was dissolved in HBSS to a concentration of 50 µg/ml and injected at 25 µg per mouse (i.p.).

PBS: NaCl 137 mM, KCl 2.7 mM, $Na_2HPO_4$ 10 mM, and $KH_2PO_4$ 1.8 mM in ultra-pure $H_2O$.

sRBC: An aliquot of sRBC was placed in a 50-ml conical tube. 25 ml of HBSS was added to the sRBC and centrifuged at 300 RCF for 5 min. The supernatant was removed from the concentrated sRBC pellet. This process was performed 3 additional times. sRBC were then counted and adjusted to $2 \times 10^9$ cells/ml in HBSS. In experiments using sRBC, mice received $1 \times 10^9$ cells via a single i.p. injection.

4.2.3: Isolation of the Spleen Capsule and Splenocytes

After euthanasia spleens were removed by an incision in the left lateral abdomen under sterile conditions, which entails spraying the area of removal with 70% ethanol and using ethanol cleaned scissors and forceps to cut through the skin, and underlying muscle and connective tissue. The spleen was placed in a 6-well plate and mechanically crushed with the blunt end of a 10 ml syringe in 2 ml of HBSS to separate the spleen capsule (insoluble tissue) from the splenocytes (contained in the disruption supernatant). The spleen capsule was removed from the supernatant using forceps and taken whole or divided into two parts using ethanol-cleaned scissors depending on the needs of the experiment Splenocytes were separated from the disruption supernatant by centrifugation at 300 RCF for 5 min and the supernatant was decanted. The separated splenocytes were then re-suspended in differing buffers and taken whole or divided into two parts depending on the needs of the experiment.

4.2.4: Preparation and Culture of Splenocytes

Two mice were killed by decapitation and their spleens removed aseptically via a single ethanol incision in the left flank, which was wetted with 70% ethanol, using ethanol-cleaned scissors. Single-cell suspensions were prepared by disrupting the spleen capsule with the blunt end of a sterile disposable 5-ml syringe in a 6-well plate in ~2 ml of RPMI-1640 media. The isolated splenocytes were then cultured in RPMI-1640 media supplemented with BCS (percentage of BCS dependent on length of culture and assay; Hyclone, Logan, UT, USA), 100 units penicillin/ml (Gibco), 100 µg

streptomycin/ml (Gibco), and 50 µM 2-ME (Gibco). Splenocytes were cultured in a humidified atmosphere at 37$^{o}$C and 5% $CO_2$.

4.2.5: Neurochemistry

All samples were placed in ice-cold tissue buffer following isolation or dissection and kept frozen at -80°C until analysis. Samples were thawed on the day of analysis and sonicated with 3 one-sec bursts (Sonicator Cell Disruptor, Heat Systems-Ultrasonic, Plainview, NY, USA) and centrifuged at 18,000 RCF for 5 min in a Beckman-Coulter Microfuge 22R centrifuge. The supernatant from the first centrifugation of the spleen capsule was removed and spun again at 18,000 RCF for 5 min in a Beckman-Coulter Microfuge 22R centrifuge before being brought up to 100 µl (q.s.) with fresh cold tissue buffer. Spleen samples were then filtered using a 0.2 µM syringe driven Millex-LG filter (Millipore, Billerica, MA).

All samples were analyzed for NE, MHPG, VMA, and/or DOPA content using HPLC-ED (Lindley et al., 1990; Eaton et al., 1994) using C18 reverse phase columns (ESA Inc., Sunnyvale, CA) combined with a low pH buffered mobile phase (0.05 M Sodium Phosphate, 0.03 M Citrate, 0.1 mM EDTA at a pH of 2.65) composed of 5-15% methanol and 0.03-0.05% sodium octyl sulfate. Oxidation of monoamines was measured at a constant potential of -0.4 V by coulometric detection using a Coulochem Electrochemical Detector (Thermo Scientific). The amount of each substance in the samples was determined by comparing peak height values (as determined by a Hewlett Packard Integrator, Model 3395) with those obtained from known standards run on the

same day. Tissue pellets remaining from preparation were dissolved in 1 N NaOH and assayed for protein using the BCA method (Noble and Bailey, 2009).

4.2.6: Western Blot

All samples were placed in ice-cold lysis buffer (water containing 1% Triton-x 100, 250 mM sucrose, 50 mM NaCl, 20 mM tris-HCl, 1 mM EDTA, 1 mM PMSF protease inhibitor cocktail, 1 mM DTT) immediately following isolation and kept frozen at -80°C until analysis. On the day of analysis samples were thawed, heated for 30 min at 100° C, sonicated for 8 sec, and spun at 12,000 RCF for 5 min. The supernatant was collected and a BCA protein assay performed (Noble and Bailey, 2009). Equal amounts of protein were separated using SDS-PAGE and transferred to PVDF-FL membranes (Millipore, Billerica, MA). The resulting membranes were reacted against antibodies for TH (AB152 1:2000, Millipore, Billerica, MA), whose intensities were normalized to β-Actin (8H10D10 1:8000, Cell Signaling, Danvers, MA) to account for loading variability. Each PVDF-FL membrane contained samples representing all experimental conditions to avoid variability due to run, transfer, or antibody exposure conditions. Blots were visualized and quantified using an Odyssey Fc Infrared Imaging system (Li-Cor, Lincoln, NE) by utilization of IRDye conjugated secondary antibodies, goat anti-Mouse 800CW (1:20,000) and/or goat anti-rabbit 680LT (1:20,000).

4.2.7: Flow Cytometry

4.2.7.1: Surface antibody labeling for flow cytometry

All staining protocols were performed in 96-well round bottom plates (BD Falcon, Franklin Lakes, NJ). Splenocytes were washed 3x with HBSS by centrifugation at 1000 RCF for 5 min, the supernatant was decanted, and the cells re-suspended in HBSS. Cultured splenocytes were then incubated for 30 min on ice in the dark in a 1x solution of near IR (APY-Cy7) live/dead stain (#L10119, Invitrogen, Grand Island, NY), a step which was omitted for splenocytes obtained directly from spleens. Following a wash in HBSS (as described above), splenocytes were then washed with FACS buffer (HBSS, 1% bovine serum albumin, 0.1% sodium azide, pH 7.6) as was done with HBSS. Surface Fc receptors were then blocked with anti-mouse CD16/CD32 [0.5 mg/ml] (#553142, BD Biosciences, Franklin Lakes, NJ) at 0.5 µl/well, IgM was blocked with anti-IgM [0.5 mg/ml] (#553425, BD Biosciences) at 1 µl/well, and IgG was blocked with anti-IgG [1.3 mg/ml] (#115-006-071, Jackson Immunoresearch, West Grove, PA) at 0.5 µl/well for 15 min each at RT. Cells were stained for 30 min at RT with the following antibody clones: CD19 (clone 6D5) [0.2 mg/ml] (Biolegend, San Diego, CA) at 1.25 µl/well and β2AR [0.25 mg/ml] (#AP7263d, Abgent, San Diego, CA) at 2 µl/ well. Cells were then washed 3x with FACS buffer. A secondary antibody for β2AR, donkey anti-rabbit DyLight 649 (clone Poly4064) [0.5 mg/ml] (Biolegend), at 0.5 µl/well was incubated for 30 min at RT. Subsequently cells were washed with FACS buffer, fixed with Cytofix (BD Biosciences) for 15 min at RT, washed 3x with FACS buffer, and finally

suspended in FACS buffer for intracellular staining. Stained and fixed cells were stored in the dark at 4°C for up to 2 weeks.

4.2.7.2: Intracellular antibody labeling for flow cytometry

Within 2 weeks of surface staining (described above), cells were washed 2x with Perm/Wash (BD) and incubated with Perm/Wash for 30 min at RT. Fluorescently labeled antibodies for IgM (Clone II/41) [0.5 mg/mL] (Biolegend) were added at 1 µl/well for 30 min. Cells were washed 2x with Perm/Wash and suspended in FACS buffer. After intracellular staining, cells were analyzed the same day.

4.2.7.3: Flow Cytometry Analysis

Fluorescent staining was analyzed using a BD Biosciences FACSCanto II flow cytometer. Data were analyzed using Kaluza (Beckman Coulter Inc., Brea, CA) or FlowJo software (Tree Star Inc., Ashland, OR). Compensation and voltage settings of fluorescent parameters were performed using fluorescence-minus-one controls. Cells were gated on singlets (forward scatter height versus area) followed by determination of live cells (low APC-Cy7 signal) only in samples obtained from splenocyte culture. Cells were then gated to select lymphocytes using forward versus side scatter. For some analyses, an additional gate was created for CD19 or β2AR expression to select for B cells or β2AR expressing cells, respectively. These sequential gates were used to identify IgM producing B cells and IgM producing B cells that express β2AR. The percentage of cells gated to individual populations relative to the entire population were

collected and analyzed. Additionally, the numerical intensity of the fluorescent signal, termed the MFI, was also quantified and analyzed.

4.2.8: ELISA

Serum IgM was detected by sandwich ELISA. In preparation, 100 µl of 1 µg/ml anti-mouse IgM (Sigma-Aldrich, St. Louis, MO) was added to wells of a 96-well microtiter plate and stored at 4°C overnight. After the pre-coating step, the plate was washed twice with 0.05% Tween-20 in PBS and three times with $H_2O$. Following this, 200 µl of 3% BSA-PBS was added to the wells and incubated at RT for 1.5 h to block nonspecific binding followed by the same washing steps described above. Serum samples were diluted and added to the coated plate (100 µl) for 1.5 h at RT. After the incubation, the plate was washed again, followed by addition of 100 µl of HRP-conjugated goat anti-mouse IgM (A8786, Sigma-Aldrich). Following the HRP incubation for 1.5 h at RT, any unbound detection antibody was washed away from the plate, and 100 µl ABTS (Roche Applied Science, Indianapolis, IN) added. The detection of the HRP substrate reaction was conducted over a one h period using a plate reader with a 405-nm filter (Bio-Tek). The KC4 computer analysis program (Bio-Tek) calculated the concentration of IgM in each sample based on a standard curve generated from the absorbance readings of known concentrations of IgM (range 6-1600 pg/ml, clone TEPC 183, Sigma-Aldrich).

### 4.2.9: ELISPOT

ELISPOT was performed as described previously (Lu et al., 2009). ELISPOT wells were coated with purified anti-mouse (Sigma-Aldrich) IgM antibody and blocked with 5% BSA. Splenocytes from freshly disrupted spleens were washed, via centrifugation as described for flow cytometry, and incubated in the ELISPOT wells for 16–20 h. Biotin-conjugated anti-mouse IgM antibody (Sigma-Aldrich, St. Louis, MO) and streptavidin-horseradish peroxidase (Sigma-Aldrich, St. Louis, MO) were sequentially added to the wells. The spots were developed with the aminoethylcarbazole staining kit (Sigma-Aldrich, St. Louis, MO). Data were collected and analyzed using the CTL ImmunoSpot system (Cellular Technology Ltd, Shaker Heights, OH).

### 4.2.10: Statistical Analysis

#### 4.2.10.1: Statistical Comparisons

Prism software version 4.0a was used to make statistical comparisons between groups using the appropriate statistical test. Differences with a probability of error of less than 5% ($p<0.05$) were considered statistically significant. Two group comparisons were done using the Student's *t*-test. Two group comparisons where in one group had more than one degree or factor were done using a One-way ANOVA followed by a Bonferroni or Tukey's post-test for multiple comparisons. Experiments in which there were two groups with more than one degree or factor in each group, such as a 2x2 design, were analyzed using a Two-way ANOVA followed by Bonferroni post-test for multiple comparisons.

4.2.10.2: aMT Experimentation

In experiments in which aMT was used to assess neuronal activity, NE concentrations from aMT treated and non-aMT (saline) treated mice were used for a regression analysis with saline animals acting as the 0 time control and aMT animals a 4 h time point. The rate constant was determined using this formula: $=(Log_{10}[B]-Log_{10}[A])/(-0.434*t)$. Where B is the concentration of NE after aMT, A is the concentration of A in saline treated animals, and t is the time of aMT treatment (Brodie et al., 1966). The slopes were compared via t-test using the mean slope, SEM, and an n equal to the total number of data points used in the analysis to account for the total number of independent measurements used to generate the regression equations. Differences with a probability of error of less than 5% were considered statistically significant.

4.2.10.3: Flow Cytometry Data Handling

Population percentage data was transformed in Excel (Microsoft Corporation, Redmond, WA) to a parametric form before ANOVA analysis using the formula: =arcsin(sqrt(DATA/100)) (Ahrens et al., 1990). Raw percentage data was used for visual representations, while statistical significance indicated on these figures was performed on the transformed data.

## 4.3: Results

### 4.3.1: Characterization of humoral immune challenge models

Initial experiments sought to determine the efficacy of sRBC and LPS to induce a humoral immune response *in vivo.* While neither sRBC nor LPS significantly changed the body weight of mice 4 days after injection (**Figure 4.1**), both immunogens were able to increase the weight of the spleen and the spleen:body weight ratio (**Figures 4.2 and 4.3**). Spleens from LPS treated mice were found to be heavier than those from sRBC treated mice (**Figures 4.2 and 4.3**). The humoral immune response of lymphocytes contained within the spleen was assessed using ELISPOT specific for IgM. Injection of either immunogen significantly increased the number of splenic IgM producing lymphocytes (**Figure 4.4**). Next the ability of LPS to induce a humoral immune response *in vitro* was evaluated using splenocytes obtained from untreated mice. Addition of LPS to the culture medium for 3 days increased the number of IgM producing B cells, indicated by surface expression of CD19 ($CD19^+$) as measured by flow cytometry (**Figure 4.5A**). The significant increase in IgM producing B cells in response to LPS *in vitro* was accompanied by a decrease in the MFI of IgM suggesting an overall decrease in the amount of IgM being produced per B cell (**Figure 4.5B**). These data establish both sRBC and LPS as immunogens able to induce a humoral immune response *in vivo* (sRBC and LPS) and *in vitro* (LPS).

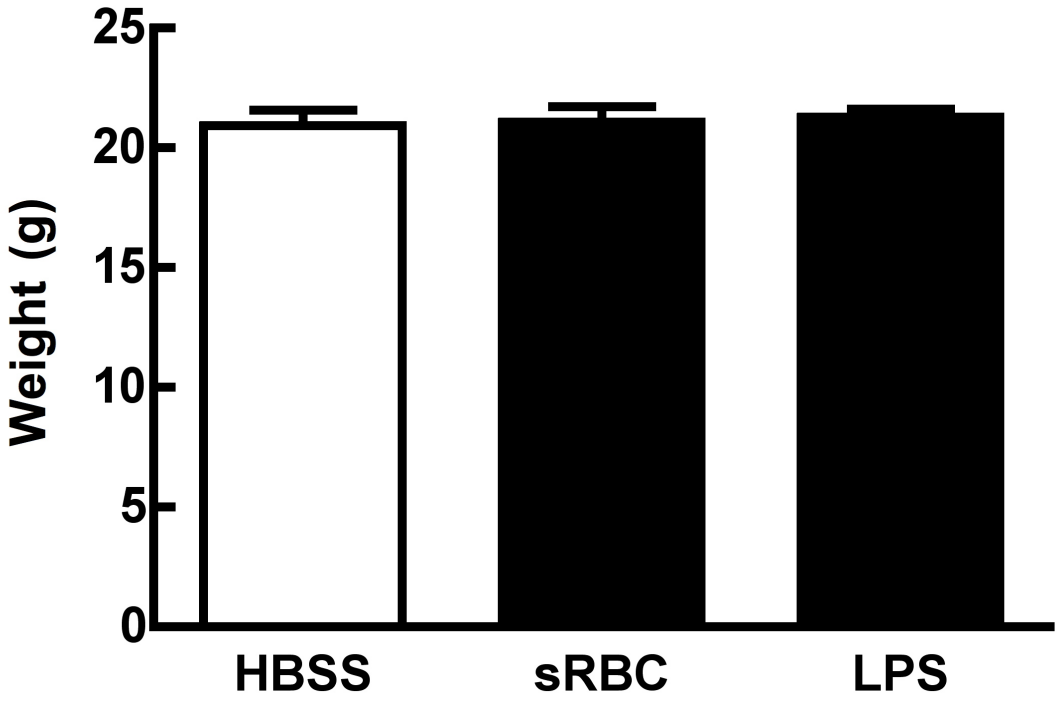


**Figure 4.1. The effect to experimental immune challenges on body weight in mice.** Female mice were injected with HBSS, sRBC ($1x10^9$ cells; i.p.), or LPS (25 μg; i.p.) and weighed 4 days later. Columns represent the average weight (g) + one SEM (n=3).

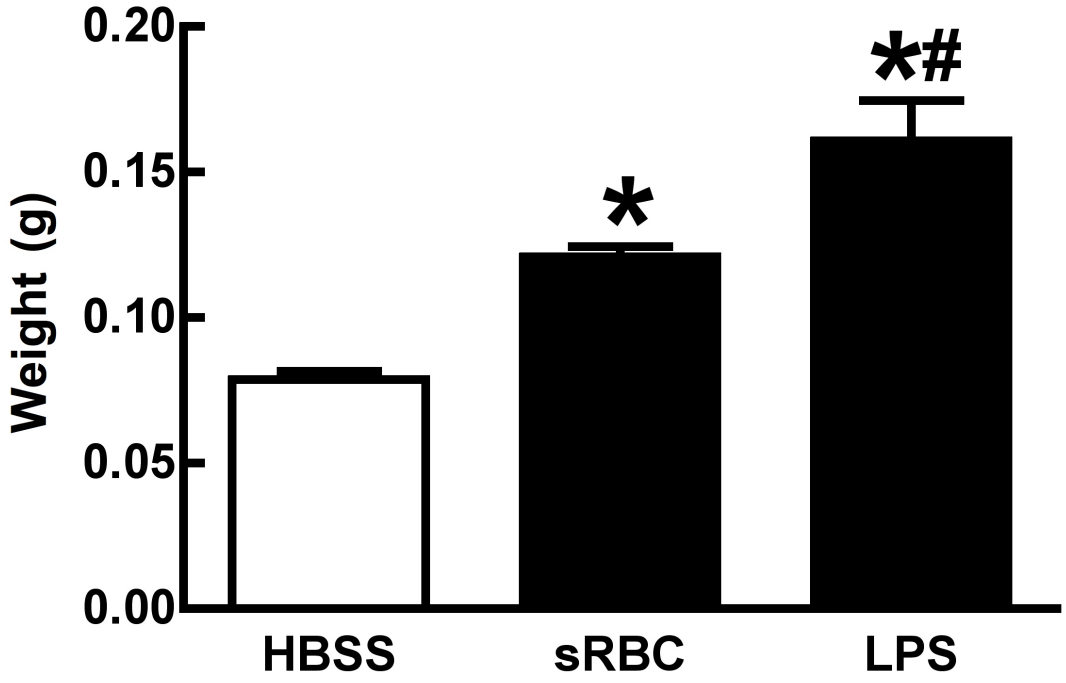


**Figure 4.2. The effect to experimental immune challenges on spleen weight in mice.** Female mice were injected with HBSS, sRBC ($1x10^9$ cells; i.p.), or LPS (25 μg; i.p.) and sacrificed 4 days later. The spleen was rapidly and aseptically removed and weighed. Columns represent the average weight (g) + one SEM (n=3). * Differs from HBSS ($p<0.05$). # Differs from sRBC ($p<0.05$).

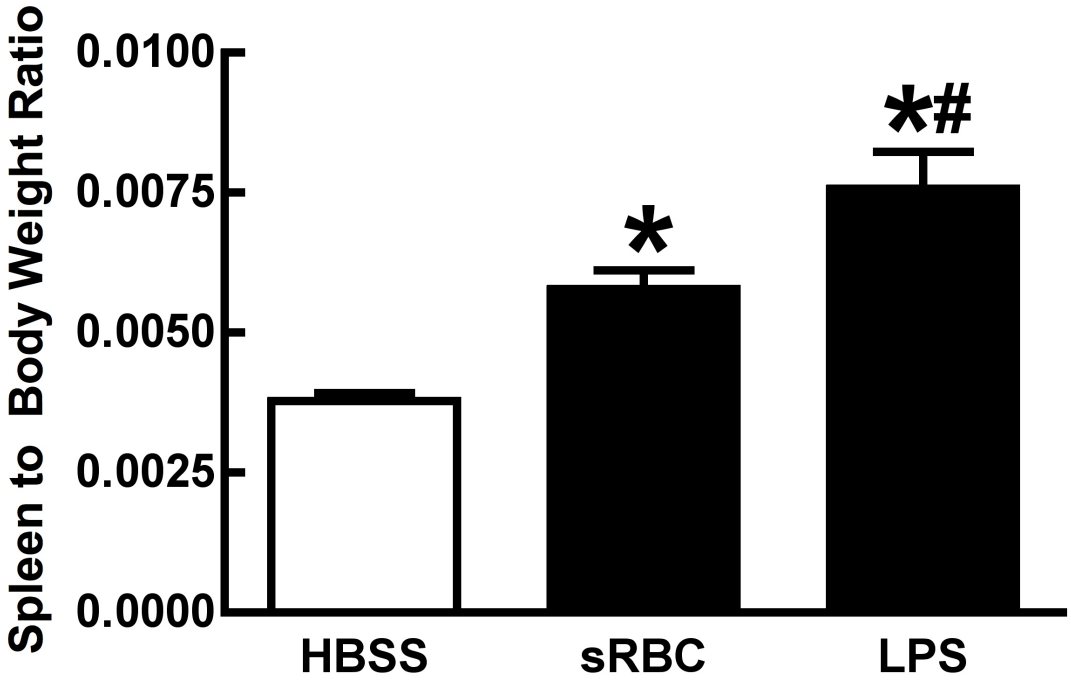


**Figure 4.3. The effect to experimental immune challenges on the spleen:body weight ratio in mice.** Female mice were injected with HBSS, sRBC ($1x10^9$ cells; i.p.), or LPS (25 μg; i.p.). Four days later the mice were sacrificed, weighed, and the spleen was weighed following rapid aseptic removal. Columns represent the average spleen:body weight ratio + one SEM (n=3). * Differs from HBSS ($p<0.05$). # Differs from sRBC ($p<0.05$).

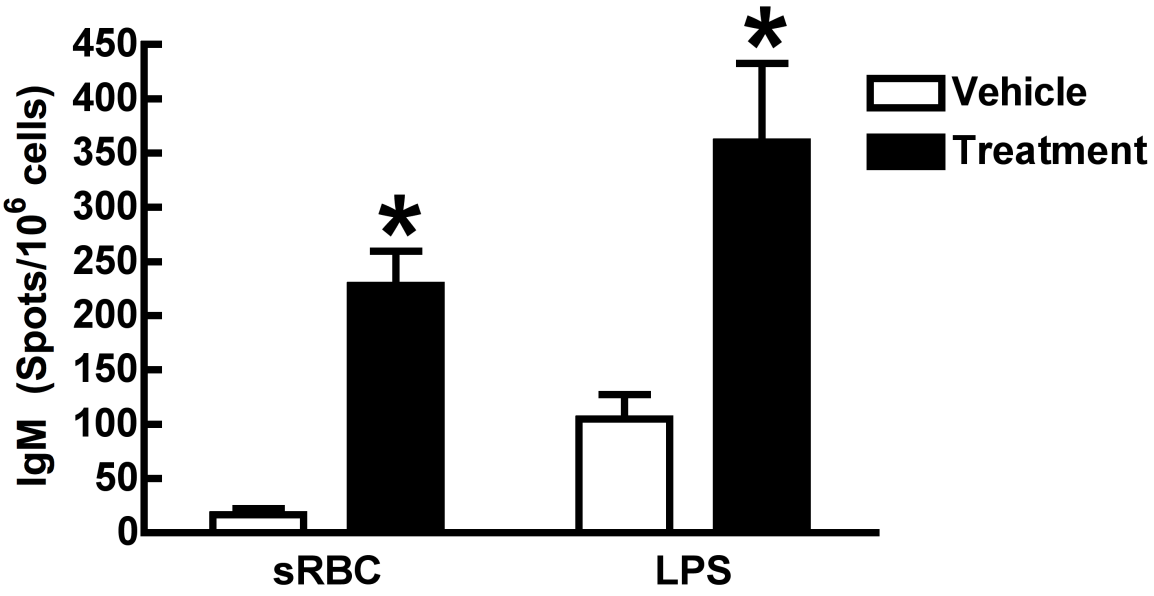


**Figure 4.4. IgM production from splenocytes from mice subject to experimental immune challenges.** Female mice were injected with sRBC ($1x10^9$ cells; i.p.), LPS (25 μg; i.p.), or vehicle (HBSS). Four days later the mice were sacrificed and the spleen was rapidly and aseptically removed. The splenocytes were isolated and subject to ELISPOT detection of IgM production. The data presented in this graph are derived from separate experiments: one in which sRBC or its vehicle was injected into mice, and another using LPS or its vehicle. Columns represent the spots generated per $10^6$ cells + one SEM (n=3). * Differs from HBSS ($p<0.05$).

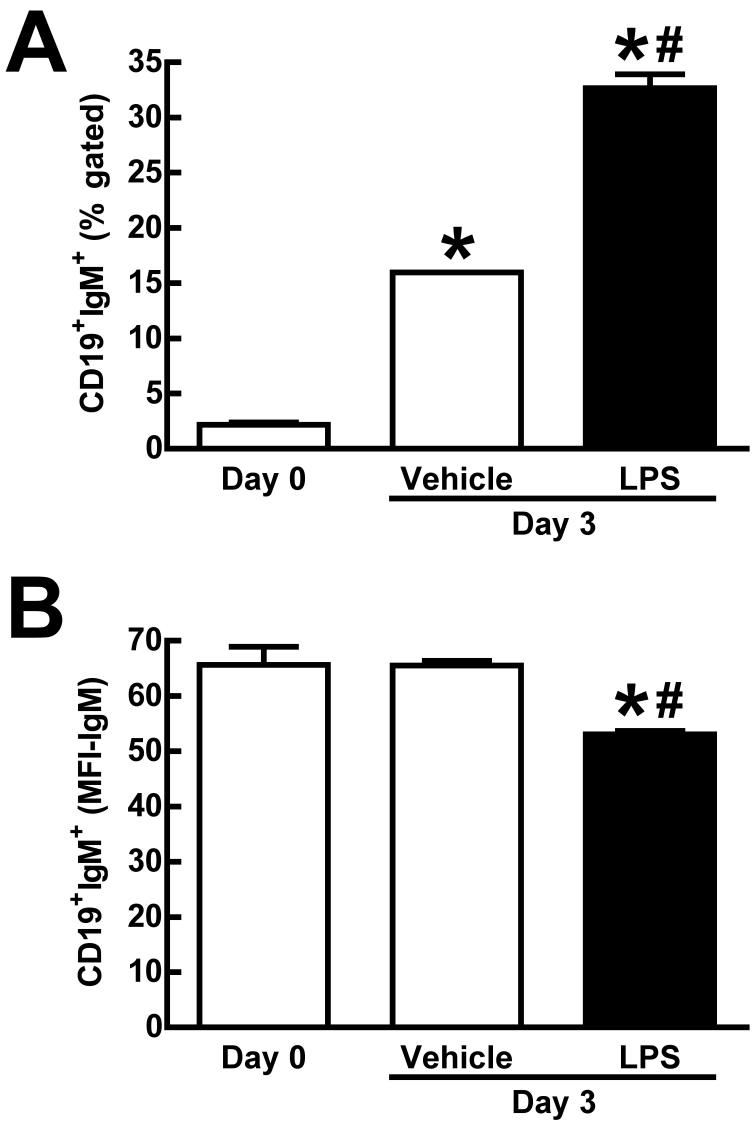


**Figure 4.5. Analysis of IgM antibody production responses in splenic B cells from mice exposed to LPS in vitro.** Isolated splenocytes were cultured in the presence of LPS (10 µg/ml), or vehicle (RPMI), for 3 days. On the 3rd day flow cytometry was used to detect CD19 (PE-Cy7) and IgM (FITC) on splenocytes. Cells were gated sequentially on singlet live lymphocytes, prior to plotting CD19 and IgM for analysis. Uncultured, freshly isolated splenocytes are designated as Day 0. All columns represent means + 1 SEM (n=3). Columns depict the percent of lymphocytes (A) or MFI of IgM (B) in lymphocytes expressing CD19 and IgM. Results are representative of at least 2 separate experiments. * Significantly differs from Day 0 ($p<0.05$). # Significantly differs from Day 3 NA ($p<0.05$).

4.3.2: Splenic sympathetic neuronal activity in response to humoral immune challenge models

Next, the activity of the sympathetic noradrenergic neurons in the spleen was assessed following T cell dependent (sRBC) and T cell independent (LPS) immune challenges *in vivo*. Neuroimmune interactions were hypothesized to occur within hours following an immune challenge; therefore the activity of splenic sympathetic noradrenergic neurons was evaluated between 90 min and 2.5 h following the injection of immunogens. Injection of sRBC increased the concentration of spleen capsule NE and splenic TH content within 90 min (**Figures 4.6 and 4.7**). The measured rate constant of NE utilization in the spleen following aMT administration was significantly elevated following the injection of sRBC (**Figure 4.8**). Injection of LPS was also able to increase the activity of splenic sympathetic noradrenergic neurons. Within 2.5 h of LPS injection spleen capsule NE concentrations and splenic TH content were increased (**Figures 4.9 and 4.10**). The rate of NE utilization was also increased in response to LPS (**Figure 4.11**). The data presented here demonstrate a correlation between splenic sympathetic neuronal activity and the initiation of a humoral immune response. The data here also suggest that increases in sympathetic neuronal activity in response to immunogens eliciting a humoral immune response are not dependent on the involvement of T cells; the activity of splenic sympathetic noradrenergic innervation increased in response to both sRBC and LPS.

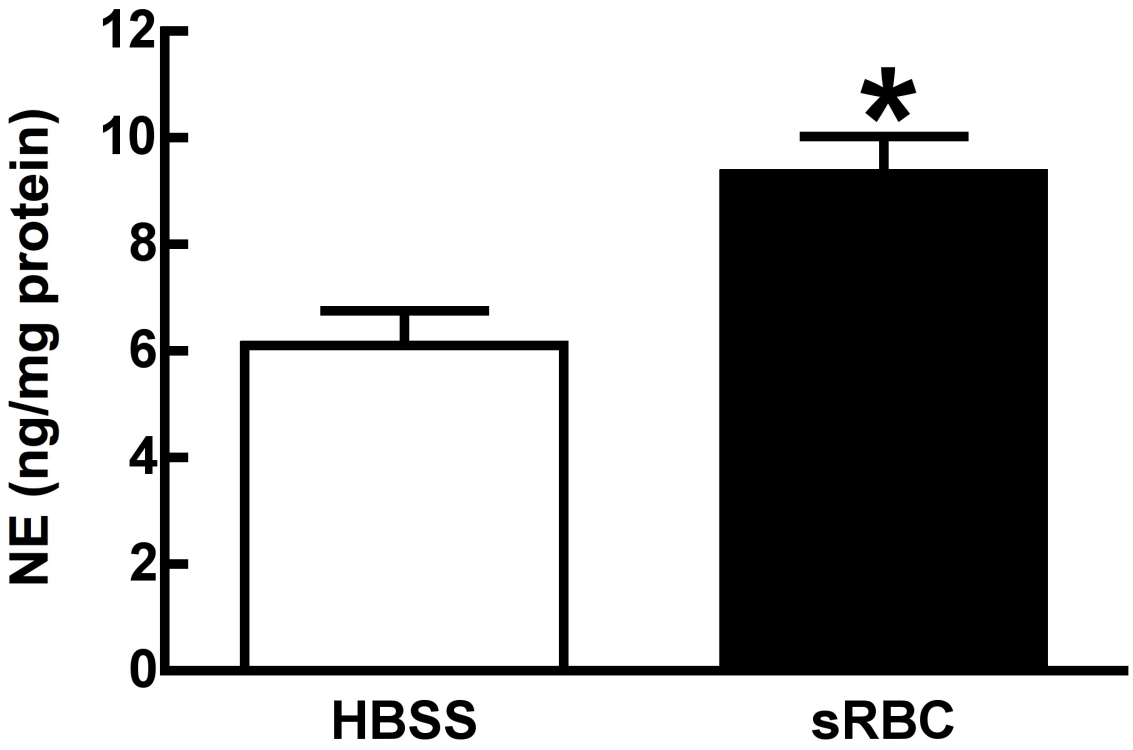


**Figure 4.6. Spleen capsule NE concentrations in response to injection of sRBC.** Female mice were injected with HBSS or sRBC ($1x10^9$ cells; i.p.). Ninety minutes later the mice were sacrificed and the spleen capsule was collected. Spleen capsule samples were prepared for and analyzed by HPLC-ED for NE as described. Columns represent average concentration of NE + one SEM (n=6-8). * Differs from HBSS ($p<0.05$).

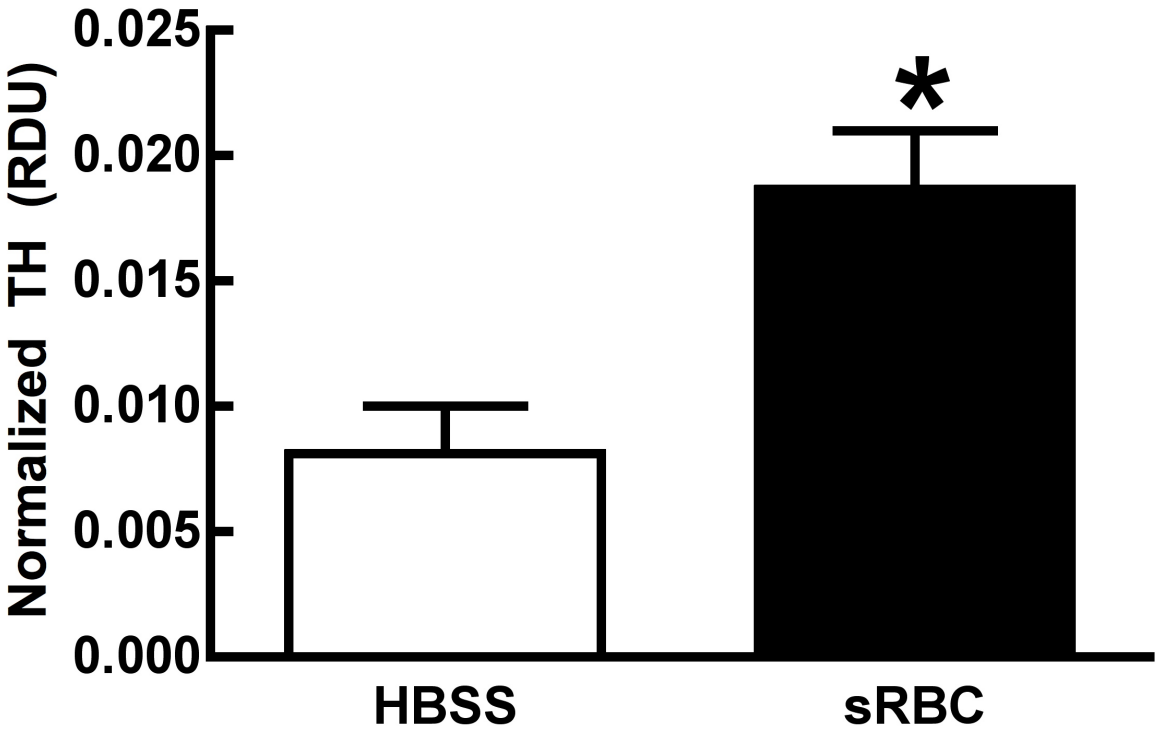


**Figure 4.7. Spleen capsule TH content in response to injection of sRBC.** Female mice were injected with HBSS or sRBC ($1x10^9$ cells; i.p.). Ninety minutes later the mice were sacrificed and the spleen capsule was collected. Spleen capsule samples were prepared for and analyzed by Western blot for TH as described in the Methods (Section 4.2.6). Columns represent the average amount of TH, normalized to β-actin, in the spleen + one SEM (n=6-8). * Differs from HBSS ($p<0.05$).

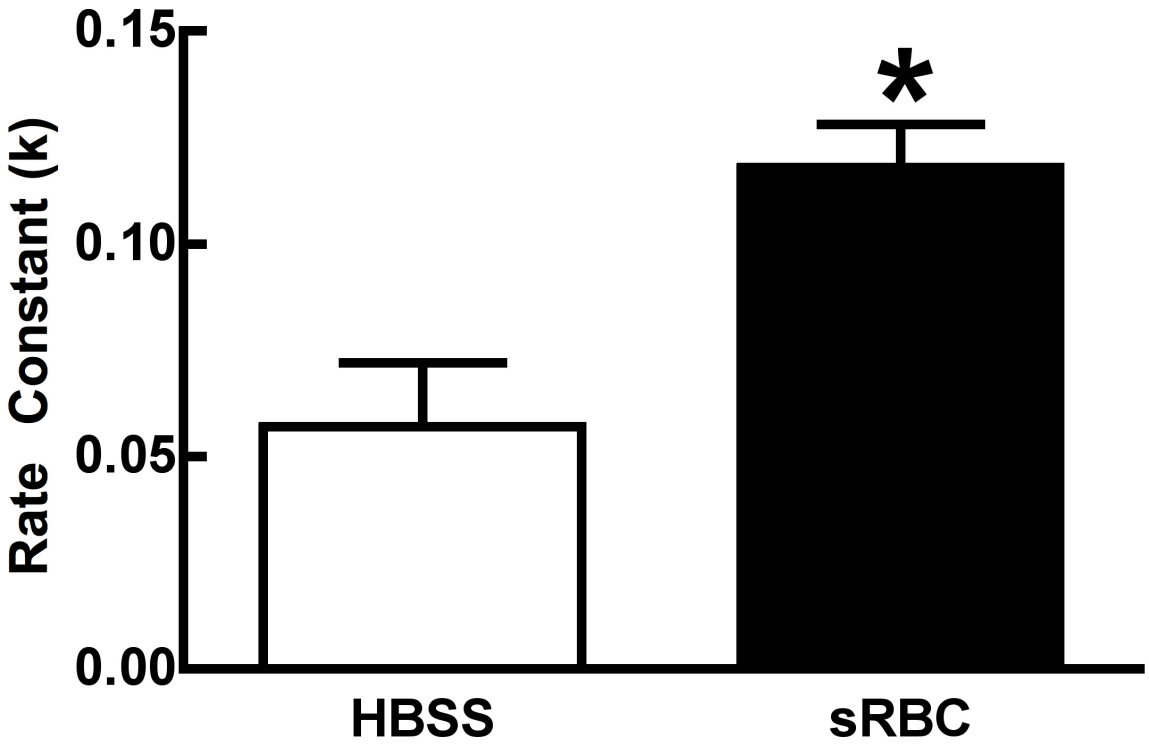


**Figure 4.8. Spleen capsule noradrenergic neuron activity in response to injection of sRBC.** Female mice received a single injection saline/aMT (300 mg/kg, i.p.) followed 2.5 hours later by single injection of HBSS or sRBC ($1x10^9$ cells; i.p.). Mice were sacrificed 90 min after the sRBC injection and the spleen capsule collected and prepared analysis of NE by HPLC-ED. Non-aMT treated mice were used for the 0 h time point and a linear regression analysis performed to determine the rate of NE utilization. Columns depict the average rate constant of NE utilization + one SEM (n=15-16). * Differs from HBSS ($p<0.05$).

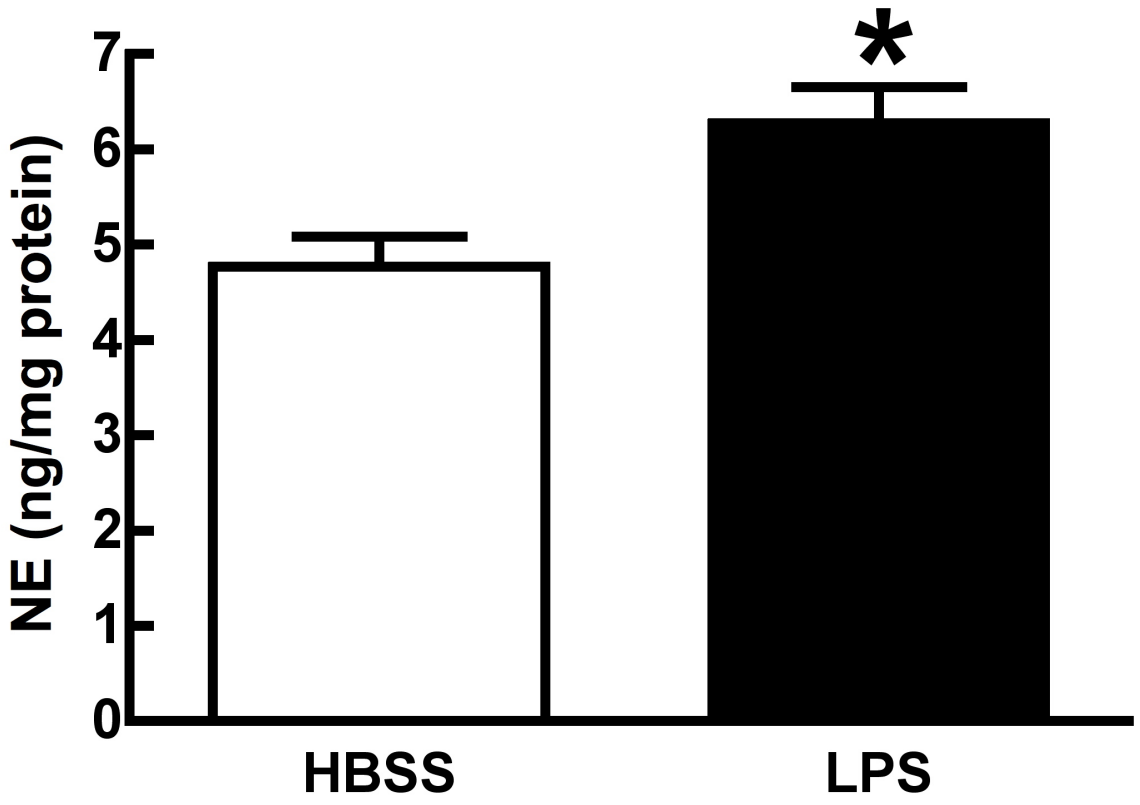


**Figure 4.9. Spleen capsule NE concentrations in response to injection of LPS.** Female mice were injected with HBSS or LPS (25 μg; i.p.). After 2.5 h the mice were sacrificed and the spleen capsule was collected. Spleen capsule samples were prepared for and analyzed by HPLC-ED for NE as described. Columns represent average concentration of NE + one SEM (n=6-8). * Differs from HBSS ($p<0.05$).

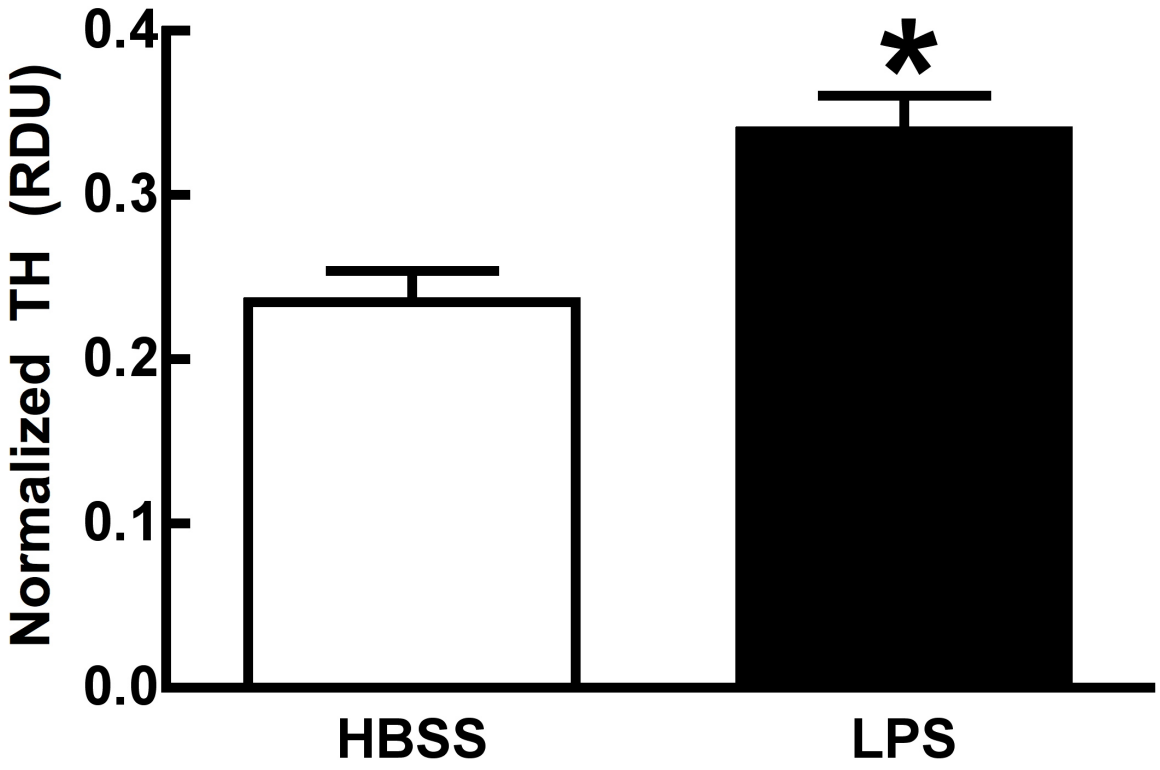


**Figure 4.10. Spleen capsule TH content in response to injection of LPS.** Female mice were injected with HBSS or LPS (25 μg; i.p.). After 2.5 h the mice were sacrificed and the spleen capsule was collected. Spleen capsule samples were prepared for and analyzed by Western blot for TH as described in the Methods (Section 4.2.6). Columns represent the average amount of TH, normalized to β-actin, in the spleen + one SEM (n=6-8). * Differs from HBSS ($p<0.05$).

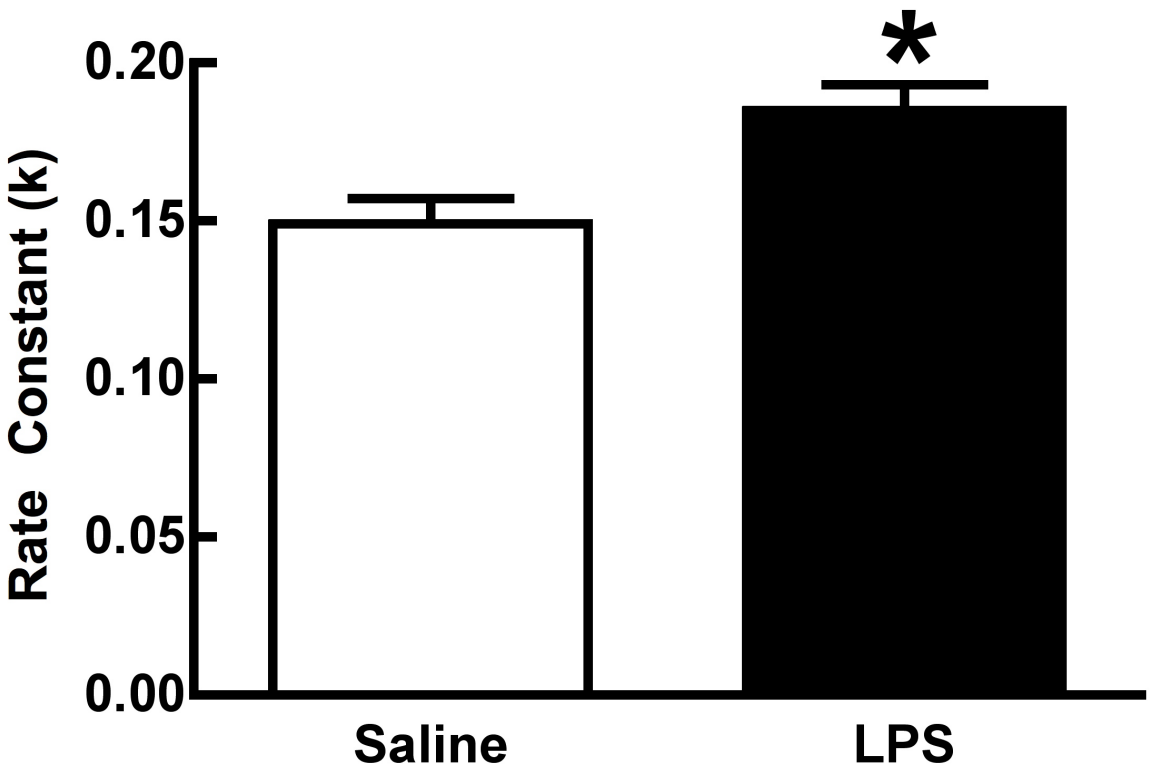


**Figure 4.11. Spleen capsule noradrenergic neuron activity in response to injection of LPS.** Female mice received a single injection saline/aMT (300 mg/kg, i.p.) immediately followed by single injection of HBSS or LPS (25 μg; i.p.). Mice were sacrificed 4 h after the LPS injection and the spleen capsule collected and prepared analysis of NE by HPLC-ED. Non-aMT treated mice were used for the 0 h time point and a linear regression analysis performed to determine the rate of NE utilization. Columns depict the average rate constant of NE utilization + one SEM (n=15-16). * Differs from HBSS ($p<0.05$).

4.3.3: β2AR expression on splenic lymphocytes

The correlation between humoral immune responses and splenic sympathetic noradrenergic activation suggests these two physiologic processes are dependent upon one another. For such a link to exist, it was hypothesized that components of the humoral immune response would be able to recognize signals from the sympathetic nervous system, including activation of adrenergic receptors. This hypothesis was tested by evaluation of β2AR expression on lymphocytes, as there is precedence for this in the literature (Sanders, 2012).

The surface expression of β2AR was assessed among lymphocytes, T cells ($CD3^+$) and B cells ($CD19^+$). Both T cells and B cells were found to express β2AR (**Figure 4.12**), however the expression of β2AR in B cells (~20%) is nearly double than that of T cells (~10%). Within the B cells, nearly all of the cells expressing β2AR also expressed MHC type II, which is involved in the antigen presenting abilities of B cells (**Figure 4.13**). These data suggest B cells are the likely targets for NE-mediated effects of the sympathetic nervous system on humoral immunity. Next, the expression of β2AR on B cells was assessed in response to LPS *in vitro*. *In vitro* LPS stimulation of splenocytes not only increased the percentage of B cells expressing β2AR over a 3 day period, but also increased the number of receptors expressed per cell as indicated by an elevation of the β2AR MFI in B cells (**Figure 4.14**). It was hypothesized that if β2AR stimulation were to have a direct effect on humoral immunity, then B cells expressing β2AR should be able to produce immunoglobulins in response to an immune challenge. In congruence with this hypothesis, β2AR expressing B cells were able to produce IgM

(**Figure 4.15A**), expand in response to *in vitro* LPS over 3 days (**Figure 4.15A**), and increase the number of β2AR expressed per cell (**Figure 4.15B**).

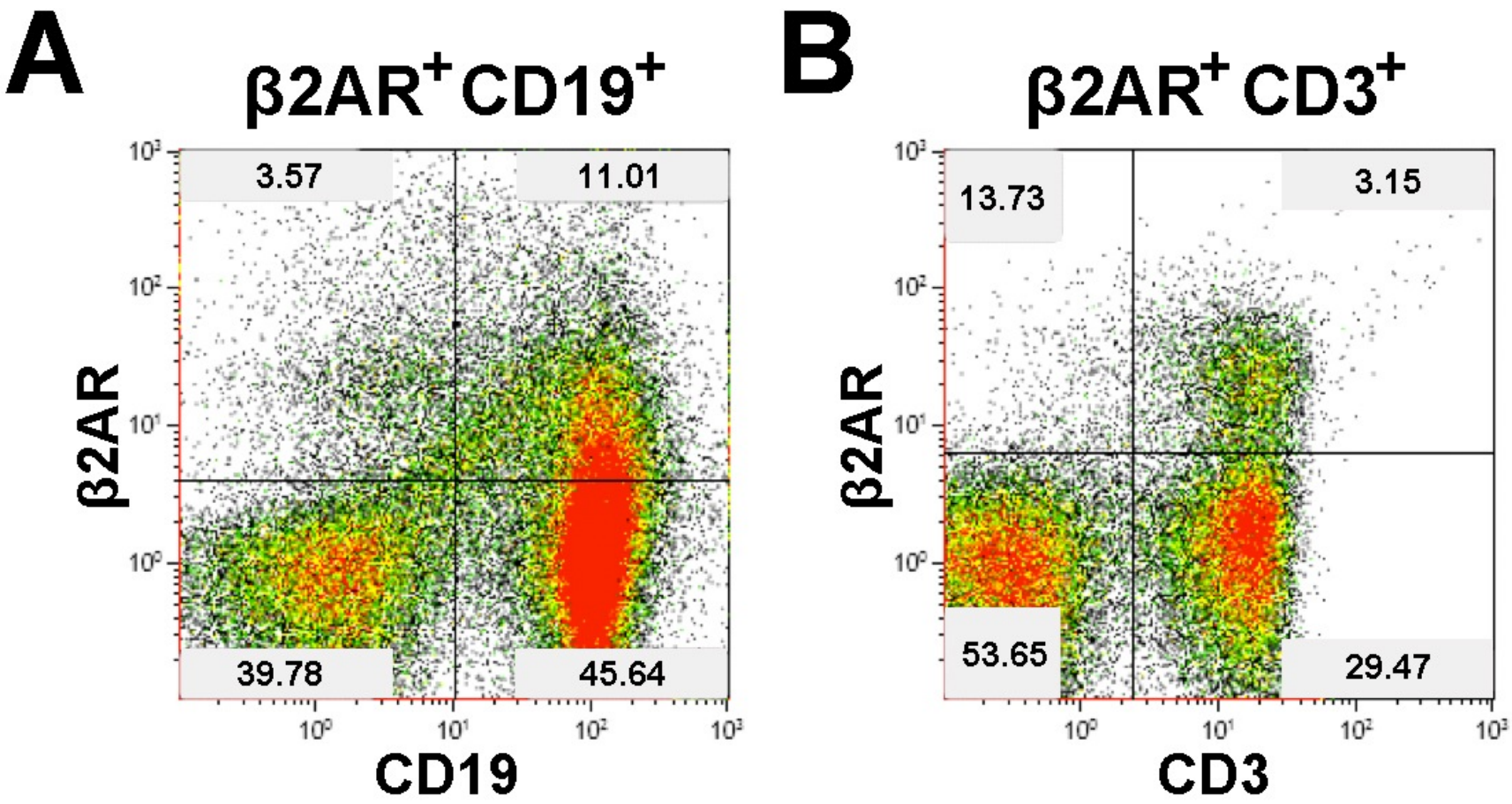


**Figure 4.12. Populations of splenic lymphocytes expressing β2AR.** Lymphocytes were isolated from spleens of untreated mice and analyzed by flow cytometry as described. Cells were gated on singlet lymphocytes prior to plotting the depicted markers. Numbers in the plot are the percent of events occurring in the respective quadrant. (A) B cells (β2AR-APC versus CD19-PE-Cy7); (B) T cells (β2AR-APC versus CD3-APC-Cy7).

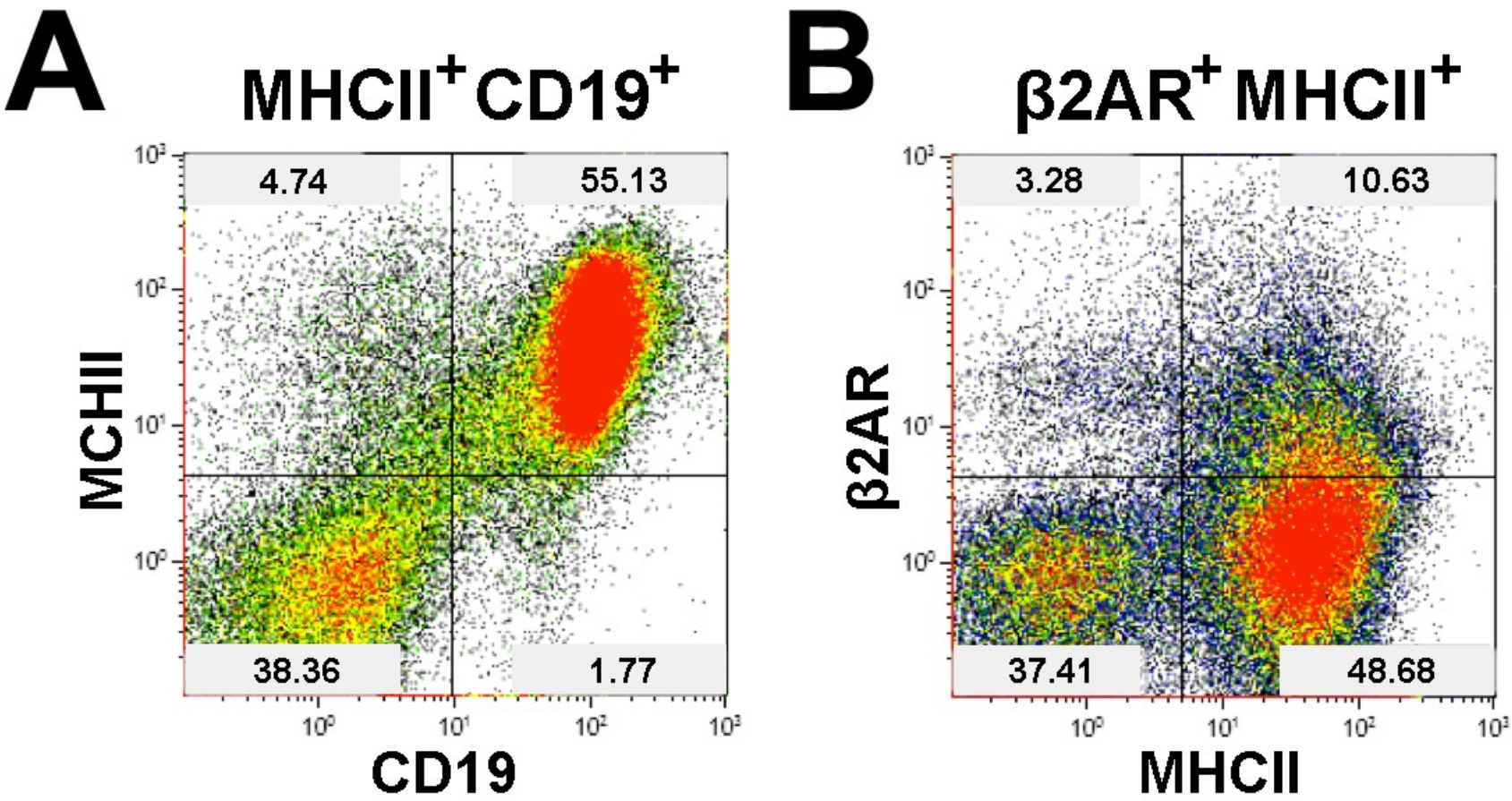


**Figure 4.13. Correlation between antigen presenting lymphocytes in the spleen and β2AR expression.** Lymphocytes were isolated from spleens of untreated mice and analyzed by flow cytometry as described. Cells were gated on singlet lymphocytes prior to plotting the depicted markers. Numbers in the plot are the percent of events occurring in the respective quadrant. (A) antigen-presenting B cells (MHCII-FITC versus CD19-PE-Cy7); (B) β2AR expressing antigen-presenting cells (β2AR-APC versus MHCII-FITC)

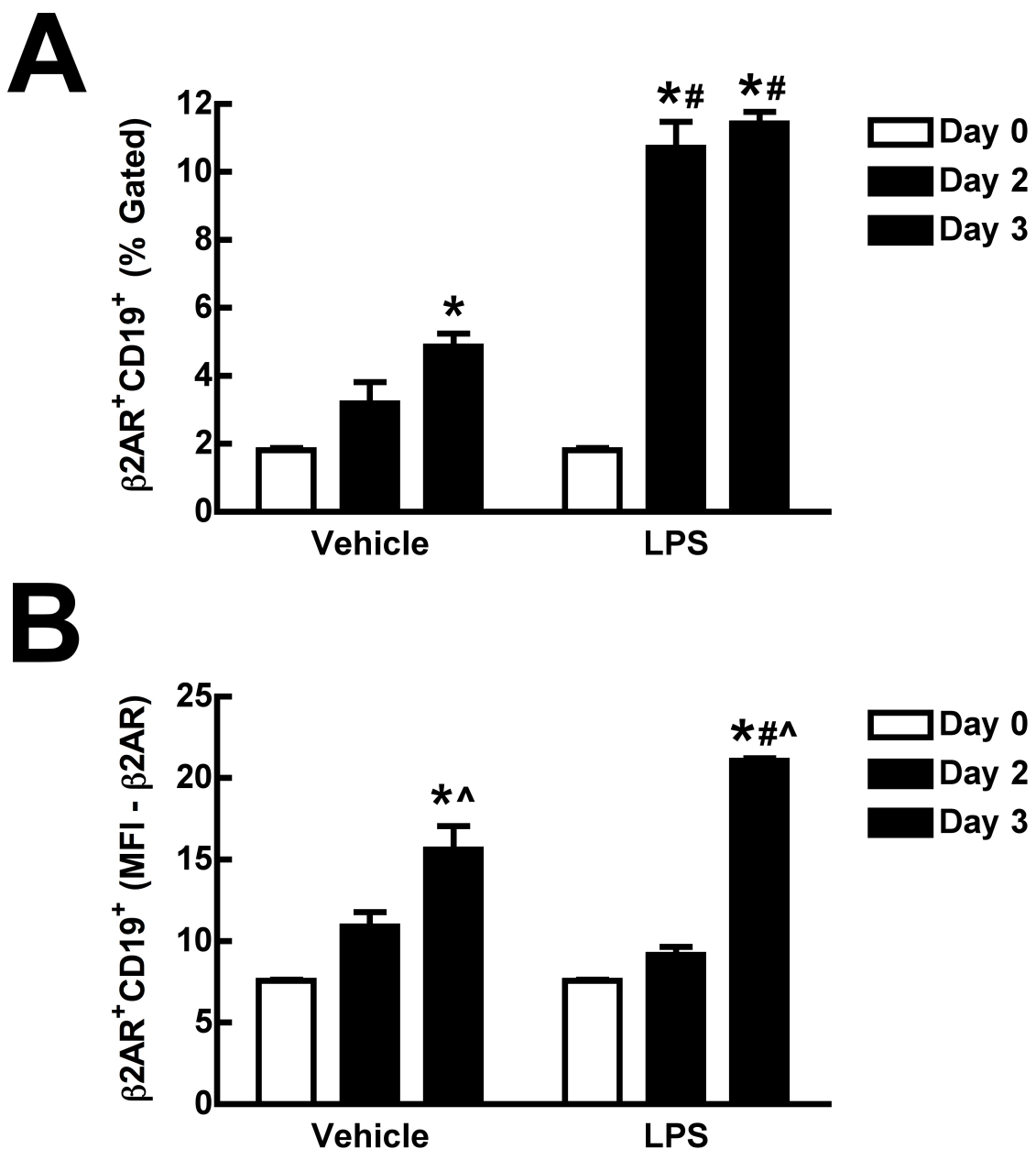


**Figure 4.14. The response of β2AR expressing splenic B cells to *in vitro* LPS administration.** Isolated splenocytes were cultured with LPS or its vehicle (RPMI) 3 days. Flow cytometry was used to assess surface β2AR and CD19 expression on lymphocytes on days 2 and 3 of culture as well as immediately after isolation (Day 0). Bars represent the average percentage of B cells expressing β2AR (A) or the MFI of β2AR on B cells (B) + one SEM. * Differs from Day 0 of the same treatment group ($p<0.05$); # Differs from the same time point in the Vehicle treated group ($p<0.05$); ^ Differs from Day 2 in the same treatment group ($p<0.05$).

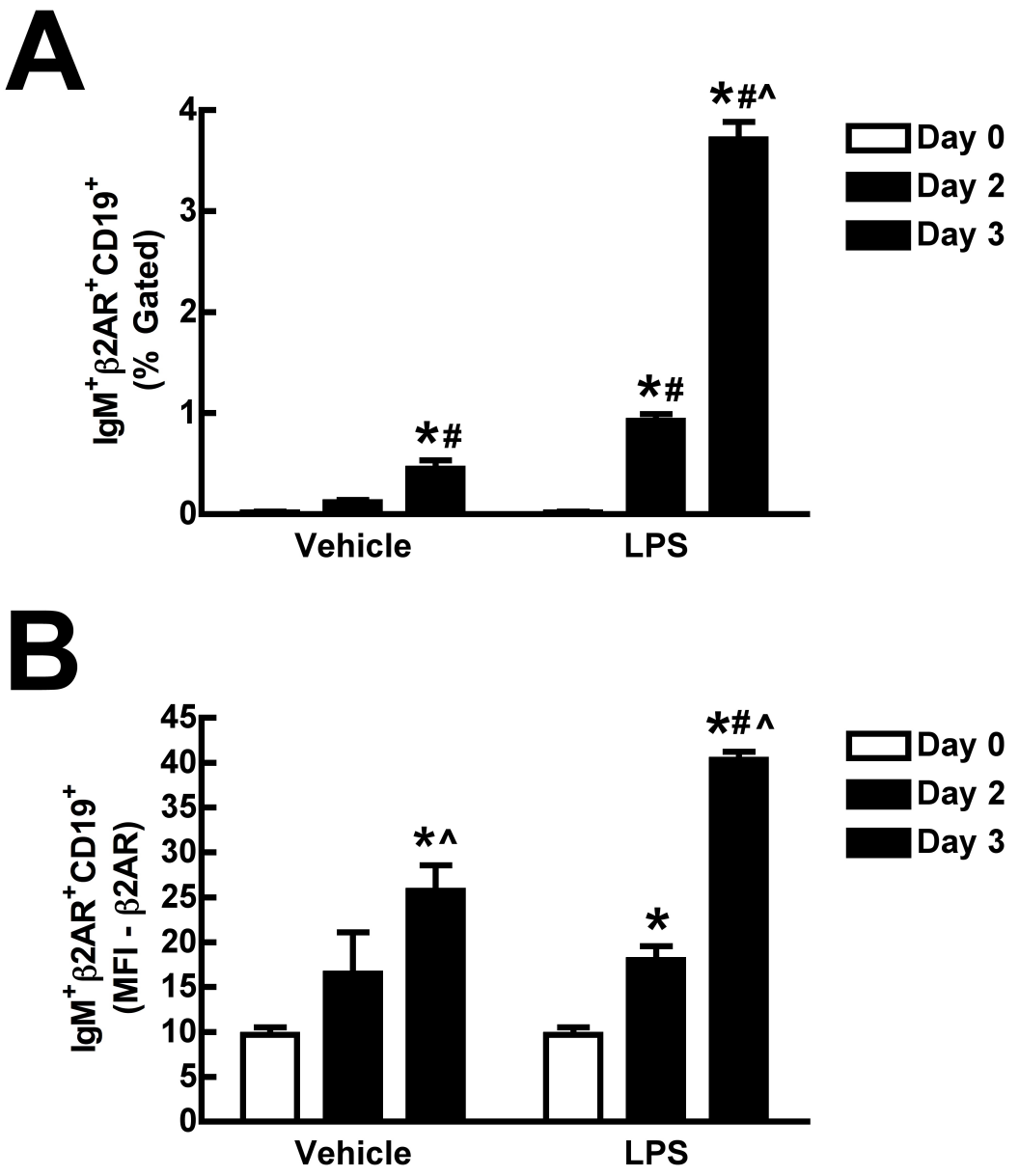


**Figure 4.15. The IgM response of B2AR expressing splenic B cells to *in vitro* LPS administration.** Isolated splenocytes were cultured with LPS or its vehicle (RPMI) 3 days. Flow cytometry was used to assess surface β2AR and CD19 expression and intracellular IgM in lymphocytes on days 2 and 3 of culture as well as immediately after isolation (Day 0). Bars represent the average percentage of IgM producing B cells expressing β2AR (A) or the MFI of IgM in the same cells (B) + one SEM. * Differs from Day 0 of the same treatment group ($p<0.05$); # Differs from the same time point in the Vehicle treated group ($p<0.05$); ^ Differs from Day 2 in the same treatment group ($p<0.05$).

4.3.4: The effect of β2AR stimulation on humoral immune responses in splenic lymphocytes

The presence of β2AR on B cells that produce IgM, coupled with the expansion of β2AR expressing cells in response to LPS, suggest NE is able to exert a direct effect in these cells. Work in this arena suggests NE stimulation of β2AR increases antibody production in response to immune challenges (Sanders, 2012). Therefore it was hypothesized NE would enhance the humoral immune response of cultured splenocytes to LPS. However, NE was not found to alter the proportion of IgM producing B cells, nor the amount of IgM per cell, at the concentrations tested (**Figure 4.16**). Furthermore, NE did not change the proportion of IgM producing B cells expressing β2AR, nor the MFI for IgM in these cells (**Figure 4.17**). To further test the effect of NE stimulation of β2AR on humoral immunity, immune challenged mice were treated with butoxamine, a β2AR antagonist, for 24 h before and after LPS. LPS significantly increased the proportion of splenic IgM producing B cells and the amount of IgM per B cell (**Figure 4.18**). This is congruent with the effects observed during *in vitro* administration of LPS. Butoxamine did not change the proportion of IgM producing B cells nor the amount of IgM per B cell (**Figure 4.18**). Interestingly, LPS did not expand the population of IgM producing B cells expressing β2AR (**Figure 4.19A**), but increased the amount of IgM per cell of this population (**Figure 4.19B**). Butoxamine also had no effect on the population of IgM producing B cells expressing β2AR (**Figure 4.19**).

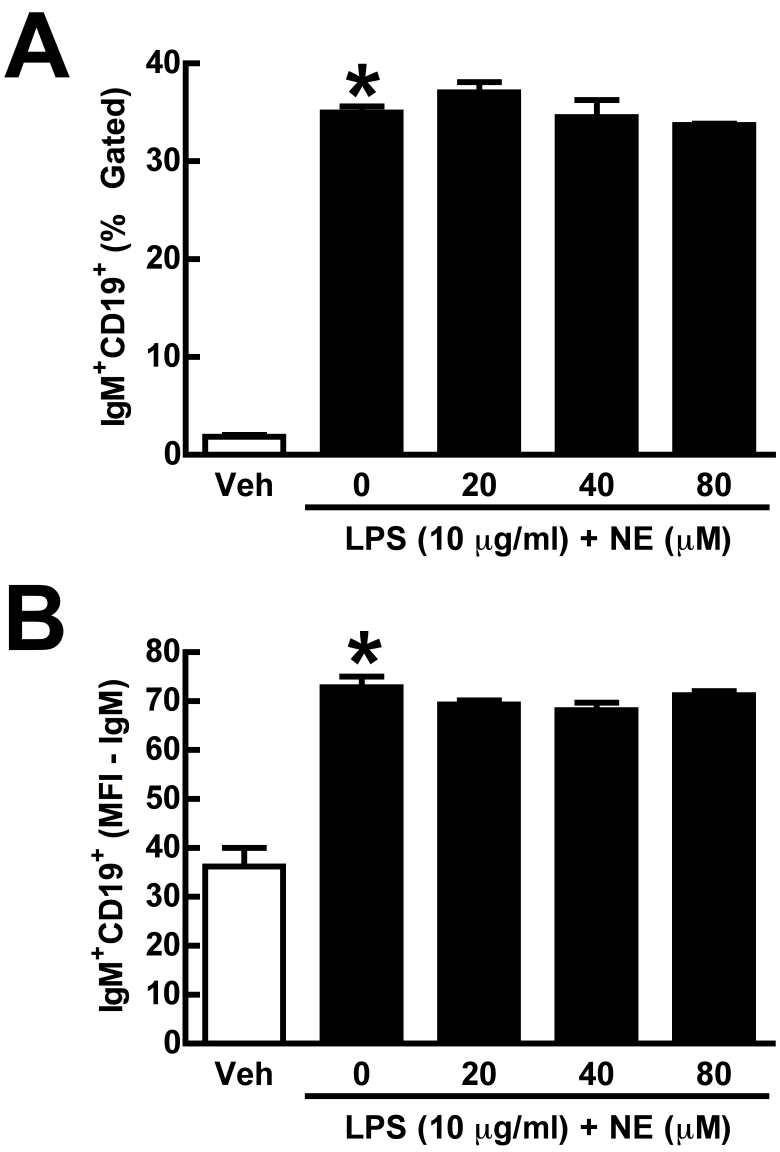


**Figure 4.16. The effect of NE on the IgM response of splenic B cells to *in vitro* LPS administration.** Isolated splenocytes were cultured with LPS or its vehicle (Veh) for 3 days. Flow cytometry was used to assess surface CD19 expression and intracellular IgM in lymphocytes after 3 days of culture. Bars represent the average percentage of IgM producing B cells (A) or the MFI of IgM in the same cells (B) + one SEM. * Differs from Veh ($p<0.05$).

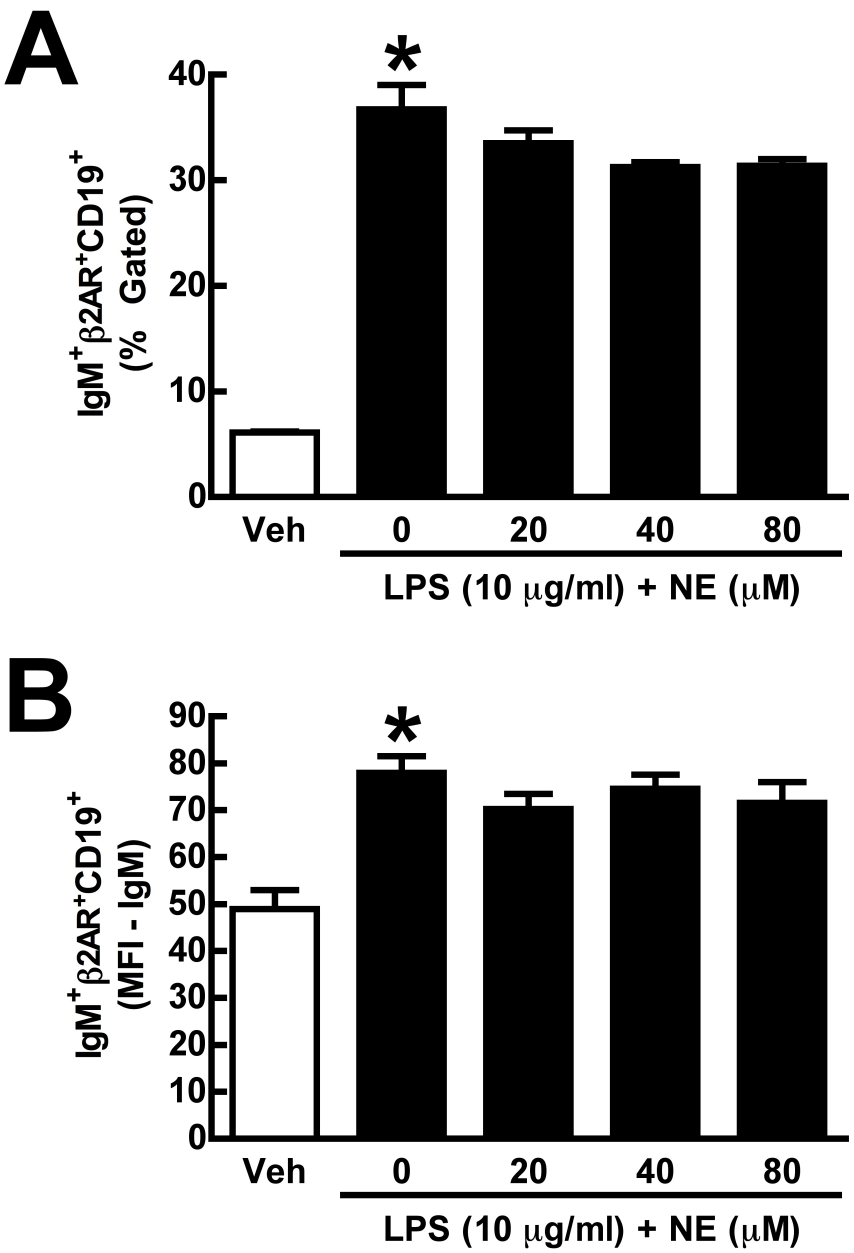


**Figure 4.17. The effect of NE on the IgM response of β2AR expressing splenic B cells to *in vitro* LPS administration.** Isolated splenocytes were cultured with LPS or its vehicle (Veh) for 3 days. Flow cytometry was used to assess surface β2AR and CD19 expression and intracellular IgM in lymphocytes after 3 days of culture. Bars represent the average percentage of IgM producing B cells expressing β2AR (A) or the MFI of IgM in the same cells (B) + one SEM. * Differs from Veh ($p<0.05$).

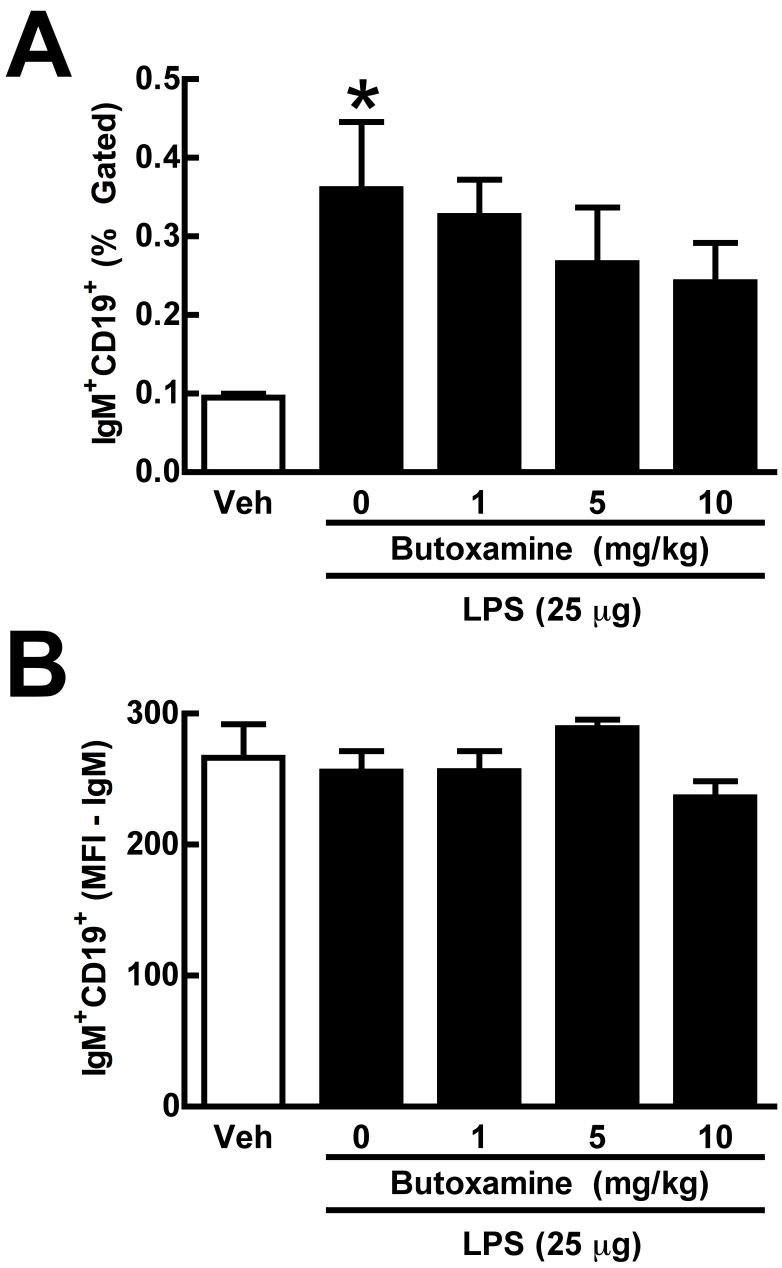


**Figure 4.18. The effect of β2AR antagonism on the IgM response of splenic B cells to *in vivo* LPS administration.** Female mice were injected 8 times with butoxamine (various doses; i.p.), or vehicle, every 6 h for 48 h. Mice received a single injection of LPS (25 μg; i.p.), or vehicle (Veh), one h prior to the 5$^{th}$ injection. Mice were sacrificed 4 days after LPS administration and their splenocytes isolated. Flow cytometry was used to assess surface CD19 expression and intracellular IgM in splenic lymphocytes. Bars represent the average percentage of IgM producing B cells (A) or the MFI of IgM in the same cells (B) + one SEM. * Differs from Veh ($p<0.05$).

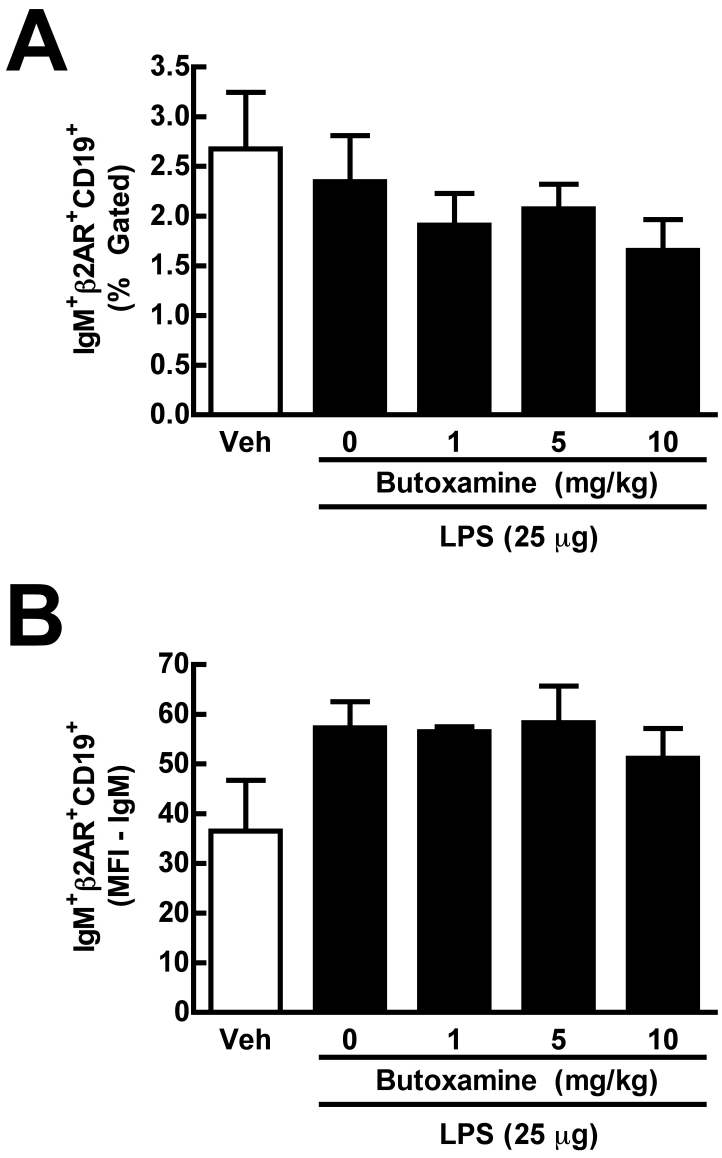


**Figure 4.19. The effect of β2AR antagonism on the IgM response of β2AR expressing splenic B to *in vivo* LPS administration.** Female mice were injected 8 times with butoxamine (various doses; i.p.), or vehicle, every 6 h for 48 h. Mice received a single injection of LPS (25 μg; i.p.), or vehicle (Veh), one h prior to the 5$^{th}$ injection. Mice were sacrificed 4 days after LPS administration and their splenocytes isolated. Flow cytometry was used to assess surface β2AR and CD19 expression and intracellular IgM in lymphocytes after 3 days of culture. Bars represent the average percentage of IgM producing B cells expressing β2AR (A) or the MFI of IgM in the same cells (B) + one SEM.

## 4.4: Discussion

The results from experiments presented in this chapter illustrate that the sympathetic nervous system is activated during an immune challenge, but noradrenergic signaling does not modulate humoral immune responses. Splenic sympathetic neurons increase their activity within hours of an immune challenge. The activation of these neurons was hypothesized to release NE to act on β2AR on lymphocytes. However, stimulation of β2AR was not found to affect the humoral response of splenic B cells.

### 4.4.1: Activation of splenic sympathetic neurons following an immune challenge eliciting a humoral response

Both sRBC and LPS induce humoral immune responses. Both immunogens increase the weight of the spleen. This increase is due to a combination of recruitment of immune cells to the spleen and the proliferation of immune cells within the spleen (Rasmussen et al., 2012). Interestingly, the increase in spleen weight was greater in LPS treated mice. LPS is a polyclonal immune stimulator, activating all B cells expressing TLR4 (Ademokun and Dunn-Walters, 2001; Lanzavecchia and Sallusto, 2007; Bekeredjian-Ding and Jego, 2009), while sRBC will only activate B cells with unique BCR that can recognize epitopes from sRBC (Ademokun and Dunn-Walters, 2001). Thus, the difference may be due to a relatively larger population of expanding cells within the spleen due to the nature of immune stimulation unique to these immunogens. This difference, however, does not translate into LPS producing more

significant responses later on as both immunogen increased the number of B cells producing IgM with relatively similar magnitudes. Despite the similarities in the humoral immune response to both of these immunogens, there is a significant difference in their action of immune stimulation.

sRBCs are a traditional soluble protein antigen requiring processing by macrophages, interactions with T cells, and eventually T cell to B cell interactions to stimulation antibody production (Ademokun and Dunn-Walters, 2001). LPS, on the other hand, is a direct stimulator of B cells. LPS bind TLR4 receptors and cross-links BCR on B cells directly causing proliferation, activation, and ultimately IgM production in the same cell (Lanzavecchia and Sallusto, 2007; Bekeredjian-Ding and Jego, 2009). Therefore, while sRBC require B cells that selectively recognize sRBC epitopes, LPS is a polyclonal B cell activator in that it activates any B cell expressing TLR4. This fact makes LPS a suitable and preferable immunogen for *in vitro* work, as demonstrated by the ability of LPS to induce and increase in the number of IgM producing cells in cultured splenocytes.

Activation of splenic sympathetic noradrenergic neurons in response to an immune challenge is T-cell independent. The injection of sRBC and LPS induce similar changes in splenic noradrenergic neurons, and both immunogens significantly increase the concentration of NE in the spleen capsule. As discussed in **Chapter 3**, increased spleen capsule NE is correlated with increased noradrenergic activity. This correlation holds true with regards to immune challenge activation in that both immunogens

increase the rate of NE utilization in the spleen. Interestingly, the amount of TH also increased in response to both immunogens.

Activity dependent increases in the content TH of catecholaminergic neurons is not a new finding (Kumer and Vrana, 1996), but the time frame of TH increases is of interest. TH within the spleen is found exclusively within the axon terminals of sympathetic neurons, the cell bodies of which lie in the pre-vertebral celiac-mesenteric ganglion plexus. Thus, due to the distance between the cell bodies and axon terminals in the spleen there is not sufficient time for increased translation and transport of TH to splenic axon terminals within 2.5 h (the longest time point of the observed effects). Feedback inhibitor stabilization of TH is more likely the cause for increased splenic TH content seen following an immune challenge (Kumer and Vrana, 1996). Thus, if no significant changes occur in the synthetic rate of TH, but there is decrease in the degradation of the enzyme this can account for the accumulation of splenic TH observed.

Phosphorylation of TH is known to occur during times of activation. This phosphorylation increases the catalytic activity of TH and leads to an increase in TH stabilizing feedback inhibitors, such as dopamine (Kumer and Vrana, 1996). Therefore, increased amounts of TH with increased catalytic activity are the potential cause for increased NE concentrations in the spleen during times of activation. Yet, the question as to how increased feedback inhibitors of TH can stabilize the protein while still allowing sufficient synthesis for the accumulation of NE. This phenomenon occurs in response to sRBC, a T-cell dependent immunogen, and LPS, a T-cell independent

immunogen. Therefore, it can be concluded that T-cell involvement is not necessary in the activation of splenic sympathetic neurons. Accordingly, LPS was used in subsequent experiments since this is a clinically relevant immunogen (Miller et al., 2005; Lanzavecchia and Sallusto, 2007), and is an effective *in vitro* model (Lee et al., 1995; Gururajan et al., 2007).

Pro-inflammatory cytokines are likely the activators of sympathetic neuronal activity during an immune challenge. The finding that T-cells are not involved in splenic sympathetic innervation raises the question: what induces sympathetic neuronal activation during an immune challenge? Due to the rapid onset of sympathetic activation following immunogen administration, the leading hypothesis is that sympathetic activity is induced by early pro-inflammatory cytokines. The most studied of these early inflammatory factors are interleukin-1β (IL-1β) and IL-6. Both of these cytokines are produced by phagocytic monocytes early in inflammatory events (Dinarello, 2004). The temporal profile of IL-1β and IL-6 production in response to an immune challenge is within hours (Kakizaki et al., 1999). This makes them prime candidates to mediate rapid and early changes in sympathetic activity.

In support of this, intraperitoneal injection of IL-1β increases the release of NE in the spleen (Shimizu et al., 1994; Kohm and Sanders, 2001). This suggests that IL-1β is the sympatho-stimulatory mediator *in vivo*. However, IL-1β is also able to stimulate the production of IL-6 from a myriad of cell types (Kauma et al., 1994; Spangelo et al., 1994; Parikh et al., 1997). This leaves open the possibility that the effects of IL-1β on sympathetic activity may be due to IL-6. Plasma and brain levels of IL-6 peak within 1-3

h following an immune challenge (Kakizaki et al., 1999), correlating with increased splenic noradrenergic activity seen in this work. Intraventricular injection of IL-6 produces increased firing of spleen capsule sympathetic neurons (Helwig et al., 2008), suggesting IL-6 may act centrally to increase NE release during an immune challenge. Taken together, these data strongly suggest that one, or both, of these cytokines are stimulating the sympathetic nervous system during an immune challenge.

4.4.2: β2AR expression on splenic B cells

Splenic B cells express β2AR and are immunologically functional. The demonstration of increased splenic sympathetic activity during an immune challenge in conjunction with NE containing axon terminals being in very close proximity to immune cells (Felten et al., 1987; Felten and Olschowka, 1987) suggests a potential interaction between sympathetic neurons and immune cells. The present study confirms observations by other investigators that β2AR are expressed by both B cells and T cells, with B cell expression being highest (Kin and Sanders, 2006). Therefore, β2AR expression on B cells was further pursued, especially with regards to humoral immunity in which the B cell plays a central role.

Co-localization of β2AR with other B cell surface markers has not been previously reported. B cells constitutively express MHCII and are considered professional antigen presenting cells (Painter and Stern, 2012). The finding that the majority of B cells expressing β2AR are also MHCII positive suggests β2AR might play a role in antigen presentation, in addition to the effects on antibody production. The data

presented here also suggest that B cells become more sensitive to NE following LPS stimulation by increasing the number of cells expressing β2AR and the amount of β2AR per B cell. This occurs within the general population of B cells as well as B cells producing IgM. The expression of β2AR on IgM producing cells further supports the hypothesis that NE stimulation of β2AR can have a direct impact on IgM production.

4.4.3: The effect of β2AR on the humoral response of splenic B cells

Stimulation of β2AR on splenic B cells does not augment IgM production in response to LPS, although β2AR expression on B cells producing IgM allows for direct interactions. NE is an endogenous agonist of β2AR and the catecholamine released by sympathetic neuron axon terminals in the spleen. Therefore, it was hypothesized that addition of NE to LPS stimulated cultured splenocytes would increase IgM production. This turned out not be the case. Despite the inability of NE to increase IgM production *in vitro*, it was postulated that perhaps the simplified conditions of splenocyte culture were not suitable to reveal the augmenting effect of β2AR stimulation. Therefore, β2AR were blocked *in vivo* during an immune challenge by LPS. LPS had previously been shown to increase splenic sympathetic activity, and therefore NE release, to augment the humoral response in the spleen. It was expected that blockade of β2AR under these conditions would decrease the humoral response of splenic B cells by blocking the effect of NE released in response to LPS. Blockade of β2AR did not significantly affect the humoral response of splenic B cells. Taken together, these data lead to the

conclusion that NE stimulation of β2AR does not augment the humoral response of splenic B cells in response to LPS.

These findings argue against a direct role for β2AR stimulation in antibody production. The question then remains as to the function of β2AR on B cells. It is demonstrated here that B cells express β2AR and these cells are immunologically functional. Furthermore, the data show that β2AR stimulation is not necessary for a normal antibody response to LPS, a T cell independent antigen. This raises the question of why the data obtained in this chapter is incongruent with the reported effect of β2AR on antibody production. A potential explanation of this discrepancy has to do with the nature of the immune challenge used. The correlation between β2AR and antibody production was explored here using LPS, a T cell independent immunogen, which induces a humoral immune response through activation of TLR4 and crosslinking of the BCR (Ademokun and Dunn-Walters, 2001; Lanzavecchia and Sallusto, 2007; Bekeredjian-Ding and Jego, 2009). However, the published research on the correlation between antibody production and β2AR has been accomplished using either T cell dependent immunogens or through direct stimulation of B cells by CD40 (Kohm et al., 2000; Kohm and Sanders, 2001; Pongratz et al., 2006; Padro et al., 2013). Therefore, it may be the case that β2AR augmentation of antibody production is specific to B cell responses in which a CD40-CD154 interaction has occurred. If this is the case, the lack of β2AR augmentation of the humoral immune response to LPS is due to the absence of CD40 being involved in this response. This hypothesis has not been directly tested and is an avenue for future research.

### 4.4.4: Conclusion

The purpose of this chapter was to test the hypothesis that β2AR stimulation on B cells by NE released in the spleen augments humoral responses. The data here demonstrate that splenic sympathetic noradrenergic activity is increased during immune challenges. Splenic B cells are shown to express β2AR and are able to produce IgM, which allows for a direct effect of NE on the effector cells of the humoral immune response. However, stimulation of the β2AR was not found to enhance the humoral immune response of splenic B cells to LPS *in vitro* or *in vivo*. Thus, the roles of β2AR on B cells and neuroimmune interactions in humoral immunity remain unclear, but the data here demonstrate that they do not directly modulate the production of antibodies in response to LPS, a T cell independent immunogen.

# REFERENCES

# REFERENCES


Ademokun AA, Dunn-Walters D. Immune Responses: Primary and Secondary. els.net. Chichester, UK: John Wiley & Sons, Ltd; 2001.

Ahrens WH, Cox DJ, Budhwar G. Use of the arcsine and square root transformations for subjectively determined percentage data. Weed Science. 1990.

Baumgarth N. Innate-Like B Cells and Their Rules of Engagement. link.springer.com.proxy2.cl.msu.edu. New York, NY: Springer New York; 2013. p. 57–66.

Bekeredjian-Ding I, Jego G. Toll-like receptors--sentries in the B-cell response. Immunology. 2009 Nov;128(3):311–23. PMCID: PMC2770679

Brodie BB, Costa E, Dlabac A, Neff NH, Smookler HH. Application of steady state kinetics to the estimation of synthesis rate and turnover time of tissue catecholamines. J Pharmacol Exp Ther. 1966 Dec;154(3):493–8.

Cesta M. Normal Structure, Function, and Histology of the Spleen. Toxicol Pathol. 2006;34(5):455–65.

Czajkowsky DM, Shao Z. The human IgM pentamer is a mushroom-shaped molecule with a flexural bias. Proc Natl Acad Sci USA. 2009 Sep 1;106(35):14960–5.

Daëron M. Fc RECEPTOR BIOLOGY - Annual Review of Immunology, 15(1):203. Annu. Rev. Immunol. 1997.

Dinarello C. Infection, fever, and exogenous and endogenous pyrogens: some concepts have changed. J Endotoxin Res. 2004;10(4):201–22.

Eaton MJ, Lookingland KJ, Moore KE. Effects of the selective dopaminergic D2 agonist quinelorane on the activity of dopaminergic and noradrenergic neurons projecting to the diencephalon of the rat. 1994 Feb 1;268(2):645–52.

Fazilleau N, Mark L, McHeyzer-Williams LJ, McHeyzer-Williams MG. Follicular helper T cells: lineage and location. Immunity. 2009 Mar 20;30(3):324–35. PMCID: PMC2731675

Felten DL, Ackerman KD, Wiegand SJ, Felten SY. Noradrenergic sympathetic innervation of the spleen: I. Nerve fibers associate with lymphocytes and macrophages in specific compartments of the splenic white pulp. J Neurosci Res.

1987;18(1):28–36, 118–21.

Felten SY, Olschowka J. Noradrenergic sympathetic innervation of the spleen: II. Tyrosine hydroxylase (TH)-positive nerve terminals form synapticlike contacts on lymphocytes in the splenic white pulp. J Neurosci Res. 1987;18(1):37–48.

Ferrero I, Michelin O, Luescher I. Antigen Recognition by T Lymphocytes. onlinelibrary.wiley.com.proxy2.cl.msu.edu. Chichester, UK: John Wiley & Sons, Ltd; 2001.

Gotch FM. T Lymphocytes: Cytotoxic. Chichester, UK: John Wiley & Sons, Ltd; 2001.

Gururajan M, Jacob J, Pulendran B. Toll-Like Receptor Expression and Responsiveness of Distinct Murine Splenic and Mucosal B-Cell Subsets. PLoS ONE. Public Library of Science; 2007 Sep 12;2(9):e863. PMCID: PMC1955832

Helwig BG, Craig RA, Fels RJ, Blecha F, Kenney MJ. Central nervous system administration of interleukin-6 produces splenic sympathoexcitation. Autonomic Neuroscience. 2008 Aug;141(1-2):104–11.

Kakizaki Y, Watanobe H, Kohsaka A, Suda T. Temporal profiles of interleukin-1beta, interleukin-6, and tumor necrosis factor-alpha in the plasma and hypothalamic paraventricular nucleus after intravenous or intraperitoneal administration of lipopolysaccharide in the rat: estimation by push-pull perfusion. Endocr J. 1999 Aug 1;46(4):487–96.

Kauma SW, Turner TT, Harty JR. Interleukin-1 beta stimulates interleukin-6 production in placental villous core mesenchymal cells. Endocrinology. 1994;134(1):457–60.

Kenter AL. Class Switch Recombination: An Emerging Mechanism - Springer. Molecular Analysis of B Lymphocyte Development and …. 2005.

Kin NW, Sanders VM. It takes nerve to tell T and B cells what to do. J Leukoc Biol. 2006 Jun;79(6):1093–104.

Kohm AP, Sanders VM. Norepinephrine: a messenger from the brain to the immune system. Immunology Today. 2000 Nov;21(11):539–42.

Kohm AP, Sanders VM. Norepinephrine and beta 2-adrenergic receptor stimulation regulate CD4+ T and B lymphocyte function in vitro and in vivo. Pharmacol Rev. 2001 Dec;53(4):487–525.

Kohm AP, Tang Y, Sanders VM, Jones SB. Activation of antigen-specific CD4+ Th2 cells and B cells in vivo increases norepinephrine release in the spleen and bone marrow. 2000 Jul 15;165(2):725–33.

Kumer SC, Vrana KE. Intricate regulation of tyrosine hydroxylase activity and gene

expression. J Neurochem. 1996 Aug 1;67(2):443–62.

Kurosaki T, Hikida M. B Lymphocytes: Receptors. eLS.

Lanzavecchia A, Sallusto F. Toll-like receptors and innate immunity in B-cell activation and antibody responses. Curr Opin Immunol. 2007 Jun;19(3):268–74.

Lee M, Yang KH, Kaminski NE. Effects of putative cannabinoid receptor ligands, anandamide and 2-arachidonyl-glycerol, on immune function in B6C3F1 mouse splenocytes. Journal of Pharmacology and Experimental …. 1995.

Lindley SE, Gunnet JW, Lookingland KJ, Moore KE. 3,4-Dihydroxyphenylacetic acid concentrations in the intermediate lobe and neural lobe of the posterior pituitary gland as an index of tuberohypophysial dopaminergic neuronal activity. Brain Res. 1990 Jan 1;506(1):133–8.

Lu H, Kaplan BLF, Ngaotepprutaram T, Kaminski NE. Suppression of T cell costimulator ICOS by Delta9-tetrahydrocannabinol. J Leukoc Biol. 2009 Feb;85(2):322–9. PMCID: PMC2631366

Meager A, Wadhwa M. An Overview of Cytokine Regulation of Inflammation and Immunity. onlinelibrary.wiley.com. Chichester, UK: John Wiley & Sons, Ltd; 2001.

Miller SI, Ernst RK, Bader MW. LPS, TLR4 and infectious disease diversity. Nat. Rev. Microbiol. 2005 Jan;3(1):36–46.

Moller G. Antigens: Thymus Independent. els.net.proxy2.cl.msu.edu. Chichester, UK: John Wiley & Sons, Ltd; 2001.

Nance DM, Sanders VM. Autonomic innervation and regulation of the immune system (1987-2007). Brain Behav Immun. 2007 Aug;21(6):736–45. PMCID: PMC1986730

Nath I. Immune Mechanisms against Intracellular Pathogens. onlinelibrary.wiley.com.proxy2.cl.msu.edu. Chichester, UK: John Wiley & Sons, Ltd; 2001.

Néron S, Nadeau PJ, Darveau A, Leblanc J-F. Tuning of CD40-CD154 interactions in human B-lymphocyte activation: a broad array of in vitro models for a complex in vivo situation. Arch. Immunol. Ther. Exp. (Warsz.). 2011 Feb;59(1):25–40.

Noble J, Bailey M. Quantitation of protein. Methods Enzymol. 2009;463:73–95.

Oikonomopoulou K, Reis ES, Lambris JD. Complement System and Its Role in Immune Responses. onlinelibrary.wiley.com. Chichester, UK: John Wiley & Sons, Ltd; 2001.

P Kane L. Lymphocyte Activation: Signal Transduction. onlinelibrary.wiley.com. Chichester, UK: John Wiley & Sons, Ltd; 2001.

Padro CJ, Shawler TM, Gormley MG, Sanders VM. Adrenergic Regulation of IgE Involves Modulation of CD23 and ADAM10 Expression on Exosomes. The Journal of Immunology. 2013 Oct 18. PMCID: PMC3842235

Painter CA, Stern LJ. Conformational variation in structures of classical and non-classical MHCII proteins and functional implications. Immunol. Rev. 2012 Nov;250(1):144–57. PMCID: PMC3471379

Parikh AA, Salzman AL, Kane CD, Fischer JE, Hasselgren PO. IL-6 production in human intestinal epithelial cells following stimulation with IL-1 beta is associated with activation of the transcription factor NF-kappa B. J Surg Res. 1997 Apr 1;69(1):139–44.

Pinaud E, Khamlichi A, Le Morvan C, Drouet M, Nalesso V, Le Bert M, et al. Localization of the 3' IgH locus elements that effect long-distance regulation of class switch recombination. Immunity. 2001 Aug 1;15(2):187–99.

Podojil JR, Kin NW, Sanders VM. CD86 and beta2-adrenergic receptor signaling pathways, respectively, increase Oct-2 and OCA-B Expression and binding to the 3'-IgH enhancer in B cells. 2004 May 28;279(22):23394–404.

Pongratz G, McAlees JW, Conrad DH, Erbe RS, Haas KM, Sanders VM. The Level of IgE Produced by a B Cell Is Regulated by Norepinephrine in a p38 MAPK- and CD23-Dependent Manner. J Immunol. 2006 Sep 1;177(5):2926–38.

Quah BJ, Parish CR. Innate Immune Mechanisms: Nonself Recognition. els.net. Chichester, UK: John Wiley & Sons, Ltd; 2001.

Rasmussen JW, Tam JW, Okan NA, Mena P, Furie MB, Thanassi DG, et al. Phenotypic, morphological, and functional heterogeneity of splenic immature myeloid cells in the host response to tularemia. Infect. Immun. 2012 Jul;80(7):2371–81. PMCID: PMC3416475

Saha B. Antigens. els.net.proxy2.cl.msu.edu. Chichester, UK: John Wiley & Sons, Ltd; 2001.

Sanders VM. The beta2-adrenergic receptor on T and B lymphocytes: Do we understand it yet? Brain Behav Immun. 2012 Feb;26(2):195–200. PMCID: PMC3243812

Schroeder HW Jr., Cavacini L. Structure and function of immunoglobulins. Journal of Allergy and Clinical Immunology. Elsevier; 2010 Feb;125(2):S41–S52.

Shimizu N, Hori T, Nakane H. An interleukin-1 beta-induced noradrenaline release in the spleen is mediated by brain corticotropin-releasing factor: an in vivo microdialysis study in conscious rats. Brain Behav Immun. 1994 Mar 1;8(1):14–23.

Spangelo BL, deHoll PD, Kalabay L, Bond BR, Arnaud P. Neurointermediate pituitary lobe cells synthesize and release interleukin-6 in vitro: effects of lipopolysaccharide and interleukin-1 beta. Endocrinology. 1994 Aug 1;135(2):556–63.

Stavnezer J, Guikema JEJ, Schrader CE. Mechanism and Regulation of Class Switch Recombination. Annu. Rev. Immunol. 2008 Apr;26(1):261–92.

Stevens S, Ong J, Kim U, Eckhardt L, Roeder R. Role of OCA-B in 3'-IgH enhancer function. J Immunol. 2000 May 15;164(10):5306–12.

Vincent-Fabert C, Fiancette R, Cogné M, Pinaud E, Denizot Y. The IgH 3' regulatory region and its implication in lymphomagenesis. Eur J Immunol. 2010 Dec 1;40(12):3306–11.

## Chapter 5: The Interaction of Endogenous CB1/CB2 Receptor Signaling and Norepinephrine in Splenic Humoral Immune Responses

### 5.1: Introduction

Cannabinoids are known immunosuppressive compounds. In humans, this can be seen as a decrease in serum lymphocytes and serum antibody concentrations in *cannabis* users (Klein et al., 1998; Pacifici et al., 2003; Gohary and Eid, 2004). Interestingly, epidemiologic studies have yet to fully identify the consequences of cannabinoid-mediated immunosuppression, despite the wealth of information in animal studies (Greineisen and Turner, 2010; Tashkin, 2013). The most well researched cannabinoid compound in this regard is THC. This compound is known to suppress both cell-mediated (Lu et al., 2009; Karmaus et al., 2012; 2013) and humoral (Schatz et al., 1993; Jan et al., 2003) adaptive immune responses in animal models.

The effects of exogenous cannabinoids occur by pharmacologically mimicking the actions of the endocannabinoids. The endocannabinoid system has largely been identified as inhibitory to the release of neurotransmitters from axon terminals as a form of retrograde trans-synaptic negative feedback. The two most well researched receptors of the endocannabinoid system are CB1 and CB2 (Mackie, 2008; Alger and Kim, 2011).

CB1 is considered to be the major neuronal cannabinoid receptor. CB1 is a G-protein coupled receptors that activate the $G_{i/o}$ pathway leading to decreased cAMP production via inhibition of adenylyl cyclase (Howlett and Mukhopadhyay, 2000; Mackie, 2008). Inhibition of cAMP production decreases protein kinase A activity resulting in a

number of downstream consequences, including a positive shift in the voltage-dependence of A-current $K^+$ channels (Childers and Deadwyler, 1996), inhibition of voltage-gate $Ca^{2+}$ channels (Felder et al., 1993; Mackie et al., 1993; 1995; Gebremedhin et al., 1999), and activation of inwardly rectifying $K^+$ channels (Mackie et al., 1995). It is by these mechanisms that CB1 activation inhibits neurotransmitter release from axon terminals.

CB1 is predominantly localized to the pre-synaptic axon terminals of neurons and found abundantly in the brain (Herkenham et al., 1991; Nyíri et al., 2005; Mackie, 2008). There is also functional evidence for CB1 regulatory processes in sympathetic axon terminals of the atria, vas deferens, and mesenteric arteries (Ishac et al., 1996; Niederhoffer and Szabo, 1999; Ralevic and Kendall, 2002). CB1 mRNA is found in the superior celiac ganglion, vas deferens, and the spleen (Ishac et al., 1996; Schatz et al., 1997). Interestingly, CB1 is also expressed by immune cells, including splenic lymphocytes, but to a much lesser extent than CB2 (Galiegue et al., 1995; Kaplan, 2012). The role of CB1 on immune cells remains somewhat controversial, but a handful of studies have shown the CB1 to mediate, at least partially, some immune effects (Kaplan, 2012). For example (Börner et al., 2008), CB1 transcription is induced by IL-4, a $T_H2$ cytokine, and once up-regulated CB1 stimulation inhibits cAMP formation and IL-2 production, a cytokine critical for T cell responses *in vivo* (Ferrero et al., 2001).

CB1 is activated by both exogenous and endogenous cannabinoids (**See Figure 1.3**). THC is a partial agonist of the CB1 receptor (Kuster et al., 1993; Pertwee, 2008).

The two most well characterized endocannabinoid compounds that bind to CB1 are AEA and 2-AG. Neither of these compounds are stored, but rather made on demand from phospholipid components found in the membrane of post-synaptic neurons (Giuffrida and Mcmahon, 2010). Once synthesized endocannabinoids travel retrogradely across the synapse to act on presynaptic CB1 receptors. Both AEA and 2-AG are partial agonists of CB1, however AEA is more selective for CB1 than 2-AG (Alger and Kim, 2011). AEA and 2-AG are rapidly degraded within minutes by the enzymes FAAH (primarily AEA) and MAGL (primarily 2-AG), thereby terminating their actions (Gerra et al., 2010; Giuffrida and Mcmahon, 2010).

CB2 is considered to be the major peripheral cannabinoid receptor. CB2 mRNA is abundant in peripheral tissues, such as the spleen, but almost completely absent from the brain (Shire et al., 1996; Griffin et al., 2000; Brown et al., 2002). Like CB1, CB2 is coupled to $G_{i/o}$ subtype G-proteins and inhibits adenylyl cyclase, preventing the formation of cAMP (Felder et al., 1995). Very different from CB1, CB2 agonism does not inhibit Q-type $Ca^{2+}$ channels, nor activate inwardly rectifying $K^{+}$ channels (Felder et al., 1995).

CB2 is expressed primarily on cells with an immunologic function, and the spleen was among the first organs shown to have abundant CB2 expression (Brown et al., 2002). CB2 is found on T-cells, B-cells, macrophages, and natural killer cells of the immune system, with B-cells having the highest expression (Galiegue et al., 1995; Schatz et al., 1997; Cabral and Griffin-Thomas, 2009).

CB2 is also activated by both exogenous and endogenous cannabinoids. THC is a partial agonist of CB2 ($K_i$ ~20 nM) (Shire et al., 1996; Griffin et al., 2000). Both AEA and 2-AG are also agonists for CB2, but 2-AG is a more selective and potent agonist than AEA and is expressed in higher quantities in the spleen, bone marrow, and gut (Tanasescu and Constantinescu, 2010; Basu et al., 2011).

The expression of CB2 on immune cells suggests a role for these receptors. A number of *in vitro* studies have been used to assess the effect of CB2 activation on a variety of immune cell functions. Stimulation of CB2 with 2-AG induces the migration of immune cell types, including B cells, monocytes/macrophages, and microglia (Basu and Dittel, 2011). However, migration of mouse macrophages in response to common chemoattractants is inhibited by synthetic CB2 agonists (Ghosh et al., 2006; Montecucco et al., 2008; Raborn et al., 2008). To date, there is no consensus regarding the effect of CB2 on immune cell migration, but it is clear from these studies that they can modulate immune cell chemotaxis. CB2 can also affect immune cell proliferation, however there is no clear consensus with studies showing both stimulatory effects on microglia (Carrier et al., 2004) and suppressive effects on $CD4^+$ T cells (Maresz et al., 2007). In contrast, the ability of CB2 receptors to inhibit cytokine production, especially pro-inflammatory cytokines (IL-10 and IL-23) has been well established (Basu et al., 2011).

The use of *in vitro* assays, while useful, cannot replicate the complexity of the immune system *in vivo*. Thus, the role of cannabinoid receptors *in vivo* has received a good deal of attention, and a wealth of studies have shown the immunosuppressive

ability of cannabis or cannabinoids (Klein et al., 1998). For example, THC was recently shown to broadly inhibit the immune response of mice to influenza infection (Karmaus et al., 2013). These results strongly suggest the site of action in this regard is inhibition of antigen presenting cell function. THC also inhibits the humoral response in mice, as demonstrated by decreasing the number of antibody producing cells in the spleen in response to sRBC administration (Schatz et al., 1993).

In addition to pharmacological experiments using CB receptor agonists, a number of studies have used mice genetically manipulated to lack the CB1 and CB2 receptors. These mice appear phenotypically normal and have a normal immune cell profile (Springs et al., 2008). Yet, in accordance with the immunosuppression observed with CB receptor stimulation, these mice demonstrate enhanced immunity. CB1/CB2 KO mice show increased numbers of antibody producing cells from the spleen in response to sRBC administration (Springs et al., 2008). Accordingly, these mice are useful in establishing the immunomodulatory role of the CB1 and/or CB2 receptors.

The purpose of this chapter is to test the hypothesis that enhanced humoral immunity in CB1/CB2 KO mice is due to increased stimulation of β2AR secondary to increased release NE from splenic sympathetic neurons. First, enhanced humoral immune responses will be evaluated in CB1/CB2 KO mice. Next, the expression of β2AR on splenic B cells will be assessed to confirm the adrenergic sensing ability of B cells in the absence of CB1/CB2. Lastly, the effect of CB1/CB2 KO on the activity of splenic sympathetic noradrenergic neurons, and subsequent β2AR stimulation, will be determined.

## 5.2: Materials and Methods

### 5.2.1: Mice

C57BL/6 WT female mice (NCI/Charles River, Portage, MI) and female CB1/CB2 KO mice were used in all experiment unless otherwise indicated. CB1/CB2 KO mice, on a C57BL/6 background, were created by Dr. Andreas Zimmer at the University of Bonn, Germany as previously described (Jarai et al., 1999; Zimmer et al., 1999; Buckley et al., 2000; Gerald et al., 2006). CB1/CB2 KO mice for these studies were obtained from Drs. Norbert Kaminski and Barbara Kaplan who maintain a breeding colony of CB1/CB2 KO mice at Michigan State University. All animals were housed two to five per cage and maintained in a sterile, temperature (22 ± 1 °C) and light controlled (12L:12D) room, and provided with irradiated food and bottled tap water *ad libitum*. All experiments used the minimal number of animals required for statistical analyses, minimized suffering, and followed the guidelines of the National Institutes of Health Guide for the Care and Use of Laboratory Animals. The Michigan State Institutional Animal Care and Use Committee approved all drug administrations and methods of euthanasia (AUF# 03/12-060-00).

#### 5.2.1.1: CB1/CB2 KO Mouse Genotyping

Polymerase chain reaction (PCR) was used to confirm knockout of CB1 and CB2 receptor genes. Genomic DNA was isolated from ~0.5 cm tail snips using 100 $\mu$l DirectPCR Lysis Reagent (Viagen Biotech, Los Angeles, CA) plus 0.1 mg/ml proteinase K. Samples were incubated overnight at 55°C followed by a 45 min incubation at 85°C.

Crude DNA extract was obtained following centrifugation at 300 RCF for 1 min. One μl of extract was used in a Taqman PCR reaction using *Cnr1* stock primers (CB1 receptor gene) or *Cnr2* (CB2 receptor gene) custom primers (Life Technologies/Applied Biosystems, Foster City, CA) (Kaplan et al., 2010). PCR primers for CB1 receptors were forward 5'-AGGAGCAAGGACCTGAGACA-3', reverse 5'-GGTCACCTTGGCGATCTTAA-3', for CB2 receptor were forward 5'-CCTGATAGGCTGGAAGAAGTATCTAC-3', reverse 5'-ACATCAGCCTCTGTTTCTGTAACC-3', neomycin cassette primers were forward 5'-ACCGCTGTTGACCGCTACCTATGTCT-3', and reverse 5'-TAAAGCGCATGCTCCAGACTGCCTT-3'. The average ± standard deviation Ct values for *Cnr1* and *Cnr2* in WT mice were 25.0 ± 0.54 and 26.0 ± 1.22, respectively. All samples obtained from CB1/CB2 KO tail snips resulted in an "undetermined" Ct value, indicating lack of expression of both *Cnr1* and *Cnr2*.

5.2.2: Materials

aMT: aMT ester (Sigma, St. Louis, MO) was dissolved in 0.9% isotonic saline to a final concentration of 30 mg/ml and administered at dose of 300 mg/kg.

Butoxamine: Butoxamine (B1385, Sigma) was dissolved in sterile isotonic saline at a concentration of 5 mg/ml and administered at doses ranging from 1-10 mg/kg (i.p.).

HBSS: 10x HBSS powder (Gibco) was diluted with ultra-pure $H_2O$ (NaCl 138 mM, KCl 5.3 mM, $Na_2HPO_4$ 0.3 mM, $NaHCO_3$ 4.2 mM, $KH_2PO_4$ 0.4 mM, and glucose 5.6 mM), autoclaved, and stored at 4° C.

Isotonic Saline: 1 L of 0.9% saline was prepared using ultra-pure $H_2O$ and 9 grams of NaCl. The solution was autoclaved and kept closed at room temperature.

LPS: LPS (*E. coli* 055:B5 catalog L2880, lot 066K4096, 5 EU/ng (Limulus lysate assay) and 10 EU/ng (chromogenic assay), Sigma, St. Louis, MO) was dissolved in RPMI-1640 at used at a final concentration of 10 μg/ml for *in vitro* studies. For *in vivo* experiments, LPS was dissolved in HBSS to a concentration of 50 μg/ml and injected at 25 μg per mouse (i.p.).

PBS: NaCl 137 mM, KCl 2.7 mM, $Na_2HPO_4$ 10 mM, and $KH_2PO_4$ 1.8 mM in ultra-pure $H_2O$.

5.2.3: Isolation of the Spleen Capsule and Splenocytes

After euthanasia spleens were removed by an incision in the left lateral abdomen under sterile conditions, which entails spraying the area of removal with 70% ethanol and using ethanol cleaned scissors and forceps to cut through the skin, and underlying

muscle and connective tissue. The spleen was placed in a 6-well plate and mechanically crushed with the blunt end of a 10 ml syringe in 2 ml of HBSS to separate the spleen capsule (insoluble tissue) from the splenocytes (contained in the disruption supernatant). The spleen capsule was removed from the supernatant using forceps and taken whole or divided into two parts using ethanol-cleaned scissors depending on the needs of the experiment. Splenocytes were separated from the disruption supernatant by centrifugation at 300 RCF for 5 min and the supernatant was decanted. The separated splenocytes were then re-suspended in differing buffers and taken whole or divided into two parts depending on the needs of the experiment.

5.2.4: Neurochemistry

All samples were placed in ice-cold tissue buffer following isolation or dissection and kept frozen at -80°C until analysis. Samples were thawed on the day of analysis and sonicated with 3 one-sec bursts (Sonicator Cell Disruptor, Heat Systems-Ultrasonic, Plainview, NY, USA) and centrifuged at 18,000 RCF for 5 min in a Beckman-Coulter Microfuge 22R centrifuge. The supernatant from the first centrifugation of the spleen capsule was removed and spun again at 18,000 RCF for 5 min in a Beckman-Coulter Microfuge 22R centrifuge before being brought up to 100 µl (q.s.) with fresh cold tissue buffer. Spleen samples were then filtered using a 0.2 µM syringe driven Millex-LG filter (Millipore, Billerica, MA).

All samples were analyzed for NE content using HPLC-ED (Lindley et al., 1990; Eaton et al., 1994) using C18 reverse phase columns (ESA Inc., Sunnyvale, CA)

combined with a low pH buffered mobile phase (0.05 M Sodium Phosphate, 0.03 M Citrate, 0.1 mM EDTA at a pH of 2.65) composed of 5-15% methanol and 0.03-0.05% sodium octyl sulfate. Oxidation of NE was measured at a constant potential of -0.4 V by coulometric detection using a Coulochem Electrochemical Detector (Thermo Scientific). The amount of NE in the samples was determined by comparing peak height values (as determined by a Hewlett Packard Integrator, Model 3395) with those obtained from known standards run on the same day. Tissue pellets were dissolved in 1 N NaOH and assayed for protein using the BCA method (Noble and Bailey, 2009).

5.2.5: Western Blot

All samples were placed in ice-cold lysis buffer (water containing 1% Triton-x 100, 250 mM sucrose, 50 mM NaCl, 20 mM tris-HCl, 1 mM EDTA, 1 mM PMSF protease inhibitor cocktail, 1 mM DTT) immediately following isolation and kept frozen at -80°C until analysis. On the day of analysis samples were thawed, heated for 30 min at 100° C, sonicated for 8 sec, and spun at 12,000 RCF for 5 min. The supernatant was collected and a BCA protein assay performed (Noble and Bailey, 2009). Equal amounts of protein were separated using SDS-PAGE and transferred to PVDF-FL membranes (Millipore, Billerica, MA). The resulting membranes were reacted against antibodies for TH (AB152 1:2000, Millipore, Billerica, MA), whose intensities were normalized to β-Actin (8H10D10 1:8000, Cell Signaling, Danvers, MA) to account for loading variability. Each PVDF-FL membrane contained samples representing all experimental conditions to avoid variability due to run, transfer, or antibody exposure conditions. Blots were

visualized and quantified using an Odyssey Fc Infrared Imaging system (Li-Cor, Lincoln, NE) by utilization of IRDye conjugated secondary antibodies, goat anti-Mouse 800CW (1:20,000) and/or goat anti-rabbit 680LT (1:20,000).

5.2.6: Flow Cytometry

5.2.6.1: Surface antibody labeling for flow cytometry

All staining protocols were performed in 96-well round bottom plates (BD Falcon, Franklin Lakes, NJ). Splenocytes were washed 3x with HBSS by centrifugation at 1000 RCF for 5 min, the supernatant was decanted, and the cells re-suspended in HBSS. Cultured splenocytes were then incubated for 30 min on ice in the dark in a 1x solution of near IR (APY-Cy7) live/dead stain (#L10119, Invitrogen, Grand Island, NY), a step which was omitted for splenocytes obtained directly from spleens. Following a wash in HBSS (as described above), splenocytes were then washed with FACS buffer (HBSS, 1% bovine serum albumin, 0.1% sodium azide, pH 7.6) as was done with HBSS. Surface Fc receptors were blocked with anti-mouse CD16/CD32 [0.5 mg/ml] (#553142, BD Biosciences, Franklin Lakes, NJ) at 0.5 µl/well, IgM was blocked with anti-IgM [0.5 mg/ml] (#553425, BD Biosciences) at 1 µl/well, and IgG was blocked with anti-IgG [1.3 mg/ml] (#115-006-071, Jackson Immunoresearch, West Grove, PA) at 0.5 µl/well for 15 min each at RT. Cells were stained for 30 min at RT with the following antibody clones: CD19 (clone 6D5) [0.2 mg/ml] (Biolegend, San Diego, CA) at 1.25 µl/well and β2AR [0.25 mg/ml] (#AP7263d, Abgent, San Diego, CA) at 2 µl/ well. Cells were then washed 3x with FACS buffer. A secondary antibody for β2AR, donkey anti-rabbit DyLight 649

(clone Poly4064) [0.5 mg/ml] (Biolegend), at 0.5 µl/well was incubated for 30 min at RT. Subsequently cells were washed with FACS buffer, fixed with Cytofix (BD Biosciences) for 15 min at RT, washed 3x with FACS buffer, and finally suspended in FACS buffer for intracellular staining. Stained and fixed cells were stored in the dark at 4$^{o}$C for up to 2 weeks.

5.2.6.2: Intracellular antibody labeling for flow cytometry

Within 2 weeks of surface staining, cells were washed 2x with Perm/Wash (BD) and incubated with Perm/Wash for 30 min at RT. Fluorescently labeled antibodies for IgM (Clone II/41) [0.5 mg/mL] (Biolegend) were added at 1 µl/well for 30 min. Cells were washed 2x with Perm/Wash and suspended in FACS buffer. After intracellular staining, cells were analyzed the same day.

5.2.6.3: Flow Cytometry Analysis

Fluorescent staining was analyzed using a BD Biosciences FACSCanto II flow cytometer. Data were analyzed using Kaluza (Beckman Coulter Inc., Brea, CA) or FlowJo software (Tree Star Inc., Ashland, OR). Compensation and voltage settings of fluorescent parameters were performed using fluorescence-minus-one controls. Cells were gated on singlets (forward scatter height versus area) followed by determination of live cells (low APC-Cy7 signal) only in samples obtained from splenocyte culture. Cells were then gated to select lymphocytes using forward versus side scatter. For some analyses, an additional gate was created for CD19 or β2AR expression to select for B

cells or β2AR expressing cells, respectively. These sequential gates were used to identify IgM producing B cells and IgM producing B cells that express β2AR. The percentage of cells gated to individual populations relative to the entire population were collected and analyzed. Additionally, the numerical intensity of the fluorescent signal, termed the MFI, was also quantified and analyzed.

5.2.7: ELISA

Serum IgM and IgG were detected by sandwich ELISA. In preparation, 100 µl of 1 µg/ml anti-mouse IgM (Sigma-Aldrich, St. Louis, MO) or 1 µg/ml anti-mouse IgG (Sigma-Aldrich) was added to wells of a 96-well microtiter plate and stored at 4$^{o}$C overnight. After the pre-coating step, the plate was washed twice with 0.05% Tween-20 in PBS and three times with $H_2O$. Following this, 200 µl of 3% BSA-PBS was added to the wells and incubated at RT for 1.5 h to block nonspecific binding followed by the same washing steps described above. Serum samples were diluted and added to the coated plate (100 µl) for 1.5 h at RT. After the incubation, the plate was washed again, followed by addition of 100 µl of HRP-conjugated goat anti-mouse IgM (A8786, Sigma-Aldrich) or HRP-conjugated goat IgG (A3673, Sigma-Aldrich). Following the HRP incubation for 1.5 h at RT, any unbound detection antibody was washed away from the plate, and 100 µl ABTS (Roche Applied Science, Indianapolis, IN) added. The detection of the HRP substrate reaction was conducted over a 1 h period using a plate reader with a 405-nm filter (Bio-Tek). The KC4 computer analysis program (Bio-Tek) calculated the concentration of IgM or IgG in each sample based on a standard curve generated from

the absorbance readings of known concentrations of IgM (range 6-1600 pg/ml, clone TEPC 183, Sigma-Aldrich) or IgG (range 3-800 pg/ml, Sigma-Aldrich).

### 5.2.8: Statistical Analysis

#### 5.2.8.1: Statistical Comparisons

Prism software version 4.0a was used to make statistical comparisons between groups using the appropriate statistical test. Differences with a probability of error of less than 5% ($p<0.05$) were considered statistically significant. Two group comparisons were done using the Student's *t*-test. Two group comparisons where in one group had more than one degree or factor were done using a One-way ANOVA followed by a Bonferroni or Tukey's post-test for multiple comparisons. Experiments in which there were two groups with more than one degree or factor in each group, such as a 2x2 design, were analyzed using a Two-way ANOVA followed by Bonferroni post-test for multiple comparisons.

#### 5.2.8.2: aMT Experimentation

In experiments in which aMT was used to assess neuronal activity, NE concentrations from aMT treated and non-aMT (saline) treated mice were used for a regression analysis with saline animals acting as the 0 time control and aMT animals a 4 h time point. The rate constant was determined using this formula: $=(\text{Log}_{10}[B]-\text{Log}_{10}[A])/(-0.434*t)$. Where B is the concentration of NE after aMT, A is the concentration of A in saline treated animals, and t is the time of aMT treatment (Brodie

et al., 1966). The slopes were compared via t-test using the mean slope, SEM, and an n equal to the total number of data points used in the analysis to account for the total number of independent measurements used to generate the regression equations. Differences with a probability of error of less than 5% were considered statistically significant.

5.2.8.3: Flow Cytometry Data Handling

Population percentage data was transformed in Excel (Microsoft Corporation, Redmond, WA) to a parametric form before ANOVA analysis using the formula: =arcsin(sqrt(DATA/100)) (Ahrens et al., 1990). Raw percentage data was used for visual representations, while statistical significance indicated on these figures was performed on the transformed data.

5.3: Results

5.3.1: Enhanced humoral immunity In CB1/CB2 KO mice

Humoral immunity in CB1/CB2 KO mice was compared with that of WT mice using antibody production from B cells and the number of B cells as indices. Here it is shown that CB1/CB2 KO have elevated serum IgM and IgG concentrations compared to WT mice, even when immunologically naïve (**Figures 5.1 and 5.2**). One potential cause for increased serum antibodies is an increase in the number of antibody producing B cells. To test this possibility the percentage of IgM producing B cells was assessed in the spleen by flow cytometry. It was discovered that CB1/CB2 KO have

more splenic IgM producing B cells than WT mice (**Figures 5.3 and 5.4**). Based upon these results, it was hypothesized that CB1/CB2 KO mice would also have enhanced humoral immunity in response to an immune challenge by LPS. Congruent with this hypothesis, serum IgM and IgG levels are elevated in LPS treated CB1/CB2 KO mice (**Figures 5.5 and 5.6**), which was associated with an increase in the population of splenic antibody producing B cells in CB1/CB2 KO mice (**Figures 5.7 and 5.8**). These data support the hypothesis that CB1/CB2 KO mice have enhanced humoral immunity, which is due, at least in part, to an increase in the number of splenic antibody producing B cells.

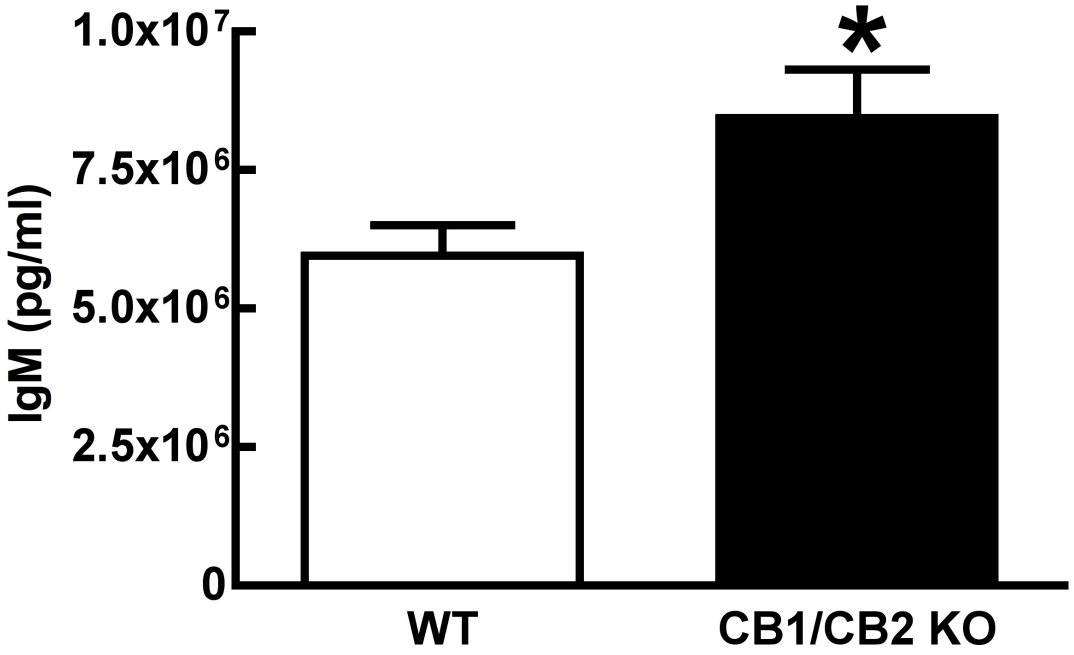


**Figure 5.1. Serum IgM concentrations in immunologically naive WT and CB1/CB2 KO mice.** The serum from female WT and CB1/CB2 KO mice collected and assayed for IgM using ELISA. Columns represent the concentration of IgM (pg/ml) + 1 SEM (n=5). * Significantly differs from WT ($p<0.05$).

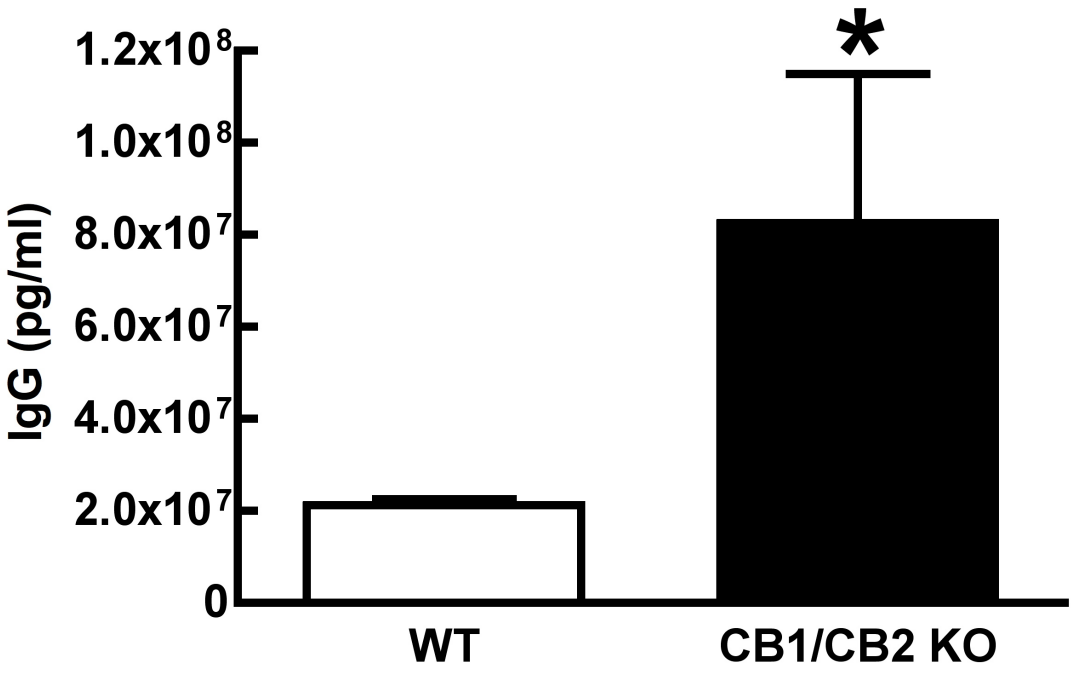


**Figure 5.2. Serum IgG concentrations in immunologically naive WT and CB1/CB2 KO mice.** The serum from female WT and CB1/CB2 KO mice collected and assayed for IgG using ELISA. Columns represent the concentration of IgG (pg/ml) + 1 SEM (n=5). * Significantly differs from WT ($p<0.05$).

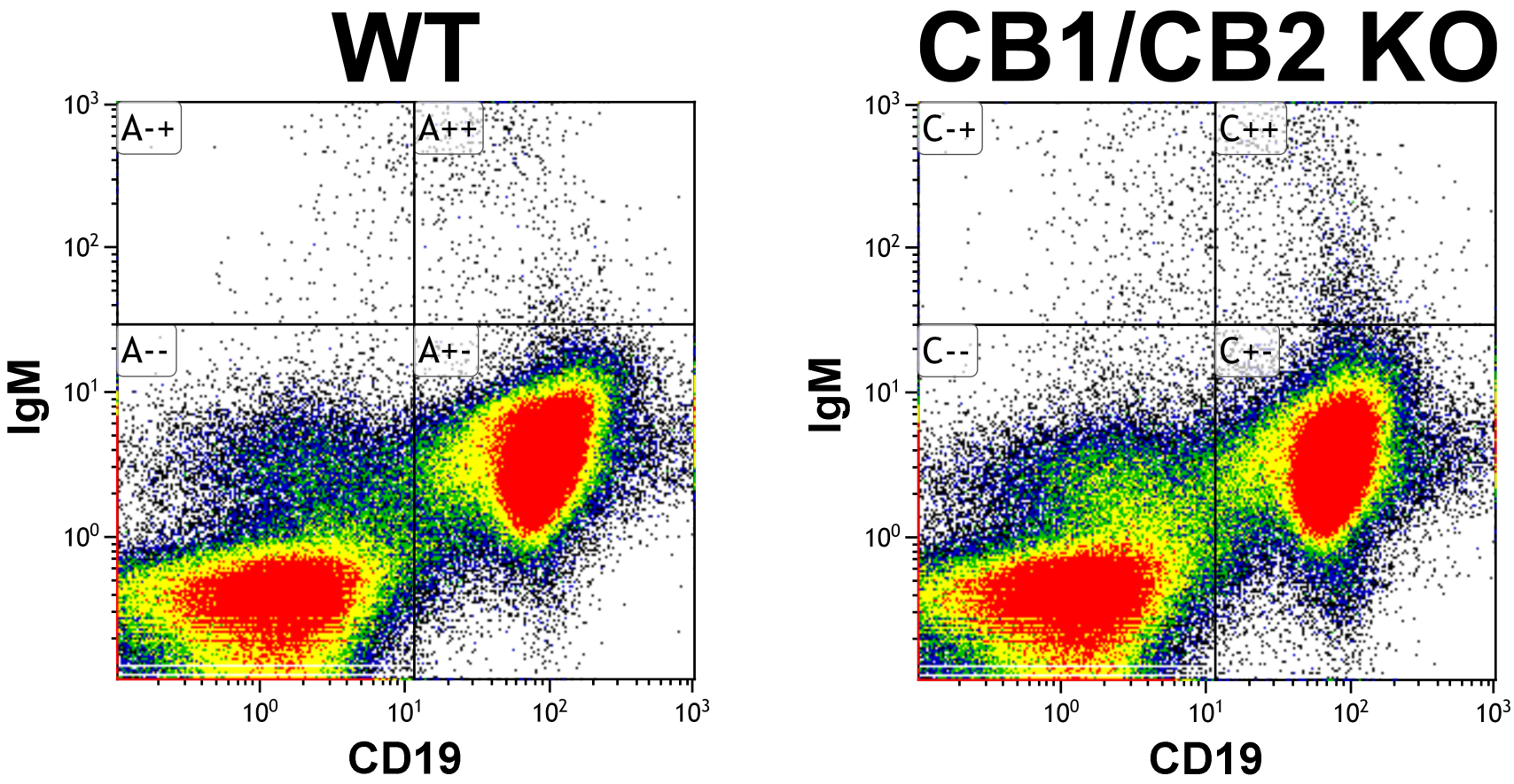


**Figure 5.3. Flow cytometric analysis of splenic IgM producing B cell populations from immunologically naïve WT and CB1/CB2 KO mice.** Lymphocytes were isolated from the spleens of untreated WT and CB1/CB2 KO mice and analyzed by flow cytometry as described. IgM (FITC) producing B cells (CD19-PE-Cy7) reside in the upper right quadrant of the displayed plots. Each plot represents the concatenated data from 3-5 mice.

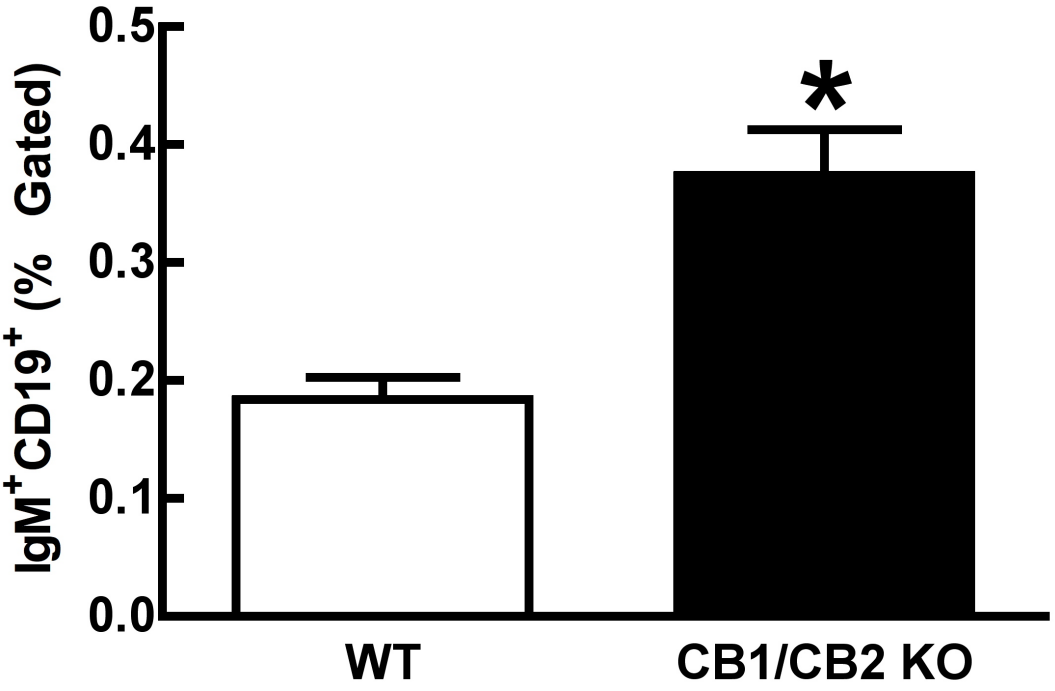


**Figure 5.4. Flow cytometric analysis of splenic IgM producing B cells from immunologically naïve WT and CB1/CB2 KO mice.** Flow cytometry was used to detect B cells (CD19-PE-Cy7) and IgM (FITC) on splenocytes freshly isolated from mice. Cells were gated sequentially on singlet live lymphocytes, prior to plotting CD19 and IgM for analysis. Columns represent the percentage of $IgM^+$ $CD19^+$ cells + 1 SEM (n=5). * Significantly differs from WT ($p<0.05$).

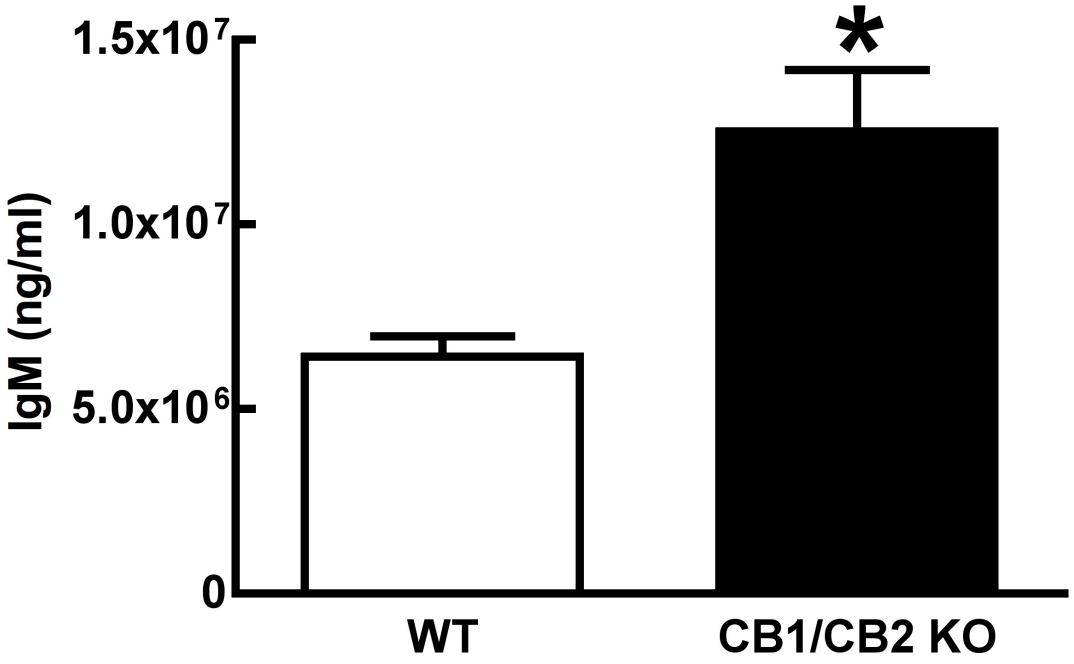


**Figure 5.5. Serum IgM concentrations in WT and CB1/CB2 KO mice treated with LPS.** Four days following an injection with LPS (25 μg; i.p.), the serum from female WT and CB1/CB2 KO mice was collected and assayed for IgM using ELISA. Columns represent the concentration of IgM (ng/ml) + 1 SEM (n=5). * Significantly differs from WT ($p<0.05$).

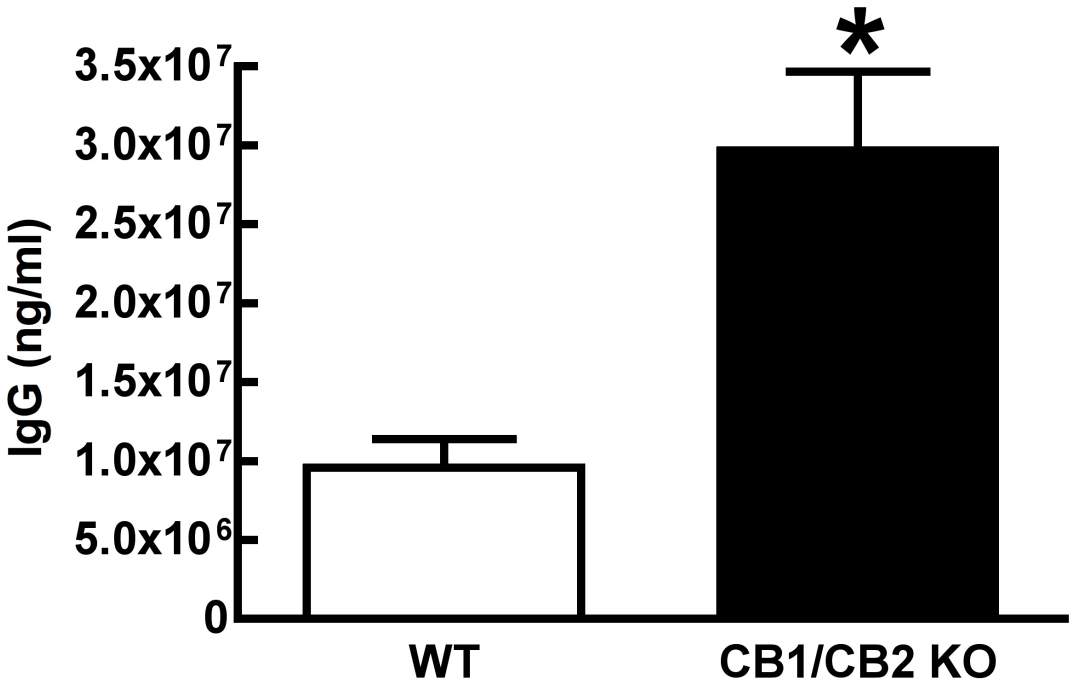


**Figure 5.6. Serum IgG concentrations in WT and CB1/CB2 KO mice treated with LPS.** Four days following an injection with LPS (25 μg; i.p.), the serum from female WT and CB1/CB2 KO mice was collected and assayed for IgG using ELISA. Columns represent the concentration of IgG (ng/ml) + 1 SEM (n=5). * Significantly differs from WT ($p<0.05$).

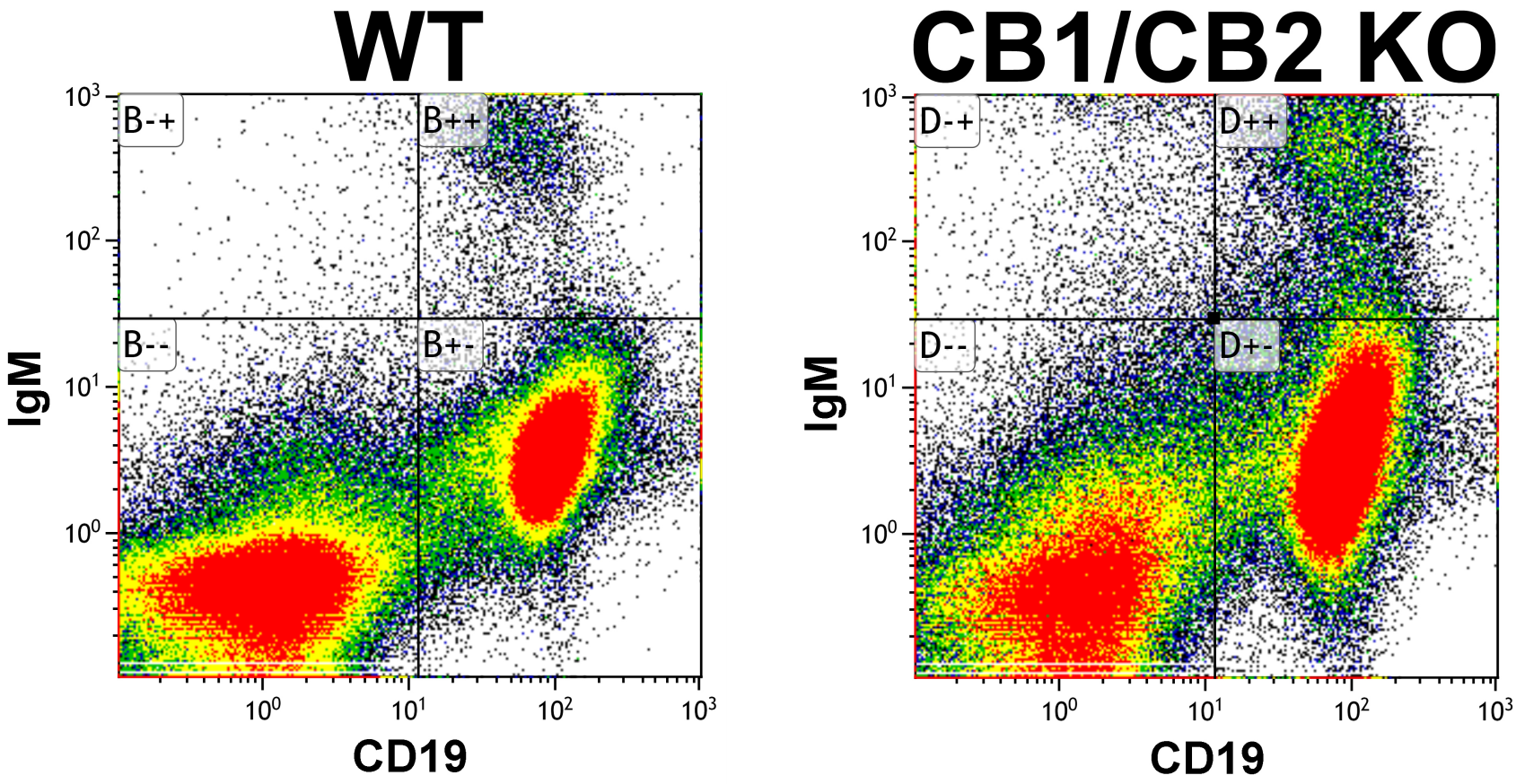


**Figure 5.7. Flow cytometric analysis of splenic IgM producing B cell populations from LPS treated WT and CB1/CB2 KO mice.** Lymphocytes were isolated from the spleens of WT and CB1/CB2 KO mice treated with LPS (25 μg; i.p.) 4 days prior and analyzed by flow cytometry as described. IgM (FITC) producing B cells (CD19-PE-Cy7) reside in the upper right quadrant of the displayed plots. Each plot represents the concatenated data from 3-5 mice.

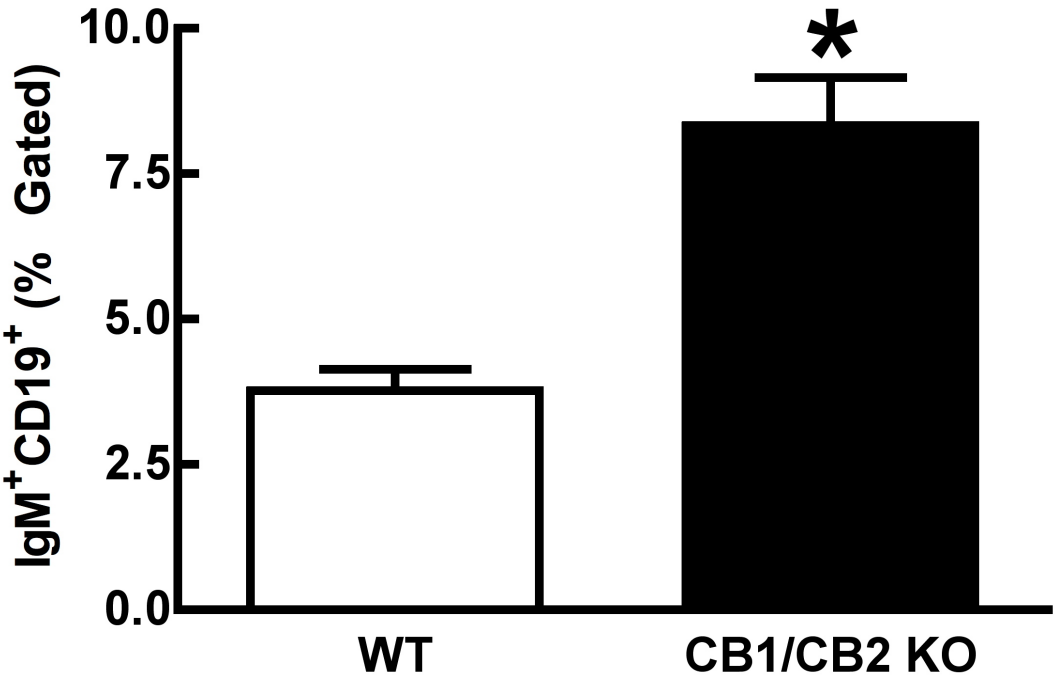


**Figure 5.8. Flow cytometric analysis of splenic IgM producing B cells from WT and CB1/CB2 KO mice treated with LPS.** Flow cytometry was used to detect B cells (CD19-PE-Cy7) and IgM (FITC) on splenocytes isolated from mice treated with LPS (25 μg; i.p.) 4 days prior. Cells were gated sequentially on singlet live lymphocytes, prior to plotting CD19 and IgM for analysis. Columns represent the percentage of $IgM^+$ $CD19^+$ cells + 1 SEM (n=5). * Significantly differs from WT ($p<0.05$).

5.3.2: Elevated β2AR expression on B cells in CB1/CB2 KO mice

The underlying hypothesis of this chapter is that CB1/CB2 KO exhibit enhanced humoral immunity due to enhanced activity of splenic sympathetic noradrenergic neurons. CB1/CB2 KO mice were confirmed to have enhanced humoral immunity. Following this, it was hypothesized that B cells from CB1/CB2 KO mice would also express β2AR, as was seen in WT mice (**Chapter 4**). It was expected that β2AR expression in CB1/CB2 KO mice would be reduced due to activity dependent down-regulation (Zastrow and Kobilka, 1992; Hudson et al., 2010) secondary to an increased rate of NE release and binding to these receptors. Flow cytometry was used to measure the expression of β2AR on B cells and it was discovered that CB1/CB2 KO have a greater population of splenic B cells expressing β2AR (**Figure 5.9**). These data suggest that either there is an interaction between cannabinoid receptors and β2AR such that the lack of CB1/CB2 allows for increased expression of β2AR on lymphocytes, or CB1/CB2 KO mice have a reduced rate of NE release from splenic sympathetic neurons resulting in up-regulation of β2AR.

It was also discovered that CB1/CB2 KO mice possess a larger percentage of β2AR expressing B cells producing IgM when immunologically naïve (**Figures 5.10 and 5.11**) and when immune challenged by LPS (**Figures 5.12 and 5.13**). Thus, the B cell population in CB1/CB2 KO mice possess an enhanced ability to sense NE, namely increased β2AR expression. Furthermore, this population with enhanced adrenergic sensing capacity is able to produce antibodies. These data, in addition to the

hypothesized effect of cannabinoid receptor knockout on NE release, support a role for β2AR activation as the cause for enhanced humoral immunity in CB1/CB2 KO mice.

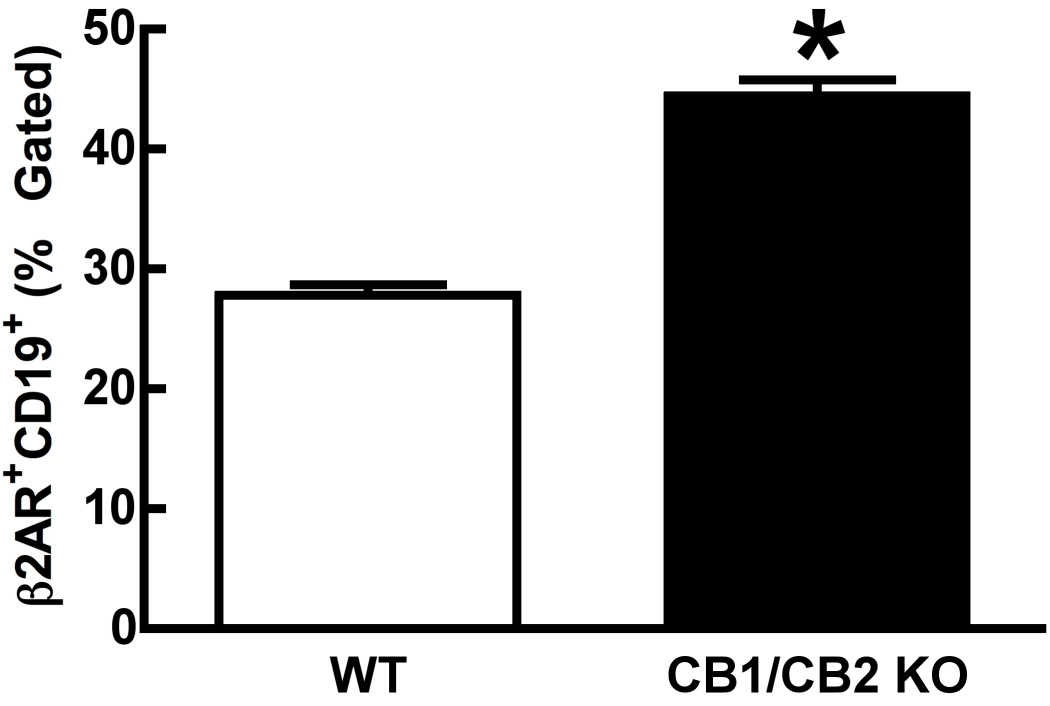


**Figure 5.9. Flow cytometric analysis of splenic B cells expressing β2AR from immunologically naive WT and CB1/CB2 KO mice.** Flow cytometry was used to detect B cells (CD19-PE-Cy7) expressing β2AR (APC) on splenocytes isolated from untreated mice. Cells were gated sequentially on singlet lymphocytes, prior to plotting CD19 and β2AR for analysis. Columns represent the percentage of $\beta2AR^+$ $CD19^+$ cells + 1 SEM (n=5). * Significantly differs from WT ($p<0.05$).

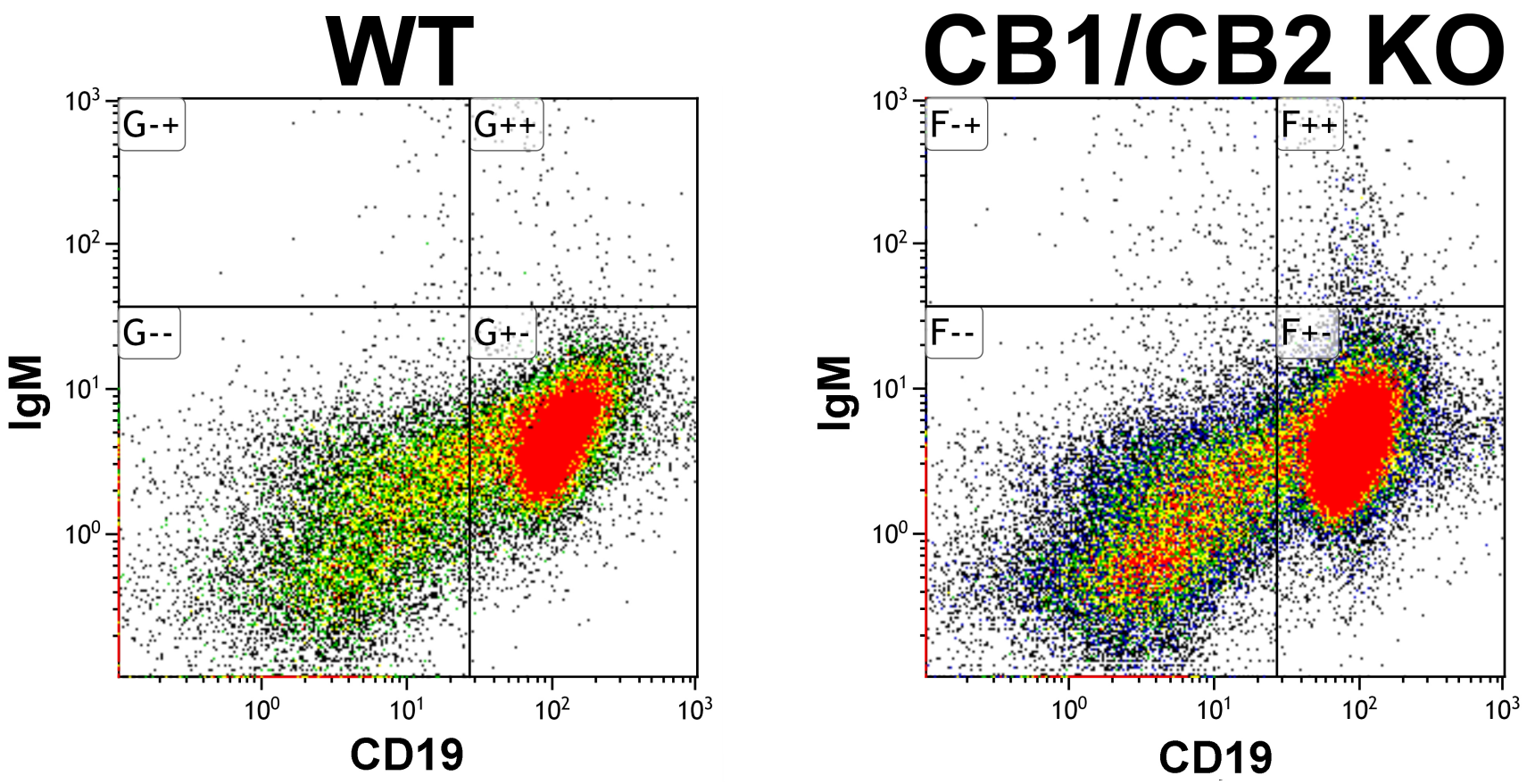


**Figure 5.10. Flow cytometric analysis of splenic IgM producing B cell populations expressing β2AR from immunologically naïve WT and CB1/CB2 KO mice.** Lymphocytes were isolated from the spleens of untreated WT and CB1/CB2 KO mice and analyzed by flow cytometry as described. Cells were gated sequentially on singlet lymphocytes expressing β2AR (APC) prior to plotting CD19 and IgM for analysis. IgM (FITC) producing B cells (CD19-PE-Cy7) reside in the upper right quadrant of the displayed plots. Each plot represents the concatenated data from 3-5 mice.

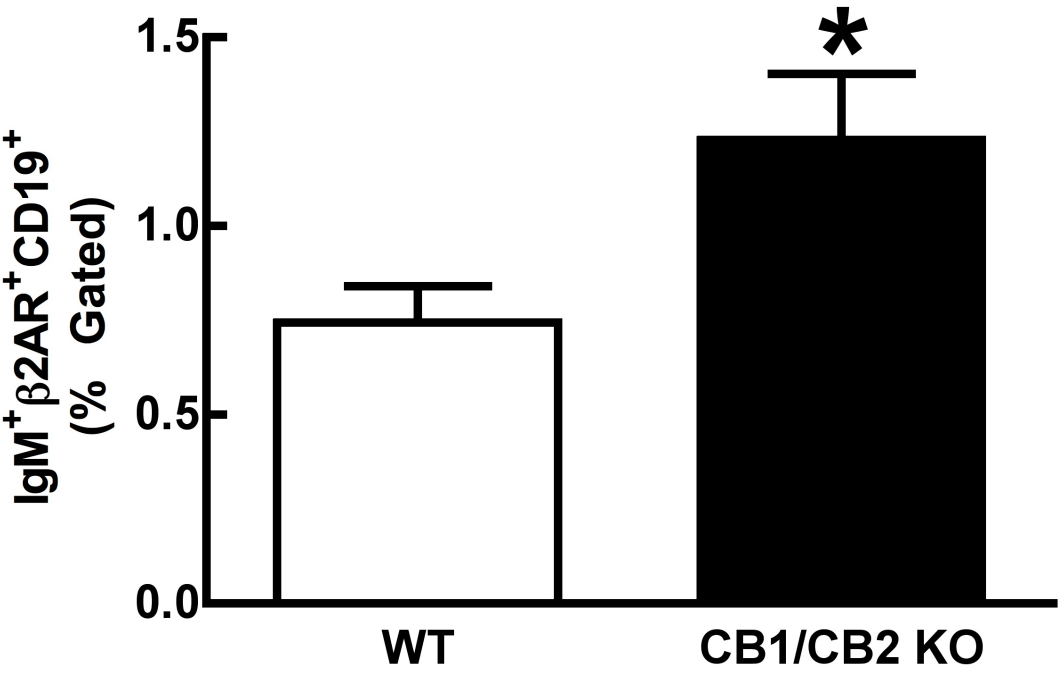


**Figure 5.11. Flow cytometric analysis of IgM producing splenic B cells expressing β2AR from immunologically naive WT and CB1/CB2 KO mice.** Flow cytometry was used to detect IgM (FITC) producing B cells (CD19-PE-Cy7) expressing β2AR (APC) on splenocytes isolated from untreated mice. Cells were gated sequentially on singlet lymphocytes expressing β2AR, prior to plotting CD19 and IgM for analysis. Columns represent the percentage of $IgM^+$ $\beta2AR^+$ $CD19^+$ cells + 1 SEM (n=5). * Significantly differs from WT ($p<0.05$).

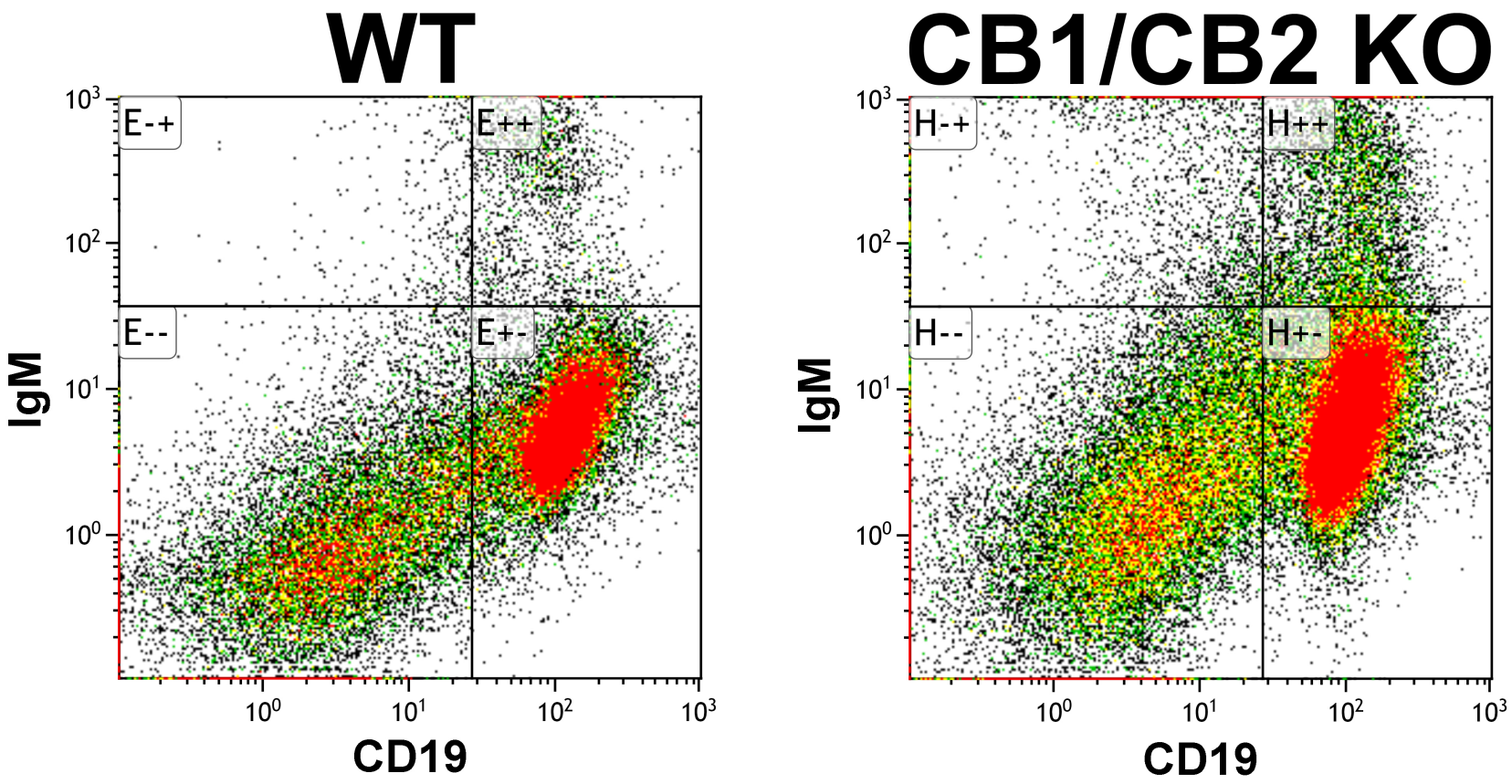


**Figure 5.12. Flow cytometric analysis of splenic IgM producing B cell populations expressing β2AR from LPS treated WT and CB1/CB2 KO mice.** Lymphocytes were isolated from the spleens of WT and CB1/CB2 KO mice treated with LPS (25 μg; i.p.) 4 days prior and analyzed by flow cytometry as described. Cells were gated sequentially on singlet lymphocytes expressing β2AR (APC) prior to plotting CD19 and IgM for analysis. IgM (FITC) producing B cells (CD19-PE-Cy7) reside in the upper right quadrant of the displayed plots. Each plot represents the concatenated data from 3-5 mice.

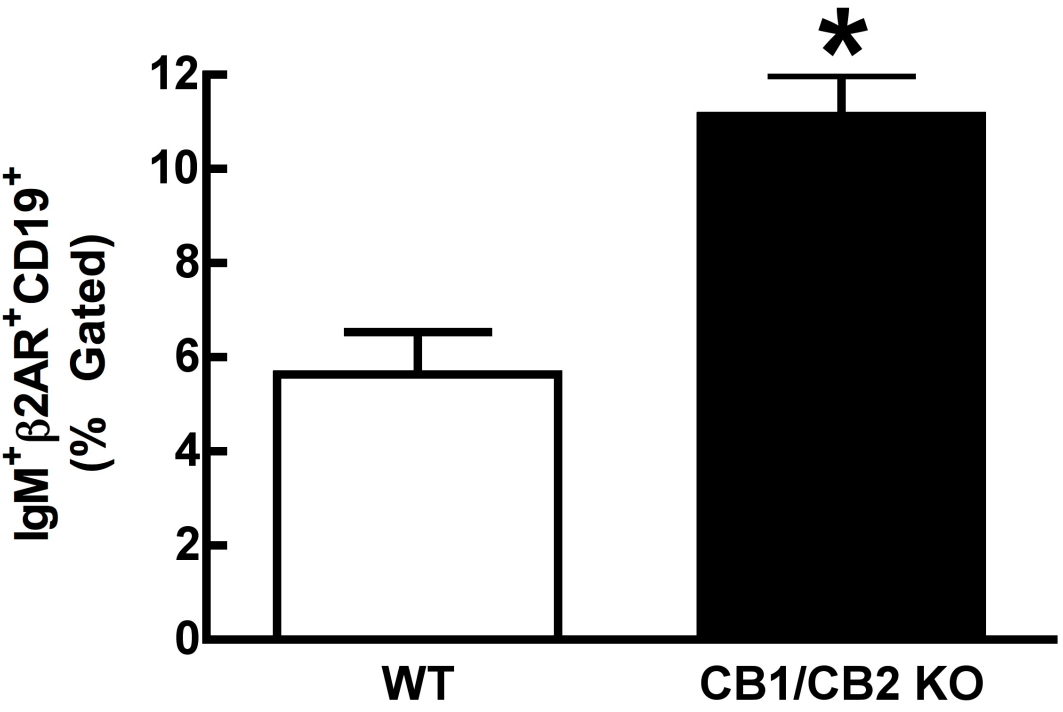


**Figure 5.13. Flow cytometric analysis of IgM producing splenic B cells expressing β2AR from WT and CB1/CB2 KO mice treated with LPS.** Flow cytometry was used to detect IgM (FITC) producing B cells (CD19-PE-Cy7) expressing β2AR (APC) on splenocytes isolated from WT and CB1/CB2 KO mice treated with LPS (25 μg; i.p.) 4 days prior. Cells were gated sequentially on singlet lymphocytes expressing β2AR, prior to plotting CD19 and IgM for analysis. Columns represent the percentage of $IgM^+$ $\beta2AR^+$ $CD19^+$ cells + 1 SEM (n=5). * Significantly differs from WT ($p<0.05$).

5.3.3: Splenic sympathetic noradrenergic neuronal activity in CB1/CB2 KO mice

Following the discovery of enhanced adrenergic sensing capacity of B cells in CB1/CB2 KO mice, the effect of cannabinoid receptor knockout on splenic sympathetic activity was tested. It was hypothesized that these mice will have enhanced splenic noradrenergic neuronal activity due to a lack of the inhibitory effects of CB1 on sympathetic axon terminals. First, it was observed that CB1/CB2 KO mice have an increased concentration of NE in the spleen capsule compared to WT (**Figure 5.14**). This data is suggestive of increased noradrenergic neuronal activity, as increased splenic NE concentrations were previously positively correlated with increased activity (**Chapters 3 and 4**). Despite elevated NE concentrations in the spleen capsule of CB1/CB2 KO mice, TH is not elevated in these mice (**Figure 5.15**). Previously it was observed that increased noradrenergic activity in the spleen capsule was correlated with increased NE concentrations and TH expression (**Chapter 4**). Therefore, the discordance of these data, in the light of the current hypothesis, was further investigated.

To this end, the rate of NE release in CB1/CB2 KO mice was assessed using the aMT method. The results revealed that under immunologically naïve conditions CB1/CB2 KO mice have a decrease in the rate constant of NE utilization in the spleen capsule, associated with increased NE concentrations (**Figure 5.16**). When challenged with LPS, there is no significant difference between WT and CB1/CB2 KO with regards to the rate of spleen capsule NE utilization (**Figure 5.17**). These data argue against a role for CB1 inhibition of NE release in the spleen, and suggest that CB1/CB2 receptors

are permissive to a regular rate of NE release as a decrease in NE utilization was observed in the spleen capsule under immunologically naïve conditions. These data do not support the hypothesis that increased NE release is the cause for enhance humoral immunity in CB1/CB2 KO mice.

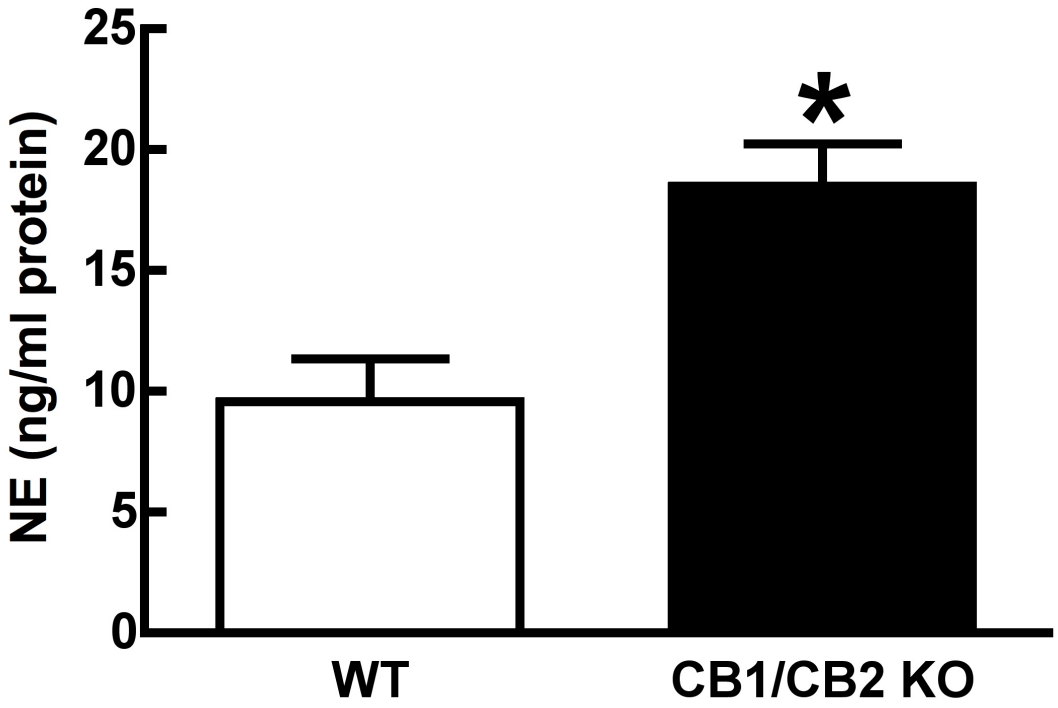


**Figure 5.14. Spleen capsule NE concentrations in immunologically naïve WT and CB1/CB2 KO mice.** The spleen capsule was collected from untreated female WT and CB1/CB2 KO mice. Spleen capsule samples were prepared for and analyzed by HPLC-ED for NE as described. Columns represent average concentration of NE + 1 SEM (n=6-8). * Differs from WT ($p<0.05$).

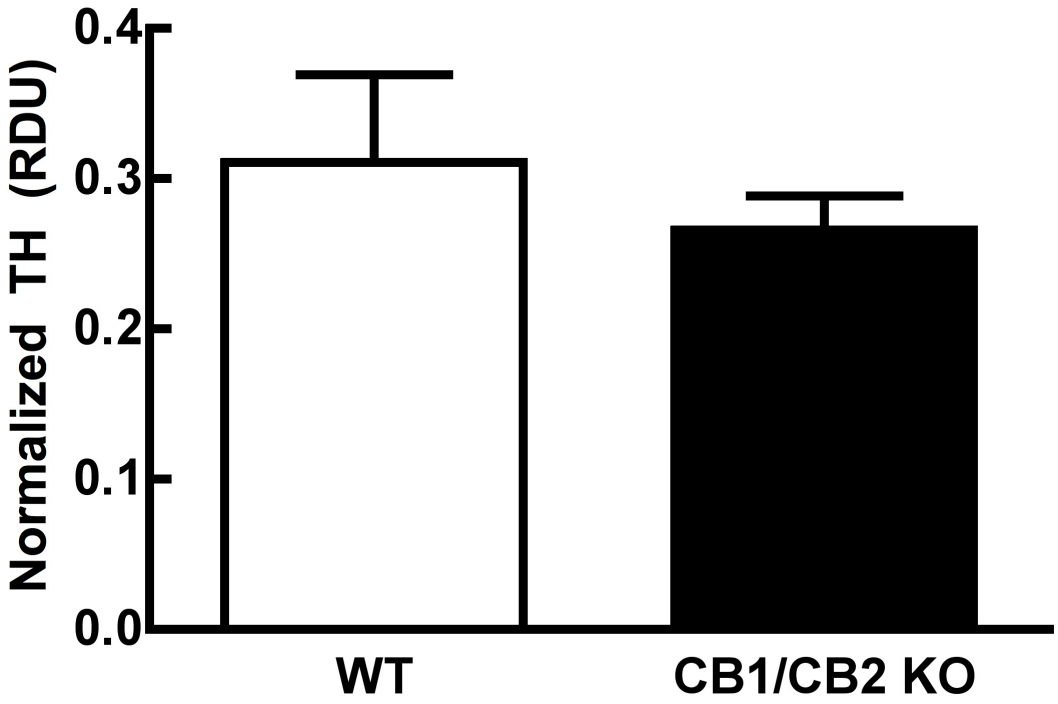


**Figure 5.15. Spleen capsule TH content in immunologically naïve WT and CB1/CB2 KO mice.** The spleen capsule was collected from untreated female WT and CB1/CB2 KO mice. Spleen capsule samples were prepared for and analyzed by Western blot for TH as described. Columns represent average normalized amount of TH in the spleen + 1 SEM (n=6-8). * Differs from WT ($p<0.05$).

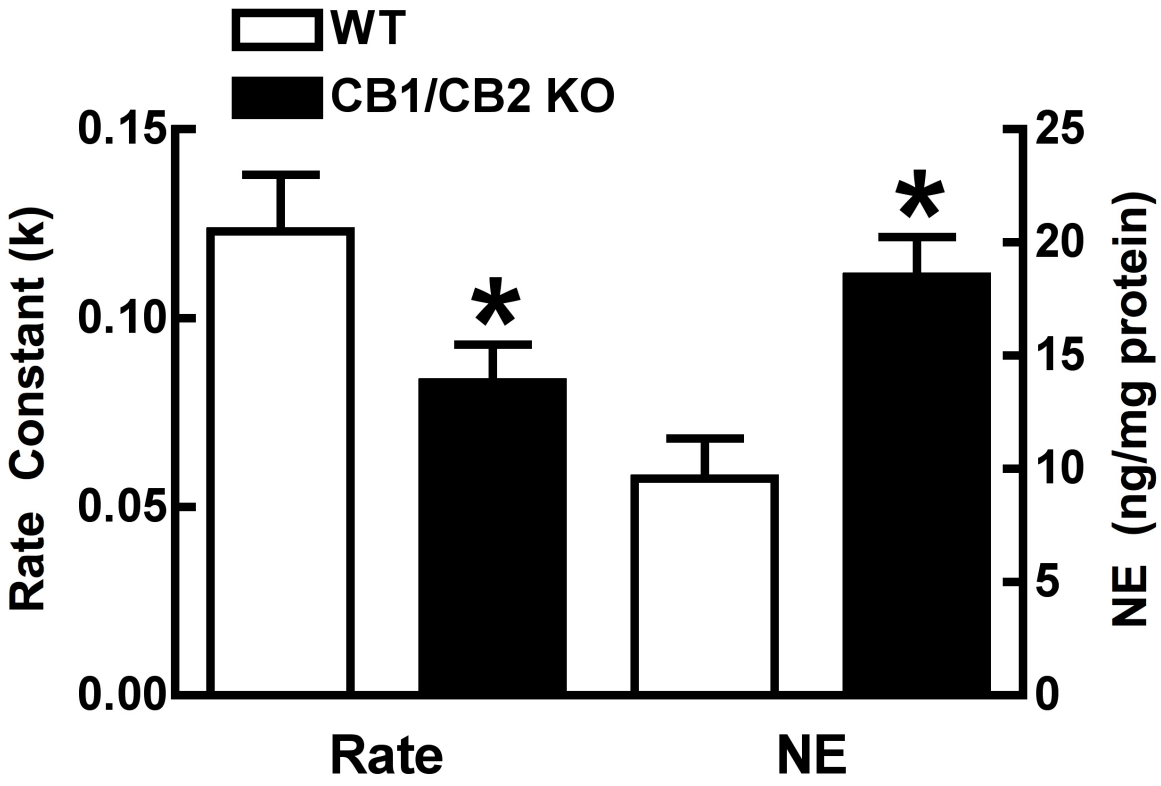


**Figure 5.16. Spleen capsule noradrenergic neuron activity in immunologically naïve WT and CB1/CB2 KO mice.** Female WT and CB1/CB2 KO mice received a single injection of saline/aMT (300 mg/kg, i.p.) and were sacrificed by decapitation 4 h later. The spleen capsule was collected and prepared for analysis of NE by HPLC-ED. Non-aMT treated mice were used for the 0 h time point and a regression analysis performed to determine the rate of NE utilization. Columns depict the average rate constant of NE utilization or the concentration of NE (ng/mg protein) in non-aMT treated mice + one SEM. * Differs from WT ($p<0.05$).

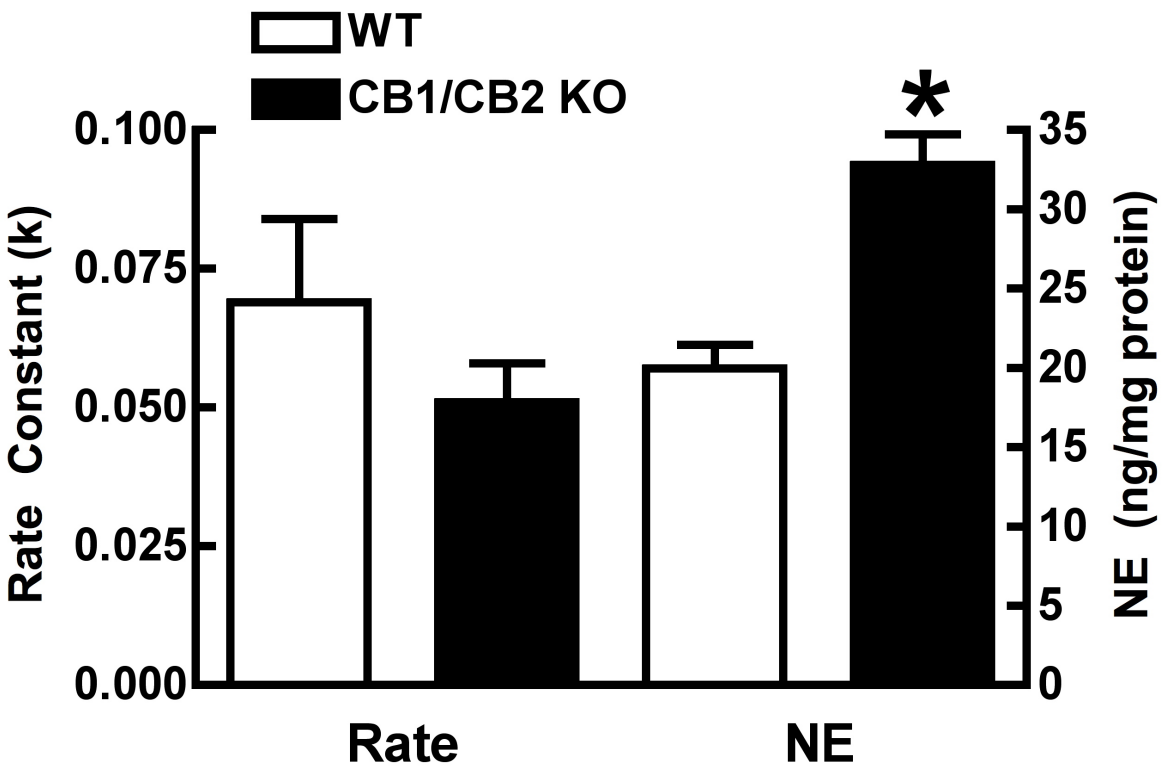


**Figure 5.17. Comparison of the effects of LPS on spleen capsule noradrenergic neuron activity in WT and CB1/CB2 KO mice.** Female WT and CB1/CB2 KO mice received a single injection of saline/aMT (300 mg/kg, i.p.) immediately followed by single injection of HBSS or LPS (25 μg; i.p.). Mice were sacrificed 4 h after the LPS injection and the spleen capsule collected and prepared analysis of NE by HPLC-ED. Non-aMT treated mice were used for the 0 h time point and a linear regression analysis performed to determine the rate of NE utilization. Columns depict the average rate constant of NE utilization or the concentration of NE (ng/mg protein) in non-aMT treated mice + one SEM. * Differs from WT ($p<0.05$).

5.3.4: Enhanced humoral immunity in CB1/CB2 KO mice is not due to increased stimulation of β2AR

Despite the finding that CB1/CB2 receptor deficiency does not affect NE release in the spleen, it was still hypothesized that β2AR may play a role in enhanced humoral immunity, based upon the finding of increased β2AR expression by splenic B cells. It was hypothesized that enhanced β2AR stimulation, due to an increased presence of these receptors on B cells, may be the cause of enhanced humoral immunity following knockout of the CB1/CB2 receptors.

To test this hypothesis β2AR were blocked by butoxamine, a β2AR specific antagonist, during an immune challenge by LPS. Serial butoxamine injections were used to antagonize β2AR for 24 h before and after an immune challenge by LPS. This time frame chosen because it had been previously published that adrenergic effects on immunity likely happen within 24 h before or after an immune challenge (Kohm and Sanders, 2001; Sanders, 2012). Consistent with data presented above, enhancement of humoral immunity in CB1/CB2 KO, as compared with WT mice, was observed in all endpoints (**Figures 5.18-21**). Butoxamine failed to alter serum concentrations of IgM (**Figure 5.18**) or IgG (**Figure 5.19**) in WT or CB1/CB2 KO mice. Moreover, antagonism of β2AR with butoxamine did not alter the percentage of B cells expressing β2AR (**Figure 5.20**), or the subset of these cells producing IgM (**Figure 5.21**) in WT or CB1/CB2 KO mice. These data are inconsistent with the hypothesis that increased β2AR expression and stimulation is responsible for enhanced humoral immunity in CB1/CB2 KO mice.

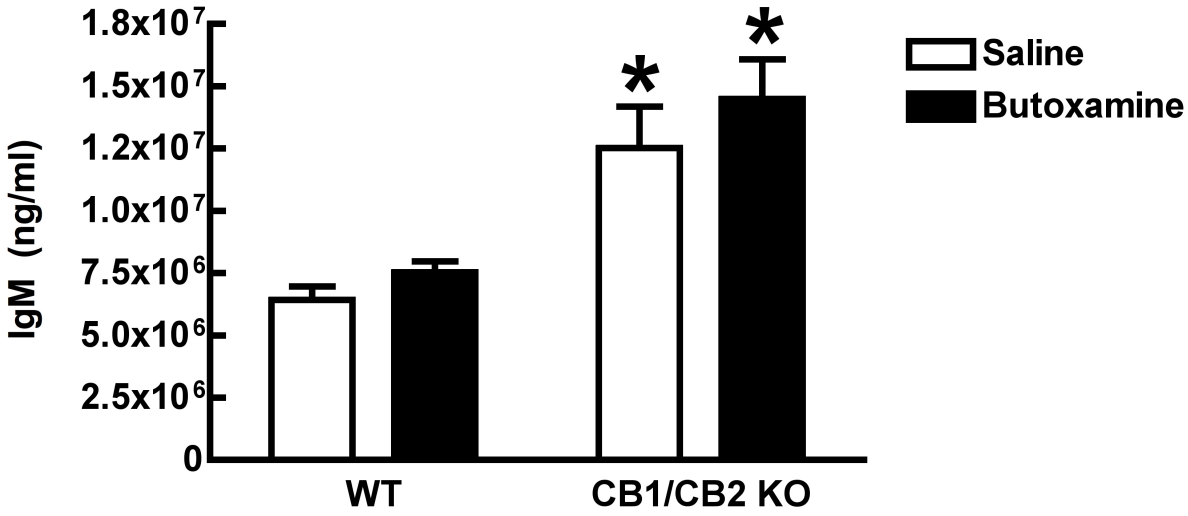


**Figure 5.18. Lack of effect of β2AR antagonism on serum IgM concentrations in LPS exposed WT and CB1/CB2 KO mice.** Female WT and CB1/CB2 KO mice were injected 8 times with butoxamine (10 mg/kg; i.p.), or vehicle, every 6 h for 48 h. Mice received a single injection of LPS (25 μg; i.p.) one h prior to the 5$^{th}$ injection and were sacrificed 4 days later. Serum was collected and assayed for IgM using ELISA. Columns represent the concentration of IgM (ng/ml) + 1 SEM (n=5). * Significantly differs from WT of the same treatment group ($p<0.05$).

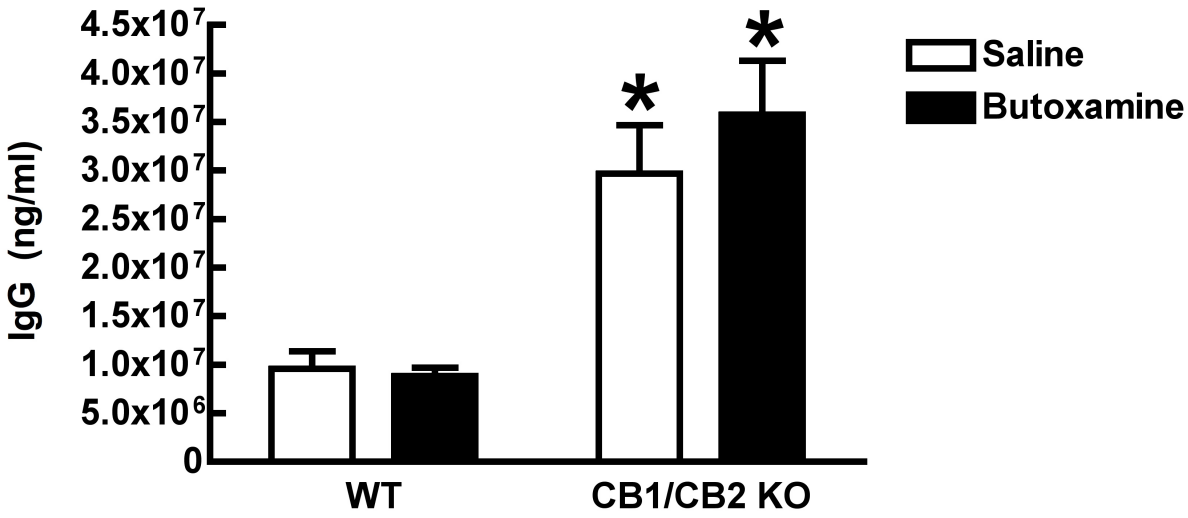


**Figure 5.19. Lack of effect of β2AR antagonism on serum IgG concentrations in LPS exposed WT and CB1/CB2 KO mice.** Female WT and CB1/CB2 KO mice were injected 8 times with butoxamine (10 mg/kg; i.p.), or vehicle, every 6 h for 48 h. Mice received a single injection of LPS (25 μg; i.p.) one h prior to the 5$^{th}$ injection and were sacrificed 4 days later. Serum was collected and assayed for IgG using ELISA. Columns represent the concentration of IgG (ng/ml) + 1 SEM (n=5). * Significantly differs from WT of the same treatment group ($p<0.05$).

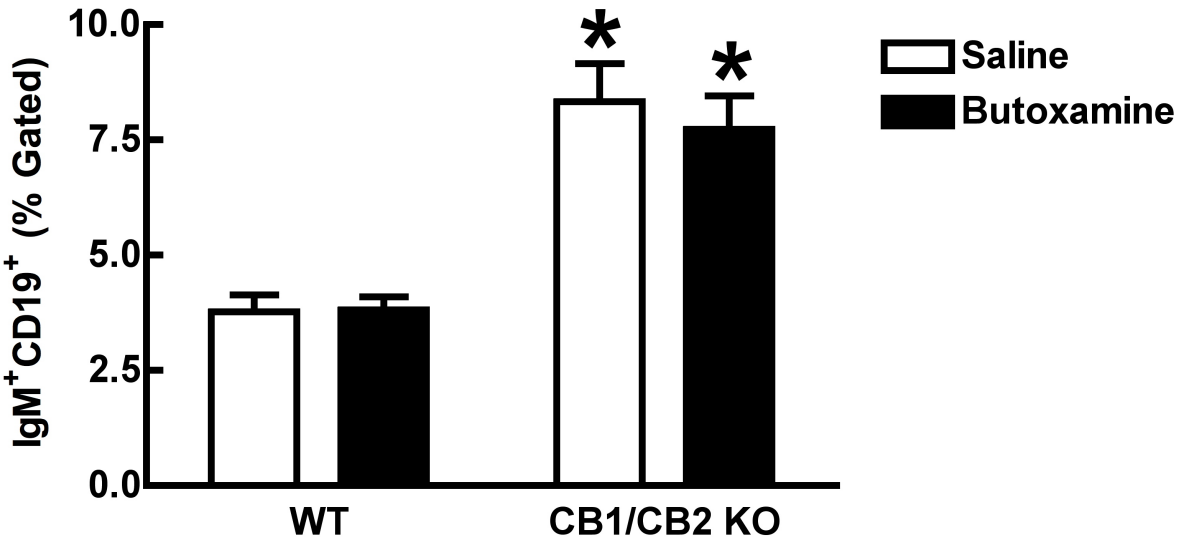


**Figure 5.20. Lack of effect of β2AR antagonism on the IgM producing B cell population in the spleen of LPS exposed WT and CB1/CB2 KO mice.** Female WT and CB1/CB2 KO mice were injected 8 times with butoxamine (10 mg/kg; i.p.), or vehicle, every 6 h for 48 h. Mice received a single injection of LPS (25 μg; i.p.) one h prior to the 5$^{th}$ injection and were sacrificed 4 days later. The splenocytes were isolated and flow cytometry was used to identify B cells (CD19-PE-Cy7) producing IgM (FITC). Cells were gated sequentially on singlet lymphocytes, prior to plotting CD19 and IgM for analysis. Columns represent the average percentage of IgM$^+$ CD19$^+$ cells + 1 SEM (n=5). * Significantly differs from WT of the same treatment group ($p<0.05$).

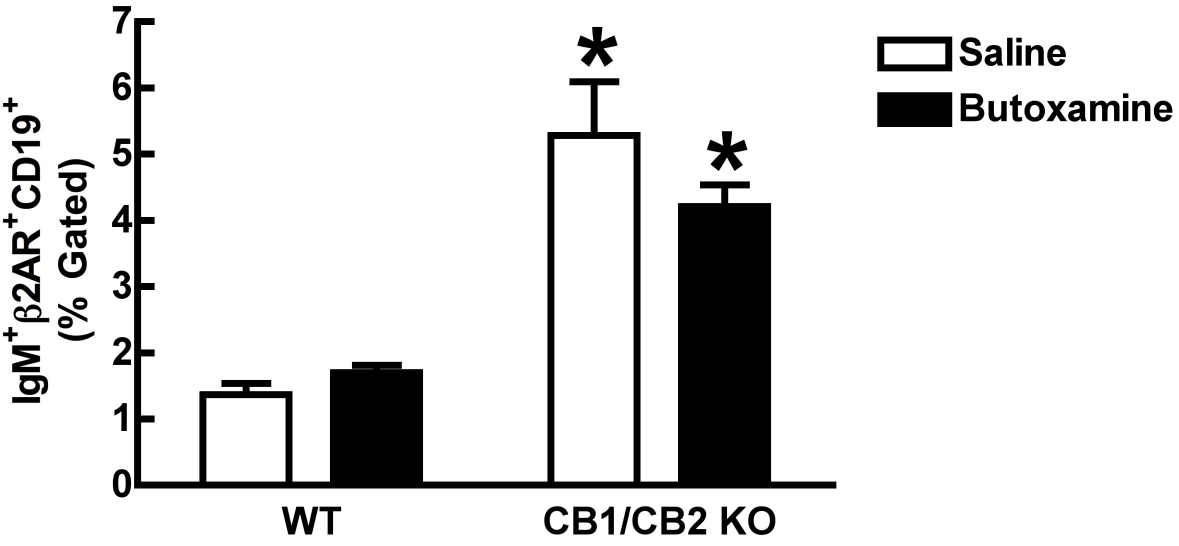


**Figure 5.21. Lack of effect of β2AR antagonism on the IgM producing B cell population expressing β2AR in the spleen of LPS exposed WT and CB1/CB2 KO mice.** Female WT and CB1/CB2 KO mice were injected 8 times with butoxamine (10 mg/kg; i.p.), or vehicle, every 6 h for 48 h. Mice received a single injection of LPS (25 μg; i.p.) one h prior to the 5$^{th}$ injection and were sacrificed 4 days later. The splenocytes were isolated and flow cytometry was used to identify β2AR (APC) expressing B cells (CD19-PE-Cy7) producing IgM (FITC). Cells were gated sequentially on singlet lymphocytes expressing β2AR prior to plotting CD19 and IgM for analysis. Columns represent the average percentage of IgM$^+$ β2AR$^+$ B cells + 1 SEM (n=5). * Significantly differs from WT of the same treatment group ($p<0.05$).

## 5.4: Discussion

In the present chapter the hypothesis was tested that enhanced humoral immunity in mice lacking the CB1 and CB2 receptor is due to increased stimulation of β2AR secondary to increased release NE from splenic sympathetic neurons. The data presented confirm that CB1/CB2 KO mice do exhibit enhanced humoral immunity. Interestingly, B cells from CB1/CB2 KO mice possess an enhanced adrenergic sensing capacity; they have an increase in B cells expressing β2AR. However, lack of CB1/CB2 does not result in increased NE release from splenic sympathetic neurons. Increased β2AR stimulation, due to increased β2AR expression, was also ruled out as a potential cause for enhanced humoral immunity in CB1/CB2 KO mice.

### 5.4.1: Enhanced humoral immunity in CB1/CB2 KO mice

Congruent with a previously published report (Springs et al., 2008), CB1/CB2 KO mice demonstrate enhanced humoral immunity. Increased serum IgM and IgG concentrations suggest several things. IgM is constitutively secreted without antigen stimulation as a form of innate immunity by innate-like B cells (Baumgarth, 2013). These IgM antibodies are termed 'natural antibodies'. Thus, elevated serum IgM in immunologically naïve CB1/CB2 KO mice suggests these receptors may be inhibitory to this specific type of immunity, a finding that is unexplored in scientific literature. However, natural antibodies are reported to be almost exclusively IgM, where as IgG is produced in response to antigenic stimulation (Zouali, 2001). Therefore, the production

of natural antibodies does not explain the elevated serum IgG in immunologically naïve CB1/CB2 KO mice.

Elevated IgG in immunologically naïve CB1/CB2 KO could have two likely sources. First, it could be due to antigenic stimulation. The only way that this is likely to be the true is if the lack of CB1 and CB2 increases the sensitivity of B cells to foreign antigens. This possibility seems unlikely to be the cause for increased IgG, though, as the elevation in IgG is approximately 4-fold higher compared to WT, whereas under true antigenic stimulation the elevation of antibodies is on the order of log-fold changes (Ademokun and Dunn-Walters, 2001). The second possible explanation for increased serum IgG is due to an increased presence of long-lived plasma cells. Plasma cells are professional antibody producing B cells produced in response to antigenic stimulation (Ademokun and Dunn-Walters, 2001; Tangye, 2011). Some plasma cells are short-lived, lasting few days to weeks, but others persist for years thereby conferring long-term immunity (Tangye, 2011). These long-lived plasma cells constitutively produce antigen specific IgG designed to speed the removal of antigens upon re-exposure (Tangye, 2011). It may be the case that lack of CB1/CB2 results in an increase in the survival or generation of these cells. This possibility seems likely to be the cause of increased IgG in immunologically naïve cells as it would likely increase IgG serum concentrations, but not at the level seen with antigenic stimulation. This suggests that CB1 and/or CB2 play a role in the formation of these specialized B cells. The effect of cannabinoids on long-term immunity is also virtually unexplored in the literature with only one report in CB2

knockout mice showing no significant effect of plasma cell generation in response to a T-cell dependent antigen (Basu et al., 2013).

Overall, however, it seems clear that CB1 and/or CB2 receptors play a role in the development and maintenance of B cells as CB1/CB2 KO mice have more splenic B cells and B cells that produce antibodies. These effects are also observed when CB1/CB2 KO mice are immune challenged by LPS, likely due to the increased number of B cells at rest resulting in more B cells that produce antibodies. This effect may be more pronounced following exposure to LPS, a polyclonal B cell stimulator, as opposed to T cell dependent immunogen requiring specific antigen recognizing T and B cell populations (Ademokun and Dunn-Walters, 2001).

### 5.4.2: β2AR expression in CB1/CB2 KO mice

Considering the hypothesis that enhanced sympathetic noradrenergic stimulation may be the underlying cause for enhanced humoral responses, it was expected that β2AR expression in CB1/CB2 KO mice would be reduced due to ligand/activity dependent down-regulation (Zastrow and Kobilka, 1992; Hudson et al., 2010). However, as demonstrated, this is not the case. The observed up-regulation of β2AR in CB1/CB2 KO mice could be due to the absence of cannabinoid receptors on B cells, most likely CB2 given it's higher expression in B cells compared to CB1 (Schatz et al., 1997). In support of this possibility, a recent study demonstrated a physical interaction between CB1 and β2AR, and this interaction was able modulate the surface expression of these receptors (Hudson et al., 2010). Thus, although CB1 and CB2 do not have 100% homology, it might be hypothesized that CB2 may also be able to alter β2AR expression

as was shown for CB1. Another potential explanation of increased β2AR is that CB1/CB2 KO mice release less NE than WT in the spleen, resulting in receptor up-regulation due to a lack of ligand-binding (Zastrow and Kobilka, 1992; Hudson et al., 2010). While obviously in direct contradiction to the original underlying hypothesis of this chapter, this explanation for increased β2AR expression turns out to be the most likely explanation given decreased NE utilization in CB1/CB2 KO mice under immunologically naïve conditions.

The increase of β2AR expressing B cells producing IgM also suggests an interaction between CB1 and/or CB2 receptors with β2AR. These data were obtained by gating for cells expressing β2AR then assessing the number of IgM producing B cells. Therefore, if β2AR expression were globally increased on all β2AR-expressing lymphocytes, the relative ratio of each cell type would not change. However, this is not the case. It appears that knockout of CB1/CB2 increases the relative proportion of these IgM producing B cells. These data cannot specifically identify the cause of this shift as both NE signaling and CB signaling are simultaneously changed in these mice. However, at least two possibilities can be considered. First, despite the reported effect of β2AR on the stimulation of antibody production, there is also evidence that β2AR stimulation may decrease proliferation in lymphocytes (Marino and Cosentino, 2011). Thus, decreased NE release in CB1/CB2 KO mice might preferentially allow for the survival of IgM producing B cells. The second possibility to be considered is a direct effect of CB2 on B cells themselves, which have been show to modulate lymphocyte proliferation (Basu and Dittel, 2011). Thus, it is possible that CB2 receptor mediated

preferential survival/proliferation of IgM producing B cells accounts for these differences.

5.4.3: Splenic sympathetic noradrenergic activity and signaling in CB1/CB2 KO mice

The lack of the CB1 and CB2 receptors does not result in increased NE release from splenic sympathetic neurons. This strongly argues against the existence of CB1 receptors on the axon terminals of spleen projection post-ganglionic sympathetic neurons, although CB1 receptor expression and regulation of neurotransmitter release in post-ganglionic sympathetic neurons is not without precedence (Ishac et al., 1996; Niederhoffer and Szabo, 1999; Ralevic and Kendall, 2002). Interestingly, the present study revealed that CB1/CB2 KO mice have lower splenic sympathetic noradrenergic activity. The explanation for this effect is unclear and may involve CNS-mediated CB1 receptor effects upstream of post-ganglionic neurons. However, the decreased release of NE from sympathetic neurons in the spleen may explain the accumulation of NE in the spleen capsule without a concomitant increase in TH enzyme content. Regardless, the lack of increased NE release in the spleen of CB1/CB2 KO leads to the acceptance of the null hypothesis regarding this explanation of enhanced humoral immunity in CB1/CB2 KO mice.

Next, due to the increased β2AR expression by B cells in CB1/CB2 KO mice, it was hypothesized that β2AR activity may still the cause of enhanced humoral immunity in these mice. It was expected that if increased β2AR stimulation was, at least in part, responsible for increased humoral immune responses in CB1/CB2 KO mice, then blockade of these receptors would significantly attenuate antibody production or reduce

the population of antibody producing cells. This hypothesis was rejected following the observation that blockade of β2AR had no observable effect in CB1/CB2 KO mice. These data also confirm what was observed in **Chapter 4**, namely that β2AR activity does not play a significant role in the humoral response to LPS.

### 5.4.4: Conclusion

The data in this chapter rule out the involvement of splenic NE release and β2AR in conferring enhanced humoral immunity in CB1/CB2 KO mice. Interestingly, B cells from CB1/CB2 KO mice possess an enhanced adrenergic sensing capacity. These data, however, do give some clues as to the underlying mechanism of enhanced humoral immunity in CB1/CB2 KO mice, namely increased 'natural antibody' production and increased long-lived plasma cell survival. Future investigation into the immunologic effects of cannabinoid receptors should be focused towards the effect of CB2 receptors on immune cells themselves, rather than the effect of CB1 modulation of local neurotransmitter release in secondary lymphoid organs, such as the spleen.

# REFERENCES

# REFERENCES


Ademokun AA, Dunn-Walters D. Immune Responses: Primary and Secondary. els.net. Chichester, UK: John Wiley & Sons, Ltd; 2001.

Ahrens WH, Cox DJ, Budhwar G. Use of the arcsine and square root transformations for subjectively determined percentage data. Weed Science. 1990.

Alger B, Kim J. Supply and demand for endocannabinoids. Trends Neurosci. 2011 Jun 1;34(6):304–15.

Basu S, Dittel BN. Unraveling the complexities of cannabinoid receptor 2 (CB2) immune regulation in health and disease. Immunol. Res. 2011 Oct;51(1):26–38.

Basu S, Ray A, Dittel BN. Cannabinoid receptor 2 is critical for the homing and retention of marginal zone B lineage cells and for efficient T-independent immune responses. The Journal of Immunology. 2011 Dec 1;187(11):5720–32. PMCID: PMC3226756

Basu S, Ray A, Dittel BN. Cannabinoid Receptor 2 (CB2) Plays a Role in the Generation of Germinal Center and Memory B Cells, but Not in the Production of Antigen-Specific IgG and IgM, in Response to T-dependent Antigens. PLoS ONE. 2013;8(6):e67587. PMCID: PMC3695093

Baumgarth N. Innate-Like B Cells and Their Rules of Engagement. link.springer.com.proxy2.cl.msu.edu. New York, NY: Springer New York; 2013. p. 57–66.

Börner C, Bedini A, Höllt V, Kraus J. Analysis of promoter regions regulating basal and interleukin-4-inducible expression of the human CB1 receptor gene in T lymphocytes. Mol Pharmacol. 2008 Mar;73(3):1013–9.

Brodie BB, Costa E, Dlabac A, Neff NH, Smookler HH. Application of steady state kinetics to the estimation of synthesis rate and turnover time of tissue catecholamines. J Pharmacol Exp Ther. 1966 Dec;154(3):493–8.

Brown SM, Wager-Miller J, Mackie K. Cloning and molecular characterization of the rat CB2 cannabinoid receptor. Biochim Biophys Acta. 2002 Jul 19;1576(3):255–64.

Buckley N, McCoy K, Mezey E, Bonner T, Zimmer A, Felder C, et al. Immunomodulation by cannabinoids is absent in mice deficient for the cannabinoid CB(2) receptor. Eur J Pharmacol. 2000 May 19;396(2-3):141–9.

Cabral GA, Griffin-Thomas L. Emerging role of the cannabinoid receptor CB2 in immune regulation: therapeutic prospects for neuroinflammation. Expert Rev Mol Med. 2009;11:e3. PMCID: PMC2768535

Carrier EJ, Kearn CS, Barkmeier AJ, Breese NM, Yang W, Nithipatikom K, et al. Cultured rat microglial cells synthesize the endocannabinoid 2-arachidonylglycerol, which increases proliferation via a CB2 receptor-dependent mechanism. Mol Pharmacol. 2004 Apr;65(4):999–1007.

Childers SR, Deadwyler SA. Role of cyclic AMP in the actions of cannabinoid receptors. Biochem Pharmacol. 1996 Sep 27;52(6):819–27.

Eaton MJ, Lookingland KJ, Moore KE. Effects of the selective dopaminergic D2 agonist quinelorane on the activity of dopaminergic and noradrenergic neurons projecting to the diencephalon of the rat. 1994 Feb 1;268(2):645–52.

Felder CC, Briley EM, Axelrod J, Simpson JT, Mackie K, Devane WA. Anandamide, an endogenous cannabimimetic eicosanoid, binds to the cloned human cannabinoid receptor and stimulates receptor-mediated signal transduction. Proc Natl Acad Sci USA. 1993 Aug 15;90(16):7656–60. PMCID: PMC47201

Felder CC, Joyce KE, Briley EM, Mansouri J, Mackie K, Blond O, et al. Comparison of the pharmacology and signal transduction of the human cannabinoid CB1 and CB2 receptors. Mol Pharmacol. 1995 Sep;48(3):443–50.

Ferrero I, Michelin O, Luescher I. Antigen Recognition by T Lymphocytes. onlinelibrary.wiley.com.proxy2.cl.msu.edu. Chichester, UK: John Wiley & Sons, Ltd; 2001.

Galiegue S, Mary S, Marchand J, Dussossoy D, Carriere D, Carayon P, et al. Expression of Central and Peripheral Cannabinoid Receptors in Human Immune Tissues and Leukocyte Subpopulations. Eur J Biochem. 1995 Aug;232(1):54–61.

Gebremedhin D, Lange AR, Campbell WB, Hillard CJ, Harder DR. Cannabinoid CB1 receptor of cat cerebral arterial muscle functions to inhibit L-type Ca2+ channel current. Am J Physiol. 1999 Jun;276(6 Pt 2):H2085–93.

Gerald T, Ward G, Howlett A, Franklin S. CB1 knockout mice display significant changes in striatal opioid peptide and D4 dopamine receptor gene expression. Brain Res. 2006 Jun 6;1093(1):20–4.

Gerra G, Zaimovic A, Gerra ML, Ciccocioppo R, Cippitelli A, Serpelloni G, et al. Pharmacology and toxicology of Cannabis derivatives and endocannabinoid agonists. Recent Pat CNS Drug Discov. 2010 Jan;5(1):46–52.

Ghosh S, Preet A, Groopman JE, Ganju RK. Cannabinoid receptor CB2 modulates the CXCL12/CXCR4-mediated chemotaxis of T lymphocytes. Mol Immunol. 2006 Jul;43(14):2169–79.

Giuffrida A, Mcmahon LR. In vivo pharmacology of endocannabinoids and their

metabolic inhibitors: therapeutic implications in Parkinson's disease and abuse liability. Prostaglandins and Other Lipid Mediators. 2010 Apr 1;91(3-4):90–103.

Gohary ME, Eid MA. Effect of cannabinoid ingestion (in the form of bhang) on the immune system of high school and university students. Human & experimental toxicology. 2004.

Greineisen WE, Turner H. Immunoactive effects of cannabinoids: considerations for the therapeutic use of cannabinoid receptor agonists and antagonists. Int Immunopharmacol. 2010 May;10(5):547–55. PMCID: PMC3804300

Griffin G, Tao Q, Abood ME. Cloning and pharmacological characterization of the rat CB(2) cannabinoid receptor. J Pharmacol Exp Ther. 2000 Mar;292(3):886–94.

Herkenham M, Lynn AB, Johnson MR, Melvin LS, de Costa BR, Rice KC. Characterization and localization of cannabinoid receptors in rat brain: a quantitative in vitro autoradiographic study. 1991 Feb 1;11(2):563–83.

Howlett AC, Mukhopadhyay S. Cellular signal transduction by anandamide and 2-arachidonoylglycerol. Chemistry and Physics of Lipids. 2000 Nov;108(1-2):53–70.

Hudson BD, Hébert TE, Kelly MEM. Physical and functional interaction between CB1 cannabinoid receptors and beta2-adrenoceptors. Br J Pharmacol. 2010 Jun;160(3):627–42. PMCID: PMC2931563

Ishac E, Jiang L, Lake K, Varga K, Abood M, Kunos G. Inhibition of exocytotic noradrenaline release by presynaptic cannabinoid CB1 receptors on peripheral sympathetic nerves. Br J Pharmacol. 1996 Aug 1;118(8):2023–8. PMCID: PMC1909901

Jan T-R, Farraj AK, Harkema JR, Kaminski NE. Attenuation of the ovalbumin-induced allergic airway response by cannabinoid treatment in A/J mice. Toxicol Appl Pharmacol. 2003 Apr 1;188(1):24–35.

Jarai Z, Wagner J, Varga K, Lake K, Compton D, Martin B, et al. Cannabinoid-induced mesenteric vasodilation through an endothelial site distinct from CB1 or CB2 receptors. Proc Natl Acad Sci U S A. 1999 Nov 23;96(24):14136–41.

Kaplan BLF. The Role of CB(1) in Immune Modulation by Cannabinoids. Pharmacol. Ther. 2012 Dec 19.

Kaplan BLF, Lawver JE, Karmaus PWF, Ngaotepprutaram T, Birmingham NP, Harkema JR, et al. The effects of targeted deletion of cannabinoid receptors CB1 and CB2 on intranasal sensitization and challenge with adjuvant-free ovalbumin. Toxicol Pathol. 2010 Apr;38(3):382–92. PMCID: PMC2941344

Karmaus PWF, Chen W, (null), Kaplan BLF, Kaminski NE. Δ9-Tetrahydrocannabinol Impairs the Inflammatory Response to Influenza Infection: Role of Antigen-Presenting Cells and the Cannabinoid Receptors 1 and 2. Toxicological Sciences. 2013. PMCID: PMC3551428

Karmaus PWF, Chen W, Kaplan BLF, Kaminski NE. Δ9-tetrahydrocannabinol suppresses cytotoxic T lymphocyte function independent of CB1 and CB 2, disrupting early activation events. J Neuroimmune Pharmacol. 2012 Dec;7(4):843–55. PMCID: PMC3266990

Klein TW, Friedman H, Specter S. Marijuana, immunity and infection. J Neuroimmunol. 1998 Mar 15;83(1-2):102–15.

Kohm AP, Sanders VM. Norepinephrine and beta 2-adrenergic receptor stimulation regulate CD4+ T and B lymphocyte function in vitro and in vivo. Pharmacol Rev. 2001 Dec;53(4):487–525.

Kuster JE, Stevenson JI, Ward SJ, D'Ambra TE, Haycock DA. Aminoalkylindole binding in rat cerebellum: selective displacement by natural and synthetic cannabinoids. J Pharmacol Exp Ther. 1993 Mar;264(3):1352–63.

Lindley SE, Gunnet JW, Lookingland KJ, Moore KE. 3,4-Dihydroxyphenylacetic acid concentrations in the intermediate lobe and neural lobe of the posterior pituitary gland as an index of tuberohypophysial dopaminergic neuronal activity. Brain Res. 1990 Jan 1;506(1):133–8.

Lu H, Kaplan BLF, Ngaotepprutaram T, Kaminski NE. Suppression of T cell costimulator ICOS by Delta9-tetrahydrocannabinol. J Leukoc Biol. 2009 Feb;85(2):322–9. PMCID: PMC2631366

Mackie K. Signaling via CNS cannabinoid receptors. Mol. Cell. Endocrinol. 2008 Apr 16;286(1-2 Suppl 1):S60–5. PMCID: PMC2435200

Mackie K, Devane WA, Hille B. Anandamide, an endogenous cannabinoid, inhibits calcium currents as a partial agonist in N18 neuroblastoma cells. Mol Pharmacol. 1993 Sep;44(3):498–503.

Mackie K, Lai Y, Westenbroek R, Mitchell R. Cannabinoids activate an inwardly rectifying potassium conductance and inhibit Q-type calcium currents in AtT20 cells transfected with rat brain cannabinoid receptor. J Neurosci. 1995 Oct;15(10):6552–61.

Maresz K, Pryce G, Ponomarev ED, Marsicano G, Croxford JL, Shriver LP, et al. Direct suppression of CNS autoimmune inflammation via the cannabinoid receptor CB1 on neurons and CB2 on autoreactive T cells. Nat. Med. 2007 Apr;13(4):492–7.

Marino F, Cosentino M. Adrenergic modulation of immune cells: an update. Amino Acids. 2011 Dec 8.

Montecucco F, Burger F, Mach F, Steffens S. CB2 cannabinoid receptor agonist JWH-015 modulates human monocyte migration through defined intracellular signaling pathways. Am J Physiol Heart Circ Physiol. 2008 Mar;294(3):H1145–55.

Niederhoffer N, Szabo B. Effect of the cannabinoid receptor agonist WIN55212-2 on sympathetic cardiovascular regulation. Br J Pharmacol. 1999 Jan;126(2):457–66.

Noble J, Bailey M. Quantitation of protein. Methods Enzymol. 2009;463:73–95.

Nyíri G, Cserép C, Szabadits E, Mackie K, Freund TF. CB1 cannabinoid receptors are enriched in the perisynaptic annulus and on preterminal segments of hippocampal GABAergic axons. Neuroscience. 2005;136(3):811–22.

Pacifici R, Zuccaro P, Pichini S, Roset PN, Poudevida S, Farré M, et al. Modulation of the immune system in cannabis users. JAMA. 2003 Apr 16;289(15):1929–31.

Pertwee RG. The diverse CB1 and CB2 receptor pharmacology of three plant cannabinoids: Δ9-tetrahydrocannabinol, cannabidiol and Δ9-tetrahydrocannabivarin. Br J Pharmacol [Internet]. 2008 Jan;153(2):199–215. Retrieved from: http://onlinelibrary.wiley.com.proxy2.cl.msu.edu/doi/10.1038/sj.bjp.0707442/full. PMCID: PMC2219532

Raborn ES, Marciano-Cabral F, Buckley NE, Martin BR, Cabral GA. The cannabinoid delta-9-tetrahydrocannabinol mediates inhibition of macrophage chemotaxis to RANTES/CCL5: linkage to the CB2 receptor. J Neuroimmune Pharmacol. 2008 Jun;3(2):117–29. PMCID: PMC2677557

Ralevic V, Kendall DA. Cannabinoids inhibit pre- and postjunctionally sympathetic neurotransmission in rat mesenteric arteries. Eur J Pharmacol. 2002 May 31;444(3):171–81.

Sanders VM. The beta2-adrenergic receptor on T and B lymphocytes: Do we understand it yet? Brain Behav Immun. 2012 Feb;26(2):195–200. PMCID: PMC3243812

Schatz A, Lee M, Condie R, Pulaski J, Kaminski N. Cannabinoid receptors CB1 and CB2: a characterization of expression and adenylate cyclase modulation within the immune system. Toxicol Appl Pharmacol. 1997 Feb 1;142(2):278–87.

Schatz AR, Koh WS, Kaminski NE. Delta 9-tetrahydrocannabinol selectively inhibits T-cell dependent humoral immune responses through direct inhibition of accessory T-cell function. Immunopharmacology. 1993 Sep;26(2):129–37.

Shire D, Calandra B, Rinaldi-Carmona M, Oustric D, Pessègue B, Bonnin-Cabanne O, et al. Molecular cloning, expression and function of the murine CB2 peripheral cannabinoid receptor. Biochim Biophys Acta. 1996 Jun 7;1307(2):132–6.

Springs AEB, Karmaus PWF, Crawford RB, Kaplan BLF, Kaminski NE. Effects of targeted deletion of cannabinoid receptors CB1 and CB2 on immune competence and sensitivity to immune modulation by Delta9-tetrahydrocannabinol. J Leukoc Biol. 2008 Dec;84(6):1574–84. PMCID: PMC2614598

Tanasescu R, Constantinescu C. Cannabinoids and the immune system: an overview. Immunobiology. 2010 Aug 1;215(8):588–97.

Tangye SG. Staying alive: regulation of plasma cell survival. Trends Immunol. 2011 Dec;32(12):595–602.

Tashkin DP. Effects of marijuana smoking on the lung. Ann Am Thorac Soc. 2013 Jun;10(3):239–47.

Zastrow von M, Kobilka BK. Ligand-regulated internalization and recycling of human beta 2-adrenergic receptors between the plasma membrane and endosomes containing transferrin receptors. J Biol Chem. 1992 Feb 15;267(5):3530–8.

Zimmer A, Zimmer AM, Hohmann AG, Herkenham M, Bonner TI. Increased mortality, hypoactivity, and hypoalgesia in cannabinoid CB1 receptor knockout mice. Proc Natl Acad Sci USA. 1999 May 11;96(10):5780–5. PMCID: PMC21937

Zouali M. Natural Antibodies. els.net. Chichester, UK: John Wiley & Sons, Ltd; 2001.

# Chapter 6: Sympathetic nervous system control of spleen contraction and the role of CB1/CB2 signaling

## 6.1: Introduction

Contraction of smooth muscle in the spleen serves two hematologic purposes. First, the spleen acts as a reservoir for RBC (Cesta, 2006). Due to the organization of the spleen, contraction of the spleen capsule reduces its overall size and volume (Davies and Withrington, 1973; Sandler et al., 1984; Cesta, 2006; Richardson et al., 2009; Seifert et al., 2012). This contraction expels the cellular contents of the spleen into the general circulation leading to an increased hematocrit of the blood. Contraction of the spleen can increase the blood hematocrit by as much as 5% in humans (Sandler et al., 1984; Bakovic et al., 2005; Richardson et al., 2007; 2009), 10% in rats (Kuwahira et al., 1999), and 16% in dogs (Sato et al., 1995), thereby increasing the oxygen carrying capacity of the blood. This is considered the primary function of spleen contraction and has been primarily studied in the context of hypoxia (Sandler et al., 1984; Sato et al., 1997; Kuwahira et al., 1999; Bakovic et al., 2003; Richardson et al., 2007; 2009). In addition to being a reservoir for RBC, the spleen is the largest secondary lymphoid organ and contains a large number of immune cells (macrophages, leukocytes, and lymphocytes) (Cesta, 2006). These cells are also released during spleen contraction (Seifert et al., 2012), but the consequences of this increased leukocyte/lymphocyte content in the blood are essentially unknown.

The second role for spleen contraction is to regulate blood flow through the spleen. Blood enters the spleen via the splenic artery which then branches into a number of trabecular arteries which eventually enter the red pulp of the spleen where they are termed central arterioles and are surrounded by lymphoid tissue, PALS (Cesta, 2006). Branches from central arterioles have several destinations including capillary beds within the white pulp (marginal zone) and the red pulp of the spleen (Schmidt et al., 1985; Satodate et al., 1986; Schmidt et al., 1993).

Blood that flows through the white pulp marginal zone and directly into venous sinuses is considered the 'fast' pathway (Cesta, 2006). As much as 90% of splenic blood flow travels through the 'fast' pathway (Schmidt et al., 1985; 1993; Cesta, 2006). Alternatively, the 'slow' pathway is blood that enters the reticular meshwork of the red pulp (Schmidt et al., 1993; Mebius and Kraal, 2005). The reticular meshwork of the red pulp is composed of reticular fibers, reticular cells, and macrophages and is the area where macrophages actively phagocytize dead and damaged erythrocytes (Saito et al., 1988; Cesta, 2006). Macrophages within the red pulp of the spleen are also constantly exposed to foreign particulates in the blood (Cesta, 2006).

Blood flow through the spleen is regulated by both arteriolar/capillary endothelial cells and red pulp reticular cell contraction (Blue and Weiss, 1981; Pinkus et al., 1986; Saito et al., 1988; Groom et al., 1991). Contraction of reticular cells surrounding capillaries and capillary endothelial cells in the red pulp serve to decrease blood flow to the reticular meshwork of the red pulp and shuttle more blood through the 'fast' pathway (Blue and Weiss, 1981; Groom et al., 1991). Contraction of reticular cells in the red pulp

likely further prevent blood from entering this area (Blue and Weiss, 1981; Pinkus et al., 1986; Saito et al., 1988). Contraction of red pulp reticular cells also participates in ejecting the cells contained within this compartment (Blue and Weiss, 1981; Pinkus et al., 1986; Saito et al., 1988).

The spleen capsule is composed of three major tissues: connective tissue, elastic tissue, and smooth muscle (Cesta, 2006). Immunohistochemical detection of smooth muscle specific myosin is demonstrative of the large amount of smooth muscle contained within the spleen capsule (Davies and Withrington, 1973; Pinkus et al., 1986; Cesta, 2006). Contractile elements are also observed in trabeculae of connective tissue that penetrate the spleen, in the periarteriolar meshwork of the white pulp in a circumferential pattern around incoming vessels, and in the reticular meshwork of the red pulp arranged in an orderly fashion parallel to the long-axis of the spleen (Blue and Weiss, 1981; Pinkus et al., 1986). Therefore, contraction of the spleen includes not only the contraction of spleen capsule smooth muscle, but also a network of contractile components throughout the spleen.

Spleen contraction is controlled by the sympathetic nervous system. NE activation of $\alpha$1AR, specifically the $\alpha 1_B$AR subtype, mediates much of sympathetically induced spleen contraction (Gillespie and Hamilton, 1966; Eltze, 1996; Aboud et al., 2012). Activation of $\alpha$1AR results in the activation of phospholipase C and generation of IP3 which then leads to the release and elevation of intracellular $Ca^{2+}$ and contraction of smooth muscle (Bootman et al., 2001; Malbon and Wang, 2001). In congruence with the ability of NE to stimulate splenic smooth muscle contraction, noradrenergic fibers

and axon terminals densely innervate the spleen capsule and periarteriolar regions of the spleen (**Chapter 3**)(Davies and Withrington, 1973; Blue and Weiss, 1981; Pinkus et al., 1986; Felten et al., 1987; Felten and Olschowka, 1987; Saito et al., 1988; Elenkov and Vizi, 1991).

Co-localized neurotransmitters in post-ganglionic sympathetic neurons other than NE also contribute to spleen contraction. NPY and ATP are commonly recognized neurotransmitters that are co-released from sympathetic neurons (Macarthur et al., 2011). NPY is a 36 amino acid peptide expressed by many post-ganglionic sympathetic neurons, including those projecting to the spleen, kidney, and mesentery (Lundberg et al., 1990; Romano et al., 1991; Chevendra and Weaver, 1992). NPY is able to induce the contraction of vascular smooth muscle through Y1 NPY receptors (Westfall et al., 1987; 1990; Zukowska-Grojec et al., 1996; Michel et al., 1998; Wiest et al., 2006). NPY also has pre-junctional effects, mediated by Y2 receptors, whereby it can autoregulate sympathetic neurotransmitter release (Westfall et al., 1987; 1990; Michel et al., 1998). Only one study has reported NPY capable of inducing spleen contraction, albeit very weakly in comparison to NE (Corder et al., 1987).

ATP released from sympathetic neurons is also able to induce the contraction of vascular smooth muscle in a variety of tissues (i.e., vas deferens, aorta, splenic nerve) through the P2X receptor (Sedaa et al., 1990; Ren and Burnstock, 1997; Burnstock and Ralevic). Extracellular ATP is quickly converted to adenosine which is then known to inhibit NE release from sympathetic neurons via an action on pre-synaptic A1 adenosine receptors, a G-coupled protein that signals through the $G_{i/o}$ pathway (Kubo and Su,

1983; Wennmalm et al., 1988; Kügelgen et al., 1992; Rongen et al., 1996; Ralevic, 2009; Macarthur et al., 2011; Burnstock and Ralevic). Interestingly, there is some precedence that activation of A1 receptors can stimulate vascular smooth muscle contraction in the spleen (Fozard and Milavec-Krizman, 1993; Tawfik et al., 2005).

To date, the effect of cannabinoids on spleen contraction has not been reported in the scientific literature. Yet, the ability of CB1 receptors to modulate neurotransmitter release from other peripheral sympathetic neurons suggests a potential effect (Ishac et al., 1996; Niederhoffer and Szabo, 1999; Ralevic and Kendall, 2002). It was originally hypothesized that NE release from sympathetic neurons in the spleens of CB1/CB2 KO mice would be increased due to the absence of pre-synaptic CB1 receptors. However, this hypothesis was not supported by the data presented in **Chapter 5** which showed that NE release in the spleen of CB1/CB2 KO mice is not elevated as compared with WT mice. With this discovery it was then hypothesized that spleen contraction would be enhanced in CB1/CB2 KO mice secondary to an increase in α1AR expression from decreased NE release. A decrease in NE release, and therefore NE binding to α1AR mediating spleen contraction, would result in increased expression of this receptor due to a lack of ligand-binding/activity dependent receptor internalization (Leeb-Lundberg et al., 1987; Malbon and Wang, 2001).

The purpose of this chapter is to test the hypothesis that spleen contraction is enhanced in CB1/CB2 KO in response to exogenously applied NE and electrically evoked neurotransmitter release. To this end, an experimental apparatus was employed in which the ability of isolated spleen to pull on a nylon string attached to an isometric

force transducer *ex vivo*. This method was used to test the contractile response of spleens from both WT and CB1/CB2 KO mice to exogenous NE and EFS-induced neurotransmitter release from splenic sympathetic axon terminals.

## 6.2: Materials and Methods

### 6.2.1: Mice

C57BL/6 WT female mice (NCI/Charles River, Portage, MI) and female CB1/CB2 KO mice were used in all experiments unless otherwise indicated. CB1/CB2 KO mice, on a C57BL/6 background, were created by Dr. Andreas Zimmer at the University of Bonn, Germany as previously described (Jarai et al., 1999; Zimmer et al., 1999; Buckley et al., 2000; Gerald et al., 2006). CB1/CB2 KO mice for these studies were obtained from Drs. Norbert Kaminski and Barbara Kaplan who maintain a breeding colony of CB1/CB2 KO mice at Michigan State University. All animals were housed two to five per cage and maintained in a sterile, temperature (22 ± 1 °C) and light controlled (12L:12D) room, and provided with irradiated food and bottled tap water *ad libitum*. All experiments used the minimal number of animals required for statistical analyses, minimized suffering, and followed the guidelines of the National Institutes of Health Guide for the Care and Use of Laboratory Animals. The Michigan State Institutional Animal Care and Use Committee approved all drug administrations and methods of euthanasia (AUF# 03/12-060-00).

6.2.1.1: CB1/CB2 KO Mouse Genotyping

PCR was used to confirm knockout of CB1 and CB2 receptor genes. Genomic DNA was isolated from ~0.5 cm tail snips using 100 *µ*l DirectPCR Lysis Reagent (Viagen Biotech, Los Angeles, CA) plus 0.1 mg/ml proteinase K. Samples were incubated overnight at 55°C followed by a 45 min incubation at 85°C. Crude DNA extract was obtained following centrifugation at 300 RCF for 1 min. One *µ*l of extract was used in a Taqman PCR reaction using *Cnr1* stock primers (CB1 receptor gene) or *Cnr2* (CB2 receptor gene) custom primers (Life Technologies/Applied Biosystems, Foster City, CA) (Kaplan et al., 2010). PCR primers for CB1 receptors were forward 5'-AGGAGCAAGGACCTGAGACA-3', reverse 5'-GGTCACCTTGGCGATCTTAA-3', for CB2 receptor were forward 5'-CCTGATAGGCTGGAAGAAGTATCTAC-3', reverse 5'-ACATCAGCCTCTGTTTCTGTAACC-3', neomycin cassette primers were forward 5'-ACCGCTGTTGACCGCTACCTATGTCT-3', and reverse 5'-TAAAGCGCATGCTCCAGACTGCCTT-3'. The average ± standard deviation Ct values for *Cnr1* and *Cnr2* in WT mice were 25.0 ± 0.54 and 26.0 ± 1.22, respectively. All samples obtained from CB1/CB2 KO tail snips resulted in an "undetermined" Ct value, indicating lack of expression of both *Cnr1* and *Cnr2*.

6.2.2: Materials

DPCPX: DPCPX (Sigma) was dissolved in DMSO to a concentration of 100 µM and used at a final concentration of 100 nM.

Krebs bicarbonate buffer: NaCl 120.0 mM, KCl 5.5 mM, $CaCl_2$ 2.5 mM, $NaH_2PO_4$ 1.2 mM, $MgCl_2$ 1.2 mM, $NaHCO_3$ 20.0 mM, and glucose 11.0 mM in ultra-pure $H_2O$.

BIBP3226: BIBP3226 (Tocris) was dissolved in DMSO to a concentration of 1 mM and used at a final concentration of 1 μM.

NE: NE (Cat# A7257, Sigma) was dissolved in RPMI media to a concentration of 1 mM and used at a final concentration between 20-80 μM. For spleen contraction studies, NE was dissolved in less than 20 ml of Krebs bicarbonate buffer that was acidified by a single drop of concentrated (18 M) HCl to a concentration of 1 mM.

Paraformaldehyde: 4% Paraformaldehyde, buffered with 0.1 M phosphate at pH 7.4, was made by combining 1:1 an 8% paraformaldehyde stock solution prepared from prills (Sigma) and a 0.2 M phosphate buffer (pH 7.4) followed by adjustment with either sodium hydroxide or concentrated phosphoric acid.

Prazosin: Prazosin (Sigma) was dissolved in DMSO to concentration of 1 mM and used at a final concentration of 1 μM.

PPADS: PPADS (Sigma) was dissolved in $H_2O$ to a concentration of 10 mM and used at a final concentration of 10 μM.

TTX: TTX (Sigma) was dissolved in $H_2O$ at a concentration of 0.3 mM and used at a final concentration of 0.3 μM.

6.2.3: Isolation of the Spleen Capsule

After euthanasia spleens were removed by an incision in the left lateral abdomen under sterile conditions, which entails spraying the area of removal with 70% ethanol and using ethanol cleaned scissors and forceps to cut through the skin, and underlying muscle and connective tissue. The spleen was placed in a 6-well plate and mechanically crushed with the blunt end of a 10 ml syringe in 2 ml of HBSS to separate the spleen capsule (insoluble tissue) from the splenocytes (contained in the disruption supernatant). The spleen capsule was removed from the supernatant using forceps and taken whole or divided into two parts using ethanol-cleaned scissors depending on the needs of the experiment.

6.2.4: Western Blot

All samples were placed in ice-cold lysis buffer (water containing 1% Triton-x 100, 250 mM sucrose, 50 mM NaCl, 20 mM tris-HCl, 1 mM EDTA, 1 mM PMSF protease inhibitor cocktail, 1 mM DTT) immediately following isolation and kept frozen at -80°C until analysis. On the day of analysis samples were thawed, heated for 30 min at 100° C, sonicated for 8 sec, and spun at 12,000 RCF for 5 min. The supernatant was collected and a BCA protein assay performed (Noble and Bailey, 2009). Equal amounts of protein were separated using SDS-PAGE and transferred to PVDF-FL membranes (Millipore,

Billerica, MA). The resulting membranes were reacted against antibodies for smooth muscle α-actin (CP47 1:5000, Millipore, Billerica, MA), or α1AR (A270 1:400, Sigma) whose intensities were normalized to GAPDH (G8795, 1:2000, Sigma) to account for loading variability. Each PVDF-FL membrane contained samples representing all experimental conditions to avoid variability due to run, transfer, or antibody exposure conditions. Blots were visualized and quantified using an Odyssey Fc Infrared Imaging system (Li-Cor, Lincoln, NE) by utilization of IRDye conjugated secondary antibodies (goat anti-Mouse 800CW (1:20,000) or goat anti-rabbit 680LT (1:20,000)) and/or HRP-conjugated anti-rabbit antibodies (1:5000; Cell Signaling) visualized using SuperSignal West Pico Chemiluminescent Substrate kit (Thermo Scientific, Rockford, IL).

### 6.2.5: Spleen Contraction Studies

#### 6.2.5.1: Preparation of Spleen Tissue for Spleen Contraction Studies

Spleens were obtained from mice euthanized by placing them in a chamber with an isoflurane soaked pad until respiration ceased as death by cervical dislocation results in less contractile responses and necessitates prolonged equilibration of the tissue (Ignarro and Titus, 1968; Wong, 1990; Eltze, 1996). Spleens were removed and connected via loops of nylon string to an isometric force transducer (Radnoti, Monrovia, CA) and placed in a 20-ml organ bath (Norman D. Erway Glass Blowing) under a resting tension of 0.8 g (7.84 millinewtons [mN]) for recording isometric contractile responses in Krebs bicarbonate buffer maintained at 37°C and gassed with 95% $0_2$ - 5% $CO_2$.

6.2.5.2: Spleen Contraction Measurement

Isometric contractions were recorded in response to EFS or direct injection of NE into the bath medium. EFS was produced by two ~1 cm custom built platinum ring electrodes placed above and below the spleen connected to a Grass S48 Stimulator (Grass Technologies, Warwick, RI). All spleens were simultaneously stimulated using a Med-Lab Stimu-Splitter II (Med-Lab Instruments). The EFS consisted of square wave pulses 0.2-0.25 ms in duration with the following characteristics: 30 V, 25 hertz (Hz), and 3 s train duration. Prior to any testing, each spleen was given at least 45 min of undisturbed time to acclimate to the *ex vivo* environment. Increased tension on the nylon string from spleen contraction resulted in deflection of a post on the isometric force transducer, the deflection of which is read as a change in voltage. This change in voltage is converted to grams at a rate of 0.28 V equaling 1 gram. All data was then converted to and expressed as mN by multiplying the gram data output by 9.8 $m/s^2$ and then multiplying by 1000.

6.2.6: Spleen Capsule Width Measurement

6.2.6.1: Hematoxylin and Eosin Staining

Mice were given a lethal dose of ketamine:xylazine (244 mg/kg:36 mg/kg; i.p.) and the spleen removed and dropped fixed in 4% paraformaldehyde. Fixed spleens were taken to the Michigan State University Department of Pathology Histology Laboratory where they were paraffin embedded, sectioned at 4 µm, and stained with hematoxylin and eosin using standard histological methodology.

6.2.6.2: Quantification of Spleen Capsule Thickness

Stained spleen sections were imaged at 40x magnification using a Nikon TE2000-S Inverted Microscope (Nikon, Melville, NY) with a Spot Insight QE camera (SPOT Imaging, Sterling Heights, MI) with SPOT 3.5.8 Imaging software (SPOT Imaging). Each spleen was imaged, focused on the spleen capsule, two times at random locations on both the internal and external side of the spleen. ImageJ software (National Institutes of Health, USA) was used to measure the width of the spleen capsule, in pixels, at four evenly spaced locations on each image. All 12 values from each spleen were then averaged and this number used as a single n for comparison between genotypes.

6.2.7: Statistical Analysis

6.2.7.1: Statistical Comparisons

Prism software version 4.0a was used to make statistical comparisons between groups using the appropriate statistical test. Differences with a probability of error of less than 5% ($p<0.05$) were considered statistically significant. Two group comparisons were done using the Student's *t*-test. Two group comparisons where in one group had more than one degree or factor were done using a One-way ANOVA followed by a Bonferroni or Tukey's post-test for multiple comparisons. Experiments in which there were two groups with more than one degree or factor in each group, such as a 2x2 design, were analyzed using a Two-way ANOVA followed by Bonferroni post-test for multiple

comparisons. Consideration for repeated measurements, as in spleen contraction studies, was given in analysis where appropriate.

## 6.3: Results

### 6.3.1: Comparison of NE-induced spleen contraction in WT and CB1/CB2 KO mice

Spleen contraction can be induced *ex vivo* in a dose dependent manner by the exogenous application of NE (**Figure 6.1**). The effective NE concentrations ranged from minimal induction of spleen contraction at 1 nM to a large induction at 1 μM, which is in coherence with previous published reports (Ignarro and Titus, 1968; Takano, 1969; Eltze, 1996; Aboud et al., 2012). Also in agreement with previous published reports, NE-induced spleen contraction was blocked by the α1AR antagonist prazosin (**Figure 6.2**) (Cambridge and Davey, 1977; Eltze, 1996; Aboud et al., 2012). An initial experiment testing the effect of repeated NE-induced stimulation of spleen capsule contraction found rapid developing desensitization at concentrations ≥100 nM (**Figure 6.3**). In a follow-up experiment, this phenomenon was found to occur at concentrations >25 nM NE (**Figure 6.4**). This desensitizing response to high-level stimulation of α1AR is post-synaptic in origin, and likely due to receptor desensitization by phosphorylation and internalization within smooth muscle (García-Sáinz et al., 2000). Thus, subsequent experiments used ≤25 nM NE to avoid agonist-induced desensitization.

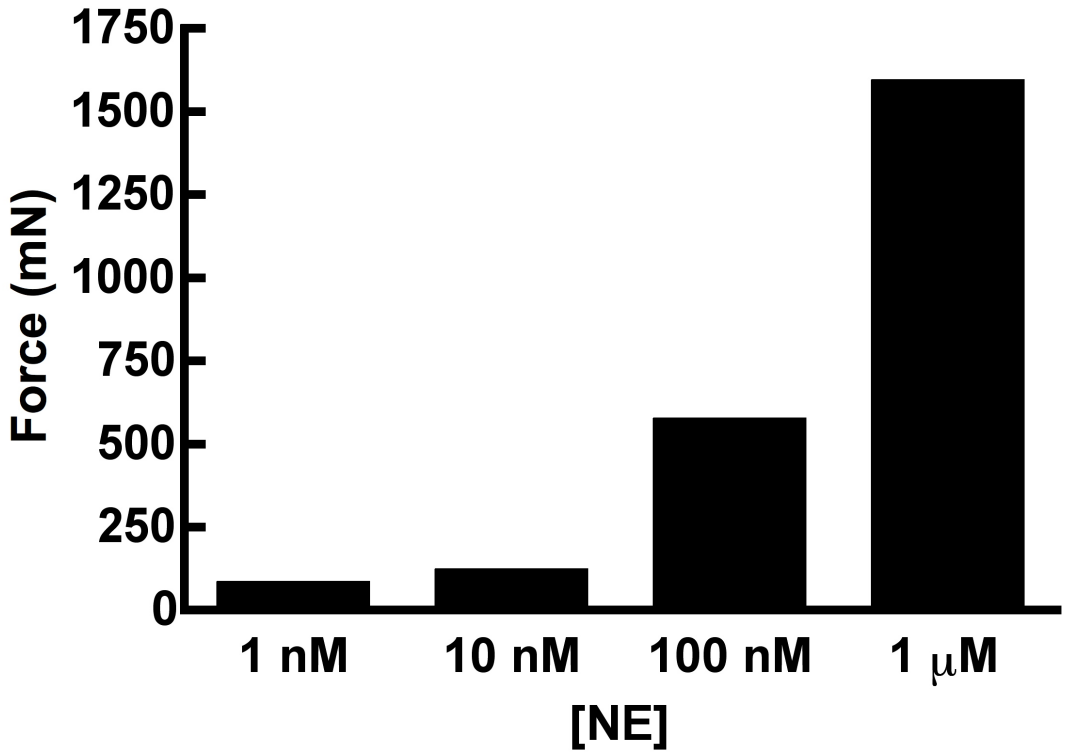


**Figure 6.1. Concentrations response of NE-induced spleen contraction.** A single spleen was removed, hung in a physiological bath, and connected to an isometric force transducer. NE was added directly to the bath medium and the resulting force of contraction was recorded to incremental NE concentrations. Columns represent the force of contraction in a single spleen to increasing concentrations of NE.

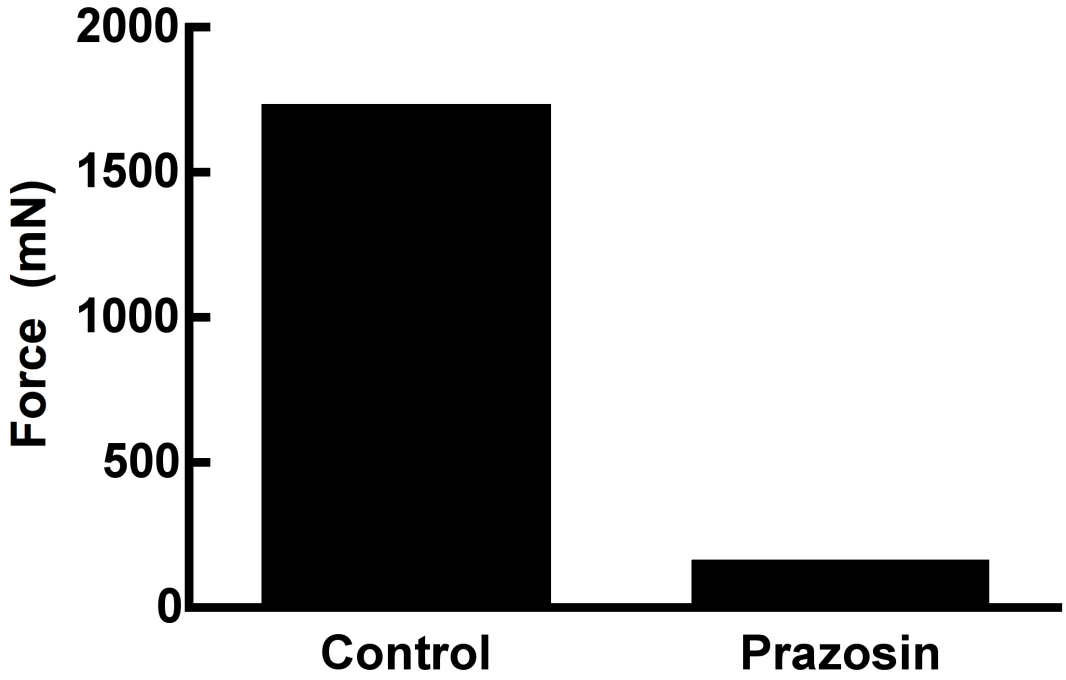


**Figure 6.2. Blockade of NE-induced spleen contraction by prazosin.** A single spleen was removed, hung in a physiological bath, and connected to an isometric force transducer. Prazosin (1.0 μM) was added 10 min before the direct addition of NE (1 μM) to the bath medium, and the resulting force of contraction was recorded. Columns represent the force of contraction in a single spleen to NE.

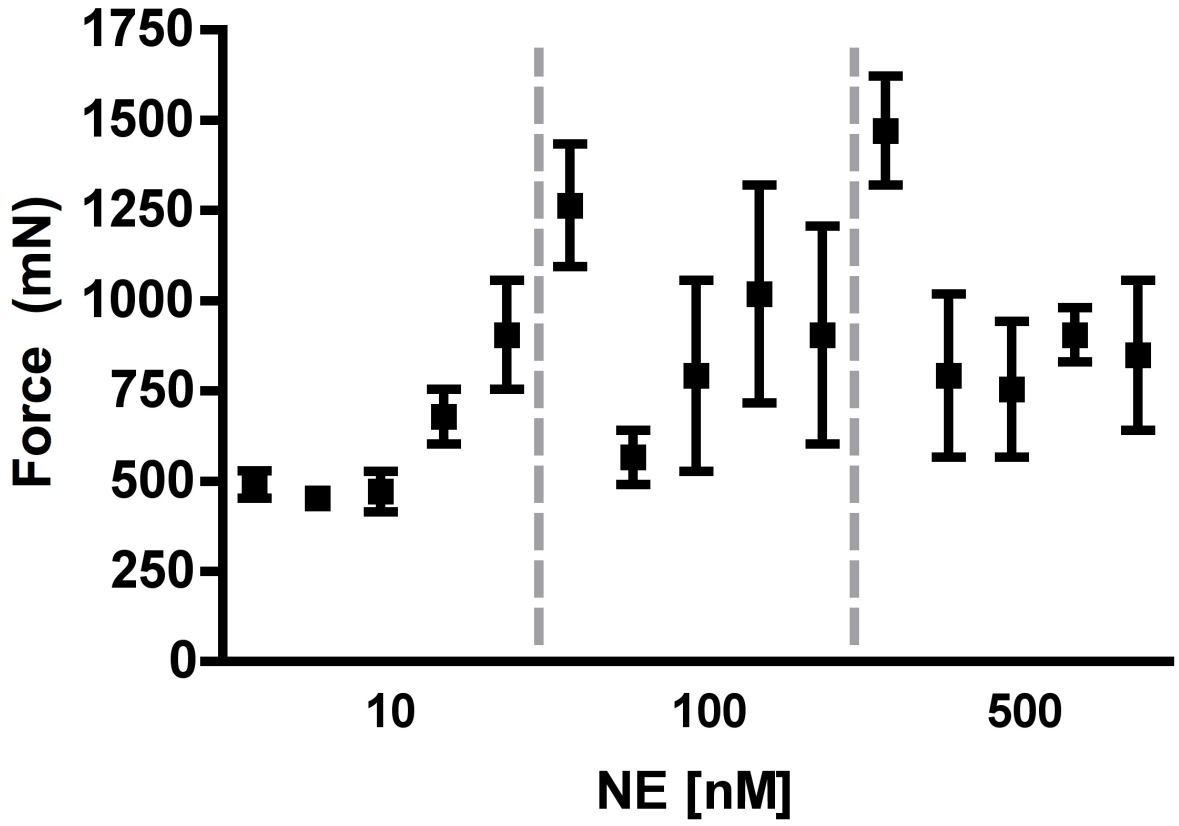


**Figure 6.3. Spleen contractions induced by repeated administration of 10, 100 or 500 nM NE.** Spleens were removed, hung in a physiological bath, and connected to an isometric force transducer. The force of contraction in response to repeated administration of increasing NE concentrations was assessed. NE was added 5 times in a row, with a 3-min wash between, for each concentration. The order of testing was from low [NE] to high [NE]. Data points represent the average force (mN) of each NE addition (in consecutive order by trial) ± one SEM (n=2).

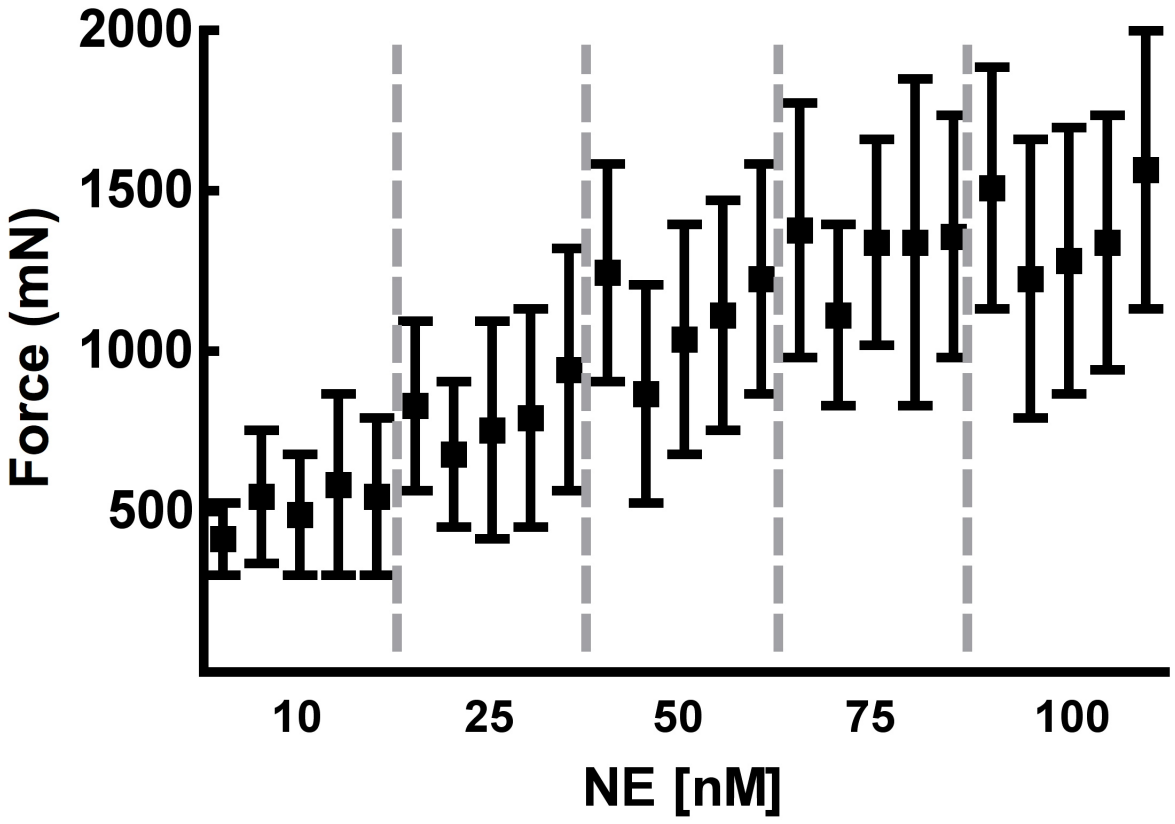


**Figure 6.4. Spleen contractions induced by repeated administration of 10-100 nM NE.** Spleens were removed, hung in a physiological bath, and connected to an isometric force transducer. The force of contraction in response to repeated administrations of increasing NE concentrations was assessed. NE was added 5 times in a row, with a 3-min wash between, for each concentration. The order of testing was from low [NE] to high [NE]. Data points represent the average force (mN) of each NE addition (in consecutive order by trial) ± one SEM (n=2).

Once it was established that NE could produce effective and reproducible spleen contractions *ex vivo,* NE-induced spleen contraction was assessed in CB1/CB2 KO mice. The working hypothesis was that spleen contraction in CB1/CB2 KO mice would be enhanced because of increased α1-adrenergic receptor expression secondary to chronically decreased spleen capsule noradrenergic sympathetic neuron activity (**Chapter 5**). Contrary to prediction, spleens from CB1/CB2 KO mice produced less forceful contractions in response to exogenous NE than those obtained from WT mice (**Figure 6.5**). The force of contraction was normalized to the weight of the spleen to control for potential differences in the absolute size and muscle mass. The spleens from CB1/CB2 KO mice also produce less force per contraction after weight normalization (**Figure 6.6**). It should be noted, too, that there is not a significant difference in spleen weight between WT and CB1/CB2 KO mice (**Figure 6.7**). These data suggest that the congenital lack of CB1 and/or CB2 receptors produces a deficit in the ability of the spleen to contract in response to NE.

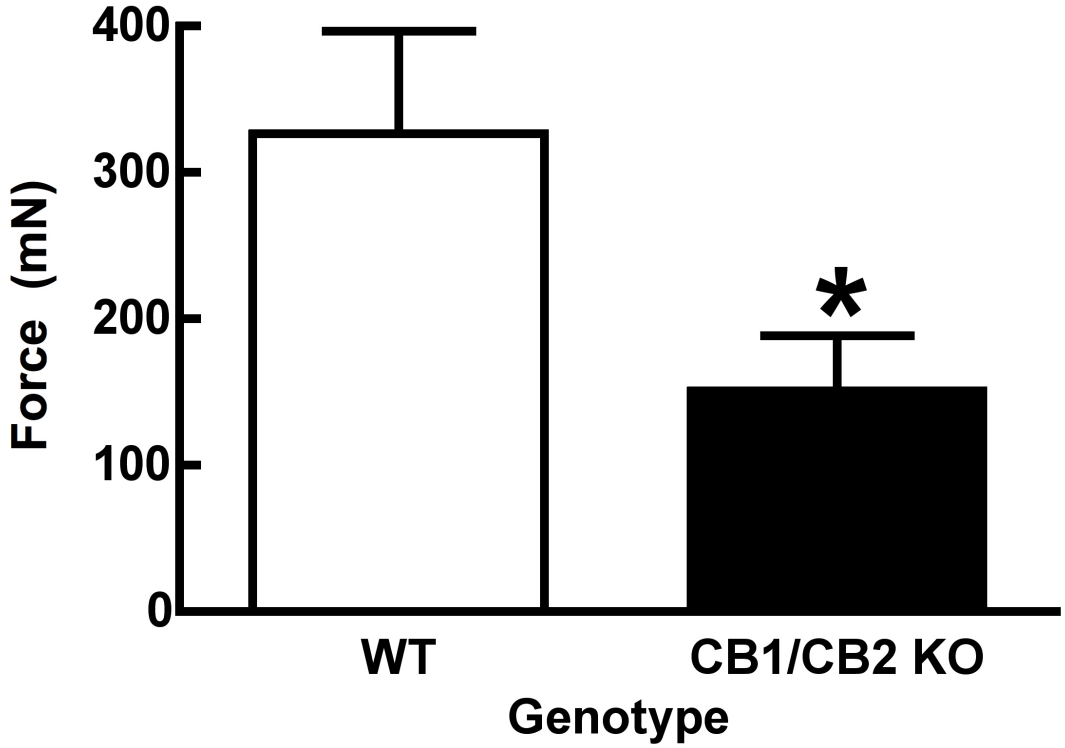


**Figure 6.5. Comparison of NE-induced spleen contraction force in WT and CB1/CB2 KO mice.** Spleens were removed, hung in a physiological bath, and connected to an isometric force transducer. The force of contraction generated by spleens in response to 25 nM NE was measured in WT and CB1/CB2 KO mice. Columns represent the average force (mN) of contraction + one SEM (n=3). * Differs from WT ($p<0.05$).

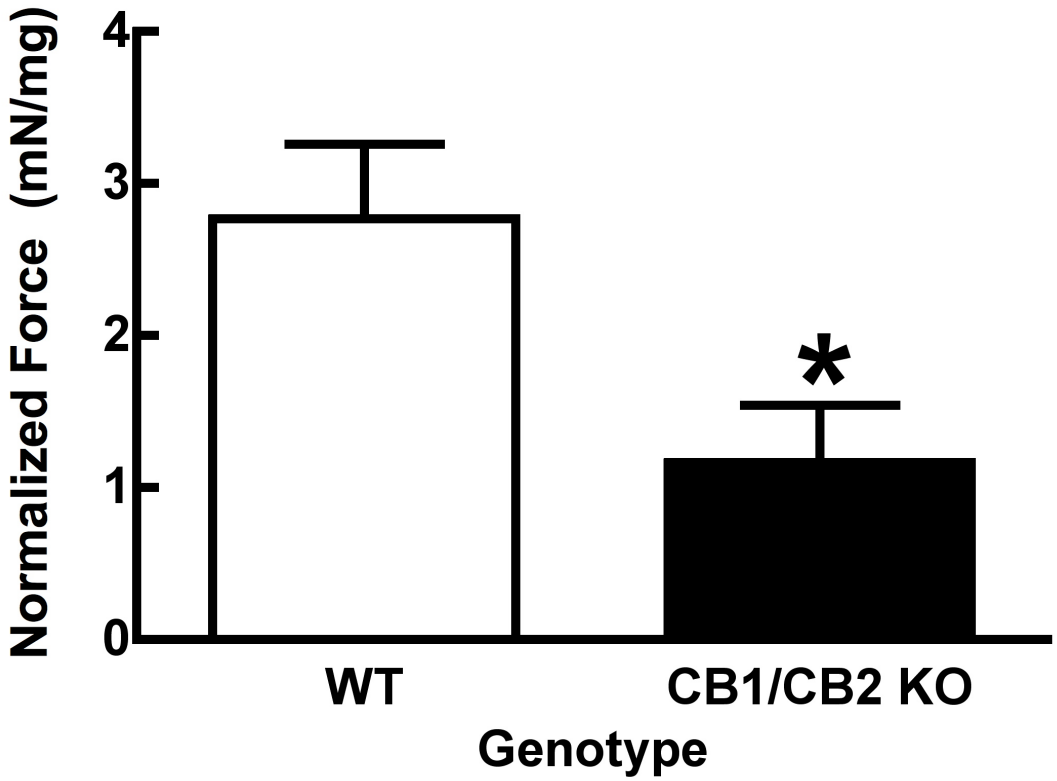


**Figure 6.6. Comparison of NE-induced weight-normalized spleen contraction force in WT and CB1/CB2 KO mice.** Spleens were removed, hung in a physiological bath, and connected to an isometric force transducer. The force of contraction generated by spleens in response to 25 nM NE was measured and normalized to the weight of the spleen in WT and CB1/CB2 KO mice. Columns represent the average weight-normalized force (mN) of contraction + one SEM (n=3). * Differs from WT ($p<0.05$).

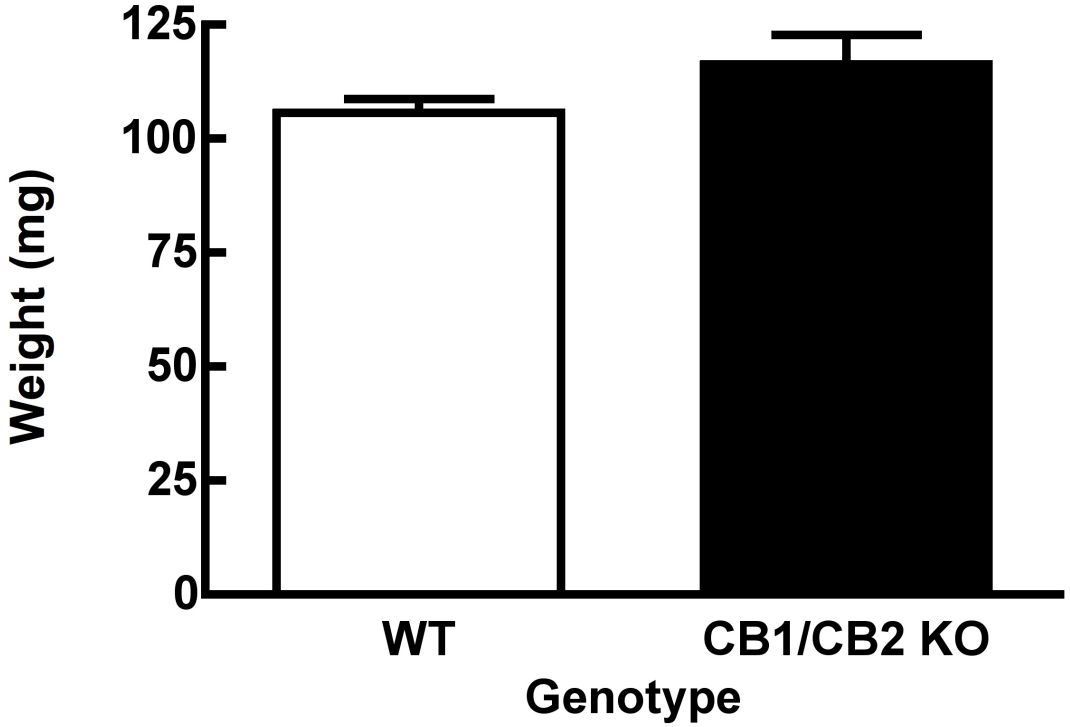


**Figure 6.7. Spleen weight comparison in WT and CB1/CB2 KO mice.** Spleens were removed and weighed. Columns represent the average weight (mg) + one SEM (n=6).

Reduced spleen contractibility in CB1/CB2 KO mice was not hypothesized to be due to a difference in the amount of smooth muscle in the spleen, as this would be expected to decrease the overall weight of the spleen. However, upon histological analysis, the thickness of the spleen capsule was significantly smaller in CB1/CB2 KO mice (**Figures 6.8 and 6.9**). A possible explanation for reduced spleen capsule thickness is a reduction in smooth muscle content. Therefore, the amount of smooth muscle in the spleen capsule was evaluated by Western blot determination of the smooth muscle specific form of $\alpha$-actin. Smooth muscle $\alpha$-actin content in the spleen capsule of CB1/CB2 KO mice was not different than that of WT mice (**Figure 6.10**).

With this data it was concluded that differences in the smooth muscle content of the spleen capsule was not a contributory factor to reduced spleen contractility in CB1/CB2 KO mice. It was hypothesized that reduced $\alpha$1AR expression might contribute to less forceful spleen contraction in mice lacking CB1/CB2. Since the contractile response of the spleen to NE is dose dependent, reduced $\alpha$1AR activity (secondary to reduced expression) would produce a reduced spleen contraction. In agreement, there is a lower amount $\alpha$1AR in the spleen capsule of CB1/CB2 KO mice as compared with WT controls (**Figure 6.11**). Collectively, these data reveal that reduced force of NE-induced spleen contractility in the absence of CB1/CB2 is due to reduced expression of $\alpha$1AR on smooth muscle in the spleen capsule.

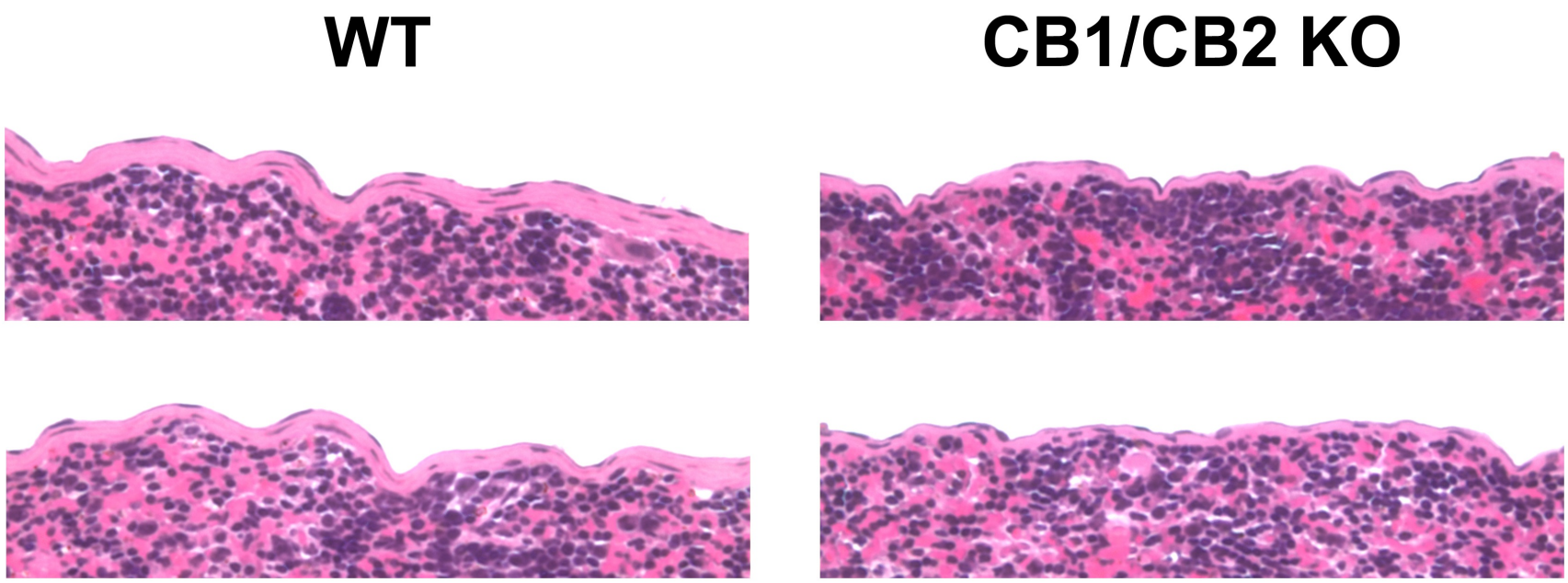


**Figure 6.8. Representative histology of the spleen capsule from WT and CB1/CB2 KO mice.** Spleens from WT and CB1/CB2 KO mice were fixed, stained with hematoxylin and eosin, and imaged at 40x magnification. Representative images of the spleen capsule from each genotype are displayed.

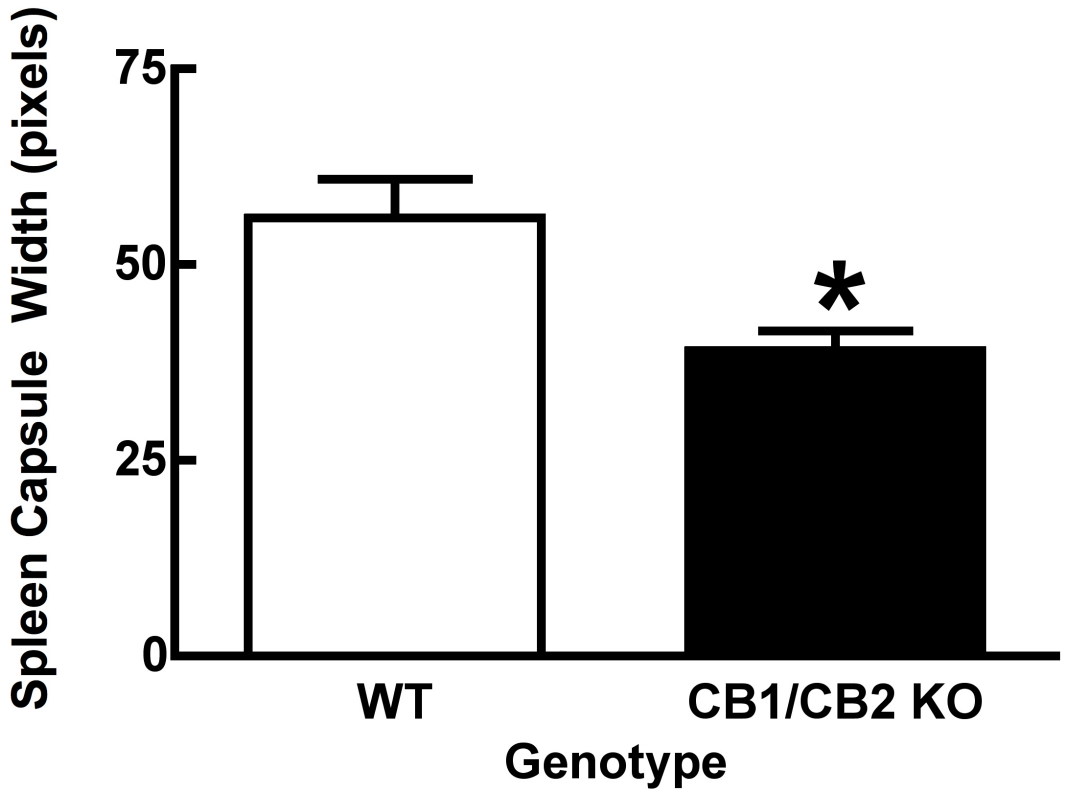


**Figure 6.9. Comparison of spleen capsule thickness in WT and CB1/CB2 KO mice.** Spleens from WT and CB1/CB2 KO mice were fixed, stained with hematoxylin and eosin, and imaged at 40x magnification. The pixel width of the spleen capsule was sampled at 12 random locations for each spleen, and the mean of these values calculated and compared statistically. Columns represent the average spleen capsule thickness (pixels) + one SEM (n=3). * Differs from WT ($p<0.05$).

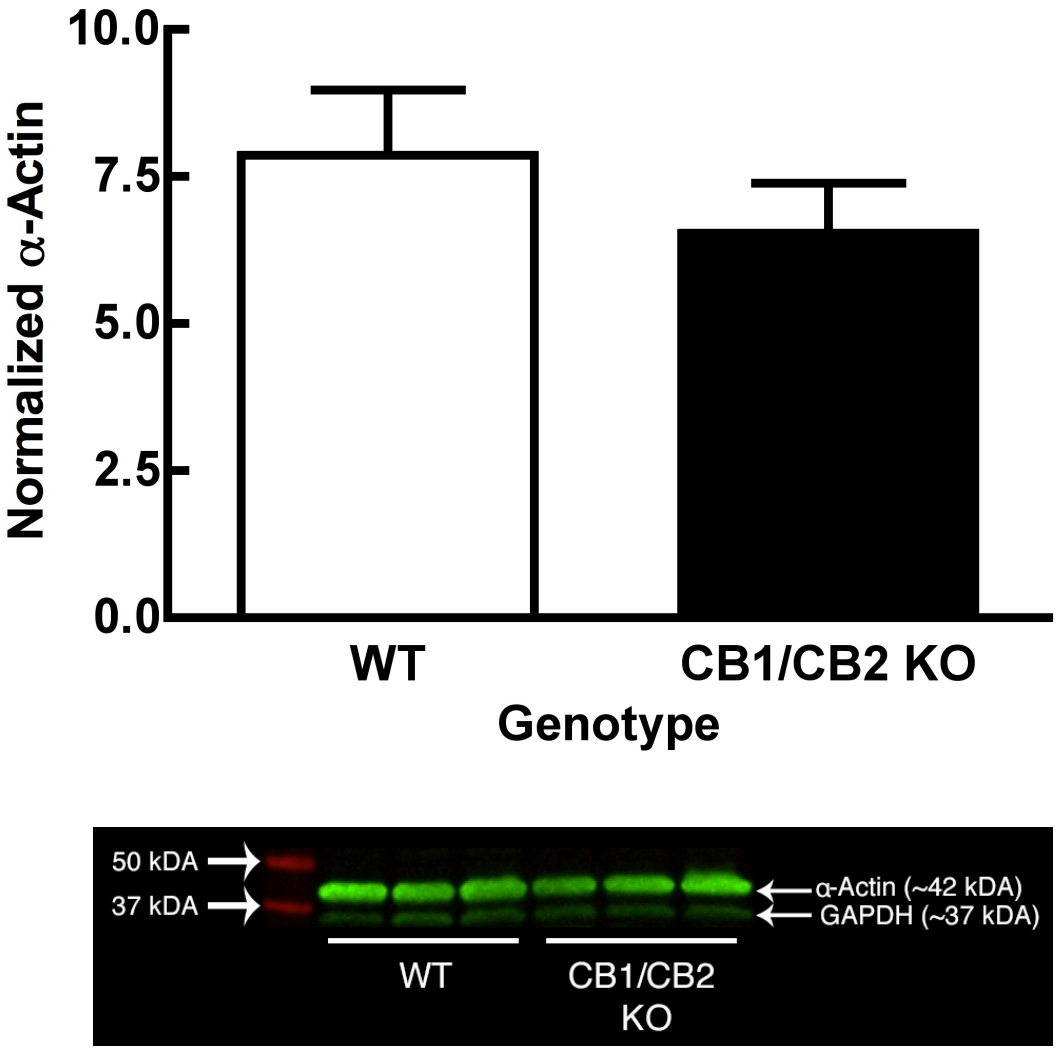


**Figure 6.10. Comparison of spleen capsule smooth muscle specific α-actin in WT and CB1/CB2 KO mice.** Spleen capsule samples from both WT and CB1/CB2 KO were prepared for analysis by Western blot for α-actin as described in the Methods (Section 6.2.4). Top: Columns represent the average amount of α-actin, normalized to GAPDH, in the spleen capsule + 1 SEM (n=5). * Differs from WT ($p<0.05$). Bottom: Representative Western blot image used for quantification.

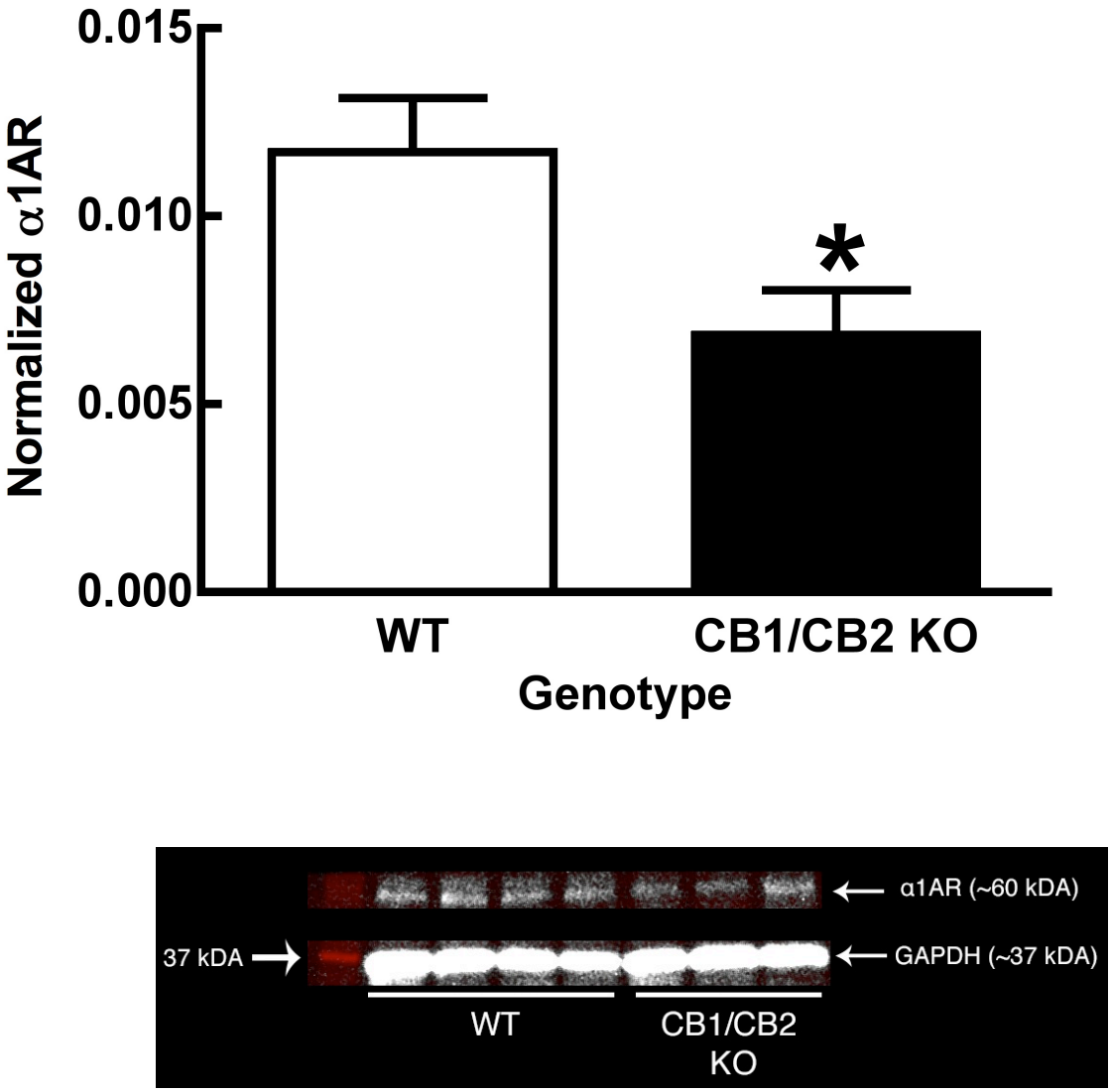


**Figure 6.11. Comparison of spleen capsule α1AR content in WT and CB1/CB2 KO mice.** Spleen capsule samples from both WT and CB1/CB2 KO were prepared for analysis by Western blot for α1AR as described in the Methods (Section 6.2.4). Top: Columns represent the average amount of α1AR, normalized to GAPDH, in the spleen capsule + 1 SEM (n=7). * Differs from WT ($p<0.05$). Bottom: Representative Western blot image used for quantification.

6.3.2: Comparison of EFS-induced spleen contraction in WT and CB1/CB2 KO mice

Following experiments utilizing exogenously applied NE, the contractile response of the spleen to EFS was investigated. The intent of electrically stimulating the spleen is to induce the release of endogenous NE and co-released neurotransmitters from sympathetic post-ganglionic axon terminals remaining in the spleen following excision. The optimization of EFS parameters was undertaken prior to experimental testing. The voltage response of spleen contraction following EFS ranged from little/no response at 10 V to a maximal response at 30 V (**Figure 6.12**). Next, it was determined that individual pulses of 0.2 ms duration induced spleen contraction through the release of neurotransmitters (as opposed to direct stimulation of voltage-gated calcium channel dependent smooth muscle contraction) since spleen contraction to EFS was blocked (zero or minimal measureable response) by TTX (**Figure 6.12**), a voltage-gated sodium channel blocker (Hille, 1975). A frequency of 25 Hz (**Figure 6.13**) and 3 sec of stimulation (**Figure 6.14**) produced optimal contraction of the spleen roughly equivalent in magnitude to that produced by 25 nM NE (**Figure 6.5**). It should be noted, however, that Hz modulation did not induce any statistically significant changes in the force of contraction (**Figure 6.13**).

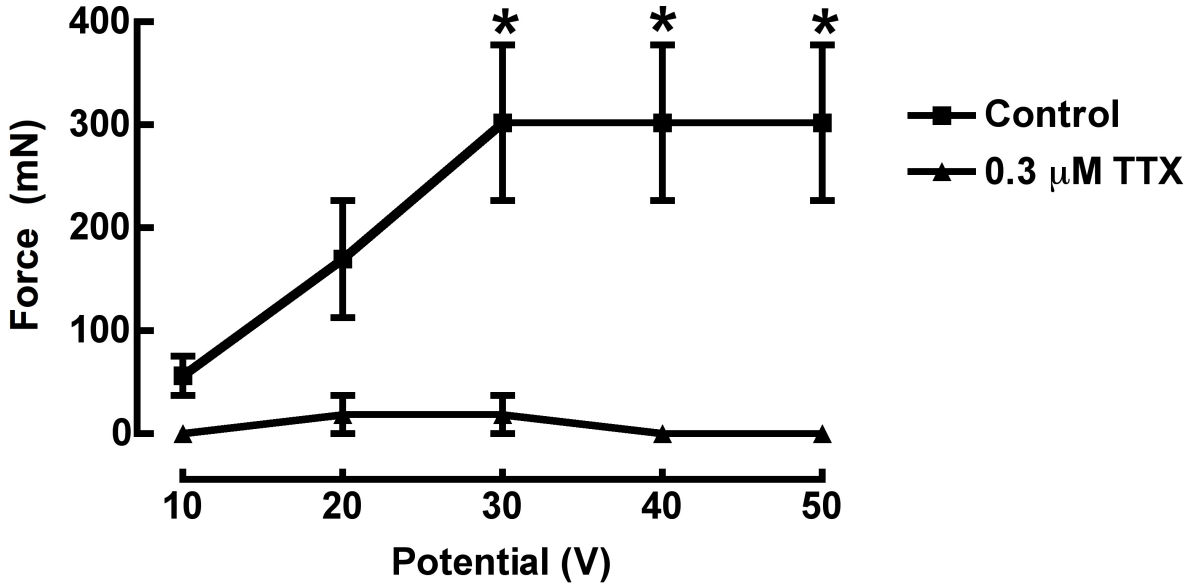


**Figure 6.12. Voltage response curve of EFS-induced spleen contraction.** Spleens from WT mice were removed, hung in a physiological bath, and connected to an isometric force transducer. The force of contraction generated by spleens was measured in response to increasing voltage and in the absence and presence of TTX (0.3 μM). EFS was done using circular platinum electrodes located above and below the spleen. Stimulation consisted of 0.2 ms square wave pulses at 20-28 mA and 8 Hz for 10 s. All data was performed in the same spleens with the control stimulations done prior to incubation with TTX and subsequent stimulation. Each point represents the average force (nM) of contraction generated ± one SEM (n=2). * Significantly differs from TTX treatment ($p<0.05$).

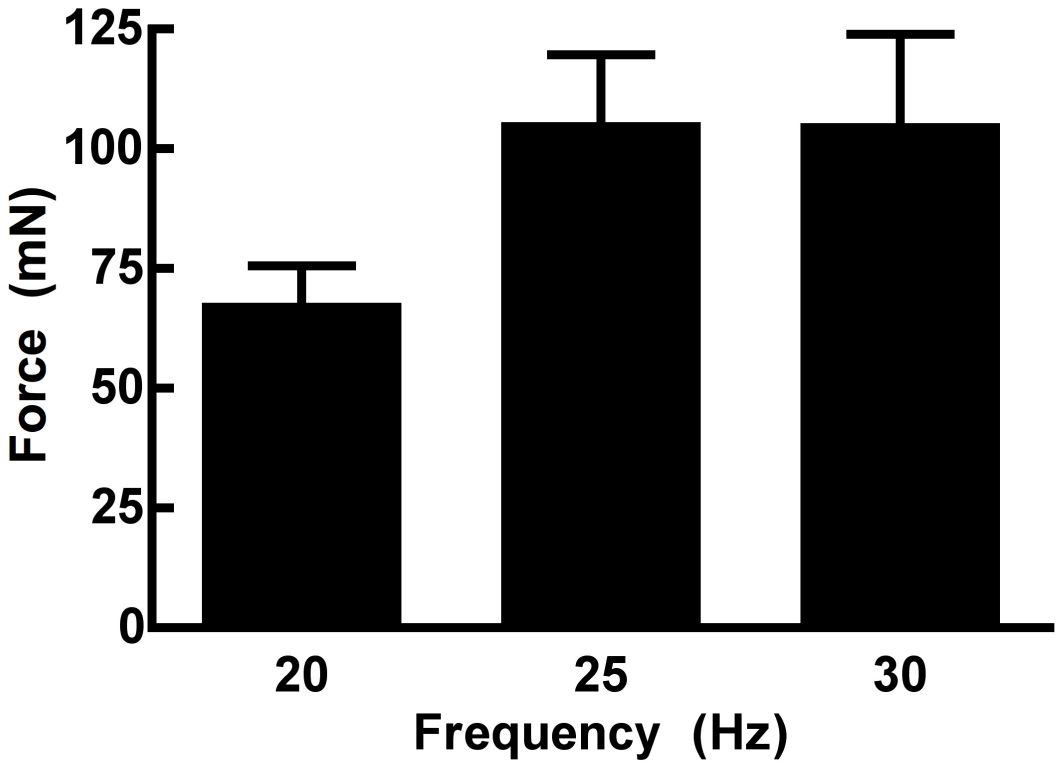


**Figure 6.13. Frequency response of EFS-induced spleen contraction**. Spleens from WT mice were removed, hung in a physiological bath, and connected to an isometric force transducer. The force of contraction generated by spleens was measured in response to increasing frequency electric pulses. EFS was done using circular platinum electrodes located above and below the spleen. The stimulation consisted of 0.2 ms square wave pulses at 20-28 mA and 40 V for 1 s. Columns represent the average force of contraction generated + one SEM (n=5).

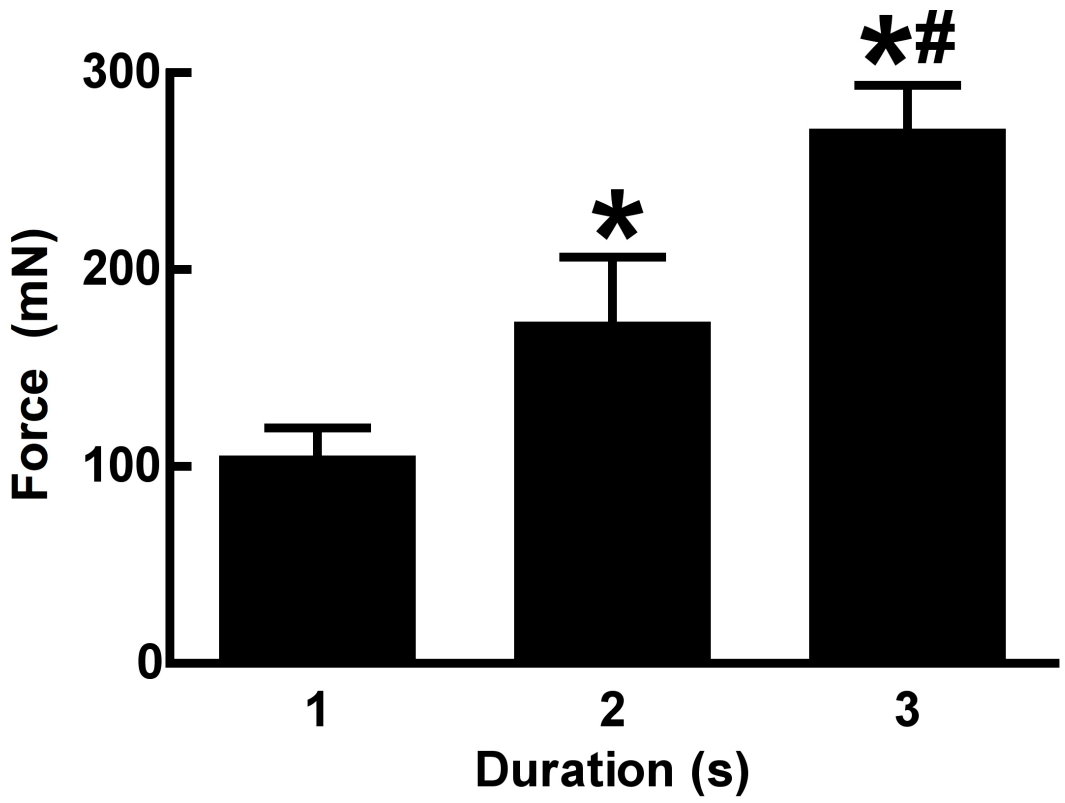


**Figure 6.14. Duration response of EFS-induced spleen contraction**. Spleens from WT mice were removed, hung in a physiological bath, and connected to an isometric force transducer. The force of contraction generated by spleens was measured in response to differing durations of stimulation. EFS was done using circular platinum electrodes located above and below the spleen. The stimulation consisted of 0.2 ms square wave pulses at 20-28 mA, 40 V, and 25 Hz. Columns represent the average force of contraction generated + one SEM (n=5). * Significantly differs from 1 s stimulation ($p<0.05$). # Significantly differs from 2 s stimulation ($p<0.05$).

After EFS parameters were established, the neurotransmitters responsible for EFS-induced spleen contraction were assessed. NE is considered to be the major neurotransmitter of sympathetic neurons (Macarthur et al., 2011), however, both ATP and NPY are well-known neurotransmitters co-released with NE from sympathetic neurons (Macarthur et al., 2011). The contribution of NE to EFS-induced spleen contraction was determined by the addition of the α1AR antagonist prazosin. Prazosin pre-treatment blocked approximately 2/3 of EFS-induced spleen contraction (**Figure 6.15**). Essentially all prazosin-insensitive spleen contraction was blocked by DPCPX (**Figure 6.15**), an adenosine A1 receptor antagonist (Fozard and Milavec-Krizman, 1993), demonstrating the role of purinergic neurotransmission in EFS spleen contraction. The contribution of NPY Y1 receptors and ATP P2X receptors, both commonly known mediators of sympathetically released NPY and ATP (Macarthur et al., 2011), were also investigated. Neither BIBP3226 (**Figure 6.16**), a Y1 receptor antagonist (Rudolf et al., 1994), nor PPADS (**Figure 6.17**), a P2X receptor antagonist (Lambrecht et al., 1992), had a significant effect on EFS-induced spleen contraction.

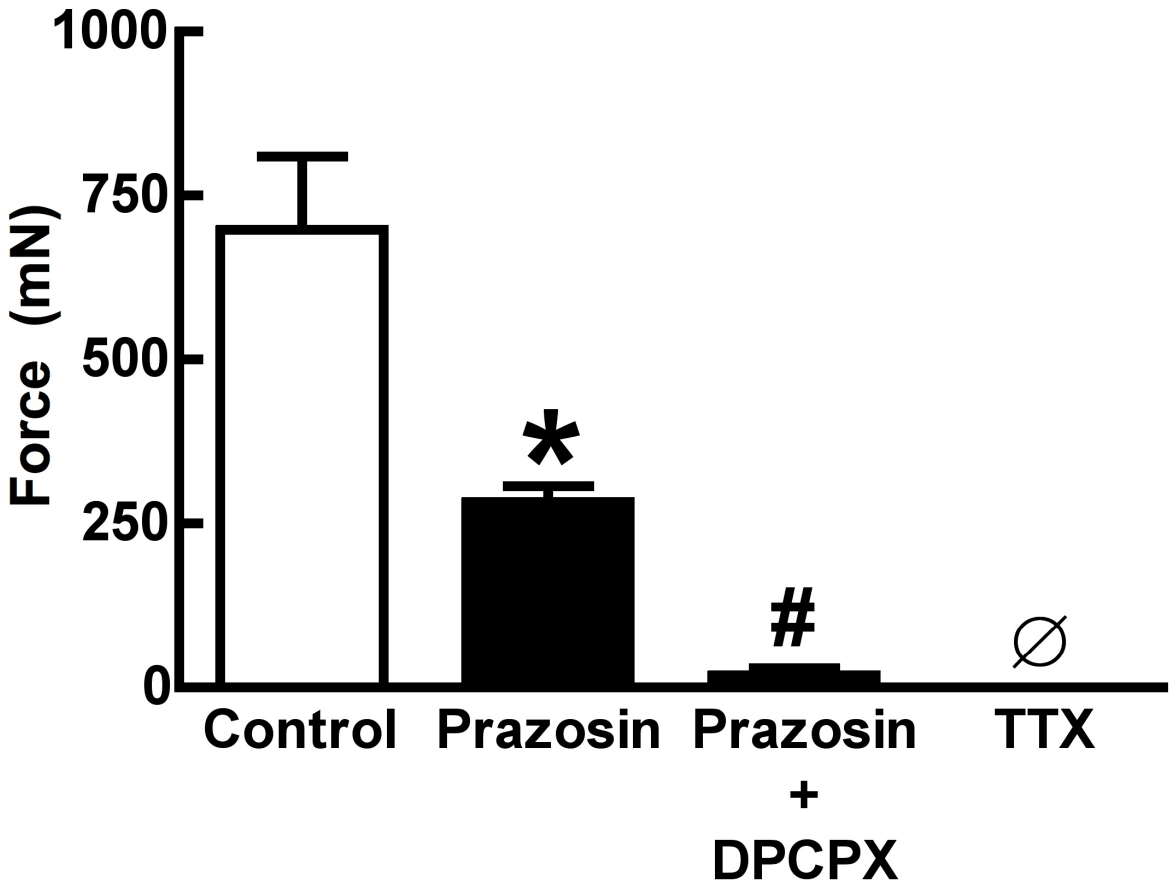


**Figure 6.15. EFS-induced spleen contraction is mediated by α1AR and adenosine A1 receptors**. Spleens from WT mice were removed, hung in a physiological bath, and connected to an isometric force transducer. The force of contraction generated by spleens was measured in response to EFS. EFS was done using circular platinum electrodes located above and below the spleen. The stimulation consisted of 0.2 ms square wave pulses with 20-28 mA at 30 V and 25 Hz for 3 s. The addition of drugs was done in the order demonstrated on the X-axis. Each drug was allowed to incubate for at least 20 min prior to EFS. The final concentrations of the individual drugs were as follows: Prazosin (P) – 1.0 μM, DPCPX (D) – 100 nM, and TTX - 0.3 μM. Columns represent the average force (mN) of contraction generated + one SEM (n=5). * Differs from Control ($p>0.05$). # Differs from Prazosin ($p>0.05$). ∅ No response.

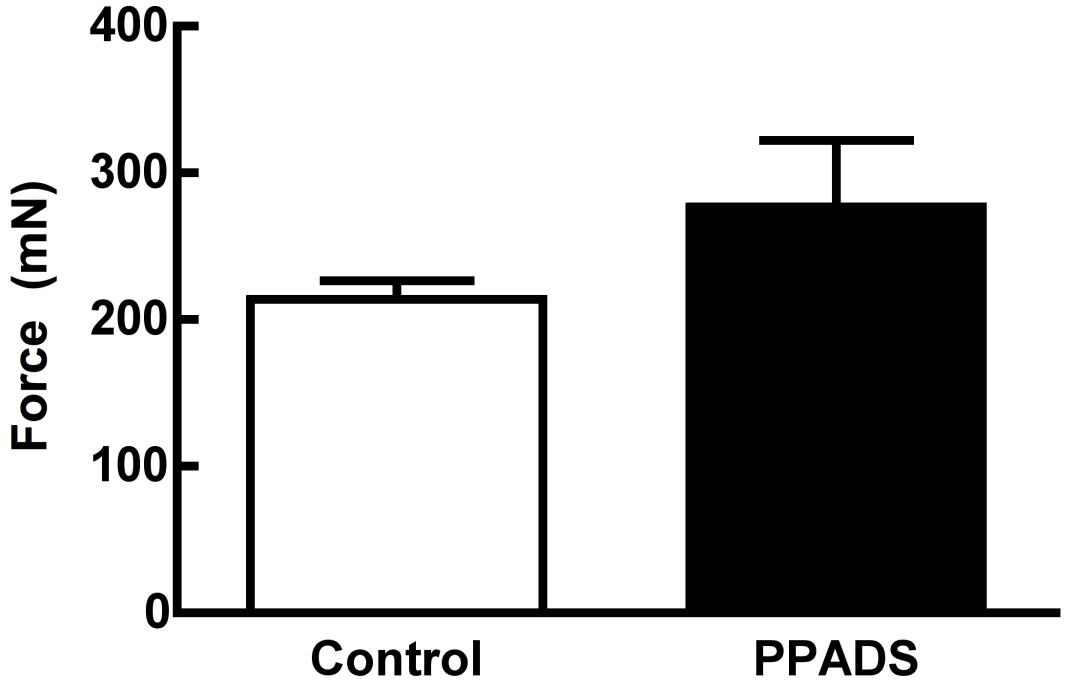


**Figure 6.16. Adenosine P2X receptors do not contribute to EFS-induced spleen contraction**. Spleens from WT mice were removed, hung in a physiological bath, and connected to an isometric force transducer. The force of contraction generated by spleens was measured in response to EFS. EFS was done using circular platinum electrodes located above and below the spleen. The stimulation consisted of 0.2 ms square wave pulses with 20-28 mA at 30 V and 25 Hz for 3 s. PPADS (10 μM) was allowed to incubate for at least 20 min prior to EFS. Columns represent the average force (mN) of contraction generated + one SEM (n=3).

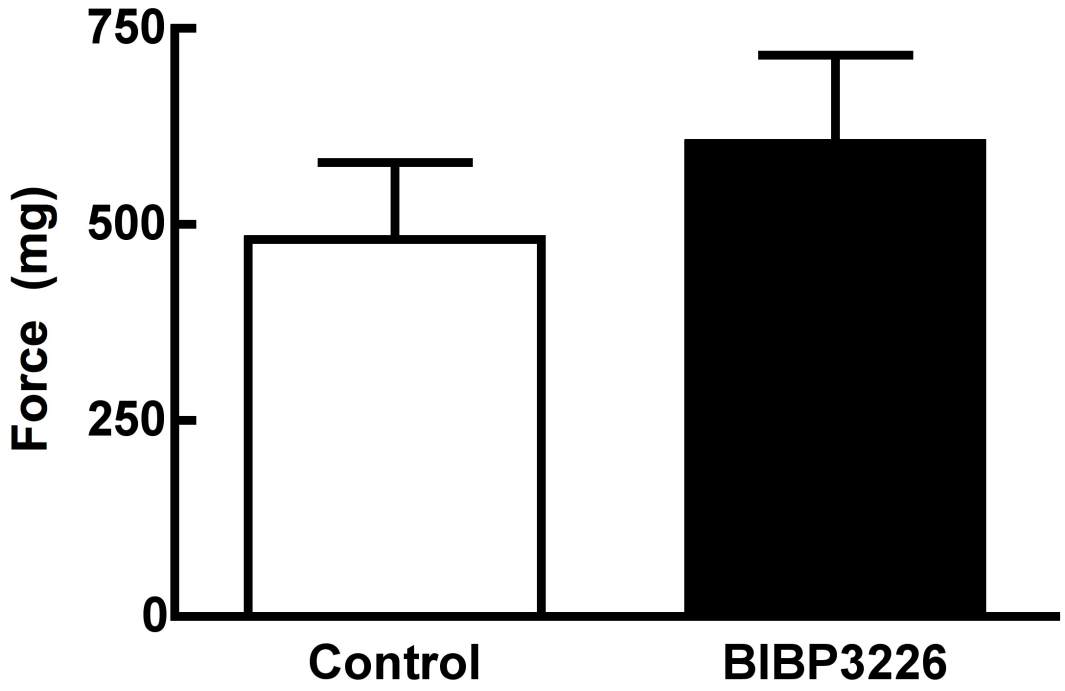


**Figure 6.17. NPY Y1 receptors do not contribute to EFS-induced spleen contraction**. Spleens from WT mice were removed, hung in a physiological bath, and connected to an isometric force transducer. The force of contraction generated by spleens was measured in response to EFS. EFS was done using circular platinum electrodes located above and below the spleen. The stimulation consisted of 0.2 ms square wave pulses with 20-28 mA at 30 V and 25 Hz for 3 s. BIBP3226 (1 μM) was allowed to incubate for at least 20 min prior to EFS. Columns represent the average force (mN) of contraction generated + one SEM (n=4).

Once the characteristics of EFS-induced spleen contraction were determined in WT mice, CB1/CB2 KO mice were investigated. It was expected that EFS-induced spleen contraction would be reduced in CB1/CB2 KO mice based on the results obtained from exogenous NE application. However, EFS-induced spleen contraction force did not differ between WT and CB1/CB2 KO mice (**Figure 6.18**). Weight-normalized EFS-induced spleen contraction also did not differ (**Figure 6.19**). These data suggest the possibility that compensatory mechanisms in CB1/CB2 KO mice act to produce normal strength spleen contraction despite reduced α1AR. This could be due to compensation by an increased contribution of adenosine – A1 receptor signaling. To determine if this is the case, the spleen contractile response to EFS was tested in WT and CB1/CB2 mice in the presence of prazosin. It was reasoned that if adenosine signaling compensates for reduced noradrenergic signaling, then in the absence of α1AR signaling the contraction of the spleen would be greater in CB1/CB2 KO than WT mice. Contrary to this hypothesis, EFS-induced spleen contraction was reduced to an equivalent extent by prazosin in both WT and CB1/CB2 KO mice (**Figure 6.20**). Thus, the non-adrenergic components of EFS-induced spleen contraction do not compensate for decreased α1AR signaling in CB1/CB2 KO mice. This may suggest that changes in the release of NE are responsible for the absence of decreased spleen contraction in response to EFS in CB1/CB2 KO mice.

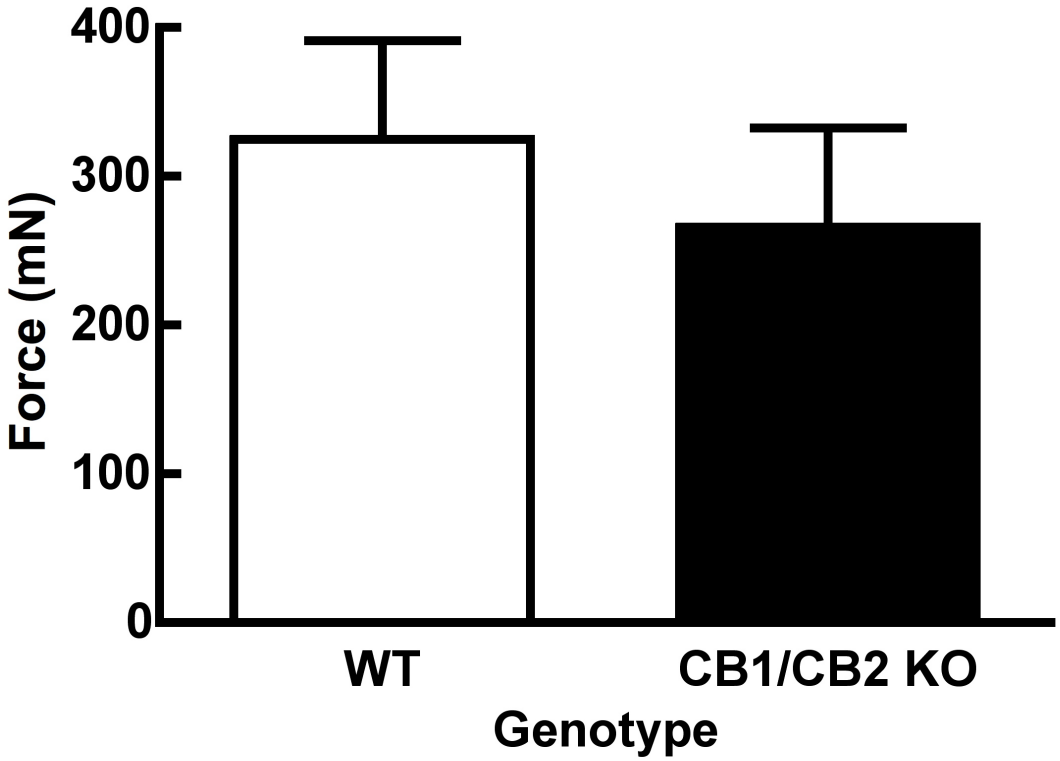


**Figure 6.18. Comparison of EFS-induced spleen contraction force in WT and CB1/CB2 KO mice.** Spleens were removed, hung in a physiological bath, and connected to an isometric force transducer. The force of contraction induced by EFS was measured in spleens from both WT and CB1/CB2 mice. EFS was done using circular platinum electrodes located above and below the spleen. The stimulation consisted of 0.2 ms square wave pulses with 20-28 mA at 30 V for 3 s at a frequency of 25 Hz. Columns represent the average force of contraction + one SEM (n=6).

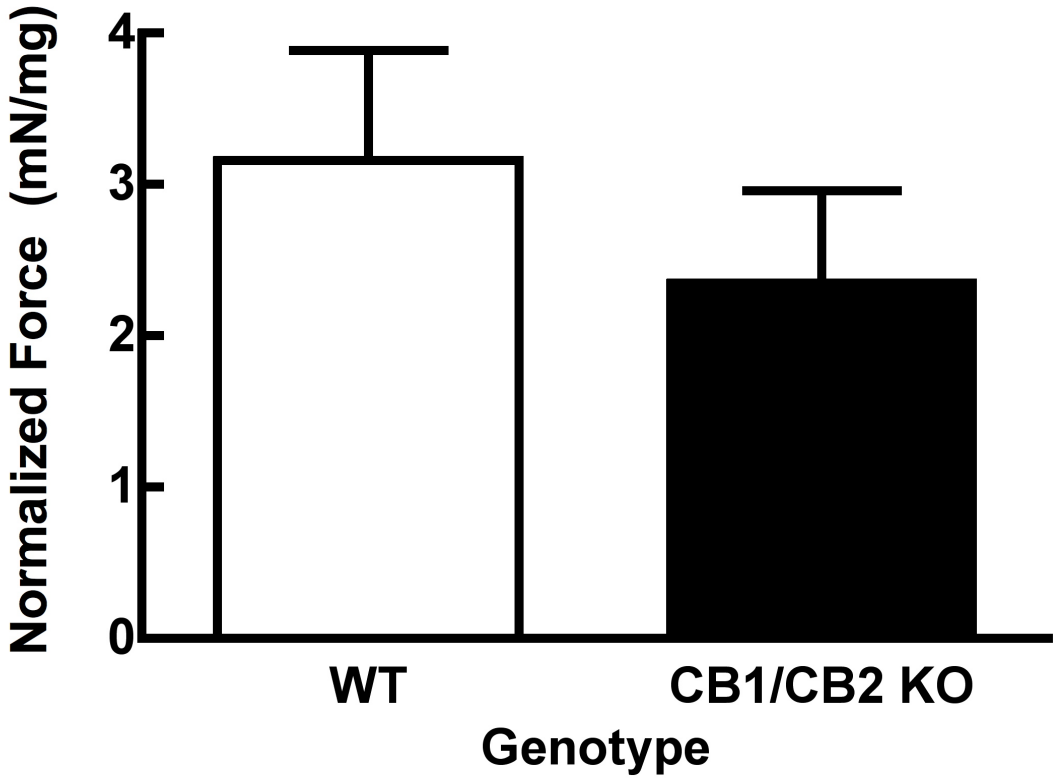


**Figure 6.19. Comparison of EFS-induced weight-normalized spleen contraction force in WT and CB1/CB2 KO mice.** Spleens were removed, hung in a physiological bath, and connected to an isometric force transducer. The force of contraction induced by EFS was measured and normalized to spleen weight for both WT and CB1/CB2 mice. EFS was done using circular platinum electrodes located above and below the spleen. The stimulation consisted of 0.2 ms square wave pulses with 20-28 mA at 30 V for 3 s at a frequency of 25 Hz. Columns represent the average weight-normalized force of contraction + one SEM (n=6).

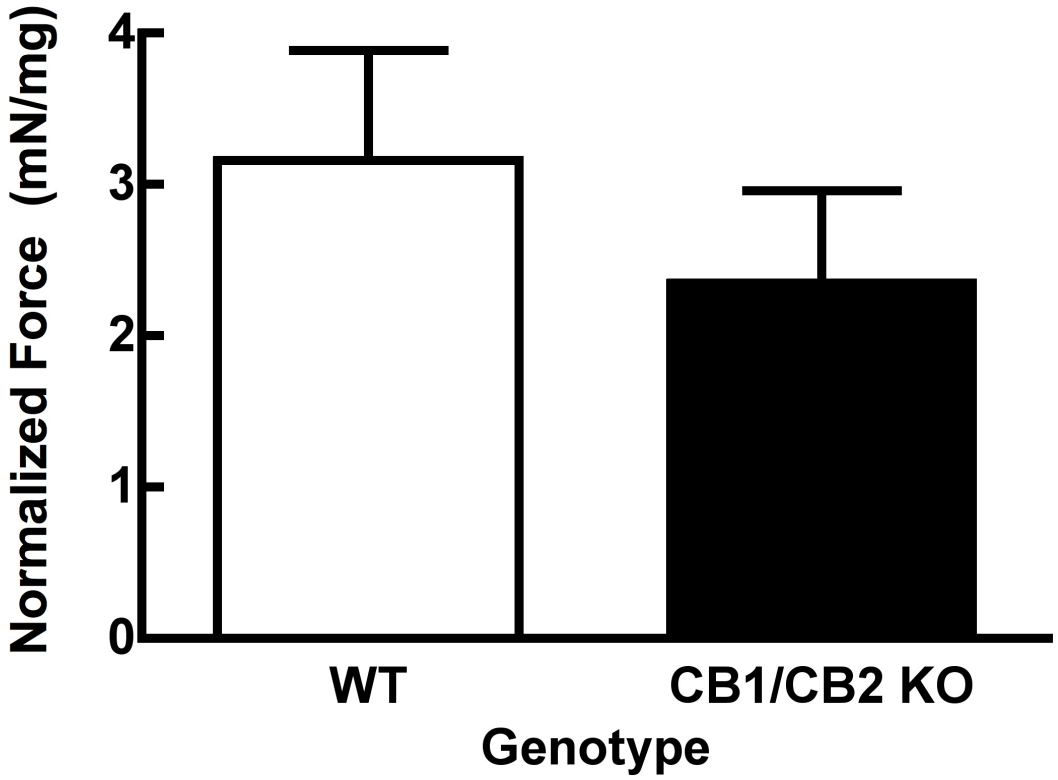


**Figure 6.20. The effect of prazosin on EFS-induced weight-normalized spleen contraction force in WT and CB1/CB2 KO mice.** Spleens were removed, hung in a physiological bath, and connected to an isometric force transducer. Prazosin (1 μM) was added to the bath medium and allowed to incubate for 20 before testing. The force of contraction induced by EFS was measured and normalized to spleen weight for both WT and CB1/CB2 mice. EFS was done using circular platinum electrodes located above and below the spleen. The stimulation consisted of 0.2 ms square wave pulses with 20-28 mA at 30 V for 3 s at a frequency of 35 Hz. Columns represent the average weight-normalized force of contraction + one SEM (n=6).

## 6.4: Discussion

The data presented in this chapter suggest that the CB1 and/or CB2 receptors are involved in the development of noradrenergic control of splenic contraction. CB1/CB2 KO mice were shown to have a decreased contractile response to exogenously applied NE that is due to a decreased expression of the α1AR in the spleen capsule. This effect, however, is absent when splenic contraction is induced by EFS. The mechanism compensating for a decrease in α1AR is not due to changes in non-adrenergic neurotransmitters.

### 6.4.1: NE-induced spleen contractility is decreased in CB1/CB2 KO mice

The data set forth here demonstrate that NE is able to contract the spleen. Furthermore the interaction between NE and spleen contraction is concentration-dependent. Spleen contraction is mediated by α1AR, as demonstrated by the ability of the pan α1AR antagonist prazosin to block this response. More specifically, other investigators have narrowed the type of α1AR to be the $\alpha 1_B$AR subtype (Eltze, 1996; Aboud et al., 2012). This specific subtype of the α1AR has previously been demonstrated to undergo phosphorylation mediated desensitization and internalization in response to NE binding (Leeb-Lundberg et al., 1987; Malbon and Wang, 2001). Internalization occurs as quickly as 5 min, which is within the time scale observed in this work (Fonseca et al., 1995). Thus, receptor phosphorylation and internalization is the likely cause for the NE-induced attenuation of spleen contraction observed at repeated high doses.

The mechanism for decreased spleen contraction force in CB1/CB2 KO mice is decreased α1AR expression on smooth muscle in the spleen capsule. This conclusion is supported by the concentration dependent increase in spleen contraction force in response to NE, and demonstrates that increasing activation of α1AR receptors results in an increased force of contraction. Thus, decreased activation of α1AR, due to decreased expression, may account for the decreased contraction observed in CB1/CB2 KO mice. This is in the face of similar weights and amounts of smooth muscle specific α-actin (Skalli et al., 1986; Johnson et al., 2010), both of which suggest an equivalent amount of smooth muscle in the spleen capsule. However, the reason for decreased α1AR expression remains unclear.

It was hypothesized that α1AR would be increased in CB1/CB2 KO mice secondary to decreased receptor stimulation, and thus decreased internalization (**Chapter 5**). However the data suggests a different interaction between α1AR expression and CB1/CB2 receptors. Whether this interaction is direct or indirect cannot be determined by the data obtained in these experiments. It remains a possibility that CB receptor expression may directly alter α1AR expression, just as was described for CB1 and β2AR (Hudson et al., 2010). While this supposition is without precedence and speculative, increasing evidence for protein-protein interactive effects between CB receptors and other G-protein coupled receptors are known (Kearn, 2005; Hudson et al., 2010; Ward et al., 2011). This hypothesis requires further investigation and likely should start with determining which receptor, CB1 or CB2, is the major mediator of decreased α1AR expression.

Interestingly, the capsule layer of the spleen in CB1/CB2 KO mice is thinner than in WT mice. The explanation for this is unclear, but does not appear to be due to differences in smooth muscle content. The other two major components of the spleen capsule are connective tissue and elastic tissue (Cesta, 2006). CB1 and CB2 have been found to have effects on the production of extracellular matrix components from fibroblast. CB1 are stimulatory to fibroblasts (Marquart et al., 2010; Lazzerini et al., 2012), whereas CB2 are inhibitory (Akhmetshina et al., 2009; Defer et al., 2009). Despite these opposing effects, these reports demonstrate that CB receptors can modulate the activity of fibroblasts. It may be the case that these effects during development account for reduced spleen capsule thickness in CB1/CB2 KO mice. Thus, an interesting line of experimentation would be to evaluate the relative contribution of CB1 and CB2 to connective tissue development in the spleen.

### 6.4.2: Normal spleen contraction in response to EFS is achieved in CB1/CB2 KO mice by a compensatory mechanism

EFS-induced spleen contraction is mediated by two different neurotransmitters. The major neurotransmitter of the sympathetic nervous system (Macarthur et al., 2011), NE, mediates approximately 2/3 of EFS-induced spleen contraction. The receptor responsible for this is the $\alpha 1_B$AR (Eltze, 1996; Aboud et al., 2012). The remaining component mediating EFS-induced spleen contraction is release of adenosine derived from the sympathetic neurotransmitter ATP (Rongen et al., 1996). Adenosine activation of A1 receptors is responsible for this action, which in agreement with other

investigators (Fozard and Milavec-Krizman, 1993). These receptors are reported to mediate a relatively small portion (18-33%) of vascular smooth muscle contraction (Tawfik et al., 2005), in agreement with the data obtained in the present study.

The compensatory mechanism whereby EFS-induced spleen contraction in CB1/CB2 KO mice is equivalent to that of WT mice does not involve changes in non-adrenergic transmission. This was demonstrated by an equivalent reduction of spleen contractile force following prazosin blockade of noradrenergic transmission through α1AR. Thus, the contribution of NE to EFS-induced spleen contraction in CB1/CB2 KO mice is equivalent to WT despite a reduction in α1AR. A possible explanation for this phenomenon is an increase in the quantal release of NE in CB1/CB2 KO mice. An increase in the amount of NE released per action potential would hypothetically stimulate more α1AR in CB1/CB2 KO mice, thus compensating for decreased α1AR expression. CB1/CB2 KO mice may indeed be primed for this scenario as splenic noradrenergic axon terminals in these mice contain more NE than WT mice (**Chapter 5**). Additionally, increased release of neurotransmitter is not without precedence as it has been shown that BDNF can increase the quantal release of glutamate in the hippocampus (Tyler and Pozzo-Miller, 2001; Amaral and Pozzo-Miller, 2012). However, while this hypothesis may explain the observed data, it is untested and requires further validation.

*6.4.3: Conclusion*

The purpose of this chapter was to test the hypothesis that spleen contraction is enhanced in CB1/CB2 KO mice presumably do to an up-regulation of α1AR expression compensating for decreased NE engagement of these receptors. First, it was demonstrated that NE can cause a concentration-dependent induction of spleen contraction via α1AR activation, but the force of contraction is reduced in CB1/CB2 KO mice. Reduced NE-induced spleen contraction in CB1/CB2 KO mice is due to decreased α1AR expression. However, EFS-induced spleen contraction in CB1/CB2 KO is not different than WT. Thus, compensatory mechanisms are able to overcome the deficit of α1AR expression in these mice. This compensation is not due to changes in adenosine stimulation of A1 adenosine receptors of EFS-induced spleen contraction.

# REFERENCES

# REFERENCES


Aboud R, Shafii M, Docherty JR. Investigation of the subtypes of α1-adrenoceptor mediating contractions of rat aorta, vas deferens and spleen. Br J Pharmacol. 2012 Jul 19;109(1):80–7.

Akhmetshina A, Dees C, Busch N, Beer J, Sarter K, Zwerina J, et al. The cannabinoid receptor CB2 exerts antifibrotic effects in experimental dermal fibrosis. Arthritis Rheum. 2009 Apr;60(4):1129–36.

Amaral MD, Pozzo-Miller L. Intracellular Ca2+ stores and Ca2+ influx are both required for BDNF to rapidly increase quantal vesicular transmitter release. Neural Plast. 2012;2012:203536. PMCID: PMC3397209

Bakovic D, Eterovic D, Saratlija-Novaković Z, Palada I, Valic Z, Bilopavlović N, et al. Effect of human splenic contraction on variation in circulating blood cell counts. Clin Exp Pharmacol Physiol. 2005 Nov;32(11):944–51.

Bakovic D, Valic Z, Eterovic D, Vukovic I, Obad A, Marinović-Terzić I, et al. Spleen volume and blood flow response to repeated breath-hold apneas. J. Appl. Physiol. 2003 Oct;95(4):1460–6.

Blue J, Weiss L. Electron microscopy of the red pulp of the dog spleen including vascular arrangements, periarterial macrophage sheaths (Ellipsoids), and the contractile, innervated reticular meshwork. Am. J. Anat. 1981 Jun;161(2):189–218.

Bootman MD, Rietdorf K, Hardy H, Dautova Y, Corps E, Pierro C, et al. Calcium Signalling and Regulation of Cell Function. els.net. Chichester, UK: John Wiley & Sons, Ltd; 2001.

Buckley N, McCoy K, Mezey E, Bonner T, Zimmer A, Felder C, et al. Immunomodulation by cannabinoids is absent in mice deficient for the cannabinoid CB(2) receptor. Eur J Pharmacol. 2000 May 19;396(2-3):141–9.

Burnstock G, Ralevic V. Purinergic Signaling and Blood Vessels in Health and Disease.

Cambridge D, Davey MJ. Prazosin, a selective antagonist of post-synaptic alpha-adrenoceptors [proceedings]. British journal of …. 1977.

Cesta M. Normal Structure, Function, and Histology of the Spleen. Toxicol Pathol. 2006;34(5):455–65.

Chevendra V, Weaver LC. Distributions of neuropeptide Y, vasoactive intestinal peptide and somatostatin in populations of postganglionic neurons innervating the rat kidney, spleen and intestine. Neuroscience. 1992 Oct;50(3):727–43.

Corder R, Lowry PJ, Withrington PG. The actions of the peptides, neuropeptide Y and peptide YY, on the vascular and capsular smooth muscle of the isolated, blood-perfused spleen of the dog. Br J Pharmacol. 1987 Apr;90(4):785–90. PMCID: PMC1917199

Davies BN, Withrington PG. The actions of drugs on the smooth muscle of the capsule and blood vessels of the spleen. Pharmacol Rev. 1973 Sep;25(3):373–413.

Defer N, Wan J, Souktani R, Escoubet B, Perier M, Caramelle P, et al. The cannabinoid receptor type 2 promotes cardiac myocyte and fibroblast survival and protects against ischemia/reperfusion-induced cardiomyopathy. FASEB J. 2009 Jul;23(7):2120–30.

Elenkov I, Vizi E. Presynaptic modulation of release of noradrenaline from the sympathetic nerve terminals in the rat spleen. Neuropharmacology. 1991 Dec 1;30(12A):1319–24.

Eltze M. Functional evidence for an alpha 1B-adrenoceptor mediating contraction of the mouse spleen. Eur J Pharmacol. 1996 Sep 12;311(2-3):187–98.

Felten DL, Ackerman KD, Wiegand SJ, Felten SY. Noradrenergic sympathetic innervation of the spleen: I. Nerve fibers associate with lymphocytes and macrophages in specific compartments of the splenic white pulp. J Neurosci Res. 1987;18(1):28–36, 118–21.

Felten SY, Olschowka J. Noradrenergic sympathetic innervation of the spleen: II. Tyrosine hydroxylase (TH)-positive nerve terminals form synapticlike contacts on lymphocytes in the splenic white pulp. J Neurosci Res. 1987;18(1):37–48.

Fonseca MI, Button DC, Brown RD. Agonist regulation of alpha 1B-adrenergic receptor subcellular distribution and function. J Biol Chem. 1995 Apr 14;270(15):8902–9.

Fozard JR, Milavec-Krizman M. Contraction of the rat isolated spleen mediated by adenosine A1 receptor activation. Br J Pharmacol. 1993 Jul 19;109(4):1059–63. PMCID: PMC2175713

García-Sáinz JA, Vázquez-Prado J, del Carmen Medina L. α1-Adrenoceptors: function and phosphorylation. Eur J Pharmacol. 2000 Feb;389(1):1–12.

Gerald T, Ward G, Howlett A, Franklin S. CB1 knockout mice display significant changes in striatal opioid peptide and D4 dopamine receptor gene expression. Brain Res. 2006 Jun 6;1093(1):20–4.

Gillespie JS, Hamilton DN. Binding of noradrenaline to smooth muscle cells in the spleen. Nature. 1966 Oct 29;212(5061):524–5.

Groom AC, Schmidt EE, MacDonald IC. Microcirculatory pathways and blood flow in spleen: new insights from washout kinetics, corrosion casts, and quantitative intravital videomicroscopy. Scanning Microsc. 1991 Mar;5(1):159–73– discussion173–4.

Hille B. The receptor for tetrodotoxin and saxitoxin. A structural hypothesis. Biophysical Journal. The Biophysical Society; 1975 Jun 1;15(6):615.

Hudson BD, Hébert TE, Kelly MEM. Physical and functional interaction between CB1 cannabinoid receptors and beta2-adrenoceptors. Br J Pharmacol. 2010 Jun;160(3):627–42. PMCID: PMC2931563

Ignarro LJ, Titus E. The presence of antagonistically acting alpha and beta adrenergic receptors in the mouse spleen. J Pharmacol Exp Ther. 1968 Mar;160(1):72–80.

Ishac E, Jiang L, Lake K, Varga K, Abood M, Kunos G. Inhibition of exocytotic noradrenaline release by presynaptic cannabinoid CB1 receptors on peripheral sympathetic nerves. Br J Pharmacol. 1996 Aug 1;118(8):2023–8. PMCID: PMC1909901

Jarai Z, Wagner J, Varga K, Lake K, Compton D, Martin B, et al. Cannabinoid-induced mesenteric vasodilation through an endothelial site distinct from CB1 or CB2 receptors. Proc Natl Acad Sci U S A. 1999 Nov 23;96(24):14136–41.

Johnson KB, Thompson JM, Watts SW. Modification of proteins by norepinephrine is important for vascular contraction. Front Physiol. 2010;1:131. PMCID: PMC3059971

Kaplan BLF, Lawver JE, Karmaus PWF, Ngaotepprutaram T, Birmingham NP, Harkema JR, et al. The effects of targeted deletion of cannabinoid receptors CB1 and CB2 on intranasal sensitization and challenge with adjuvant-free ovalbumin. Toxicol Pathol. 2010 Apr;38(3):382–92. PMCID: PMC2941344

Kearn CS. Concurrent Stimulation of Cannabinoid CB1 and Dopamine D2 Receptors Enhances Heterodimer Formation: A Mechanism for Receptor Cross-Talk? Molecular Pharmacology. 2005 Feb 9;67(5):1697–704.

Kubo T, Su C. Effects of adenosine on [3H]norepinephrine release from perfused mesenteric arteries of SHR and renal hypertensive rats. Eur J Pharmacol. 1983 Feb 18;87(2-3):349–52.

Kuwahira I, Kamiya U, Iwamoto T, Moue Y, Urano T, Ohta Y, et al. Splenic contraction-induced reversible increase in hemoglobin concentration in intermittent hypoxia. J. Appl. Physiol. 1999 Jan;86(1):181–7.

Kügelgen von I, Späth L, Starke K. Stable adenine nucleotides inhibit [3H]-noradrenaline release in rabbit brain cortex slices by direct action at presynaptic adenosine A1-

receptors. Naunyn-Schmied Arch Pharmacol. 1992 Aug;346(2):187–96.

Lambrecht G, Friebe T, Grimm U, Windscheif U, Bungardt E, Hildebrandt C, et al. PPADS, a novel functionally selective antagonist of P2 purinoceptor-mediated responses. Eur J Pharmacol. 1992 Jul 7;217(2-3):217–9.

Lazzerini PE, Natale M, Gianchecchi E, Capecchi PL, Montilli C, Zimbone S, et al. Adenosine A2A receptor activation stimulates collagen production in sclerodermic dermal fibroblasts either directly and through a cross-talk with the cannabinoid system. J. Mol. Med. 2012 Mar;90(3):331–42.

Leeb-Lundberg LM, Cotecchia S, DeBlasi A, Caron MG, Lefkowitz RJ. Regulation of adrenergic receptor function by phosphorylation. I. Agonist-promoted desensitization and phosphorylation of alpha 1-adrenergic receptors coupled to inositol phospholipid metabolism in DDT1 MF-2 smooth muscle cells. J Biol Chem. 1987 Mar 5;262(7):3098–105.

Lundberg JM, Franco-Cereceda A, Lacroix JS, Pernow J. Neuropeptide Y and sympathetic neurotransmission. Ann N Y Acad Sci. 1990;611:166–74.

Macarthur H, Wilken GH, Westfall TC, Kolo LL. Neuronal and non-neuronal modulation of sympathetic neurovascular transmission. Acta Physiol (Oxf). 2011 Sep;203(1):37–45. PMCID: PMC3139802

Malbon CC, Wang H-Y. Adrenergic Receptors. onlinelibrary.wiley.com. Chichester, UK: John Wiley & Sons, Ltd; 2001.

Marquart S, Zerr P, Akhmetshina A, Palumbo K, Reich N, Tomcik M, et al. Inactivation of the cannabinoid receptor CB1 prevents leukocyte infiltration and experimental fibrosis. Arthritis Rheum. 2010 Nov;62(11):3467–76.

Mebius RE, Kraal G. Structure and function of the spleen. Nat Rev Immunol. Nature Publishing Group; 2005 Aug;5(8):606–16.

Michel MC, Beck-Sickinger A, Cox H, Doods HN, Herzog H, Larhammar D, et al. XVI. International Union of Pharmacology recommendations for the nomenclature of neuropeptide Y, peptide YY, and pancreatic polypeptide receptors. Pharmacol Rev. 1998 Mar;50(1):143–50.

Niederhoffer N, Szabo B. Effect of the cannabinoid receptor agonist WIN55212-2 on sympathetic cardiovascular regulation. Br J Pharmacol. 1999 Jan;126(2):457–66.

Noble J, Bailey M. Quantitation of protein. Methods Enzymol. 2009;463:73–95.

Pinkus GS, Warhol MJ, O'Connor EM, Etheridge CL, Fujiwara K. Immunohistochemical localization of smooth muscle myosin in human spleen, lymph node, and other

lymphoid tissues. Unique staining patterns in splenic white pulp and sinuses, lymphoid follicles, and certain vasculature, with ultrastructural correlations. Am. J. Pathol. 1986 Jun;123(3):440–53. PMCID: PMC1888274

Ralevic V. Purines as Neurotransmitters and Neuromodulators in Blood Vessels. CVP. 2009 Jan 1;7(1):3–14.

Ralevic V, Kendall DA. Cannabinoids inhibit pre- and postjunctionally sympathetic neurotransmission in rat mesenteric arteries. Eur J Pharmacol. 2002 May 31;444(3):171–81.

Ren LM, Burnstock G. Prominent sympathetic purinergic vasoconstriction in the rabbit splenic artery: potentiation by 2,2′-pyridylisatogen tosylate - Ren - 2009 - British Journal of Pharmacology - Wiley Online Library. Br J Pharmacol. 1997.

Richardson MX, de Bruijn R, Schagatay E. Hypoxia augments apnea-induced increase in hemoglobin concentration and hematocrit. Eur. J. Appl. Physiol. 2009 Jan;105(1):63–8.

Richardson MX, Lodin A, Reimers J, Schagatay E. Short-term effects of normobaric hypoxia on the human spleen. Eur. J. Appl. Physiol. Springer-Verlag; 2007 Nov 28;104(2):395–9.

Romano TA, Felten SY, Felten DL, Olschowka JA. Neuropeptide-Y innervation of the rat spleen: another potential immunomodulatory neuropeptide. Brain Behav Immun. 1991 Mar;5(1):116–31.

Rongen GA, Lenders JW, Lambrou J, Willemsen JJ, Van Belle H, Thien T, et al. Presynaptic inhibition of norepinephrine release from sympathetic nerve endings by endogenous adenosine. Hypertension. 1996 Apr;27(4):933–8.

Rudolf K, Eberlein W, Engel W, Wieland HA, Willim KD, Entzeroth M, et al. The first highly potent and selective non-peptide neuropeptide Y Y1 receptor antagonist: BIBP3226. Eur J Pharmacol. 1994 Dec 27;271(2-3):R11–3.

Saito H, Yokoi Y, Watanabe S, Tajima J, Kuroda H, Namihisa T. Reticular meshwork of the spleen in rats studied by electron microscopy. Am. J. Anat. 1988 Mar;181(3):235–52.

Sandler MP, Kronenberg MW, Forman MB, Wolfe OH, Clanton JA, Partain CL. Dynamic fluctuations in blood and spleen radioactivity: splenic contraction and relation to clinical radionuclide volume calculations. J. Am. Coll. Cardiol. 1984 May;3(5):1205–11.

Sato N, Shen YT, Kiuchi K, Shannon RP, Vatner SF. Splenic contraction-induced increases in arterial O2 reduce requirement for CBF in conscious dogs. American

Journal of Physiology - Heart and Circulatory Physiology. American Physiological Society; 1995 Aug 1;269(2):H491–H503.

Sato S, Steeber DA, Jansen PJ, Tedder TF. CD19 expression levels regulate B lymphocyte development: human CD19 restores normal function in mice lacking endogenous CD19. J Immunol. 1997 May 15;158(10):4662–9.

Satodate R, Tanaka H, Sasou S, Sakuma T, Kaizuka H. Scanning electron microscopical studies of the arterial terminals in the red pulp of the rat spleen. Anat. Rec. 1986 Jul;215(3):214–6.

Schmidt EE, MacDonald IC, Groom AC. Microcirculation in mouse spleen (nonsinusal) studied by means of corrosion casts. Journal of morphology. 1985.

Schmidt EE, MacDonald IC, Groom AC. Comparative aspects of splenic microcirculatory pathways in mammals: the region bordering the white pulp. Scanning Microsc. 1993 Jun;7(2):613–28.

Sedaa KO, Bjur RA, Shinozuka K, Westfall DP. Nerve and drug-induced release of adenine nucleosides and nucleotides from rabbit aorta. J Pharmacol Exp Ther. 1990 Mar;252(3):1060–7.

Seifert HA, Hall AA, Chapman CB, Collier LA, Willing AE, Pennypacker KR. A transient decrease in spleen size following stroke corresponds to splenocyte release into systemic circulation. J Neuroimmune Pharmacol. 2012 Dec;7(4):1017–24. PMCID: PMC3518577

Skalli O, Ropraz P, Trzeciak A, Benzonana G, Gillessen D, Gabbiani G. A monoclonal antibody against alpha-smooth muscle actin: a new probe for smooth muscle differentiation. J. Cell Biol. 1986 Dec;103(6 Pt 2):2787–96. PMCID: PMC2114627

Takano S. A study on the contraction of spleen strips in kids and dogs, with special reference to the cholinergic and adrenergic receptors. Jpn. J. Pharmacol. 1969 Dec;19(4):563–8.

Tawfik HE, Schnermann J, Oldenburg PJ, Mustafa SJ. Role of A1 adenosine receptors in regulation of vascular tone. Am J Physiol Heart Circ Physiol. 2005 Mar;288(3):H1411–6.

Tyler WJ, Pozzo-Miller LD. BDNF enhances quantal neurotransmitter release and increases the number of docked vesicles at the active zones of hippocampal excitatory synapses. Journal of Neuroscience. 2001 Jun 15;21(12):4249–58. PMCID: PMC2806848

Ward RJ, Pediani JD, Milligan G. Heteromultimerization of cannabinoid CB(1) receptor and orexin OX(1) receptor generates a unique complex in which both protomers are

regulated by orexin A. Journal of Biological Chemistry. 2011 Oct 28;286(43):37414–28. PMCID: PMC3199489

Wennmalm M, Fredholm BB, Hedqvist P. Adenosine as a modulator of sympathetic nerve-stimulation-induced release of noradrenaline from the isolated rabbit heart. Acta Physiol. Scand. 1988 Apr;132(4):487–94.

Westfall TC, Carpentier S, Chen X, Beinfeld MC, Naes L, Meldrum MJ. Prejunctional and postjunctional effects of neuropeptide Y at the noradrenergic neuroeffector junction of the perfused mesenteric arterial bed of the rat. Journal of Cardiovascular Pharmacology. 1987 Dec;10(6):716–22.

Westfall TC, Chen XL, Ciarleglio A, Henderson K, Del Valle K, Curfman-Falvey M, et al. In vitro effects of neuropeptide Y at the vascular neuroeffector junction. Ann N Y Acad Sci. 1990;611:145–55.

Wiest R, Jurzik L, Moleda L, Froh M, Schnabl B, Hörsten SV, et al. Enhanced Y1-receptor-mediated vasoconstrictive action of neuropeptide Y (NPY) in superior mesenteric arteries in portal hypertension. Journal of Hepatology. 2006 Mar;44(3):512–9.

Wong KK. Bethanechol induced contraction in mouse spleen. Chin J Physiol. 1990;33(2):161–7.

Zimmer A, Zimmer AM, Hohmann AG, Herkenham M, Bonner TI. Increased mortality, hypoactivity, and hypoalgesia in cannabinoid CB1 receptor knockout mice. Proc Natl Acad Sci USA. 1999 May 11;96(10):5780–5. PMCID: PMC21937

Zukowska-Grojec Z, Dayao EK, Karwatowska-Prokopczuk E, Hauser GJ, Doods HN. Stress-induced mesenteric vasoconstriction in rats is mediated by neuropeptide Y Y1 receptors. Am J Physiol. 1996 Feb;270(2 Pt 2):H796–800.

## Chapter 7: General Discussion and Concluding Remarks

The spleen is a visceral abdominal organ with both hematologic and immune functions that is innervated by the sympathetic nervous system. Cannabinoid receptors are present throughout the body of mammals, including in the spleen. The multi-functional role of splenic sympathetic innervation is not completely understood, and the effects of cannabinoids on the function of splenic sympathetic innervation are not known. The present dissertation characterizes the physiology of splenic noradrenergic sympathetic innervation and explores its role in both immunologic and hematologic functions. The effects of CB1 and CB2 deficiency on both the immunologic and hematologic functions of these neurons were also examined. Understanding the role of endocannabinoid signaling is significant considering the increase in medicinal use of cannabinoids and can inform the scientific and medical community of the possible ramifications of cannabinoid use and abuse.

### 7.1: Anatomy and physiology of splenic noradrenergic post-ganglionic neurons

Innervation of the spleen is heterogeneous, the targets of innervation being the spleen capsule and parenchymal tissue surrounding arterioles. This innervation is sympathetic in origin and noradrenergic in nature. This was confirmed by visualization with TH immunostaining and a lack of finding significant amounts of either DA or epinephrine in the spleen by HPLC-ED,

confirming the findings of other investigators (Felten et al., 1987; Felten and Olschowka, 1987; Nance and Sanders, 2007; Olofsson et al., 2012). A major function of noradrenergic innervation to the spleen is control of smooth muscle contraction, which expels the cellular content of the spleen and regulates blood flow through the spleen (Blue and Weiss, 1981; Pinkus et al., 1986; Saito et al., 1988; Groom et al., 1991). Therefore the distribution of noradrenergic terminals in the spleen is not surprising. Finding noradrenergic nerve terminals in the lymphocyte-rich PALS (Felten and Olschowka, 1987; Cesta, 2006) supports the hypothesis of an immunologic function for noradrenergic innervation of the spleen (Sanders, 2012). The paucity of noradrenergic axon terminals, catecholamine synthetic machinery (TH), and NE in the remainder of the spleen parenchyma suggests no direct role for noradrenergic innervation in these regions.

The basal metabolic and synthetic activity of noradrenergic neurons in the spleen capsule is lower than the PVN. This was illustrated by differences in the concentration of NE metabolites and suggests NE axon terminals in the PVN are more metabolically active than those in the spleen. However, differences in the concentration of these metabolites may simply be due to the size difference. The ratio of total metabolite content to total primary catecholamine content is more suited for conclusions with regards to metabolic activity (Lookingland et al., 1991). Interestingly, the VMA/NE ratio was not different between these tissues, whereas the MHPG/NE ratio was lower in the spleen. This difference may be due to the tissue location where VMA and MHPG are respectively created. VMA synthesis

is mostly dependent upon extra-neuronal conversion of MHPG, whereas MHPG synthesis is largely dependent upon neuronal MAO activity (Lookingland et al., 1991; Karhunen et al., 1994; Hayley et al., 2001; Oh-hashi et al., 2001; Eisenhofer et al., 2004; Myöhänen et al., 2010; Siraskar et al., 2011) making it a better indicator of the metabolic capacity of neurons. Thus, the large difference in the MHPG/NE ratio is more telling of a reduced metabolic rate in splenic sympathetic neurons. Furthermore, increased accumulation of DOPA following blockade of NE synthesis with NDS-1015 suggests a faster rate of NE synthesis in axon terminals of the PVN versus the spleen capsule under basal conditions.

The rate of NE release in the spleen is lower compared to the PVN. This was determined using the aMT method, which has a number of advantages compared to electrophysiology or microdialysis, such as being able to measure the activity of two different sites in the body in the same animal (Lee et al., 1992; Helwig et al., 2008), the amount of time required, and not requiring the insertion of large microdialysis probes (Olive et al., 2000; Ortega et al., 2012; CMA Microdialysis). Using this method, the rate of noradrenergic activity in the PVN was found to be much faster than that of the spleen.

The rate of NE release from splenic noradrenergic sympathetic neurons is regulated by α2AR autoreceptors. This was demonstrated by measuring the effect of the α2AR antagonist idazoxan on the activity of spleen capsule noradrenergic neurons. These receptors are act much like D2-autoreceptors in that their stimulation on pre-synaptic terminals decreases the synthesis and

release of neurotransmitters (Khan et al., 2002; Marino and Cosentino, 2013). Thus antagonism of these receptors leads to an increased release of NE and demonstrates the ability of these neurons to self-regulate their activity.

Interestingly, the activity of splenic noradrenergic neurons is coupled to increases in the concentration of NE and TH in the spleen. Normally under basal conditions, the coupling of NE synthesis and release maintains a steady-state amount of stored NE in the axon terminals (Brodie et al., 1966; Lookingland et al., 1991). For example, during times of activation the amount of NE does not change in the PVN, demonstrating the maintenance of steady-state NE concentrations in a central noradrenergic nucleus (Lookingland et al., 1991). Yet during increased neuronal activity the amount of NE significantly increases in the spleen capsule. Thus, it appears that in splenic noradrenergic neurons the synthetic capacity out-paces the release of NE leading to accumulation during activation. Activity dependent increases in the activity of TH are a known phenomenon in catecholaminergic neurons (Kumer and Vrana, 1996). The enzyme activity of TH can be increased in response to neuronal activation via phosphorylation (Kumer and Vrana, 1996). However, the phosphorylation of TH also reduces the stability of the phosphorylated enzyme (not due to degradation of the entire protein) (Lazar et al., 1981; Vrana et al., 1981; Vrana and Roskoski, 1983). On the other hand, TH stability is increased by feedback inhibitors, such as DA (Kumer and Vrana, 1996). Therefore, it may be the case that two different

mechanisms are occurring simultaneously to cause both increased TH activity and increased stability of this enzyme.

During times of activation the rate of NE production is out-pacing the rate of NE release due to increased enzyme activity by phosphorylation, thus explaining the increase in spleen capsule NE during activation. During the times of increased production, however, there should also be an increase in the synthesis of feedback inhibitors of TH, such as DA, which stabilize TH proteins. This occurs by DA forming a complex with ferric iron within the active site of the enzyme. The binding of this complex serves to not only decrease the catalytic activity of TH, but also yields a very stable form of the enzyme that can be reversibly activated (Okuno and Fujisawa, 1991). This may explain the increase in splenic TH during times of activation. What is unclear, however, is how increased synthesis of NE can occur in the presence of increased TH-stabilizing feedback inhibitors that should shut down the production of NE due to phosphorylation induced increases in TH catalytic activity.

This paradoxical aspect of splenic noradrenergic neuron physiology requires further investigation and presents a number of future directions to explore. For instance, changes in the rate of TH synthesis could be measured in spleen capsule during times of activity by measuring the accumulation of DOPA following blockade of L-AAAD (Lookingland and Moore, 2005). If phosphorylation-dependent increases the catalytic activity are occurring, then it would be expected that DOPA accumulation would occur quicker during

activation. However, other causes for NE accumulation in the spleen are also possible. For instance, increased NE storage, due to increased vesicular number and size, or displacement of co-released transmitters, effectively increasing the storage available for NE, could also account for this phenomenon. Ultrastructural analysis by electron microscopy of NE containing terminals in the spleen capsule would reveal differences due to these factors. In addition to these experiments, differences in the ability of feedback inhibitors, such as DA, to inhibit and stabilize isolated TH from the brain spleen might be assessed. This may reveal differences in the sensitivity of TH from different tissues to feedback inhibitors, or even reveal differences in DA-mediated stabilization.

7.2: Immunologic function of splenic noradrenergic post-ganglionic neurons

The activity of splenic noradrenergic neurons is increased in response to humoral immune challenges regardless of T-cell involvement. Both sRBC and LPS induce humoral immune responses. sRBC are a traditional soluble protein antigen requiring processing by macrophages, interactions with T cells, and eventually T cell to B cell interactions to stimulate antibody production (Ademokun and Dunn-Walters, 2001). LPS, on the other hand, is a direct stimulator of B cells. LPS binds TLR4 receptors and cross-links BCR on B cells to directly cause proliferation, activation, and IgM production in the same cell (Lanzavecchia and Sallusto, 2007; Bekeredjian-Ding and Jego, 2009). Therefore, while sRBC require both T and B cells that selectively recognize

sRBC epitopes, LPS is a polyclonal B cell activator by activating any B cell expressing TLR4. Both sRBC and LPS were found to significantly increase the rate of NE release in the spleen capsule. This demonstrates that humoral immunogen induced increases in the activity of splenic sympathetic noradrenergic neurons does not depend on the involvement of T cells.

Pro-inflammatory cytokines, such as IL-1β and IL-6, are the likely activators of sympathetic neuronal activity during an immune challenge. Peripheral injection of IL-1β increases the release of NE in the spleen (Shimizu et al., 1994; Kohm and Sanders, 2001). However, IL-1β also stimulates the production of IL-6 from a myriad of cell types (Kauma et al., 1994; Spangelo et al., 1994; Parikh et al., 1997) leaving open the possibility that the effects of IL-1β on sympathetic activity may be due to IL-6. In support of this hypothesis, central injection of IL-6 produces increased firing of spleen capsule sympathetic neurons (Helwig et al., 2008). The role for each of these specific cytokines could be tested using biological inhibitors. For instance, the administration of MP161-1, an IL-6 receptor neutralizing antibody (Uchiyama et al., 2008; Tomiyama-Hanayama et al., 2009), prior to an immune challenge would be expected to inhibit sympathetic activation in the periphery if IL-6 is the sympatho-stimulatory factor. If MR161-1 is unable to block sympathetic nervous system stimulation then it might reasonably be assumed that IL-1β is the mediating factor, leading to a similar experiment using a blockade of IL-1β effects.

Splenic B cells express β2AR and are immunologically functional. The observations by other investigators were confirmed in that β2AR are expressed by both B cells and T cells, with B cell expression being highest (Kin and Sanders, 2006). The data presented here also suggest that B cells become more sensitive to NE following LPS stimulation by increasing the number of cells expressing β2AR and the amount of β2AR per B cell. This also occurs within the population of B cells producing IgM. Thus, changes in the expression of β2AR on B cells, and on IgM producing cells, supports the hypothesis that NE stimulation of β2AR can have a direct impact on IgM production. Unfortunately, stimulation of β2AR on splenic B cells does not augment IgM production in response to LPS.

The question then remains as to the function of β2AR on B cells. It was demonstrated here that B cells express β2AR and are immunologically functional. However, the data show that β2AR stimulation is not necessary for normal antibody responses to LPS, a T cell independent antigen. This raises the question of why the data obtained is seemingly incongruent with the reported effect of β2AR on antibody production (Kohm and Sanders, 2001; Nance and Sanders, 2007; Sanders, 2012). The explanation may lie in the nature of the immune challenge used. The correlation between β2AR and antibody production was explored in this dissertation using LPS, a T cell independent immunogen, which induces a humoral immune response through activation of TLR4 and crosslinking of the BCR in the absence of other co-stimulators, such as CD40

(Ademokun and Dunn-Walters, 2001; Lanzavecchia and Sallusto, 2007; Bekeredjian-Ding and Jego, 2009).

On the other hand, the published research correlating antibody production and β2AR utilized either T cell dependent immunogens or direct stimulation of B cells by CD40 (Kohm et al., 2000; Kohm and Sanders, 2001; Pongratz et al., 2006; Padro et al., 2013). Therefore, it may be the case that β2AR augmentation of antibody production is specific to B cell responses in which a CD40-CD154 interaction is required, such as during immune responses requiring T cells involvement (Ademokun and Dunn-Walters, 2001; Néron et al., 2011). If this is the case, the lack of β2AR augmentation of the humoral immune response to LPS is due to the absence of CD40 being involved in this response. This hypothesis has not been directly tested and is an avenue for future research. To test this hypothesis, *in vitro* stimulation of β2AR could be compared in the face of immunologic stimulation by both LPS and CD40. It would be expected that β2AR stimulation would augment humoral immune responses to CD40, but not to LPS. This could then be further tested *in vivo* by blocking β2AR in mice immunized with sRBC and LPS. It would be expected in this case that blockade of β2AR signaling would decrease antibody production in sRBC, but not LPS, mice.

## 7.3: The role of CB1 and CB2 on the immunologic role of noradrenergic splenic sympathetic innervation

Congruent with a previously published report (Springs et al., 2008), CB1/CB2 KO mice demonstrate enhanced humoral immunity. This is a partially manifested in the present studies by higher plasma IgM and IgG in immunologically naïve CB1/CB2 KO mice. IgM is constitutively secreted without antigen stimulation, termed 'natural antibodies', as a form of innate immunity by innate-like B cells (Baumgarth, 2013). Thus, elevated plasma IgM in immunologically naïve CB1/CB2 KO mice suggests these receptors are inhibitory to this specific type of immunity, a finding that is unexplored in scientific literature. This hypothesis could be tested by chronically treating mice with THC, a non-selective CB1/CB2 agonist, under immunologically naïve conditions and then testing for the presence of natural antibodies and natural antibody producing cells in the spleen. These innate-type B cells are known as Marginal Zone B cells, identified by an $IgM^{high}$ $IgD^{low}$ $CD21^{high}$ $CD23^{low}$ phenotype, and B-1a cells, identified by expressing CD19 and CD5 (Zouali, 2001). If this hypothesis is correct, then it is expected that THC treatment would cause a decrease in plasma IgM as well as a decrease in marginal zone B cells and B-1a cells. If this is found to be the case, then the contribution of CB1 versus CB2 on this effect could be explored using individual CB receptor KO mice, or receptor specific pharmacologic agents.

IgG, on the other hand, is produced in response to antigenic stimulation (Zouali, 2001). Therefore, 'natural antibody' production does not explain elevated plasma IgG in immunologically naïve CB1/CB2 KO mice. The most likely explanation for increased plasma IgG is an increased presence of long-lived plasma cells. Plasma cells can be short-lived (days to weeks) or persist for years (conferring long-term immunity) (Ademokun and Dunn-Walters, 2001; Tangye, 2011). These long-lived plasma cells constitutively produce antigen specific IgG to speed the removal of antigens upon re-exposure (Tangye, 2011). It may be the case that CB1/CB2 deficiency results in an increase in the survival or generation of these cells. This possibility seems very likely to be the cause of increased IgG in immunologically naïve mice as this would be expected to increase IgG plasma concentrations, but not at the level seen with antigenic stimulation. This suggests that CB1 and/or CB2 play an inhibitory role in the function of formation of these specialized B cells.

The effect of cannabinoids on long-term immunity are also virtually unexplored in the literature with only one report in CB2 knockout mice showing no significant effect of plasma cell generation in response to a T-cell dependent antigen (Basu et al., 2013). A simple experiment to test this hypothesis would be to measure and compare the number of plasma cells in the spleen and bone marrow of WT and CB1/CB2 KO mice. This could be accomplished using CD138, a marker for plasma cells (O'Connell et al., 2004). CB1/CB2 KO mice are expected to have an increased number of CD138 positive lymphocytes if this

hypothesis is correct. If KO of CB1/CB2 results in an increased presence of plasma cells, then a role for each specific receptor could be explored using CB1 or CB2 KO mice using a similar approach.

Alternatively, the use of CB1 and CB2 specific antagonists could be utilized. To do this, antagonists of CB1 or CB2 would be administered prior to an immune challenge. After sufficient time has passed for the differentiation of plasma cells (4 days), the effect of the individual receptor antagonists would be tested by comparing the size of the CD138 lymphocyte population in untreated and antagonist treated mice. It would be expected in this case that mice treated with the antagonist of the CB receptor responsible for inhibiting plasma cell differentiation would have an increased population of plasma cells.

Considering the hypothesis that enhanced sympathetic noradrenergic stimulation may be the underlying cause for enhanced humoral responses, it was expected that β2AR expression in CB1/CB2 KO mice would be reduced due to ligand/activity dependent down-regulation (Zastrow and Kobilka, 1992; Hudson et al., 2010). Contrary to expectation, β2AR expression is elevated on B cells in CB1/CB2 KO mice. The most likely explanation for this phenomenon is the release of less splenic NE than in WT mice. This is hypothesized to result in β2AR receptor up-regulation due to a lack of ligand-binding, or rather decreased ligand-dependent internalization (Zastrow and Kobilka, 1992; Hudson et al., 2010). This hypothesis requires further experimentation and could be tested several ways. For instance, the administration of an $\alpha$2AR antagonist, which

increases the release of NE from splenic sympathetic neurons, would be expected to result in a decrease of β2AR expression on B cells. Alternatively, an α2AR agonist, which is expected to decrease the release of NE from splenic sympathetic neurons, would be expected to increase the expression of β2AR on B cells. These experiments would demonstrate the direct correlation between splenic NE release and the expression of β2AR on B cells, providing support for the above hypothesis.

The results obtained in this dissertation argue against the regulation of splenic post-ganglionic sympathetic neurons by CB1. CB1 are pre-synaptically expressed receptors known to inhibit the release of neurotransmitters from peripheral sympathetic neurons (Ishac et al., 1996; Niederhoffer and Szabo, 1999; Ralevic and Kendall, 2002). It was expected that the absence of CB1 inhibitory actions on splenic sympathetic neurons would result in increased NE release. This was not found to be true and therefore argues against the ability of CB1 to regulate splenic sympathetic neurons.

Interestingly, it was found that CB1/CB2 KO mice actually have lower splenic sympathetic noradrenergic activity. The explanation for this effect is unclear and may involve CNS-mediated CB1 receptor effects upstream of post-ganglionic neurons. However, decreased release of NE from sympathetic neurons in the spleen may explain the accumulation of NE in the spleen capsule without a concomitant increase in TH enzyme content. Regardless, the results regarding the rate of NE in the spleen of CB1/CB2 KO mice leads to the

acceptance of the null hypothesis regarding the absence of CB1 inhibition on NE release in the spleen as a mechanism for enhanced humoral immunity in CB1/CB2 KO mice.

Due to the increased β2AR expression of B cells in CB1/CB2 KO mice, it was hypothesized that β2AR activity may still be the cause for enhanced humoral immunity in these mice. It was expected that if increased β2AR stimulation were at least partly responsible for increased humoral immune responses in CB1/CB2 KO mice, then blockade of these receptors would significantly attenuate antibody production in response to LPS. This hypothesis was rejected following the observation that blockade of β2AR had no observable effect in LPS-treated CB1/CB2 KO mice. Yet, as discussed above, β2AR stimulation is likely not involved in the humoral response to LPS. Therefore, this hypothesis needs to be revisited in response to an immunogen for which β2AR plays a role in modulating humoral responses, such as sRBC or CD40 stimulation.

Collectively, the data presented in this dissertation are consistent with the conclusion that enhanced humoral immunity in the absence of CB1/CB2 is not due to dis-inhibition of splenic sympathetic noradrenergic neurons. Given that CB1 is the predominant neuronal receptors, this also suggests that enhanced humoral immunity in CB1/CB2 KO mice is not due to the absence of this receptor (Mackie, 2008). Therefore, CB2 signaling directly on cells of the immune system (Schatz et al., 1997; Tanasescu and Constantinescu, 2010) is the likely immunosuppressive mediator of the endocannabinoid system.

Future work should be directed towards this possibility by utilizing tools such as CB2 KO mice or CB2 specific agonists and antagonists. Assessing the activity of splenic sympathetic neurons in CB2 KO mice could rule out any contributing effect of this receptor to the function of these neurons. Of particular interest is the interaction between B2AR and CB2 receptors. The expression of β2AR on B cells should be evaluated in CB2 KO mice to determine if the lack of CB2 modulates the its expression. Furthermore, the effect of β2AR stimulation in response to appropriate immunogens can be evaluated in the absence of CB2 or during pharmacologic activation/inhibition of CB2. Beyond these studies, an interesting point of investigation is the effect of CB2 on the transcription of the 3'-IgH enhancer. It is unknown if the actions of CB2 are able to directly inhibit 3'-IgH enhancer activity to mediate cannabinoid-mediated suppression of antibody production.

7.4: Sympathetic control of spleen contraction

Spleen contraction is mediated by two different neurotransmitters. NE can induce spleen contraction and is responsible for approximately 2/3 of EFS-induced spleen contraction. NE-induced spleen contraction is mediated by α1AR, as demonstrated by the ability of the pan α1AR antagonist prazosin to block this response. More specifically, the type of α1AR mediating this effect is the $\alpha 1_B$AR subtype (Eltze, 1996; Aboud et al., 2012). This specific subtype of the α1AR has previously been demonstrated to undergo phosphorylation mediated

desensitization and internalization in response to NE binding, occurring as quickly as 5 min after binding (Leeb-Lundberg et al., 1987; Fonseca et al., 1995; Malbon and Wang, 2001). Thus, receptor internalization is the likely cause for the NE-induced attenuation of spleen contraction observed at repeated high concentrations of exogenous NE.

The other neurotransmitter mediating spleen contraction is adenosine derived from ATP (Rongen et al., 1996). Results from the present studies reveal that adenosine activation of A1 receptors is responsible for this action, which is in agreement with other investigators (Fozard and Milavec-Krizman, 1993). A1 receptors are also known to mediate a relatively small portion (18-33%) of vascular smooth muscle contraction (Tawfik et al., 2005).

7.5: The role of CB1 and CB2 in spleen contraction

The spleens from CB1/CB2 KO mice produce less force during contraction than WT in response to NE. The mechanism for this phenomenon is decreased α1AR expression on smooth muscle in the spleen capsule of CB1/CB2 KO mice. In support of this conclusion, NE induces a concentration-dependent increase in spleen contraction force, which demonstrates that increasing activation of α1AR receptors results in increased force of contraction. Thus, decreased activation of α1AR, due to decreased expression, likely accounts for the decreased contraction observed in CB1/CB2 KO mice. This is despite similar weights and similar amounts of smooth muscle specific α-actin (Skalli et al., 1986; Johnson et

al., 2010), both of which suggest an equivalent amount of smooth muscle in the spleen capsule of WT and CB1/CB2 KO mice.

The reason for decreased spleen capsule α1AR expression in CB1/CB2 KO mice remains unclear. It was hypothesized that α1AR would be increased in CB1/CB2 KO mice secondary to decreased receptor stimulation from decreased NE release. However, this does not appear to be the case since α1AR are decreased, not increased, in CB1/CB2 deficient mice. Thus, mechanisms other than ligand-mediated receptor internalization are likely at play. Whether this effect is direct or indirect cannot be determined by the data obtained in these experiments. It is possible that CB receptors directly alter α1AR expression, just as has been recently described for CB1 and β2AR (Hudson et al., 2010). While this supposition is without precedence and speculative, increasing evidence for protein-protein interactive effects between CB receptors and other G-protein coupled receptors are known (Kearn, 2005; Hudson et al., 2010; Ward et al., 2011). This hypothesis requires further investigation and likely should start with determining which receptor, CB1 or CB2, is the major mediator of decreased α1AR expression through the use of selective CB1 and CB2 antagonists or mouse models employing specific knockout of CB1 or CB2.

The compensatory mechanism whereby EFS-induced spleen contraction in CB1/CB2 KO mice is equivalent to that of WT mice does not involve changes in non-adrenergic transmission. Prazosin blockade of noradrenergic transmission reduces EFS-induced spleen contraction to an equivalent extent in both WT and

CB1/CB2 KO mice. Thus, the contribution of NE to EFS-induced spleen contraction in CB1/CB2 KO mice is equivalent to WT, despite the reduction in α1AR. This phenomenon may be due to an increase in the quantal release of NE in CB1/CB2 KO mice. Increased NE released per action potential would hypothetically stimulate more α1AR in CB1/CB2 KO mice, thus compensating for lower α1AR expression. In fact, CB1/CB2 KO mice may be primed for this scenario as the axon terminals of splenic sympathetic neurons in these mice contain more NE than WT mice. Increased release of neurotransmitters is not without precedence. For instance, BDNF can increase the quantal release of glutamate in the hippocampus (Tyler and Pozzo-Miller, 2001; Amaral and Pozzo-Miller, 2012).

This hypothesis may explain the observed data and could be further validated using microdialysis. It would be expected if this were true the concentration of captured NE in the dialysate from spleens of CB1/CB2 KO mice would be higher than those from WT spleen in response to sympathetic neuron excitation. Alternatively, an electrochemical method utilizing boron-doped diamond nanoelectrodes, which can quantify the amount of NE released from *in situ* neurons, could be utilized to compared the quantal release of NE in the spleens of WT and CB1/CB2 KO mice (Dong et al., 2011). The mechanism underlying this hypothesis could then be studied by ultrastructure analysis of splenic sympathetic neuron axon terminals using electron microscopy. If this hypothesis is true then the size of synaptic vesicles or the number of docking

synaptic vesicles should be increased in splenic sympathetic axon terminals of CB1/CB2 KO mice compared to WT.

Interestingly, the capsule of the spleen in CB1/CB2 KO mice is thinner than WT mice, but not due to differences in smooth muscle content. The other two major tissues of the spleen capsule are connective tissue and elastic tissue (Cesta, 2006). CB1 and CB2 have demonstrated effects on the production of extracellular matrix components from fibroblast. CB1 are stimulatory to fibroblasts (Marquart et al., 2010; Lazzerini et al., 2012), whereas CB2 are inhibitory (Akhmetshina et al., 2009; Defer et al., 2009). Despite these opposing effects, these reports demonstrate that CB receptors can modulate the activity of fibroblasts. It may be the case that CB1 and/or CB2 receptors allow for an appropriate amount, or structure, of extracellular material and these effects during development account for reduced spleen capsule thickness in CB1/CB2 KO mice. Alternative to changes in the amount or structure of extracellular material, changes in the number, or cytoarchitecture, of cells in the spleen capsule could account for a decreased thickness of the spleen capsule of CB1/CB2 KO mice. However, any changes in the cytoarchitecture would likely not affect smooth muscle cells, as they are able to contract and have a nominal amount of α-actin. An interesting line of experimentation would be to evaluate the relative contribution of CB1 and CB2 to connective tissue development in the spleen. This line of investigation could initiated by histologically evaluating the

structure and development of the spleen capsule in the individual CB1 and CB2 KO mice.

7.6: Significance of cannabinoid use and abuse

*Cannabis,* or marijuana, has been used by humans for over 5000 years, the earliest recorded use of *cannabis* fibers occurred circa 4,000 B.C. (Zuardi, 2008). The use of marijuana for medicinal and possibly spiritual purposes arose in China and the Himalayas as far back as 2000 B.C. (Kalant, 2001; Zuardi, 2008). Over time marijuana has been used by a multitude of cultures for spiritual, religious, medicinal, and recreational purposes. Even today cannabis is still widely used. In fact, in the U.S., where marijuana is illegal according to federal law, it is the most widely used illicit drug with an estimated ~17.4 million people using marijuana every month (National Institute on Drug Abuse, 2013). Additionally, studies show that approximately 1/3 of $12^{th}$ grade students have tried marijuana (National Institute on Drug Abuse, 2013).

Despite the illegal status given to *cannabis* by multiple national governments (Hall and Diehm, 2014), the use of marijuana persists and may be gaining mainstream acceptance (Swift, 2014). In support of this, 20 U.S. states and the District of Columbia have approved measures allowing for the possession and growing of marijuana for medicinal purposes (WhiteHouse.gov, 2014). Two of these states, Colorado and Washington, have legalized the recreational use of marijuana, which is an indicator of increasing popular support

for the use of marijuana (Wollner, 2014; 2014). In South America, Paraguay recently legalized the production and sale of marijuana (Watts, 2014).

In addition to the acceptance of marijuana in a modern social context, cannabinoid-based compounds are finding acceptance in modern Western medicine. The U.S. Food and Drug Agency (FDA) has approved several cannabinoid-based compounds for medicinal use and prescription. Dronabinol is synthetically created THC and is approved by the FDA for the control of nausea and vomiting in cancer patients undergoing chemotherapy as well as an appetite stimulant in patients with AIDS (Galal et al., 2009). In the United Kingdom, a drug named nabiximols (Sativex®), which is a mixture of THC and another *cannabis*-derived cannabinoid called cannabidiol (CBD), is approved for the control of spasticity in multiple sclerosis patients (Pharmaceuticals, 2011).

Despite the increasing acceptance and popularity of marijuana, the biological ramifications of cannabinoid use are not completely understood. This is particularly true for the actions of cannabinoids outside the brain. As has been discussed, cannabinoid receptors are found not only in the CNS, but also throughout the body (Schatz et al., 1997; Ralevic and Kendall, 2002; Cabral et al., 2008; Mackie, 2008; Cabral and Griffin-Thomas, 2009; Atwood and Mackie, 2010; Kaplan, 2012). The presence of peripherally located cannabinoid receptors suggests a role for both exogenous and endogenous cannabinoids at these sites. Understanding the role of endocannabinoid signaling is significant by itself, but is also able to inform the scientific and medical community of the

possible ramifications of cannabinoid use and/or abuse, which remains a persistent world-wide issue (Degenhardt et al., 2013).

With particular reference to work in this dissertation, the immunologic function of cannabinoids is of clinical interest. The use of potentially immunosuppressive cannabinoids needs to be evaluated and understood as these compounds are already potentially being given to immunocompromised patients with AIDS or undergoing chemotherapy (Galal et al., 2009). However, what may be even more relevant is the potential impact of cannabinoids in new and chronic users of *cannabis* as it become increasingly popular and available.

The effect of cannabinoids on the contraction of the spleen is wholly untouched by the scientific community. The work in this dissertation, while of scientific interest, is difficult as yet to relate to a clinic or biologic effect. This may be simply due to the lack of understanding regarding the function of spleen contraction as a whole. Of particular interest are the consequences of spleen contraction on immune function. It has been demonstrated that immune cells from the spleen are released in response to spleen contraction (Seifert et al., 2012). Yet it is unknown if this release of immune cells is beneficial or detrimental to immunity. It can be hypothesized that increasing the number of circulating macrophages and lymphocytes can increase the probability of these cells to interact with an immunogen thus initiating immune responses more quickly to infection. On the other, the dispersion of immune cells from their close packed environment of the spleen may impede the requirement for these cells to

interact with each other in the process of an immune response. Which of these hypothesized effects are true or predominant is unknown and presents an interesting avenue for future research. Regardless, cannabinoid receptors definitely play a role in regulating the contraction of the spleen and warrants further investigation.

## 7.7: Concluding Remarks

The spleen is a multifunction organ that sits at a unique intersection between the circulatory, immune, and neurologic systems. The work in this dissertation endeavored to shed light on the interaction of the sympathetic nervous system in the spleen with these other vital biologic systems. In addition, the role of CB1/CB2 signaling was explored as it relates the function of splenic sympathetic noradrenergic innervation. Specifically it was found that splenic noradrenergic neurons do not play a role in T cell independent humoral immunity, and that both NE and adenosine mediate spleen contraction. It was concluded that splenic sympathetic noradrenergic neurons likely are not regulated by CB1 and that cannabinoid-mediated immunosuppression of humoral immunity is likely due solely to CB2 on immune cells. It was also found that CB1/CB2 play a permissive role in maintaining the relationship between NE release from splenic sympathetic neurons and spleen contraction. These findings add to the knowledge base regarding both the spleen and extra-CNS cannabinoid effects and can be built upon for a more complete understanding of these systems.

# REFERENCES

# REFERENCES


Aboud R, Shafii M, Docherty JR. Investigation of the subtypes of α1-adrenoceptor mediating contractions of rat aorta, vas deferens and spleen. Br J Pharmacol. 2012 Jul 19;109(1):80–7.

Ademokun AA, Dunn-Walters D. Immune Responses: Primary and Secondary. els.net. Chichester, UK: John Wiley & Sons, Ltd; 2001.

Akhmetshina A, Dees C, Busch N, Beer J, Sarter K, Zwerina J, et al. The cannabinoid receptor CB2 exerts antifibrotic effects in experimental dermal fibrosis. Arthritis Rheum. 2009 Apr;60(4):1129–36.

Amaral MD, Pozzo-Miller L. Intracellular Ca2+ stores and Ca2+ influx are both required for BDNF to rapidly increase quantal vesicular transmitter release. Neural Plast. 2012;2012:203536. PMCID: PMC3397209

Atwood BK, Mackie K. CB2: a cannabinoid receptor with an identity crisis. Br J Pharmacol. 2010 Mar 4;160(3):467–79.

Basu S, Ray A, Dittel BN. Cannabinoid Receptor 2 (CB2) Plays a Role in the Generation of Germinal Center and Memory B Cells, but Not in the Production of Antigen-Specific IgG and IgM, in Response to T-dependent Antigens. PLoS ONE. 2013;8(6):e67587. PMCID: PMC3695093

Baumgarth N. Innate-Like B Cells and Their Rules of Engagement. link.springer.com.proxy2.cl.msu.edu. New York, NY: Springer New York; 2013. p. 57–66.

Bekeredjian-Ding I, Jego G. Toll-like receptors--sentries in the B-cell response. Immunology. 2009 Nov;128(3):311–23. PMCID: PMC2770679

Blue J, Weiss L. Electron microscopy of the red pulp of the dog spleen including vascular arrangements, periarterial macrophage sheaths (Ellipsoids), and the contractile, innervated reticular meshwork. Am. J. Anat. 1981 Jun;161(2):189–218.

Brodie BB, Costa E, Dlabac A, Neff NH, Smookler HH. Application of steady state kinetics to the estimation of synthesis rate and turnover time of tissue catecholamines. J Pharmacol Exp Ther. 1966 Dec;154(3):493–8.

Cabral GA, Griffin-Thomas L. Emerging role of the cannabinoid receptor CB2 in

immune regulation: therapeutic prospects for neuroinflammation. Expert Rev Mol Med. 2009;11:e3. PMCID: PMC2768535

Cabral GA, Raborn ES, Griffin L, Dennis J, Marciano-Cabral F. CB 2receptors in the brain: role in central immune function. Br J Pharmacol. 2008 Jan;153(2):240–51. PMCID: PMC2219530

Cesta M. Normal Structure, Function, and Histology of the Spleen. Toxicol Pathol. 2006;34(5):455–65.

CMA Microdialysis. Microdialysis Probes [Internet]. CMA Microdialysis AB. [cited 2013 Dec 18]. Retrieved from: http://www.microdialysis.com/probe_brochure.pdf?cms_fileid=2772532331977349a4a942f6d40fafca

Defer N, Wan J, Souktani R, Escoubet B, Perier M, Caramelle P, et al. The cannabinoid receptor type 2 promotes cardiac myocyte and fibroblast survival and protects against ischemia/reperfusion-induced cardiomyopathy. FASEB J. 2009 Jul;23(7):2120–30.

Degenhardt L, Whiteford HA, Ferrari AJ, Baxter AJ, Charlson FJ, Hall WD, et al. Global burden of disease attributable to illicit drug use and dependence: findings from the Global Burden of Disease Study 2010. Lancet. 2013 Nov 9;382(9904):1564–74.

Dong H, Wang S, Galligan JJ, Swain GM. Boron-doped diamond nano/microelectrodes for biosensing and in vitro measurements. Front Biosci (Schol Ed). 2011;3:518–40.

Eisenhofer G, Kopin IJ, Goldstein DS. Catecholamine metabolism: a contemporary view with implications for physiology and medicine. 2004 Sep 1;56(3):331–49.

Eltze M. Functional evidence for an alpha 1B-adrenoceptor mediating contraction of the mouse spleen. Eur J Pharmacol. 1996 Sep 12;311(2-3):187–98.

Felten DL, Ackerman KD, Wiegand SJ, Felten SY. Noradrenergic sympathetic innervation of the spleen: I. Nerve fibers associate with lymphocytes and macrophages in specific compartments of the splenic white pulp. J Neurosci Res. 1987;18(1):28–36, 118–21.

Felten SY, Olschowka J. Noradrenergic sympathetic innervation of the spleen: II. Tyrosine hydroxylase (TH)-positive nerve terminals form synapticlike contacts on lymphocytes in the splenic white pulp. J Neurosci Res. 1987;18(1):37–48.

Fonseca MI, Button DC, Brown RD. Agonist regulation of alpha 1B-adrenergic receptor subcellular distribution and function. J Biol Chem. 1995 Apr 14;270(15):8902–9.

Fozard JR, Milavec-Krizman M. Contraction of the rat isolated spleen mediated by adenosine A1 receptor activation. Br J Pharmacol. 1993 Jul 19;109(4):1059–63. PMCID: PMC2175713

Galal A, Slade D, Gul W, El-Alfy A, Ferreira D, Elsohly M. Naturally occurring and related synthetic cannabinoids and their potential therapeutic applications. Recent Pat CNS Drug Discov. 2009 Jun 1;4(2):112–36.

Groom AC, Schmidt EE, MacDonald IC. Microcirculatory pathways and blood flow in spleen: new insights from washout kinetics, corrosion casts, and quantitative intravital videomicroscopy. Scanning Microsc. 1991 Mar;5(1):159–73–discussion173–4.

Hall K, Diehm J. The World's Most Marijuana-Friendly Countries (INFOGRAPHIC) [Internet]. huffingtonpost.com. 2014 [cited 2014 Jan 10]. Retrieved from: http://www.huffingtonpost.com/2013/08/27/marijuana-world-map-_n_3805800.html

Hayley S, Lacosta S, Merali Z, van Rooijen N, Anisman H. Central monoamine and plasma corticosterone changes induced by a bacterial endotoxin: sensitization and cross-sensitization effects. Eur J Neurosci. 2001 Mar;13(6):1155–65.

Helwig BG, Craig RA, Fels RJ, Blecha F, Kenney MJ. Central nervous system administration of interleukin-6 produces splenic sympathoexcitation. Autonomic Neuroscience. 2008 Aug;141(1-2):104–11.

Hudson BD, Hébert TE, Kelly MEM. Physical and functional interaction between CB1 cannabinoid receptors and beta2-adrenoceptors. Br J Pharmacol. 2010 Jun;160(3):627–42. PMCID: PMC2931563

Ishac E, Jiang L, Lake K, Varga K, Abood M, Kunos G. Inhibition of exocytotic noradrenaline release by presynaptic cannabinoid CB1 receptors on peripheral sympathetic nerves. Br J Pharmacol. 1996 Aug 1;118(8):2023–8. PMCID: PMC1909901

Johnson KB, Thompson JM, Watts SW. Modification of proteins by norepinephrine is important for vascular contraction. Front Physiol. 2010;1:131. PMCID: PMC3059971

Kalant H. Medicinal use of cannabis: History and current status. Pain Res Manag.

2001;6(2):80–91.

Kaplan BLF. The Role of CB(1) in Immune Modulation by Cannabinoids. Pharmacol. Ther. 2012 Dec 19.

Karhunen T, Tilgmann C, Ulmanen I, Julkunen I, Panula P. Distribution of catechol-O-methyltransferase enzyme in rat tissues. J. Histochem. Cytochem. 1994 Aug;42(8):1079–90.

Kauma SW, Turner TT, Harty JR. Interleukin-1 beta stimulates interleukin-6 production in placental villous core mesenchymal cells. Endocrinology. 1994;134(1):457–60.

Kearn CS. Concurrent Stimulation of Cannabinoid CB1 and Dopamine D2 Receptors Enhances Heterodimer Formation: A Mechanism for Receptor Cross-Talk? Molecular Pharmacology. 2005 Feb 9;67(5):1697–704.

Khan ZP, Ferguson CN, Jones RM. Alpha-2 and imidazoline receptor agonistsTheir pharmacology and therapeutic role. Anaesthesia. 2002 Apr 6;54(2):146–65.

Kin NW, Sanders VM. It takes nerve to tell T and B cells what to do. J Leukoc Biol. 2006 Jun;79(6):1093–104.

Kohm AP, Sanders VM. Norepinephrine and beta 2-adrenergic receptor stimulation regulate CD4+ T and B lymphocyte function in vitro and in vivo. Pharmacol Rev. 2001 Dec;53(4):487–525.

Kohm AP, Tang Y, Sanders VM, Jones SB. Activation of antigen-specific CD4+ Th2 cells and B cells in vivo increases norepinephrine release in the spleen and bone marrow. 2000 Jul 15;165(2):725–33.

Kumer SC, Vrana KE. Intricate regulation of tyrosine hydroxylase activity and gene expression. J Neurochem. 1996 Aug 1;67(2):443–62.

Lanzavecchia A, Sallusto F. Toll-like receptors and innate immunity in B-cell activation and antibody responses. Curr Opin Immunol. 2007 Jun;19(3):268–74.

Lazar MA, Truscott RJW, Raese JD, Barchas JD. Thermal Denaturation of Native Striatal Tyrosine Hydroxylase: Increased Thermolability of the Phosphorylated Form of the Enzyme. J Neurochem. 1981 Feb;36(2):677–82.

Lazzerini PE, Natale M, Gianchecchi E, Capecchi PL, Montilli C, Zimbone S, et al.

Adenosine A2A receptor activation stimulates collagen production in sclerodermic dermal fibroblasts either directly and through a cross-talk with the cannabinoid system. J. Mol. Med. 2012 Mar;90(3):331–42.

Lee TH, Ellinwood EH Jr., Einstein G. Intracellular recording from dopamine neurons in the substantia nigra: double labelling for identification of projection site and morphological features. Journal of Neuroscience Methods. 1992 Jul;43(2-3):119–27.

Leeb-Lundberg LM, Cotecchia S, DeBlasi A, Caron MG, Lefkowitz RJ. Regulation of adrenergic receptor function by phosphorylation. I. Agonist-promoted desensitization and phosphorylation of alpha 1-adrenergic receptors coupled to inositol phospholipid metabolism in DDT1 MF-2 smooth muscle cells. J Biol Chem. 1987 Mar 5;262(7):3098–105.

Lookingland KJ, Ireland LM, Gunnet JW, Manzanares J, Tian Y, Moore KE. 3-Methoxy-4-hydroxyphenylethyleneglycol concentrations in discrete hypothalamic nuclei reflect the activity of noradrenergic neurons. Brain Res. 1991 Sep 13;559(1):82–8.

Lookingland KJ, Moore KE. Chapter VIII Functional neuroanatomy of hypothalamic dopaminergic neuroendocrine systems. Handbook of chemical neuroanatomy. 2005.

Mackie K. Signaling via CNS cannabinoid receptors. Mol. Cell. Endocrinol. 2008 Apr 16;286(1-2 Suppl 1):S60–5. PMCID: PMC2435200

Malbon CC, Wang H-Y. Adrenergic Receptors. onlinelibrary.wiley.com. Chichester, UK: John Wiley & Sons, Ltd; 2001.

Marino F, Cosentino M. Adrenergic modulation of immune cells: an update. Amino Acids. 2013 Jul;45(1):55–71.

Marquart S, Zerr P, Akhmetshina A, Palumbo K, Reich N, Tomcik M, et al. Inactivation of the cannabinoid receptor CB1 prevents leukocyte infiltration and experimental fibrosis. Arthritis Rheum. 2010 Nov;62(11):3467–76.

Myöhänen TT, Schendzielorz N, Männistö PT. Distribution of catechol-O-methyltransferase (COMT) proteins and enzymatic activities in wild-type and soluble COMT deficient mice. J Neurochem. 2010 Mar 31.

Nance DM, Sanders VM. Autonomic innervation and regulation of the immune system (1987-2007). Brain Behav Immun. 2007 Aug;21(6):736–45. PMCID: PMC1986730

National Institute on Drug Abuse. Marijuana Abuse. 2013 Jul 24;:1–12. Retrieved from: http://www.drugabuse.gov/sites/default/files/rrmarijuana.pdf

Néron S, Nadeau PJ, Darveau A, Leblanc J-F. Tuning of CD40-CD154 interactions in human B-lymphocyte activation: a broad array of in vitro models for a complex in vivo situation. Arch. Immunol. Ther. Exp. (Warsz.). 2011 Feb;59(1):25–40.

Niederhoffer N, Szabo B. Effect of the cannabinoid receptor agonist WIN55212-2 on sympathetic cardiovascular regulation. Br J Pharmacol. 1999 Jan;126(2):457–66.

O'Connell FP, Pinkus JL, Pinkus GS. CD138 (syndecan-1), a plasma cell marker immunohistochemical profile in hematopoietic and nonhematopoietic neoplasms. Am. J. Clin. Pathol. 2004 Feb;121(2):254–63.

Oh-hashi Y, Shindo T, Kurihara Y, Imai T, Wang Y, Morita H, et al. Elevated Sympathetic Nervous Activity in Mice Deficient in  CGRP. Circ. Res. 2001 Nov 23;89(11):983–90.

Okuno S, Fujisawa H. Conversion of tyrosine hydroxylase to stable and inactive form by the end products. J Neurochem. 1991 Jul;57(1):53–60.

Olive MF, Mehmert KK, Hodge CW. Microdialysis in the mouse nucleus accumbens: a method for detection of monoamine and amino acid neurotransmitters with simultaneous assessment of locomotor activity. Brain Res. Brain Res. Protoc. 2000 Feb;5(1):16–24.

Olofsson PS, Rosas-Ballina M, Levine YA, Tracey KJ. Rethinking inflammation: neural circuits in the regulation of immunity. Immunol. Rev. 2012 Jul;248(1):188–204.

org D, editor. Marijuana Legalization in Washington State and Colorado | Drug Policy Alliance [Internet]. drugpolicy.org. 2014 [cited 2014 Jan 10]. Retrieved from: http://www.drugpolicy.org/resource/marijuana-legalization-washington-state-and-colorado

Ortega JE, Katner J, Davis R, Wade M, Nisenbaum L, Nomikos GG, et al. Modulation of neurotransmitter release in orexin/hypocretin-2 receptor knockout mice: a microdialysis study. J Neurosci Res. 2012 Mar;90(3):588–96.

Padro CJ, Shawler TM, Gormley MG, Sanders VM. Adrenergic Regulation of IgE Involves Modulation of CD23 and ADAM10 Expression on Exosomes. The Journal of Immunology. 2013 Oct 18. PMCID: PMC3842235

Parikh AA, Salzman AL, Kane CD, Fischer JE, Hasselgren PO. IL-6 production in human intestinal epithelial cells following stimulation with IL-1 beta is associated with activation of the transcription factor NF-kappa B. J Surg Res. 1997 Apr 1;69(1):139–44.

Pharmaceuticals G. Sativex. 2011;(3/8/2012).

Pinkus GS, Warhol MJ, O'Connor EM, Etheridge CL, Fujiwara K. Immunohistochemical localization of smooth muscle myosin in human spleen, lymph node, and other lymphoid tissues. Unique staining patterns in splenic white pulp and sinuses, lymphoid follicles, and certain vasculature, with ultrastructural correlations. Am. J. Pathol. 1986 Jun;123(3):440–53. PMCID: PMC1888274

Pongratz G, McAlees JW, Conrad DH, Erbe RS, Haas KM, Sanders VM. The Level of IgE Produced by a B Cell Is Regulated by Norepinephrine in a p38 MAPK- and CD23-Dependent Manner. J Immunol. 2006 Sep 1;177(5):2926–38.

Ralevic V, Kendall DA. Cannabinoids inhibit pre- and postjunctionally sympathetic neurotransmission in rat mesenteric arteries. Eur J Pharmacol. 2002 May 31;444(3):171–81.

Rongen GA, Lenders JW, Lambrou J, Willemsen JJ, Van Belle H, Thien T, et al. Presynaptic inhibition of norepinephrine release from sympathetic nerve endings by endogenous adenosine. Hypertension. 1996 Apr;27(4):933–8.

Saito H, Yokoi Y, Watanabe S, Tajima J, Kuroda H, Namihisa T. Reticular meshwork of the spleen in rats studied by electron microscopy. Am. J. Anat. 1988 Mar;181(3):235–52.

Sanders VM. The beta2-adrenergic receptor on T and B lymphocytes: Do we understand it yet? Brain Behav Immun. 2012 Feb;26(2):195–200. PMCID: PMC3243812

Schatz A, Lee M, Condie R, Pulaski J, Kaminski N. Cannabinoid receptors CB1 and CB2: a characterization of expression and adenylate cyclase modulation within the immune system. Toxicol Appl Pharmacol. 1997 Feb 1;142(2):278–87.

Seifert HA, Hall AA, Chapman CB, Collier LA, Willing AE, Pennypacker KR. A transient decrease in spleen size following stroke corresponds to splenocyte release into systemic circulation. J Neuroimmune Pharmacol. 2012 Dec;7(4):1017–24. PMCID: PMC3518577

Shimizu N, Hori T, Nakane H. An interleukin-1 beta-induced noradrenaline release in the spleen is mediated by brain corticotropin-releasing factor: an in vivo microdialysis study in conscious rats. Brain Behav Immun. 1994 Mar 1;8(1):14–23.

Siraskar B, Völkl J, Ahmed MSE, Hierlmeier M, Gu S, Schmid E, et al. Enhanced catecholamine release in mice expressing PKB/SGK-resistant GSK3. Pflugers Arch. 2011 Dec;462(6):811–9.

Skalli O, Ropraz P, Trzeciak A, Benzonana G, Gillessen D, Gabbiani G. A monoclonal antibody against alpha-smooth muscle actin: a new probe for smooth muscle differentiation. J. Cell Biol. 1986 Dec;103(6 Pt 2):2787–96. PMCID: PMC2114627

Spangelo BL, deHoll PD, Kalabay L, Bond BR, Arnaud P. Neurointermediate pituitary lobe cells synthesize and release interleukin-6 in vitro: effects of lipopolysaccharide and interleukin-1 beta. Endocrinology. 1994 Aug 1;135(2):556–63.

Springs AEB, Karmaus PWF, Crawford RB, Kaplan BLF, Kaminski NE. Effects of targeted deletion of cannabinoid receptors CB1 and CB2 on immune competence and sensitivity to immune modulation by Delta9-tetrahydrocannabinol. J Leukoc Biol. 2008 Dec;84(6):1574–84. PMCID: PMC2614598

Swift A. For First Time, Americans Favor Legalizing Marijuana [Internet]. gallup.com. 2014 [cited 2014 Jan 10]. Retrieved from: http://www.gallup.com/poll/165539/first-time-americans-favor-legalizing-marijuana.aspx

Tanasescu R, Constantinescu C. Cannabinoids and the immune system: an overview. Immunobiology. 2010 Aug 1;215(8):588–97.

Tangye SG. Staying alive: regulation of plasma cell survival. Trends Immunol. 2011 Dec;32(12):595–602.

Tawfik HE, Schnermann J, Oldenburg PJ, Mustafa SJ. Role of A1 adenosine receptors in regulation of vascular tone. Am J Physiol Heart Circ Physiol. 2005 Mar;288(3):H1411–6.

Tomiyama-Hanayama M, Rakugi H, Kohara M, Mima T, Adachi Y, Ohishi M, et al. Effect of interleukin-6 receptor blockage on renal injury in apolipoprotein E-deficient mice. AJP: Renal Physiology. 2009 Sep 1;297(3):F679–84.

Tyler WJ, Pozzo-Miller LD. BDNF enhances quantal neurotransmitter release

and increases the number of docked vesicles at the active zones of hippocampal excitatory synapses. Journal of Neuroscience. 2001 Jun 15;21(12):4249–58. PMCID: PMC2806848

Uchiyama Y, Yoshida H, Koike N, Hayakawa N, Sugita A, Nishimura T, et al. Anti-IL-6 receptor antibody increases blood IL-6 level via the blockade of IL-6 clearance, but not via the induction of IL-6 production. Int Immunopharmacol. 2008 Nov 1;8(11):1595–601.

Vrana KE, Allhiser CL, Roskoski R. Tyrosine hydroxylase activation and inactivation by protein phosphorylation conditions. J Neurochem. 1981 Jan;36(1):92–100.

Vrana KE, Roskoski R. Tyrosine hydroxylase inactivation following cAMP-dependent phosphorylation activation. J Neurochem. 1983 Jun;40(6):1692–700.

Ward RJ, Pediani JD, Milligan G. Heteromultimerization of cannabinoid CB(1) receptor and orexin OX(1) receptor generates a unique complex in which both protomers are regulated by orexin A. Journal of Biological Chemistry. 2011 Oct 28;286(43):37414–28. PMCID: PMC3199489

Watts J. Uruguay legalises production and sale of cannabis | World news | The Guardian [Internet]. theguardian.com. 2014 [cited 2014 Jan 4]. Retrieved from: http://www.theguardian.com/world/2013/dec/11/uruguay-cannabis-marijuana-production-sale-law

WhiteHouse.gov. Marijuana Resource Center: State Laws Related to Marijuana | The White House [Internet]. whitehouse.gov. 2014 [cited 2013 Dec 31]. Retrieved from: http://www.whitehouse.gov/ondcp/state-laws-related-to-marijuana

Wollner A. Public Support For Marijuana Legalization Hits Record High : It's All Politics : NPR [Internet]. npr.org. 2014 [cited 2014 Jan 10]. Retrieved from: http://www.npr.org/blogs/itsallpolitics/2013/10/22/239847084/public-support-for-marijuana-legalization-hits-record-high

Zastrow von M, Kobilka BK. Ligand-regulated internalization and recycling of human beta 2-adrenergic receptors between the plasma membrane and endosomes containing transferrin receptors. J Biol Chem. 1992 Feb 15;267(5):3530–8.

Zouali M. Natural Antibodies. els.net. Chichester, UK: John Wiley & Sons, Ltd; 2001.

Zuardi AW. Cannabidiol: from an inactive cannabinoid to a drug with wide spectrum of action. Rev Bras Psiquiatr [Internet]. 2008 Sep;30(3):271–80. Retrieved from: http://eutils.ncbi.nlm.nih.gov/entrez/eutils/elink.fcgi?dbfrom=pubmed&id=18833429&retmode=ref&cmd=prlinks

npr.org [Internet]. [cited 2013 Dec 31]. Retrieved from: http://www.npr.org